ISSMGE Technical Committee TC 209
Offshore Geotechnics

PROCEEDINGS OF TC 209 WORKSHOP
18TH ICSMGE - PARIS, 4 SEPTEMBER 2013

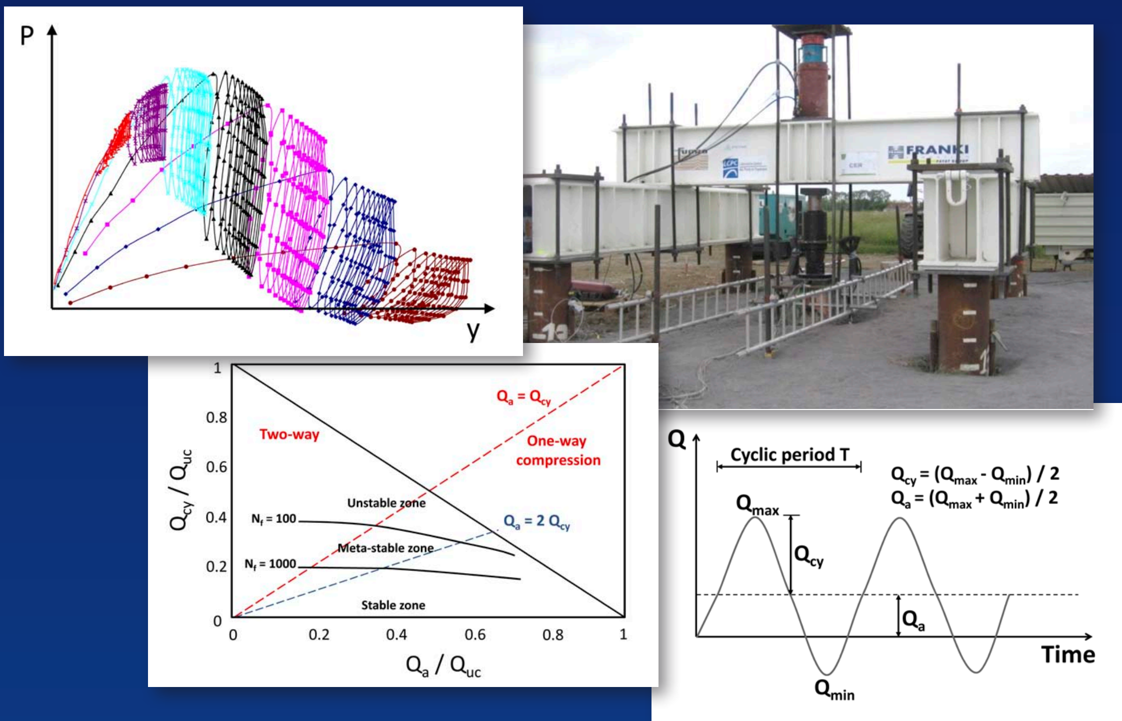

DESIGN FOR CYCLIC LOADING: PILES AND OTHER FOUNDATIONS

Edited by: Alain PUECH

Presses des Ponts

ISSMGE Technical Committee TC 209 – Offshore Geotechnics

Proceedings of TC 209 Workshop
18th ICSMGE, Paris 4 September 2013

DESIGN FOR CYCLIC LOADING: PILES AND OTHER FOUNDATIONS

Edited by Alain PUECH

SIMSG ISSMGE

Presses des Ponts

IREX
Institut pour la recherche appliquée et l'expérimentation en génie civil

ISBN 978-2-85978-479-9

Presses des Ponts
15, rue de la Fontaine-au-Roi
75127 Paris Cedex 11

Foreword

The International Society for Soil Mechanics and Geotechnical Engineering (ISSMGE) and its Technical Committee 209 (TC 209) on Offshore Geotechnics are proud to sponsor this workshop and the publication of this volume. At the beginning of his term, ISSMGE President Professor Jean-Louis Briaud set out clear objectives for all Technical Committees. Amongst others, they were urged to disseminate their knowledge and practices to the membership of the ISSMGE and encouraged to establish guidelines and technical recommendations within their subject area. There lies the impetus for this workshop.

First Andersen, Puech, and Jardine, in a superb tour de force, summarize forty years of successful practice in the design of a wide variety of offshore structures under cyclic loads, starting with the 1970s gravity-based structures of the North Sea and expanding to the deepwater areas of the world basins and more recently to the offshore renewable energy sector.

Second, Puech and Garnier generously share and summarize the latest advancements from the SOLCYP Joint Industry Project for piles under axial and lateral cyclic loads. Further findings from SOLCYP are also included in six additional papers.

Each of the ISSMGE technical committee's subject area includes unique aspects of geotechnics and not all knowledge is directly transferable and applicable from one community to the other. Nevertheless, we trust that other areas of geotechnics will capitalize on the experience and recommendations presented herein and avoid repeating similar learning curves. We also believe that onshore codes and standards would benefit from improved guidance on cyclic loading and its effects, as offered in this volume.

Last, ISSMGE TC 209 is grateful to IREX for funding the publication of this volume, to all the authors who shared their knowledge and experience, and to Alain Puech, for his leadership and dedication to make this workshop a reality.

Philippe Jeanjean
Chairman, ISSMGE TC 209 on Offshore Geotechnics.

Editorial Address

Pile design for cyclic loading is still a challenging issue. The offshore oil and gas industry has developed standards which include recommendations for the cyclic design of jacket pile foundations. However, limitations of the proposed procedures are recognised. The design of monopiles, tripod piles and jacket piles for offshore wind turbines is often governed by cyclic loading and more demanding procedures are required. In the building and civil engineering industries, the potential detrimental effect of cyclic loading on pile capacity and displacement is noted in most international codes but no specific procedure for taking these effects into account is proposed.

A collaborative research and development project called SOLCYP was launched in France in 2008, with the aim of understanding the phenomena which govern pile response under axial or lateral cyclic loading and developing advanced design methodologies. The project, partially sponsored by MEDDE (Ministry for Sustainable Development) and ANR (National Research Agency), is driven by IREX (the French Institute for Experimental Research in civil engineering) and uses a combination of field tests, model tests and theoretical approaches.

A major part of the testing was completed by the end of 2012 and a number of papers presenting results from the SOLCYP project were accepted for publication at the 18th ICSMGE. The new format adopted for the Paris 2013 Conference provided the great opportunity of organising, under the umbrella of TC 209, a workshop dedicated to "Design for cyclic loading: piles and other foundations".

IREX is proud of sponsoring this edition of the TC 209 Workshop Proceedings which includes:
– "Cyclic resistant geotechnical design and parameter selection for offshore engineering and other applications " prepared by K. Andersen (NGI), A. Puech (Fugro GeoConsulting) and R. Jardine (Imperial College London) on behalf of TC 209;
– Two original papers by A. Puech and J. Garnier, prepared for the TC 209 Workshop, which summarise the main findings of the SOLCYP pile tests and show how they can be used to develop advanced methodologies for axial and lateral cyclic pile design.

Six short papers are included in this document, which are English translations of papers originally published in French as part of the 18th ICSMGE Conference Proceedings.

We believe that gathering this information into a single publication will provide the geotechnical foundation designer with unique and useful data and recommendations for designing piles and other foundations under cyclic loading.

Lastly, we are grateful to Meriam Kkemakhem-Ben Amor and Laura Connochie for their contribution to the preparation of this document.

Alain Puech
Technical Director, SOLCYP project

Brice Delaporte
Technical Director, IREX

Table of contents

Cyclic resistant geotechnical design and parameter selection for offshore engineering and other applications

Dimensionnement aux chargements cycliques et sélection des paramètres pour l'ingénierie des fondations offshore et autres applications

Knut H. Andersen, Alain A. Puech and Richard J. Jardine
Norwegian Geotechnical Institute, Oslo, Norway; Fugro GeoConsulting, Nanterre, France and Imperial College London

ABSTRACT: Cyclic loading due to wind, wave and wind-turbine loading is of crucial importance in offshore foundation engineering. Designers often have to consider cyclic bearing capacity and stiffness, as well as permanent displacements due to cycling and potentially changing patterns of soil reaction stresses. These features are illustrated by drawing on offshore engineering prototype observations, field, model and soil element testing studies before setting out cyclic design procedures for gravity base foundations, suction anchors, monopiles and deep driven piles. Similar approaches may be used to consider the geotechnical effects of cycling imposed by seasons, earthquakes, ice, machinery or other processes in applications ranging from sea barriers to large bridges and foundations to roads or high-speed trains. A main objective has been to offer guidance for obtaining the soil parameters for design of foundations under cyclic loading.

RÉSUMÉ : Les chargements cycliques induits par le vent, la houle et le fonctionnement des éoliennes sont d'une importance capitale pour l'ingénierie des fondations offshore. Le concepteur doit le plus souvent considérer la capacité portante et la raideur cycliques mais aussi les déplacements permanents engendrés par les cycles et de possibles évolutions des réactions du sol. Ces particularités sont illustrées par un panorama d'observations recueillies sur des prototypes de structures offshore et de résultats d'essais in situ, sur modèles et sur échantillons de sol. On décrit ensuite les procédures de dimensionnement sous chargement cyclique des fondations de plates-formes gravitaires, d'ancres à succion, de monopieux d'éoliennes et de pieux battus de grandes longueurs. Des approches similaires peuvent être utilisées pour prendre en compte les effets géotechniques des charges cycliques imposées par les variations saisonnières, les séismes, les glaces, les machineries et autres processus tels que rencontrés dans les ouvrages de défense à la mer, les grands ponts ou les fondations de routes et de trains à grande vitesse. L'objectif principal a été de proposer des recommandations pour l'obtention des paramètres de sol nécessaires pour le dimensionnement des fondations sous chargements cycliques.

KEYWORDS: cyclic loading, foundation design, laboratory testing, soil parameters

MOTS-CLES: chargement cyclique, dimensionnement de fondations, essais de laboratoire, paramètres de sol

1 INTRODUCTION

This document has been prepared under the auspices of ISSMGE TC-209, which is concerned with advancing offshore geotechnical engineering. Its main aim is to contribute to comprehensive cyclic design guidance for offshore and other civil engineering applications.

The offshore oil and gas industry has advanced cyclic design in recent decades, developing procedures for considering the effects of large cyclic loads caused principally by waves and wind. Well-established guidance is available for Gravity Base Structure (GBS) and other shallow foundation types, in API RP 2GEO, 2011; DNV Foundations, 1992. Jardine et al 2012 summarise equivalent developments in cyclic assessment methods for offshore piled foundations. The offshore wind-turbine industry is also adapting cyclic design methodologies: see DnV-OS-J101, 2010 or BSH, 2007.

Far less attention is given currently to cyclic loading in general civil engineering and building foundation guidelines. National codes and Eurocode 7 reflect a generally lower level of elaboration. Closer attention is paid to the topic in earthquake geotechnical engineering, pavement studies and in foundation design for heavy rotating machines. Andersen (2009) emphasized cases where cyclic loading is important for coastal structures (harbour facilities, breakwaters, storm surge barriers etc.) and also foundations, slopes, embankments and cuts subjected to variable seasonal, wind, operating or seismic loads. The present lack of guidance regarding piles under cyclic loading is being addressed in the ambitious SOLCYP Research and Development project (Puech et al., 2012) underway in France that considers a wide range of applications including high rise towers and chimneys, energy transport pylons, high-speed train infrastructure and crane foundations, as well as offshore energy facilities. Results from SOLCYP are incorporated into this paper.

The paper describes how foundation design can be approached when cyclic loading is important, summarises some relevant calculation procedures and focuses on reporting current best offshore practice for determining cyclic design parameters. The latter has developed through advanced laboratory testing, performed on high quality samples, combined with model and full-scale field studies. In-situ testing based approaches have yet to be developed comprehensively, although this avenue may prove more promising in the future.

Ten main sections are set out between this introduction and the final conclusions covering:

- The range of offshore foundation types considered
- Cyclic loading characteristics
- The key aspects to consider in cyclic design

- Calculation procedures for offshore shallow foundations and suction anchors
- Calculation procedures for offshore piles
- Cyclic soil parameters required for foundation design
- Derivation of cyclic soil parameters from laboratory tests
- Guidance on interpreting and presenting results
- Existing data bases of cyclic loading test results
- Application to other types of structures and cyclic regimes, describing how cyclic design methodologies can be applied to applications outside offshore engineering, noting the broader spread of cyclic loading regimes and the potential demands of the mainstream civil engineering industry.

2 OFFSHORE FOUNDATION TYPES

The choice of cyclic design procedure depends on the foundation type under consideration. This paper follows the historical development of offshore cyclic design development, starting with large North Sea Gravity Base Structures (GBS) (Andersen, 1976), before extending to suction anchor cases (Andersen and Jostad, 1999) and then offshore piles. The first two, relatively shallow (low depth L to Diameter D ratio), applications illustrate the NGI's 'cyclic contour diagram network' method for addressing soil behaviour and foundation response. Low L/D skirted foundations, offshore jacket mud-mats and sea-bed templates can be analysed in similar ways, as may suction anchors and even monopiles.

The piling sections that follow draw on an earlier paper (Jardine et al., 2012) that focused on deeper foundations and argued that closer attention should be given to cyclic resistance in routine practice. Most offshore jackets and floating structures rely on piles with $10 < L/D < 70$. The piles usually comprise open ended steel tubes, although bored piles are used in some special applications. Pile driving adds complexity, setting up new stress conditions at the soil/pile interface. The effective stresses generated redistribute with time in the soil mass and over the pile surface during loading. While different approaches are available for low 'L/D' foundations, wind-turbine monopiles and sometimes even suction caissons have also been analysed by extending conventional offshore pile methods. This practice is also discussed, referring to recent research.

3 CYCLIC LOADS

The term "cyclic" loading is used generically to characterise variable loads that have clearly repeated patterns and a degree of regularity in amplitude and return period. Cyclic loads can be essentially of environmental origin (seasons, waves, tide, current, wind, earthquakes, ice sheets) or anthropogenic (due to traffic, blasting operations, plant operations or rotating machinery).

Cyclic loading characteristics vary considerably between cases as illustrated by Figure 3.1. For example, seasons cycle over months, tidal forces usually follow 12 hour periods, while large sea-waves cycle over 10-20s and earthquake periods are far shorter. The durations of extreme cycling events also vary, ranging from 1 to 2 days for an offshore design storm to less than 1 minute for most earthquakes. Design critical cases range from a few extreme cycles to millions of low level fluctuations.

The most severe cyclic storm or earthquake load histories are often composed of a succession of irregular amplitude waves that are distributed relatively randomly with time. However, the cyclic field, laboratory-model and soil-element tests that are conducted to explore cyclic loading effects are usually restricted to tests that can be conducted within limited time-frames and at cyclic rates that allow suitable control, precision and data capture rates. The most common practice is to conduct uniform cycling with load or displacement series' that employ a fixed frequency and regular amplitude. Such regular-cycle tests can be defined by their number of cycles N, period (T), average load (Q_a), cyclic load amplitude (Q_{cy}) - or their displacement equivalents (Figure 3.2).

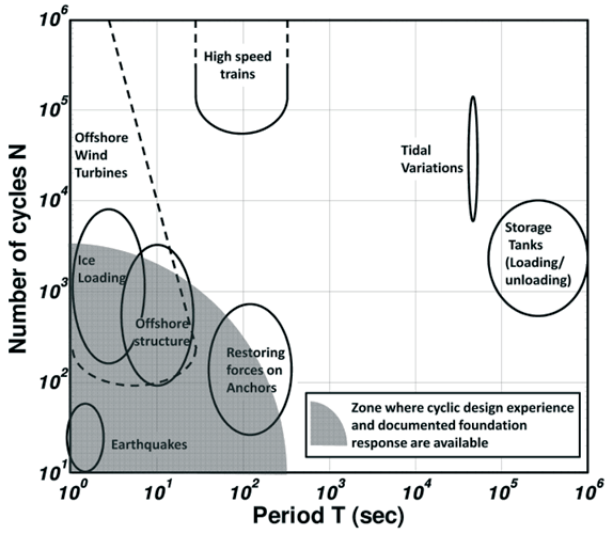

Figure 3.1: Periods and number of cycles characterising typical cyclic loading events.

Regular cyclic loading can be symmetrical ($Q_a = 0$) but is more normally non-symmetrical due to a non-zero average component. Even GBS cases have dead-weight vertical or steady current/wind components. One-way loading imposes $Q_{cy} < Q_a$ while two-way loading leads to $Q_{cy} > Q_a$. Cycle-counting methods (often derived from 'rainflow' analyses, see ASTM E1049-85 which may overestimate number of large waves) are often used to transform the expected field cyclic load histories into idealised series' of regular cycles that may be matched with the outcomes of the uniform cycling imposed in laboratory or field tests performed to aid practical cyclic design.

There are cases where two or more cyclic loading frequencies need to be considered simultaneously. This can occur with offshore wind power structures, for example, that are subject to cycling forced by wind and waves periods as well as secondary cycles related to their rotor rotation frequencies. Another cause of multi-mode cycling can be the combination of an external forcing frequency and cyclic motions set up by the structure resonating at a frequency determined by its own weight and stiffness. The foundation of the Great Belt bridge in Denmark provides one example where design had to address actions from floating and breaking ice sheets that imposed load cycles with periods of about 10s that generated significant bridge pier vibrations. The latter, secondary, foundation loading cycled at a higher frequency of about 1Hz; Andersen, 2009.

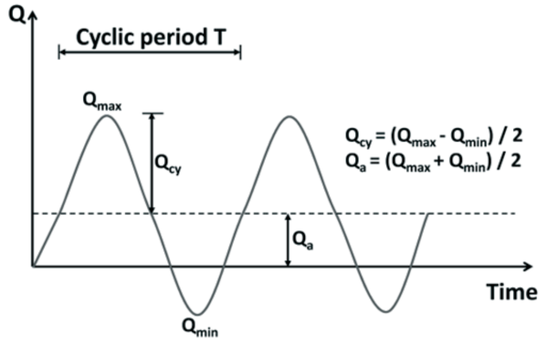

Figure 3.2: Cyclic loading definitions. Note Q_a is often referred in the literature to as $Q_{average}$, Q_{ave} , Q_{av} or Q_{mean}, and Q_{cy} as Q_{cyc}, Q_{cyclic} or Q_c

4 FOUNDATION DESIGN ASPECTS

The major requirements to be addressed in cyclic foundation design are: (1) ensuring sufficient bearing capacity; (2) making sure that cyclic displacements are tolerable; (3) providing equivalent soil spring stiffnesses for use in dynamic soil-structure analyses; (4) assessing whether long term settlements due to permanent straining during cyclic loading are tolerable, (5) considering also movements developed post-cycling through creep and pore pressure dissipation, and (6) assessing how the base and side soil reaction stresses developed at the soil-structure interface may change due to cycling. These aspects are outlined briefly below and discussed in more detail by Andersen (2004).

4.1 *Capacity*

Cyclic bearing capacities must be sufficient to (i) carry the structure and its external cyclic loads and keep deformations within acceptable limits, while (ii) maintaining a sufficient reserve against uncertainty in soil conditions and parameters, calculation method performance and loading. The ultimate capacity developed under cyclic loading can differ considerably from the monotonic (drained or potentially undrained) loading capacity. One example is shown in Figure 4.1, which compares the capacities developed under cyclic and monotonic loading in two model tests footing on clay. The capacity developed under some dozens of high-level cycles is smaller than the monotonic capacity in this case. However, the relative capacities depend on the number of cycles, the ratio between cyclic and average loads, the composition of the cyclic amplitudes and the load period. Rate effects can cause the capacity developed under a small number of fast cycles to exceed the monotonic capacity; the monotonic capacity can also be improved in some cases by pre-applying many low-level cycles and allowing creep and drainage.

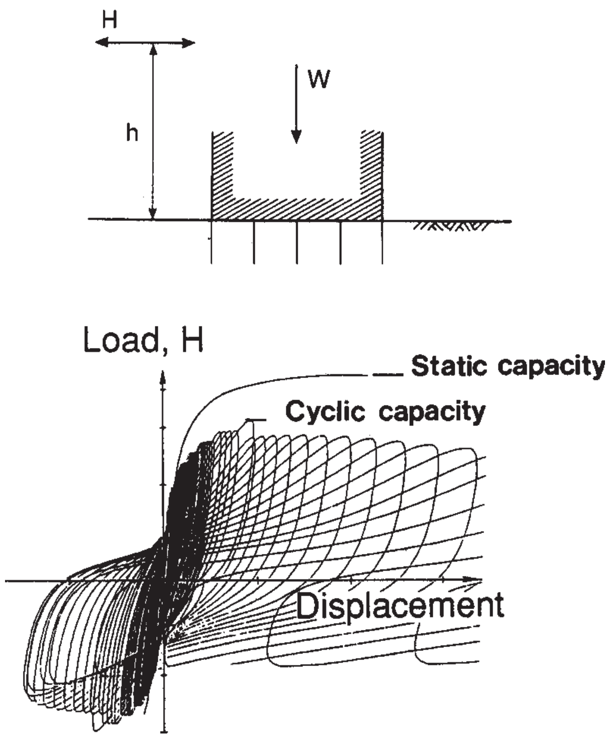

Figure 4.1: Results from model tests with monotonic and cyclic loading of a 0.4m diameter footing with 0.1m long skirts in a soft clay with Ip=28% and shear strength of about 10kPa (Dyvik et al. 1989)

Another example is shown in Figure 4.2a, which compares the cyclic and monotonic axial loading responses of a (D=420mm, L=13.5m) bored pile installed in the highly overconsolidated Flanders clay at Merville (Northern France). This system is relatively resistant to one-way cyclic loading. However, batches of cycles applied (at 0.5 Hz) to give load maxima amounting to 90% of the static capacity led to failure by steadily accumulating permanent displacements. The static capacities were defined by relatively rapid incremental loading tests typically achieving failure in 30 minutes.

Jardine et al. (2012) show that axial capacity degradation is more severe with sensitive clays and in soils (such as sands) that have higher interface shear friction angles, δ. Figure 4-2b compares the static and cyclic response of two identical piles (D=420mm, L=8m) bored in dense Flanders sand at Loon-Plage, near Dunkirk in Northern. France. The sand has far higher δ angles than the plastic Merville clay. One-way (first time) cyclic loading on pile F5 generated large permanent displacements at loads well below the static capacity (about 1100kN) developed in a conventional incremental static test on a control pile (F4) after a displacement of 0.1D.

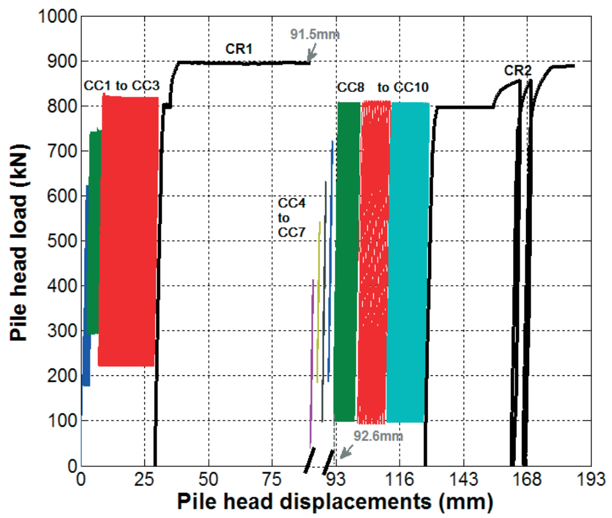

Figure 4.2a: Cyclic field tests on a bored pile in Flanders clay (Benzaria et al., 2013). CC: cyclic tests each with N = 1000, CR: monotonic rapid tests. Pile loaded in compression

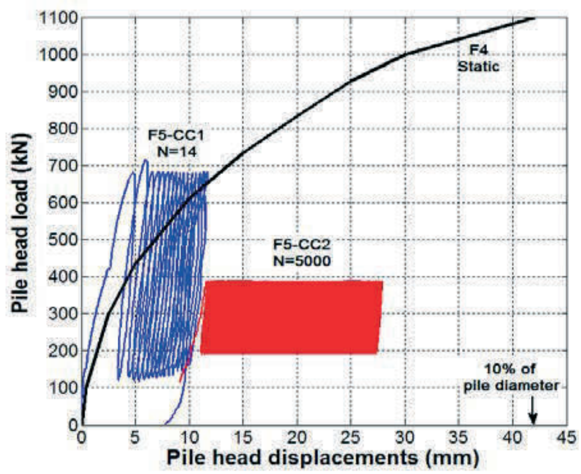

Figure 4.2b: Field tests on two identical piles bored in dense Flanders sands (Benzaria et al., 2013). Static (F4) and cyclic (F5) responses. Piles loaded in compression

It is also well established that high-level two-way loading leads to far more marked capacity losses than one-way loading: see the Haga clay or Dunkirk sand driven pile cases reviewed by Jardine et al. (2012).

4.2 *Cyclic displacements*

Structural serviceability and fatigue life may be sensitive to the displacements experienced under cycling. These issues are critical with wind-turbines, for example, while cyclic movements have to be contained. Limits have to be maintained with other offshore platform types to control stresses in structural elements or in connections with wells, risers or pipelines.

The North Sea Brent B Condeep platform provides an illustration. In this case, the oil wells positioned beneath the base were considered liable to distress if horizontal seafloor displacements exceeded 150mm. Design calculations indicated that the foundation scheme should be able to keep cyclic horizontal displacements and rotations within tolerable values (≈ 65mm and ≈ $7 \cdot 10^{-4}$ radians respectively) even if the design storm arrived during the first winter after platform installation. Analysis indicated that movements would be reduced by around 70% if the design storm developed after full dissipation of the pore pressures set up in the underlying stiff glacial clay and dense sand layers by the platform's weight: see Figure 4.3. Later field monitoring showed that the prototype foundation was approximately 30% softer for horizontal displacements and approximately 5% stiffer for rotations than anticipated in design.

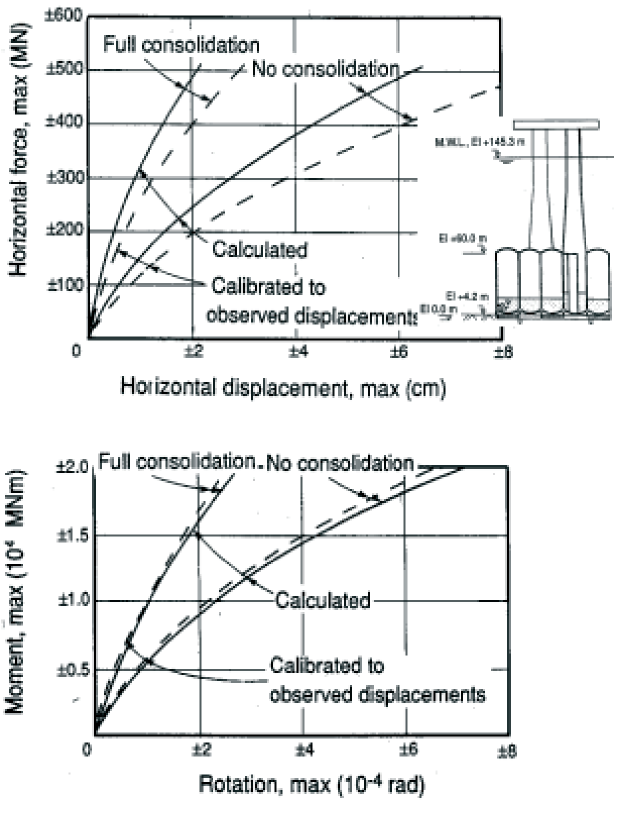

Figure 4.3: Cyclic displacements of the Brent B Condeep platform at seafloor elevation (Andersen & Aas 1980). Design loads comprise a horizontal load of 500MN and moment of $2 \cdot 10^4$ MNm

The SOLCYP group show that high level axial or lateral cyclic loading can generate large permanent displacements with bored piles. Figure 4.2 demonstrated the results of axial cyclic loading field tests on 420mm diameter piles in sand and overconsolidated clay, while lateral cyclic loading centrifuge tests performed on low OCR kaolin are presented in Figure 4.4 for a pile with 0.9m equivalent prototype diameter.

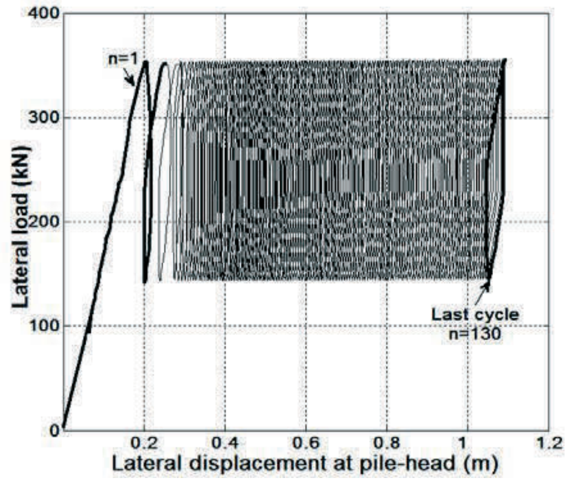

Figure 4.4: Centrifuge tests in low OCR kaolin; equivalent prototype pile diameter = 0.9m; one-way horizontal loading; cyclic displacements

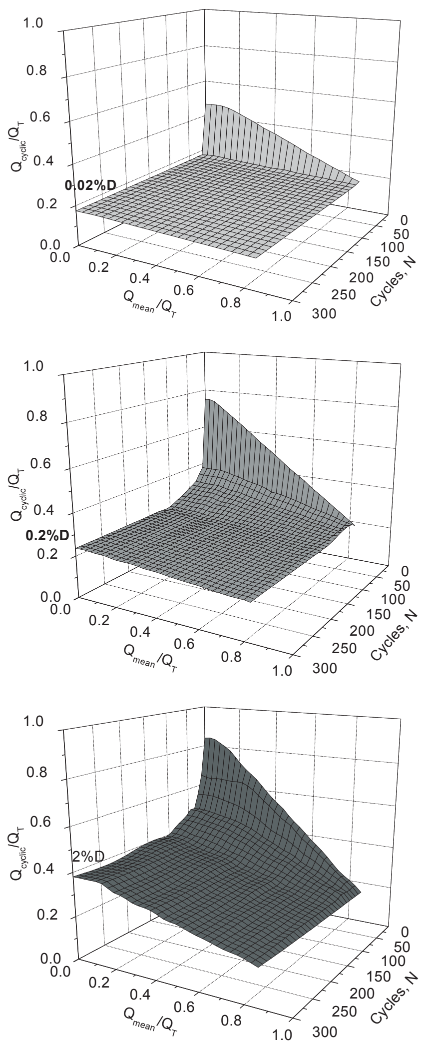

Fig. 4.5: Permanent displacements as functions of N and cyclic loading parameters from metastable and unstable axial cycling tests on 19m long, 456mm diameter, steel tubular piles driven in dense Dunkirk sand. Note Q_T = tension capacity; Rimoy et al., 2013

Jardine and Standing (2000 and 2012) and Jardine et al. (2006) report trends from multiple axial cyclic loading tests on 456mm diameter, 19m long steel tubular piles driven at the Dunkirk test site. Rimoy et al. (2013) show that permanent displacements depend systematically on the cyclic loading level, degree of cyclic stability and number of cycles. Figure 4.5 shows the conditions under which permanent pile head displacements accumulated in individual cyclic tests to reach 0.02% D (top), 0.2% D (middle) and 2% D (bottom) where D = pile diameter.

Rimoy et al. (2013) also showed that pile stiffness under cyclic loading was also highly non-linear at Dunkirk, although less affected by the numbers of cycles imposed until failure is approached. The upper part of Figure 4.6 highlights the stiffness non-linearity by showing how the overall pile head secant stiffness k = Q/δ (where Q = load and δ pile head displacement, both are sum of average and cyclic components) fell with load during the first-time monotonic testing of piles R2 to R6. The k values are normalized by a reference value (k_{ref}) defined from the first load step (that applied Q_{ref} = 200 kN) while loads Q are normalized by Q_{ref}. These patterns are typical for large pile and other foundation types; see Jardine et al. (1986 and 2005b).

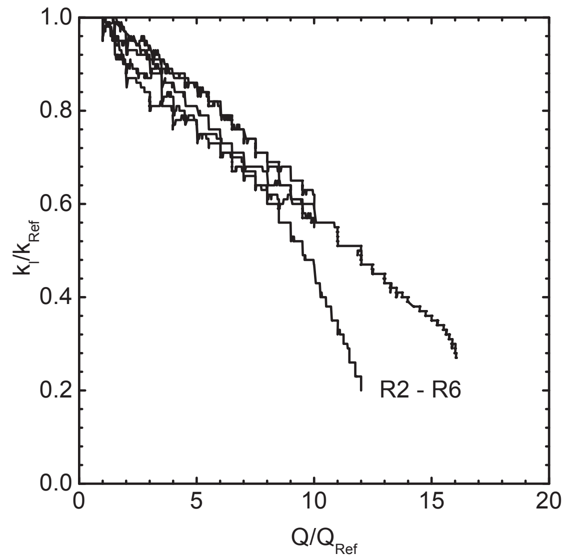

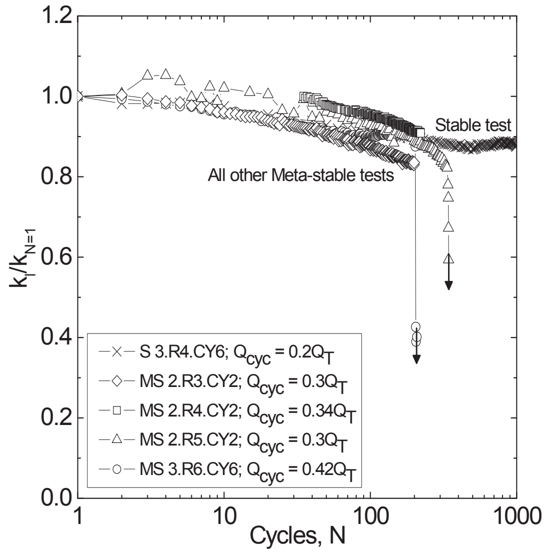

Fig. 4.6: Axial stiffness characteristics from static and metastable cyclic tests on steel piles driven in Dunkirk dense sand; Rimoy et al., 2013

The lower traces in Figure 4.6 show how axial stiffness varied with N in five typical stable and metastable tests, normalized by $k_{N=1}$, the (non-linear) stiffness developed over first cycle; after Rimoy et al 2013. The stiffness under cyclic loading showed only modest reductions (< 20%) over hundreds of cycles. However, sudden stiffness reductions were seen over the final few cycles of the two tests that developed full cyclic failure.

4.3 *Equivalent cyclic soil spring stiffnesses*

A key task in offshore design is to avoid damaging resonant motions developing under cyclic loading. The Brent B Condeep GBS platform monitoring data shown in Figure 4.7 indicate an example where the first resonance periods for the combined soil-structure system were found to be 1.78s, 1.71s and 1.19s respectively, all falling well below the predominant wave load period range (10s to 15s). The structural stiffness and weight changes associated with moving to progressively deeper water conditions lead to increasing resonant periods that eventually approach the wave load period, which encourages dynamic load amplification and structural problems. Such trends apply to all slender structures as their slenderness ratio (L/D) increases.

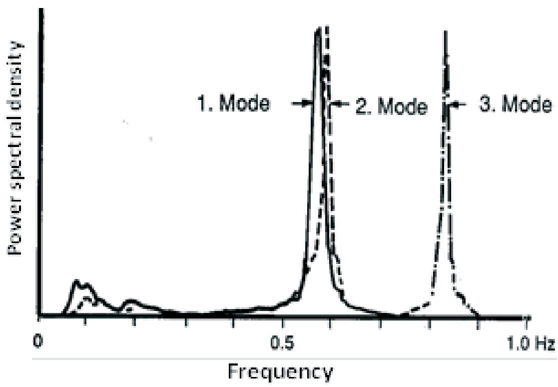

Figure 4.7: Measured acceleration spectra from the Brent B Condeep gravity base platform (Hansteen, 1980)

The resonant frequencies of wind-turbines, for example, are sensitive to their horizontal foundation stiffness characteristics. Monopiles based offshore often have embedded diameters in excess of 5 meters and slenderness ratios in the range of 5 to 10. They are designed to work as 'soft-stiff' structures, with first natural frequencies that fall between their two critical excitation frequency bands (1P and 3P) in order to avoid resonance. The 1P and 3P excitation frequencies are functions of the operational rotor rate, which for modern turbines is typically between 7 and 12 rpm (Andersen et al., 2012). As illustrated in Figure 4.8, the first natural frequency is constrained within a narrow band and needs to be known with a high level of confidence. Any initial stiffness estimation errors could have significant consequences, as can any long-term cyclic effects that change the foundation frequencies and move an initially optimally designed system towards resonance and fatigue problems. One possible remedial measure might be to alter the operational rotor frequency.

It is common when assessing structural dynamic characteristics to sub-divide the interacting soil and structural domains and consider each separately. Soils conditions are often represented in dynamic structural analyses by equivalent 'soil springs' whose stiffnesses have to be specified from independent simplified geotechnical analyses. As noted above, foundation stiffness behaviour may be highly non-linear and great care is needed to derive appropriate simplified 'spring' characteristics.

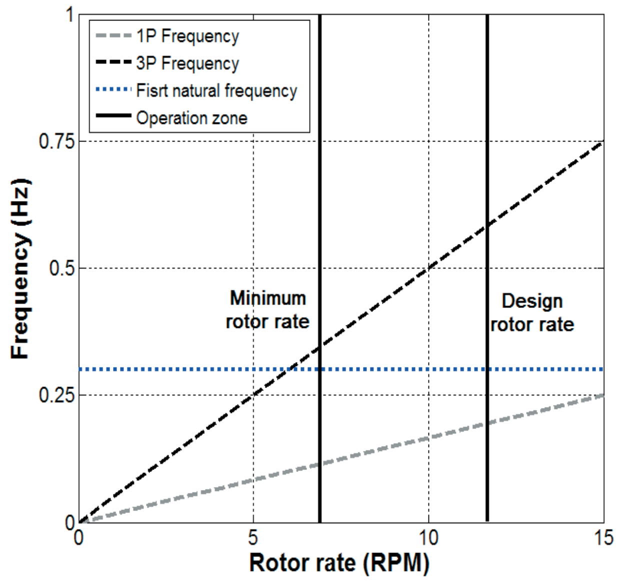

Figure 4.8: Simplified Campbell diagram for wind turbine soft-stiff design (after Andersen et al., 2012).

4.4 *Permanent displacements due to cyclic loading*

Cyclic loads add to permanent loads in causing permanent deformations that may distress structural elements or connections to offshore platforms. Significant settlements also reduce the free-board between the deck and the sea. Similarly, wind-power structures have to maintain strictly set verticality limits under markedly non-symmetrical cyclic loading conditions.

The deformations developed due to cyclic loading can be separated into two components; (1) those due to permanent strains developed during the cyclic loading and (2) strains due to dissipation of cyclically induced pore pressure and creep. Settlement due to cyclic loading is illustrated in Figure 4.9, reporting the response of the Ekofisk Oil Storage Tank during first its installation and ballasting, and then a severe storm in late 1973. The settlements increased sharply by ≈ 60mm during the November storms.

As discussed above, piles develop significant permanent displacements under high level cyclic axial loading. Similar trends apply under lateral loading, with displacement rates that depend on the loading style and loading severity. Centrifuge test data from lateral loading tests on normally consolidated soft kaolin are presented in Figure 4.10a as an example. Non-symmetrical horizontal loading generated large permanent lateral pile head displacements which trebled within 500 cycles. The additional displacements naturally lead to large increases in maximum pile bending moments. The latter feature can also be important under even relatively low-level cycling, as illustrated in Figure 4.10b with measurements from a second lateral loading set of cyclic centrifuge tests on piles installed in medium-dense fine Fontainebleau NE34 sand.

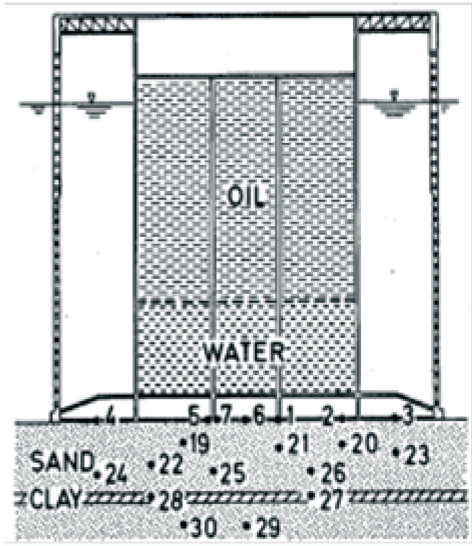

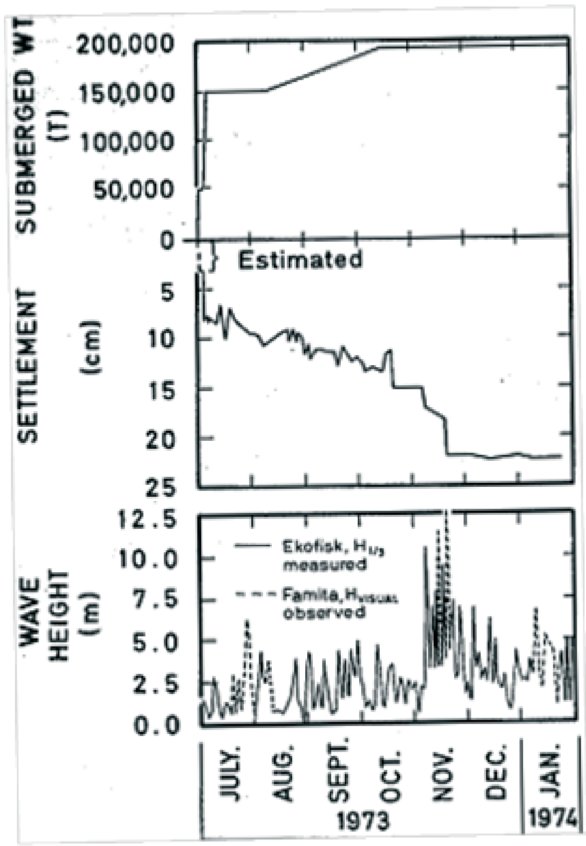

Figure 4.9: Measured settlements of the Ekofisk oil storage tank during installation, ballasting and storm loading (Clausen et al., 1975)

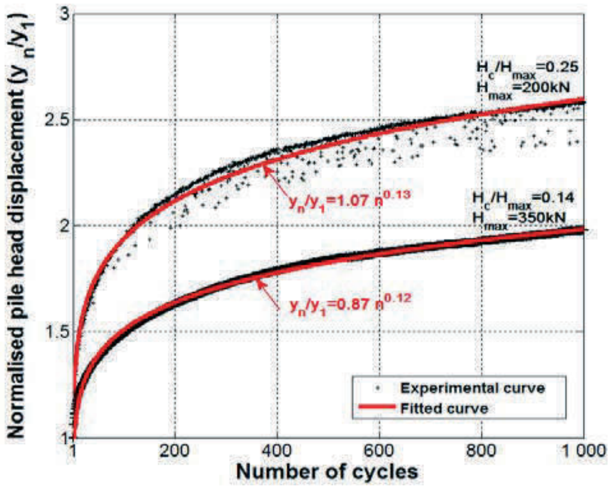

a) Horizontal displacements (y_N) normalised by y_1 displacement for first cycle against N (Khemakhem, 2012) from high-level centrifuge lateral loading tests on Kaolin at OCR = 1

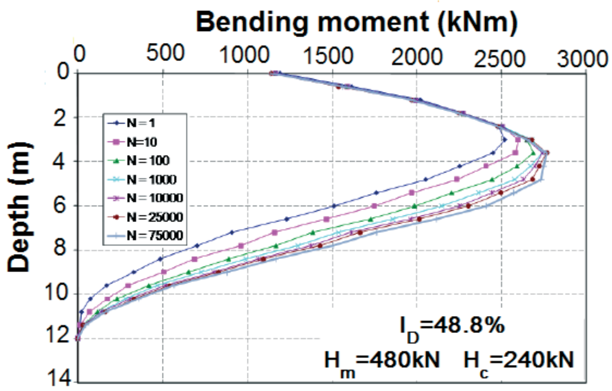

b) Bending moment in piles varying with number of cycles N from low level centrifuge lateral loading tests on medium dense sand (Rakotonindriana, 2009)

Figure 4.10: Results of centrifuge model tests on piles subject to cyclic horizontal loading

4.5 *Soil reaction stresses*

The above lateral pile loading cases provide examples of stiffness degradation under cyclic loading changing the lateral soil-structure contact pressure distributions and raising bending stresses within the (pile) structure. Analogous changes may develop through load cycling on the pressure distributions developed across the bases and sides of GBS foundations or suction caisson due to creep, consolidation and cyclic loading. Such changes have to be addressed to ensure that the structural design is sufficiently robust to cope with long-term soil pressure distributions and stiffness characteristics.

5 CALCULATION PROCEDURES FOR OFFSHORE SHALLOW FOUNDATIONS AND SUCTION ANCHORS

5.1 *Capacity*

Capacity is assessed by applying limit equilibrium, plastic limit or finite element procedures. Limit equilibrium and plastic limit methods involve assuming a failure mechanism and optimising the solution, searching for the most critical case. Examples of trial limit equilibrium failure surfaces are shown in Figure 5.1 for shallow foundation and anchor examples. Such analyses normally use simplified 2D models and account for 3D-effects by adding additional 'side shear' forces that are calibrated against 3D finite element analyses (e.g. Schjetne and Lauritzsen, 1976; Andersen and Jostad, 1999). However, the critical failure mechanism emerges in elastic-plastic finite element analyses without the user having to making any prior assumption; both 2D and 3D finite element analyses are practically feasible.

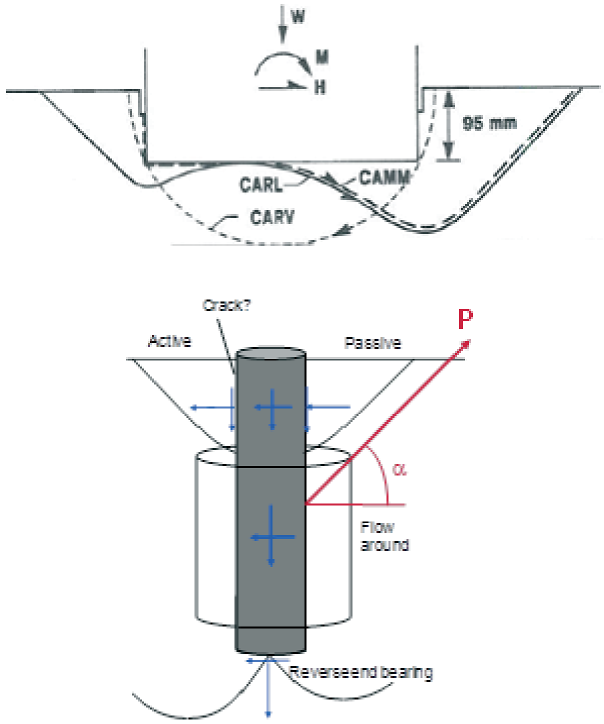

Figure 5.1: Examples of potential limit equilibrium failure surfaces

Finite element analyses also reveal details of the stress paths imposed on the underlying soil and around any potential failure mechanism. Six stress components have to be specified to describe the stress state fully at any given point, which reduces to four in 2-D plane stress/strain or axially symmetric cases. The familiar stress path parameters $q = (\sigma_1 - \sigma_3)$, $p' = (\sigma'_1 + \sigma'_2 + \sigma'_3)/3$ (or $t = q/2$ and $s' = (\sigma'_1 + \sigma'_3)/2$) describe the stress conditions of Triaxial Compression (TC) or Triaxial Extension (TE) tests fully, where α (the orientation of σ_1 relative to the vertical) and $b = (\sigma_2 - \sigma_3)/(\sigma_1 - \sigma_3)$ are fixed as α = 0, b = 0 for TC and as α = 90°, b = 1 for TE respectively. But α and b can vary freely under more general 2-D stress conditions and it is necessary to track these variations. Direct Simple Shear (DSS) involve α and b changes. However, it is not possible with most apparatus to define the full (q, p′, α, b) DSS stress paths.

Figure 5.2 shows an example of an analysis reported by Jardine et al. (1997) that presents the contours of α that apply beneath a trapezoidally loaded shallow foundation on low OCR clay. The σ_1 axis is vertical under the centre line but rotates under the edges to eventually become horizontal outside the loaded area. Such stress axis rotation implies an associated rotation of potential slip failure plane orientations. The same analysis showed the 'b' parameter changing from an initial value of 0 to ≈ 0.4 as loading progresses.

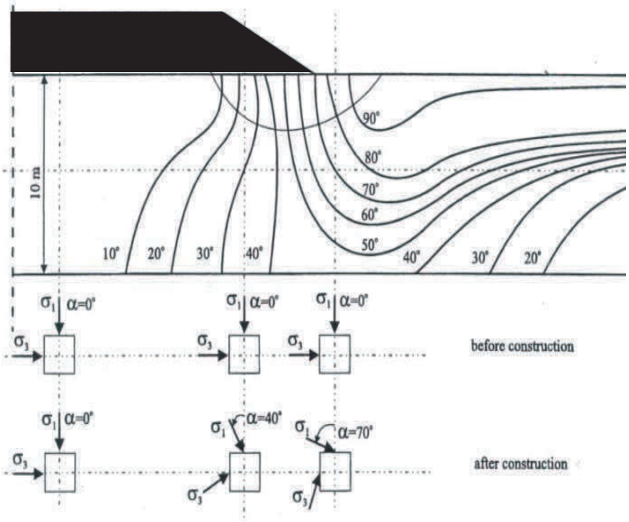

Figure 5.2: Contours of α (the orientation of σ_1 relative to the vertical underneath a trapezoidally loaded shallow foundation on low OCR clay; after Jardine et al., 1997. Note that σ_2 parameter b also changes to ≈ 0.4.

Advanced laboratory tests show that soil response, and in particular undrained shear strength, depends critically on the imposed combinations of q/p′, α (effects of direction, or anisotropy) (e.g. Bjerrum 1973) and b (effects of σ_2). Jardine et al 1997 report undrained shear strengths measured with Hollow Cylinder Apparatus (HCA) that can vary b and α over a wide range. Figure 5.3 illustrates multiple tests conducted by Menkiti 1995 on K_0 consolidated samples of HK, a clay-sand, tested at OCR = 1 in which 'b' was kept at a nominally plane strain value (b = 0.5) in tests that imposed a range of α values (between 0 and 90°). The s_u values obtained, expressed as ratios to the vertical effective consolidation stresses, show strong anisotropy with s_u/σ'_v falling continuously with α. The same figure shows data from DSS tests conducted in the HCA and TC and TE tests on K_0 consolidated samples that were conducted in both the HCA and in standard triaxial cells. The triaxial shear strengths fall below the plane strain HCA values, while the HCA simple shear failure develops with α ≈ 25°, rather than at α > 45° as assumed conventionally.

The s_u/σ_v' pattern shown in Figure 5.3 is typical of low OCR soils as is illustrated in Figure 5.4 by similar sets of data from 'plane strain' HCA tests conducted at OCR = 1 on clay, clay-sand and loose sand; similar results are found with HPF4 rock-flour silt (Zdravkovic and Jardine 2000). Nishimura et al. 2007 and Brosse 2013 show that highly overconsolidated natural stiff clays and mudrocks also have markedly anisotropic plane strain shear strengths, although they tend to develop their s_u minima around α ≈ 45°: see Figure 5.5. Other HCA tests conducted with constant α values but with variable b ratios show that the relative magnitude of σ_2 also affects the shear strengths. Zdravkovic et al. (2001) reported advanced finite element analyses with anisotropic soil models that demonstrated how the observed behaviour impacts significantly on the 3-D bearing capacity of offshore suction caisson anchors.

Simple shear tests can be undertaken in the HCA (see Nishimura et al., 2007 or Anh-Minh et al., 2011) under fully defined stress conditions. Such tests show that the peak horizontal shear stresses τ_{vh} usually falls below the true t_{max} and that the α values at which τ_{vh} reaches its maximum vary with K_0, shifting from around 25° at OCR = 1 (see Figure 5.3) to around 65° in very high OCR specimens; the b values typically fall between 0.35 and 0.65, depending also on K_o and OCR.

HCA and stress path triaxial experiments that include multi-axis bender element arrangements also show that soils' non-linear stiffness characteristics are often markedly anisotropic from small strains to large: see Zdravkovic and Jardine (1997), Kuwano and Jardine (2002), Gasparre et al. (2007), or Jardine (2013).

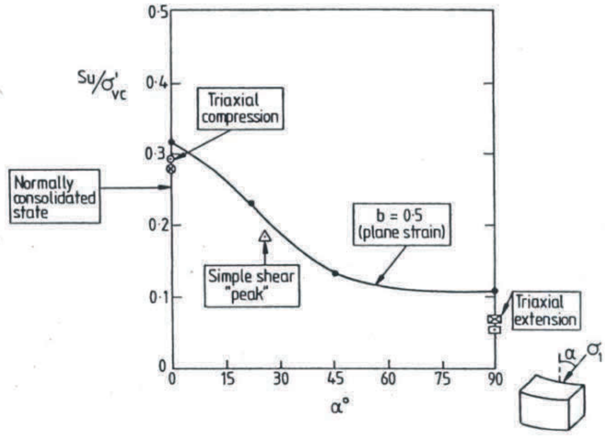

Figure 5.3: Variation with α of s_u/σ_v' in plane strain (b = 0.5) HCA tests on normally (K_0) consolidated HK clay-sand, CAU TC, TE and HCA SS shear strengths also shown; Jardine and Menkiti, 1999

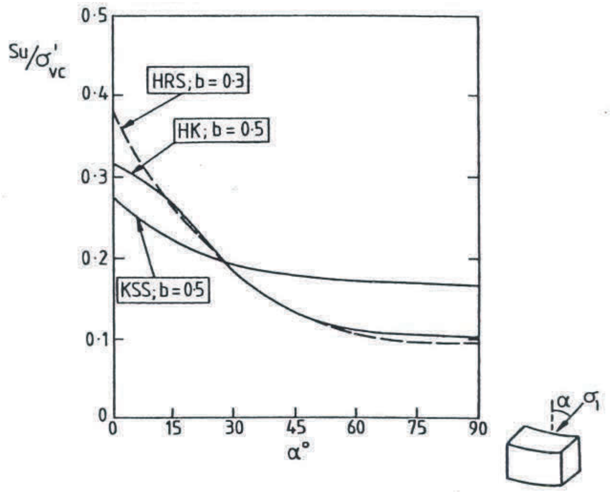

Figure 5.4: Variation with α of s_u/σ_v' developed in HCA tests (with b = 0.5) for normally (K_0) consolidated clay sand (HK), kaolin-silt-sand (KSS) and Ham River Sand (HRS); Jardine and Menkiti, 1999

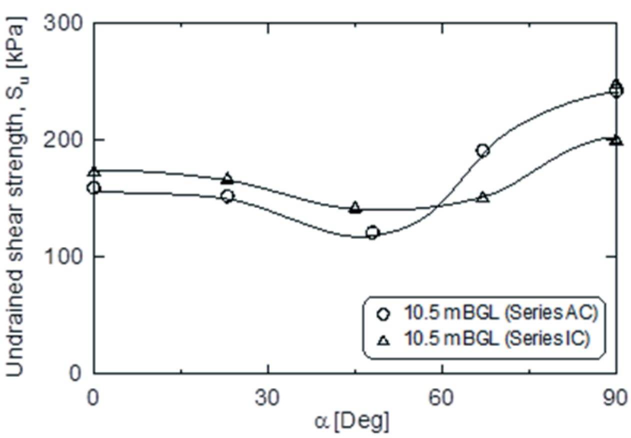

Figure 5.5: Variation with α of su developed in HCA tests (with b = 0.5) for high OCR stiff natural London clay; Nishimura et al., 2007

The stiffness and shear strength anisotropy of soils can be modified by consolidation to differently oriented effective stress regimes. While this may be achieved readily with sands, larger consolidation strains are required with clays. Figure 5.6 illustrates how this may be achieved in HCA tests, where b and α may be changed during consolidation to new values that may be maintained or modified during subsequent shear tests. Figure 5.7 illustrates the considerable impact on the s_u/σ_v' - α relationships seen in HCA tests on normally consolidated loose sands and dense silts in tests that rotated α to the full series of possible orientations prior to shearing under similar α values. Pre-shearing towards the final ultimate σ'_1 orientation clearly increases the subsequent undrained shear strength. Zdravkovic and Jardine (2001) provide further details of these experiments.

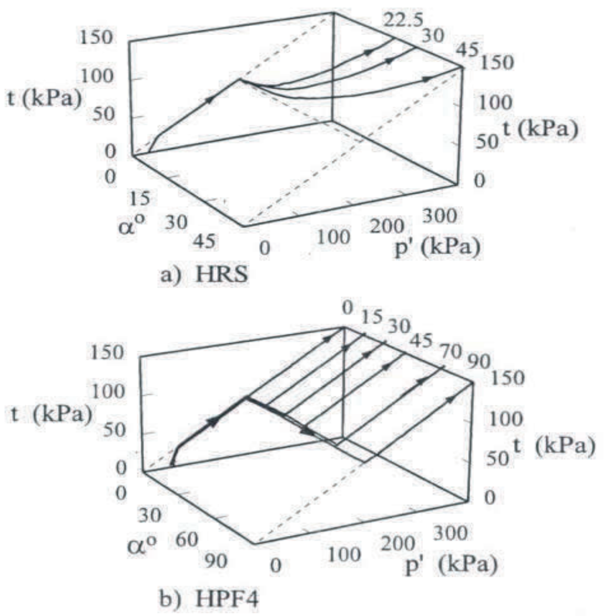

Figure 5.6: Effective stress paths applied in HCA tests on Ham River Sand (HSR) or HPF4 silt involving σ1 axis rotation during consolidation to a range of αc orientations, prior to shearing with b = 0.5 and σ1 axis orientation αs = αc; Jardine et al., 1997

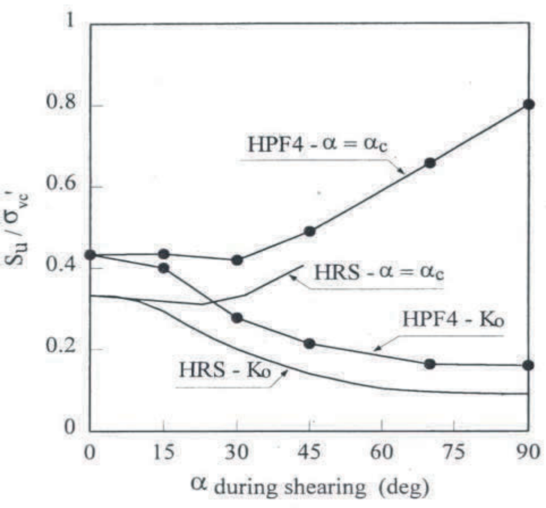

Figure 5.7: Variation of su/σv′ with αs from HCA tests on Ham River Sand (HSR) and HPF4 silt involving either (i) K0 (αc = 0) consolidation, or (ii) consolidation involving the σ1 axis rotated to = αc prior to shearing with b = 0.5 at range of αs orientations; Jardine et al., 1997

HCA testing is not employed widely in practical site characterisation. Anisotropy usually has to be gauged by performing simpler tests TC, TE or CAU tests on K_0 consolidated samples. The shear strengths established from CAU TC, TE and DSS tests cover a range of σ_1 orientations (representing a spread of α angles) and therefore reflect anisotropy. They may also provide conservative estimates for plane strain shear strengths. But because the tests each impose different b values at failure they inevitably mix the effects of anisotropy with those of relative σ_2 magnitude.

The NGI has developed and applied a simplified 'contour diagram' framework to (i) characterize and define potentially anisotropic soil behaviour under cyclic loading and (ii) undertake design with calculation procedures based on this framework; Andersen et al. (1988); Andersen (2009). Figure 5.8 illustrates the modes of shearing engaged around a potential shallow foundation failure mechanism, indicating which regions compare best with the conditions applying in the simplified DSS, TC CAU and TE CAU laboratory tests discussed above. The contour diagram framework defines the cyclic shear strength and the average, permanent and cyclic shear strains as functions of average and cyclic shear stresses and number of cycles. The shear stress and shear strain components are defined in Figure 5.9, and examples of contour diagrams for cyclic shear strength are presented in Figures 5.10 and 5.11. $\tau_{f,cy}/s_u$ is the normalised cyclic shear strength and γ_a/γ_{cy} represents the failure mode, i.e. the average and cyclic shear strains at failure. Examples showing contours of average and cyclic shear strains as function of average and cyclic shear stresses are presented later in Figures 5.14 and 5.15. Reference is made to Andersen et al. (1988) and Andersen (2009) for further explanation.

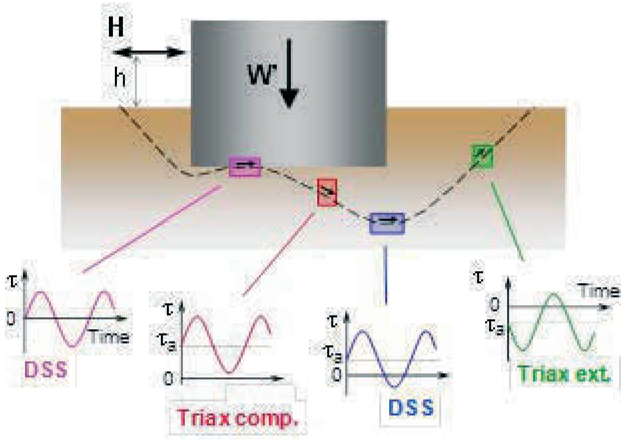

Figure 5.8: Stress conditions beneath a shallow foundation under cyclic loading (Andersen, 2009)

The calculation procedures based on the contour diagram framework have been used extensively in practical design of GBS foundations, suction anchors and monopiles for offshore wind power structures. Among these procedures is a limit equilibrium method to calculate the bearing capacity of foundations or pull-out capacity of anchors subjected to a combination of average and cyclic loading (Andersen and Lauritzsen, 1988). The procedure is based on (1) the condition that the average shear stress along the critical slip surface is in equilibrium with the average loads, and that the cyclic shear strength along the critical slip surface is in equilibrium with the maximum loads (sum of average and cyclic), and (2) the assumption of shear strain compatibility along the critical slip surface of both the average and cyclic shear strain components.

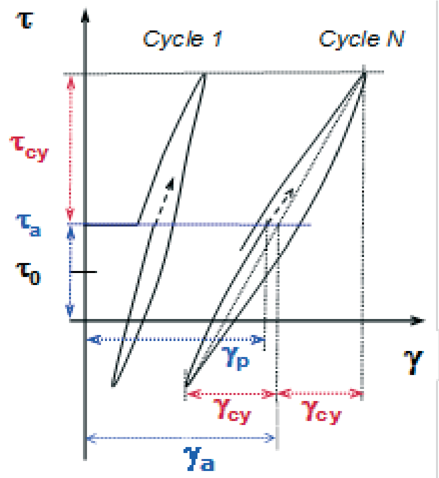

Figure 5.9: Definition of shear stresses and shear strains under cyclic loading (Andersen, 2009)

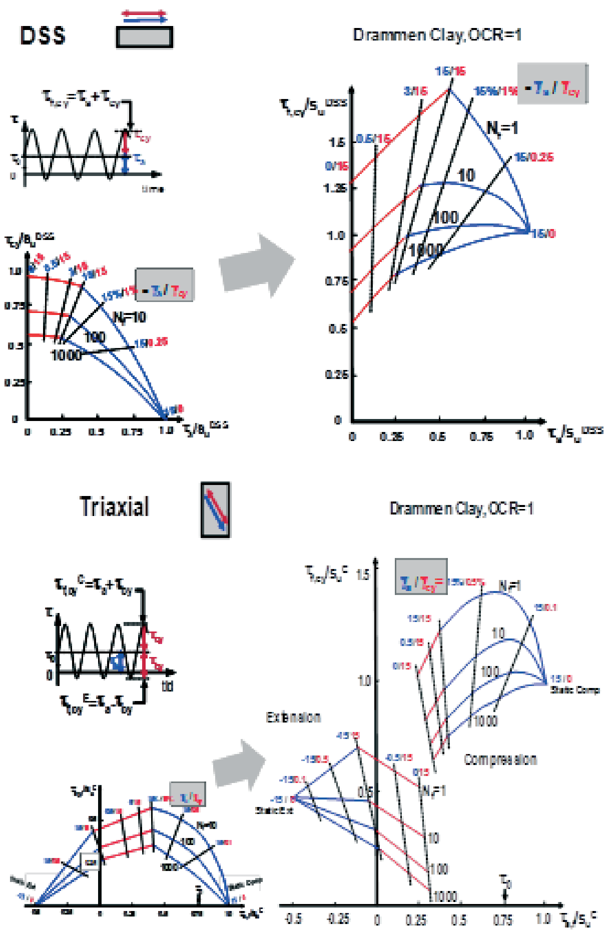

Figure 5.10: Examples of cyclic shear strength contour diagrams for DSS and triaxial stress paths (Andersen, 2009). Red indicates cyclic shear strain and range where failure mode is cyclic shear strain. Blue indicates average shear strain and range where failure mode is average shear strain (compression or extension)

In addition to the capacity, the strain contour analysis gives information on whether the failure mode involves large cyclic or permanent displacements. An approximation that simplifies the calculation is to assume that the ratio between the local cyclic and average shear stresses matches that ratio between the applied cyclic and average environmental loads. However, this simplification does not account for strain compatibility and the associated potential redistribution of the stress regime and inevitably sacrifices solution accuracy.

The wave trains that build up in offshore storms, and hence the cyclic shear stresses developed in soil foundation elements, usually vary from one wave, or cycle, to the next. The test results from regular, uniformly cycling, laboratory tests cannot be applied to model such storm sequences directly. It is usual to transform the storms spectrum of waves into equivalent batches of regular uniform waves, assuming that the damage can be represented by an equivalent number, N_{eq}, of uniform waves. This is achieved by considering the maximum cyclic shear stress that will give the same cyclic shear strain (Andersen, 1976) or the same cyclically induced pore pressure (Andersen et al., 1992) as the true loading composition. The transformation is based on the assumption that the normalized cyclic shear stress composition, $\tau_{cy}/\tau_{cy,max}$, is the same as the normalized resultant of the cyclic load composition, $|\mathbf{F}_{cy}|/|\mathbf{F}_{cy,max}|$ in all the governing soil elements. $\tau_{cy,max}$ can then vary from one element to another, but N_{eq} will be the same in all soil elements.

Pore pressure is used by NGI as the key 'memory parameter' for cyclic degradation in cases where drainage occurs during the storm. One can then calculate the net pore pressure generated by the cyclic loading and the simultaneous pore pressure dissipation. Contour diagrams of the type presented in Figure 5.11 provide the basis for the NGI accumulation procedures and Figure 5.12 presents an example.

Most cases involving clays do not experience significant pore pressure dissipation during the design storm, and it can be more convenient to use the cyclic shear strain as the cyclic degradation 'memory parameter'. One difficulty with the pore pressure approach in clays is that accurate pore pressure measurements are hard to make in laboratory during rapid cyclic testing due to the system compliance and time-lag problems inherent in conventional testing (see Gibson, 1963). Local pore pressure measurement techniques may overcome such problems: see Hight (1982).

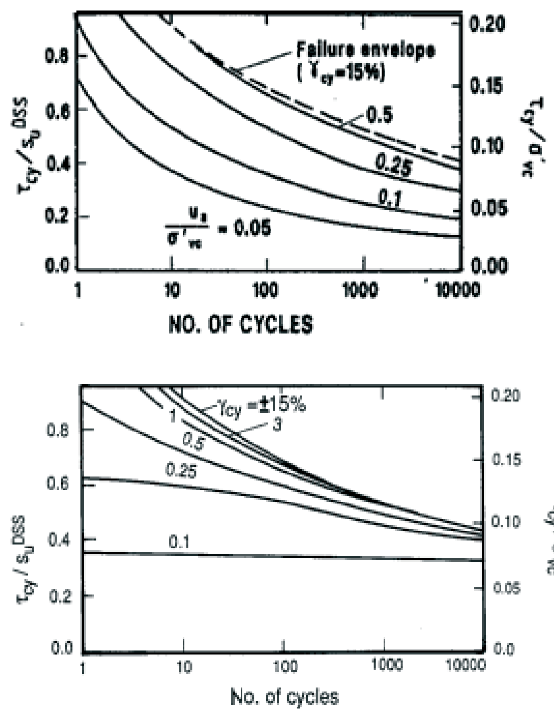

Figure 5.11: Examples of diagrams with permanent pore pressure (upper) and cyclic shear strain (lower) as function of cyclic shear stress and number of cycles. DSS tests with τa = 0 on Drammen Clay (Andersen, 2004)

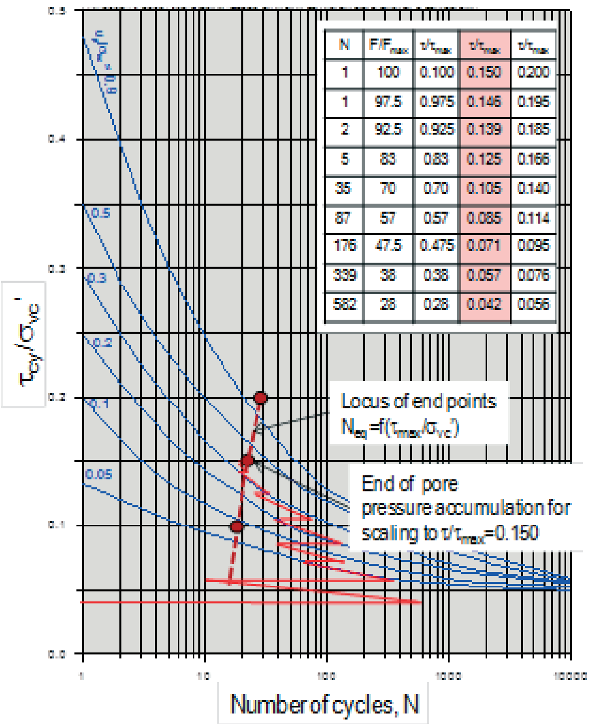

N	F/F_{max}	τ/τ_{max}	τ/τ_{max}	τ/τ_{max}
1	100	0.100	0.150	0.200
1	97.5	0.975	0.146	0.195
2	92.5	0.925	0.139	0.185
5	83	0.83	0.125	0.166
35	70	0.70	0.105	0.140
87	57	0.57	0.085	0.114
176	47.5	0.475	0.071	0.095
339	38	0.38	0.057	0.076
582	28	0.28	0.042	0.056

Figure 5.12: Example of pore pressure accumulation for a case with no drainage

It has become more common during the last decade to use the finite element method to determine not only displacements but also the bearing capacity of offshore structures; see for example Andresen et al. (2010). Displacements and capacities have been calculated with the NGI approach by assuming a constant N_{eq} for all the elements in the soil volume (see Andersen and Hoeg, 1991) with N_{eq} determined as described above.

Both the limit equilibrium and the finite element approaches described above have shown favourable agreement with results from model tests (e.g. Andersen et al., 1989; Jostad and Andresen, 2009). However, the assumption of a constant N_{eq} within the soil volume may underestimate (with some geometries) the effects of stress redistribution and progressive failure. A new finite element code, UDCAM, has been developed by NGI where the accumulation of pore pressure or cyclic shear strain is determined and continuously updated in each integration point based on the calculated cyclic shear stress in that point (Grimstad et al., 2013). UDCAM has a 3D formulation to aid analysis of monopile foundations for offshore wind-turbine structures. An extension of UDCAM to include pore pressure dissipation and redistribution during cyclic loading (PDCAM) is being developed. Grimstad et al. (2013) present examples where UDCAM is used to successfully back-calculate a GBS model test with cyclic loading and a 3D analysis of an offshore wind turbine monopile under cyclic environmental loads. Redistribution of pore pressure can be important at sites involving inter-layered clays and sands. Pore pressures generated by cyclic loading in cyclically susceptible sand and silt layers can flow into clay layers, leading to loss of shear strength. This redistribution process can be modelled in the finite element analyses.

Both limit equilibrium and finite element analyses need shear strength input data. As shown in Figure 5.10, the cyclic shear strength depends on the ratio between cyclic and average shear stresses, the simplified stress path (TC, TE, DSS), and number of cycles. Cyclic pore pressure generation and consolidation analyses involving reloading modulus and coefficient of consolidation are also required when the pore pressure procedure is applied and when drainage may be significant.

Andersen and Jostad (1999, 2002 and 2004) argue from model and field tests that the vertical resistance of skirted foundations and anchors is controlled during installation in low OCR, sensitive, clays by a large shear strain disturbance process that takes clay in the interface shear zone to a 'remoulded' state. It is necessary in design to model the set-up that takes places after installation at the interface and in the disturbed zone close to the skirt wall. DSS tests on reconsolidated remoulded samples are performed to indicate the shear strength that develops within such zones. The importance of modelling the set-up increases with increasing foundation L/D ratio. While set-up is most important in relation to vertical capacity, the degree of shaft adherence also affects the lateral capacity. This may be appreciated by noting that (in spatially uniform soil) the lateral capacity bearing capacity factor $N_c = q_f/s_u$ of a cylinder increases approximately from 9 to 12 between the 'smooth' case (where no shear stress can develop at the interface) and the 'fully rough' case when the full s_u is available in shear at the interface to help resist lateral motion.

The set-up of skirts penetrated into clay depends on the ratio between remoulded shear strength, the virgin loading consolidation characteristics of remoulded clay, the unload/reload loading consolidation characteristics of intact clay, and any thixotropic strength gain characteristics of the remoulded clay. A procedure to determine the set-up for skirts penetrated into clay is given in Andersen and Jostad (2002), who also recommend set-up factors for cases where site specific calculations are not performed. Clukey et al. (2013) summarize comparisons between calculated set-up factors and those measured in prototype and model tests, finding a reasonable match with current experience, which relates mainly to soft clays. As explained later in relation to driven piles, such procedure may be less applicable for low sensitivity, overconsolidated clays and soils that develop low residual shear strength shear surfaces with low φ′ and δ values in their interface shear zone. The latter characteristics are best captured by interface ring shear tests rather than DSS or other low displacement undrained tests on remoulded samples.

Suction anchors installed by under-pressure, are relatively light and the 'still-water average' vertical shaft shear stress that has to be carried to support their weight is normally small compared to their shaft shear capacity. More significant 'average' still-water shaft stresses may have to be carried by skirted foundations, such as subsea templates, if they are not penetrated to depths that bring their base plates into full contact with the soil. Such maintained shear stresses pre-shear the interface shear zone soil close to the skirt wall, effectively rotating the σ'_1 orientation α during consolidation. As shown earlier, consolidation involving α rotation modifies the anisotropy of low OCR soils and can enhance undrained shear strength of low OCR soils, leading to additional long term shear strength gains in a spread of applications, including shallow foundation problems; e.g. Zdravkovic and Jardine (2001). Such effects can be modelled to some extent in pre-sheared DSS tests designed to match field conditions.

Pore pressure can be adopted as a memory parameter to define N_{eq} in cyclic analyses of large offshore foundations, provided that conditions remain undrained in the surrounding ground over any given single cycle. However, partial (or even full) drainage can apply with high permeability soils (such as clean sand) and short drainage paths. The operational field shear strength of dense sand may then be limited by the soil's inability to sustain any negative pore pressures set up by constrained dilatancy. This limitation is illustrated for triaxial and DSS stress paths in Figure 5.13. The limiting shear strengths may be defined by the slopes of the respective failure lines and the assumed drained stress loading path directions.

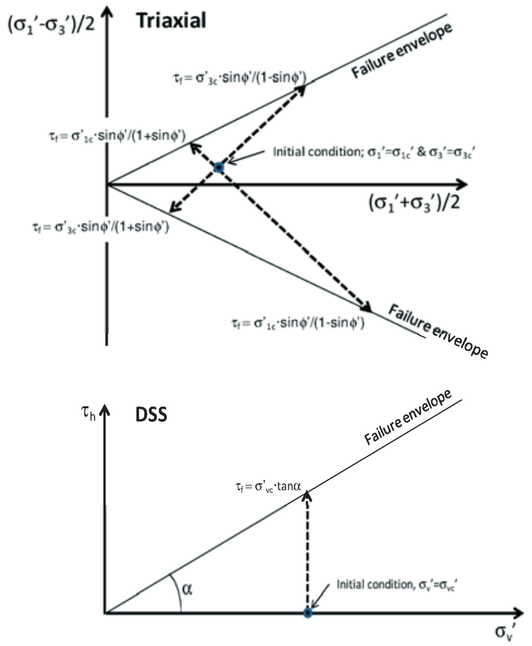

Figure 5.13: Shear strength for different stress paths when dilatancy in dense sand is not relied upon

5.2 *Cyclic displacements*

Structural assessments often require predictions for the horizontal, vertical and rotational cyclic displacements developed under the maximum wave or working load conditions. It is normally assumed that the maximum wave develops at the end of the design storm peak, at a stage when the prior cyclic degradation is most severe. Cyclic displacement assessments are generally not required for anchors because the movements are small compared to those developed in their flexible mooring chains.

Cyclic displacements are normally calculated by finite element methods. The effect of cyclic loading can be accounted for by an equivalent number of cycles approach, as set out Section 5.1. It has usually been assumed in the NGI approach that N_{eq} is constant within the whole soil volume. N_{eq} is then determined before starting the finite element analysis and is used to establish the cyclic stress-strain-strength data that is needed as input to the numerical analysis. As with capacity, the calculation accuracy can be improved by considering the effects of pore pressure or cyclic shear strain accumulation at each integration point in the finite element code. It is also important to model the set-up along any skirt walls.

The NGI finite element approach relies on functions being pre-specified from tests that relate average and cyclic shear strains to the applied average and cyclic shear stresses and number of cycles. As with the bearing capacity cases, different relationships are specified from multiple cyclic TC, TE and DSS tests run with suitable combinations of average and cyclic shear stresses. The finite element programme interpolates for stress conditions in between those specified based on the inclination of the major principal stress. The calculations thus account to some degree for the four-dimensional (q, p′, α and b) stress regime imposed in the field.

The laboratory results are visualised as shown in the examples in Figures 5.14 and 5.15. Pore pressure generation due to cyclic loading and consolidation characteristics are combined in cases where drainage needs to be considered. Simplifications can sometimes be made. For example, the cyclic stress-strain relationship may not always depend unduly on average shear stress. When this is evident from tests, it may be possible to calculate cyclic displacements by considering only the cyclic loading components.

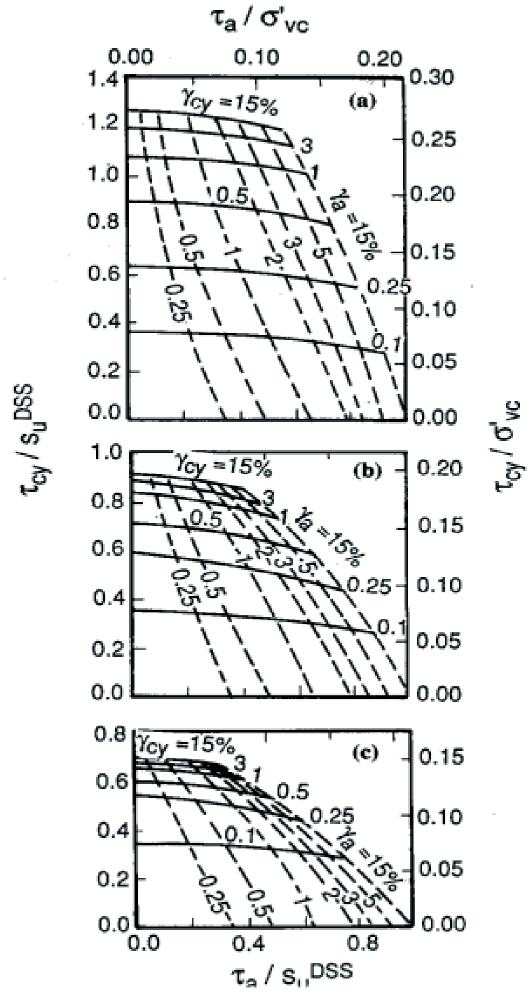

Figure 5.14: Examples of cyclic shear strain contour diagrams for DSS type stress paths on normally consolidated Drammen Clay.
a) N=1, b) N=10, c) N=100 cycles (Andersen, 2004)

The structural displacements result from the integration of strains over the entire soil volume. It is essential to define the highly non-linear shear stress-strain curve over the full strain range from the initial (very limited) linear G_{max} range up to large strain failure. Even if the strains become small at some distance from the structure, they may affect a large volume and make a significant contribution to the overall displacements. In cases where pore pressures dissipate significantly during cycling the soil's non-linear bulk stiffness and consolidation characteristics have also to be considered.

5.3 *Permanent displacements due to cyclic loading*

The permanent displacements developed due to cyclic loading result from: (1) straining (principally in shear) during the cycling, (2) subsequent volume changes due to dissipation of cyclically induced pore pressure and (3) drained and undrained creep. In the NGI approach, the permanent displacements developed during cycling are normally output from the finite element analyses used to calculate cyclic displacements, as described in Section 5.2 above.

Assessment of permanent displacement caused by pore pressure dissipation requires a semi-coupled finite element consolidation formulation, as in the code PDCAM mentioned in Section 5.1. Approximate calculations can also be made assuming 1D-conditions beneath the foundation in cases where assessing the central settlements is the main aim. Simplified creep assessments can also be made for such cases.

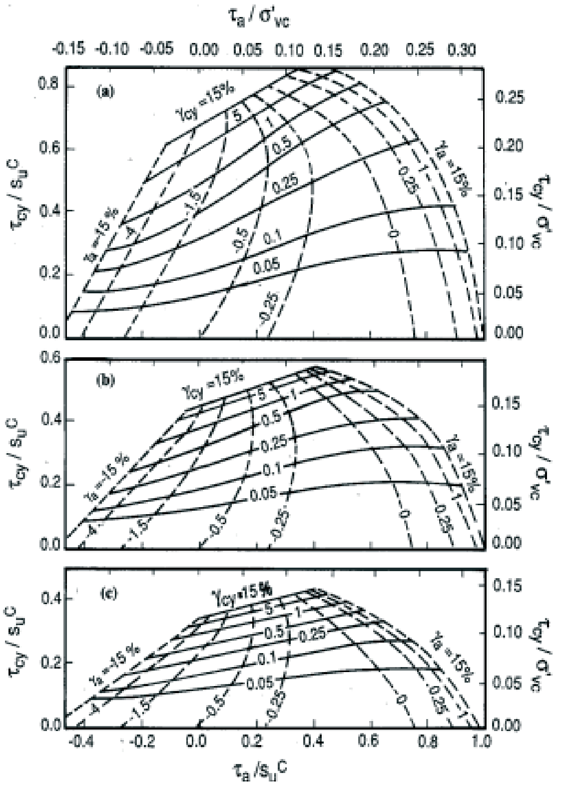

Figure 5.15: Examples of cyclic shear strain contour diagrams for triaxial type stress path on normally consolidated Drammen Clay.
a) N=1, b) N=10, c) N=100 cycles (Andersen, 2004)

The soil behaviour characteristics input into the analyses are the same as visualised and described for cyclic displacements assessment in Section 5.2, except that additional information is required about (1) the pore pressure generated by the cyclic loading and (2) the soils' reconsolidation characteristics. Examples of pore pressure diagrams are given in Figures 5.16 and 5.17, which follow the contoured format adopted earlier for shear strains in Figures 5.14 and 5.15.

Alternative displacement and stiffness calculation methods:

Still more advanced treatments are becoming feasible that may eventually provide the means to model together non-linear, hysteretic and anisotropic cyclic pore pressure generation and straining responses of soils with time dependent drainage. Such treatments must incorporate fully coupled treatments along with high-fidelity cyclic constitutive models that can be calibrated or checked directly against advanced laboratory tests.

At present such models are not applied in routine offshore practice. However, Wichtman (2005) reviews alternative explicit methods (including Boukovalas et al., 1984; Gotschol, 2002; Kaggwa et al., 1991 and Diyaljee and Raymond, 1982) and notes "a need for an explicit model exists which delivers the accumulation rates of the volumetric and the deviatoric strains".

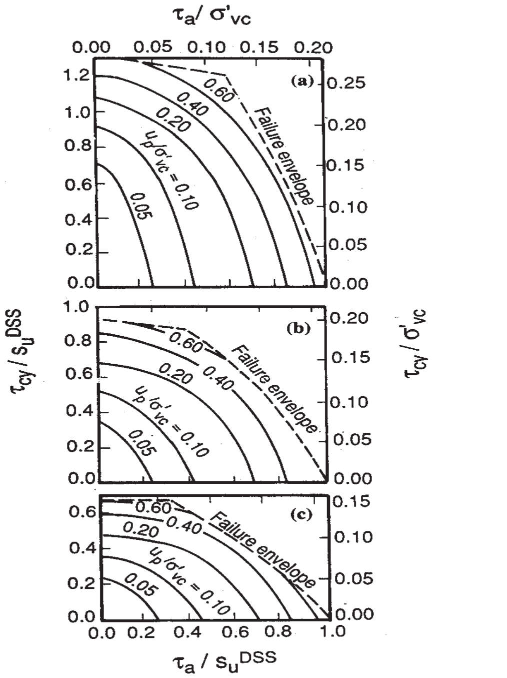

Figure 5.16: Examples of pore pressure contour diagrams for DSS type stress paths on normally consolidated Drammen Clay.
a) N=1, b) N=10, c) N=100 cycles (Andersen, 2004)

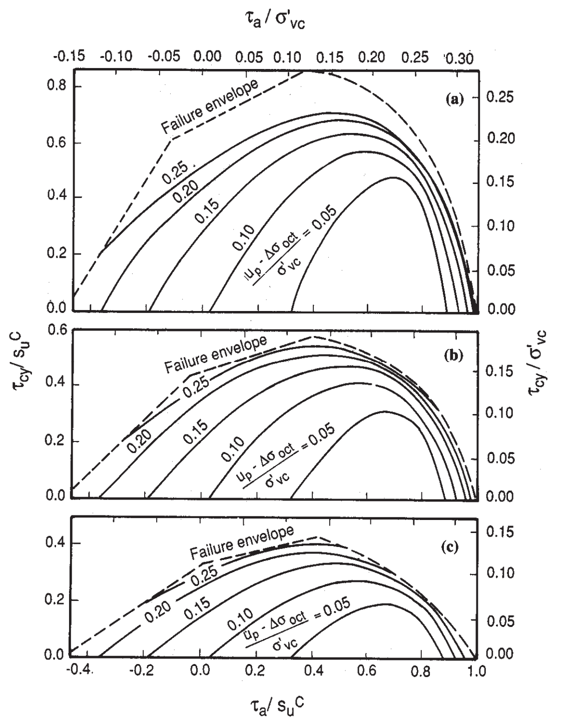

Figure 5.17: Examples of pore pressure contour diagrams for triaxial type stress path on normally consolidated Drammen Clay.
a) N=1, b) N=10, c) N=100 cycles (Andersen, 2004)

More challenging, implicit "time domain" procedures, (where each cycle is calculated with an appropriate constitutive model and iterated over many small strain increments) have also been implemented in finite element programs intended, in particular, for earthquake geotechnical engineering applications. Each cycle is calculated with an appropriate constitutive model and iterated over many small strain increments. Examples of elasto-plastic models (such as Prevost, 1977; Mroz et al., 1978; Chaboche, 1994), endochronic models (Valanis and Lee, 1984) or hypoplastic models (e.g. Gudehus, 1996 or Niemunis and Herle, 1997) have been proposed. This procedure becomes difficult after a significant number of cycles (say 50) because (i) computational resource costs become high and (ii) and errors can accumulate with the constitutive models and integration algorithms that may be employed. When considering large numbers of cycles, the explicit procedure appears more robust and appropriate. Wichtman, Niemunis and Triantafyllidis (2004) have recently developed a procedure that combines implicit and explicit elements. Careful validation will naturally be required to assess the new methods' reliability and predictive capabilities before they are adopted for routine use.

5.4 *Equivalent cyclic soil spring stiffnesses*

Equivalent overall soil spring stiffnesses, which are defined as the overall (secant) ratios between the amplitudes of particular components of cyclic foundation and the resulting displacement amplitudes, can be assessed from the output of the finite element analyses described in Section 5.2 and exported for use in soil-structure interaction analyses. However, as emphasised earlier, the soil response is likely to be highly non-linear and no single stiffness can match behaviour fully from small loads up to the maximum. Secant stiffnesses defined from the extreme maximum load case will be too soft to match the response seen at lower, more frequently encountered, cyclic loading levels. Interaction is necessary with structural engineers to ensure compatibility between the geotechnical and the dynamic analysis cases and parameter sets.

One simplified approach that has been applied in dynamic analyses of large diameter GBSs on clay is to calculate an 'operational' stiffness by inputting (over the peak period of the storm) into the cyclic finite element analyses an 'operational' cyclic load calculated as the Root Mean Square (RMS - equivalent to a standard deviation, as applied in alternating current electrical engineering) cyclic deviation from the mean load. The stress strain input is similarly defined in terms of RMS for the cyclic load composition in the peak period of the storm. The finite element output gives equivalent RMS displacements and stiffnesses, working from the soil cyclic data described in Section 5.2. Further details can be found in Andersen (1991).

Foundation damping behaviour, which can also be important, may be calculated from the finite element analyses by integrating the damping expected in each element over the soil volume. Such calculations have been implemented in the finite element program INFIDEL (Hansteen, 1991), which also performs stiffness calculations according to the method described above. INFIDEL can consider circular and elliptic geometries with axisymmetric or non-axisymmetric loads and with elastic far field elements that can extend to infinity horizontally. Such analyses require soil damping functions related to stresses or strains and the number of applied cycles.

The analyses described above give secant stiffnesses. The load-displacement relationships applying to individual cycles may also be established by applying Masing's rule and calculating the relative area retained within the load-displacement loop as the ratio.

6 CALCULATION PROCEDURES FOR PILES

The Commentary section of the industry standard recommendations (API RP2GEO 2011) for offshore design recognises several methods to calculate static axial pile capacity and lateral loading response. The API axial approach for clay relies on UU triaxial shear strength measurements. Alternative approaches that are used in some North Sea and other applications are the ICP-05 effective stress approach (Jardine et al., 2005), which combines an holistic approach to YSR assessment with sensitivity and interface shear measurements (and CPT measurements for base resistance), and the NGI-05 total stress procedure (Karlsrud et al., 2005) which relies on UU shear strength and plasticity index although Karlsrud (2012) proposed that the NGI-05 clay method for clays should be based on DSS undrained shear strength tests. API RP2GEO (2011) indicates a preference in sands for the Commentary 'CPT methods' which all require high quality CPT data, while the ICP-05 sand method also requires interface shear tests.

Methods for addressing cyclic loading, however, are not equally well developed. Review of (i) cyclic load tests on piles and (ii) cyclic loading on piled structures led Jardine et al. (2012) to conclude that cyclic loading effects can be more important for pile capacity than has been appreciated conventionally, particularly for structures with high ratios of cyclic to average loads. They argue that current design practice needs to be reconsidered and start by relating potential effects of axial load cycling to the static axial capacity considerations.

Jardine et al. (2012) argue that cyclic pile capacity depends on effective stresses, which can change due to stress redistribution and/or pore pressure generation. Storm loading conditions will usually lead to a principally undrained response and potential excess pore pressure generation in clays. When the permeability of sand is high enough to give drained conditions during storms, volume changes can develop that provide scope for possible radial straining close to the pile shaft. If the response is dilative, as it may be at high shear stresses in dense sand, the expanding interface shear zone reacts against the surrounding soil mass and generates radial stress increases. The reverse applies when the sand close to the shaft contracts under cyclic loading. However, as reviewed by Sim et al. (2013), the soil near to the pile shaft is subject to tight kinematic controls. Effective stress changes can develop in both sands and clays through constrained dilation without the necessity for any excess pore pressure changes.

6.1 *Effects of axial cycling on axial capacity*

Jardine et al. (2012) recommend that a graduated cyclic assessment process should be applied to evaluate cyclic effects of axially loaded piles (Figure 6.1), starting with simple summary interaction diagrams that relate the cyclic capacity to the static capacity and progress, if required, to full analyses of site specific soil-structure analyses considering local storm loading.

Examples of interaction diagrams for driven and jacked displacement piles are given in Figures 6.2, 6.3 and 6.4, which show results of in situ load tests on piles driven in clay, and Figures 6.5, 6.6 and 6.7 which show results of model or in-situ tests on displacement piles in sand. The Haga clay has medium plasticity, moderate sensitivity and is lightly over consolidated. Onsøy is a plastic, normally consolidated clay, while Lierstranda clay has low plasticity and low OCR. The Tilbrook Grange profile consists of low plasticity, very stiff, glacial till overlying highly plastic, high OCR, Jurassic Oxford clay; both strata have high OCR. Fontainebleau NE34 sand is a fine grained industrial silica sand that is widely used for centrifuge and other model studies in France and elsewhere, which was air-pluviated in a dense to medium-dense state for the model experiments reported. As mentioned earlier, Dunkirk sand is a fine principally silica shallow marine deposit from Northern France that is considered typical of Southern North Sea sands and has a predominantly medium-dense to dense site profile: see Jardine et al. (2006). Labenne sand is a loose to very loose dune sand from SW France.

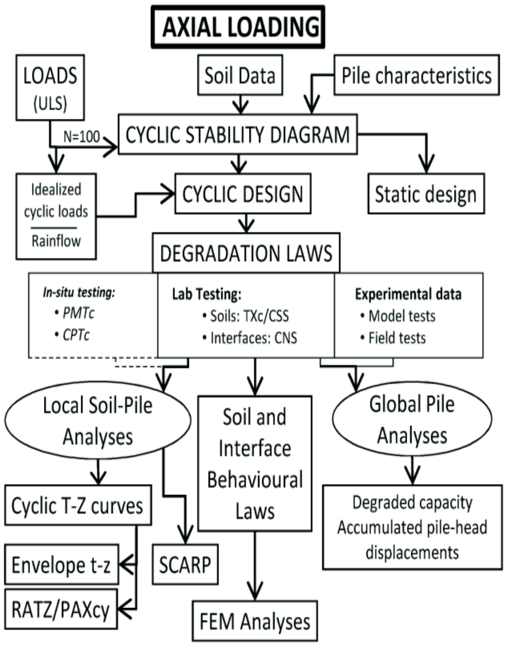

Figure 6.1: SOLCYP graduated design approach for piles under axial cyclic loading (Jardine et al., 2012)

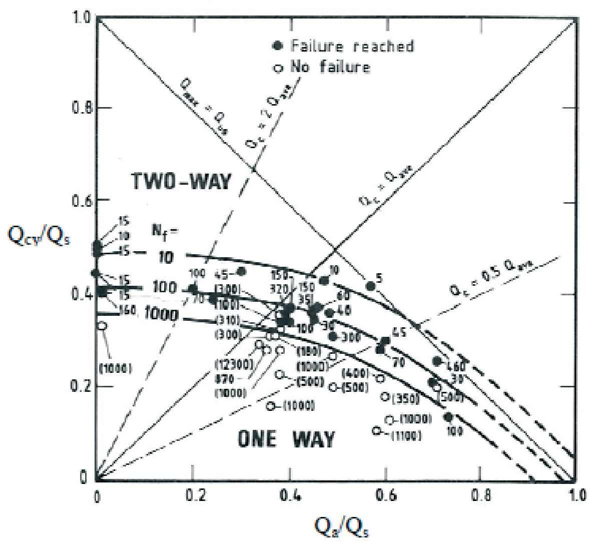

Figure 6.2: Interaction diagram with number of cycles to failure N_f at Haga as function of Q_a and Q_{cy} normalized by static tension capacity Qs (Karlsrud and Haugen, 1985b)

Equivalent interaction diagrams for bored piles are presented later in Section 11.

The interaction diagrams show the combination of average (Q_a) and cyclic (Q_{cy}) loads, normalised by the static shaft capacity (often defined in tension) that cause failure after a given number of cycles. For historical reasons the diagrams apply alternative forms. Figures 6.3, 6.4 and 6.8 plot cyclic failure load, Q_{max} rather than Q_{cy} on the vertical axis as in the other pile and soil element tests. However, as $Q_{max}=Q_a+Q_{cy}$ the two plot types contain the same information. The Haga clay set displayed in Figure 6.2 represent the most comprehensive set of available cyclic field test data.

Practical considerations lead to most axial cyclic pile load tests involving just one-way loading with $Q_{cy} < Q_a$. Such conditions plot in the lower right quadrant of interaction diagrams where cyclic degradation is at its least severe. While such data often plot close to the first diagonal 'no-damage' line potentially significant shaft capacity degradation (up to 25%) is seen under such conditions in some soils. High level cycling with low values of Q_a/Q_a leads to more severe effects in the two-way sector where failure can develop within 100 cycles under maximum loads less than one-half of the static capacity. Lehane et al. (2003) report field tests on pile groups installed in soft Kinnegar clay-silt, interpreting the results to show that both static shaft capacity and cyclic performance are affected negatively by group interaction.

In general, axial cycling affects sands and sensitive low OCR clays that have high drained peak friction angles, φ´, and interface shear δ values more severely than most other deposits. Carbonate sands are especially sensitive to cycling. Problematic low plasticity clays also exist that show high φ´ and δ values but develop low axial static capacities and are highly susceptible to cyclic loading. Normalized cyclic loading levels exist below which large numbers of cycles can be applied without impacting significantly on load-displacement behaviour. These 'zero damage' curves are most favourable in high OCR clays that develop low δ values resulting from residual shear surfaces during installation and under loading. Low level cycling can enhance pile capacity (Jardine and Standing, 2012).

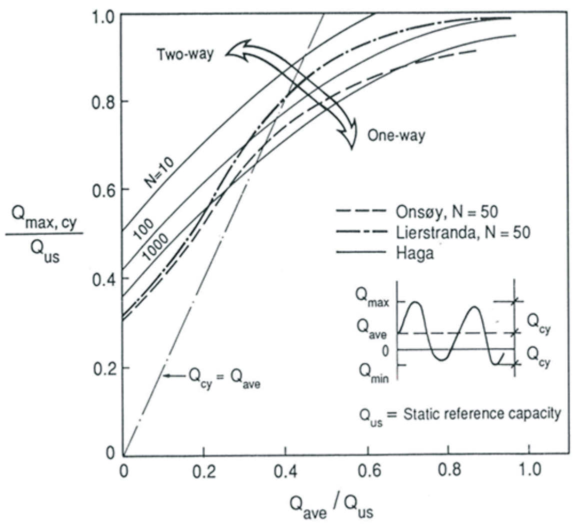

Figure 6.3: Interaction diagram with comparison of Onsøy and Lierstranda cyclic axial pile test capacities with Haga (Karlsrud et al., 1992b)

The interaction diagrams illustrate the crucial importance of knowing, even for screening assessments, the likely static axial shaft capacities, cyclic loading components and numbers of cycles. Interaction diagrams provide simple and helpful guidance when these parameters are known and good matches exist with the soil conditions at each site under review. But care must be taken to allow for a range of soil responses. For example, piles driven in high OCR plastic London or Flandrian clays (at Canons Park or Merville) provide contours that plot above those for Haga in Figure 6.2, while the contours for the more susceptible Lierstranda or Onsøy sites pass well below the Haga trends. A comparison of the positions of these sites N_f =

50 failure curves is given in Figure 6.8. It is interesting to observe in Figure 6.6 that the normalised cyclic behaviour of the piles in the loose to very loose Labenne dune sand does not seem to be significantly lower than in the medium dense to dense Dunkirk marine sand.

Cyclic interaction diagrams can be predicted by a range of procedures when suitable cyclic pile test data is unavailable. Karlsrud and Haugen (1985) matched their Haga clay cyclic pile tests results with site-specific monotonic and cyclic DSS laboratory tests. Their 'DSS' and 'pile test' cyclic failure interaction diagrams developed the same normalised patterns, provided the axes were normalized by the appropriate monotonic DSS strength or the pile shaft tension capacity respectively. This held true whether the DSS tests were conducted on intact or remoulded clay.

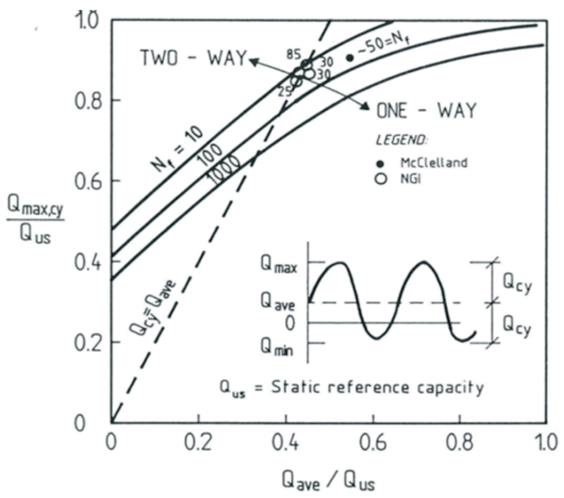

Figure 6.4: Interaction diagram with comparison of Tilbrook Grange and Haga cyclic axial pile test capacities (Nowacki et al., 1992).

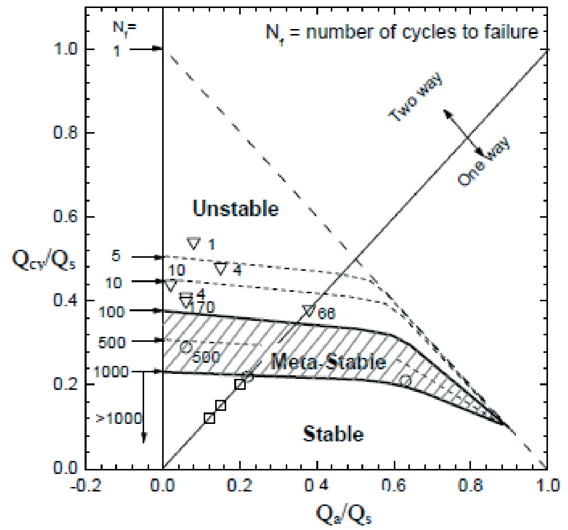

Figure 6.5: Shaft interaction diagram with number of cycles to failure Nf from Mini-ICP piles installed in medium dense Fontainebleau NE 34 sand under a vertical confining pressure of 150 kPa in the large INPG calibration chamber; after Rimoy et al., 2012.

Cyclic capacity clearly depends on the number of cycles N applied. In a design storm the cyclic load will vary from one cycle to the next, and the design storm composition needs to be transformed into a regular cyclic loading history by an equivalent number of cycles approach. This can be achieved with an accumulation procedure, using contour diagrams with either pore pressure, cyclic shear strain or shaft capacity damage as the memory parameter, as explained previously for shallow foundations.

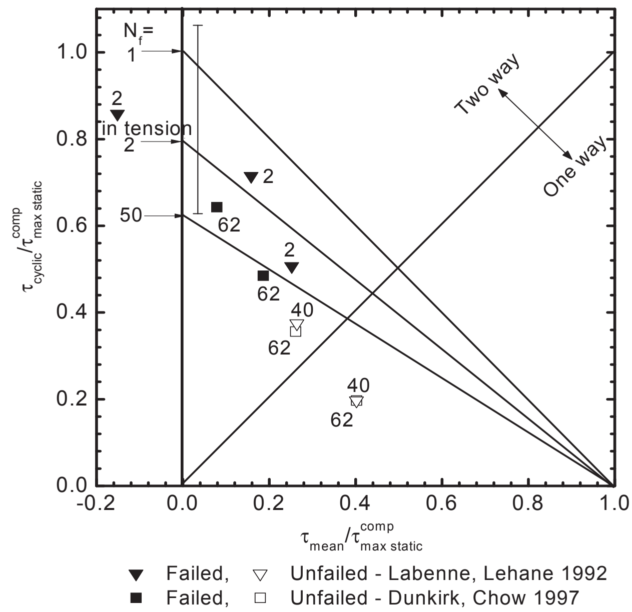

Figure 6.6: Interaction diagram with local cyclic shaft failure from ICP tests in sand at Labenne (loose to very loose dune sand) and Dunkirk (medium dense to dense marine sand). Open symbols = unfailed, interpreted from tests by Lehane 1992 and Chow 1997. (ICP = Imperial College Pile).

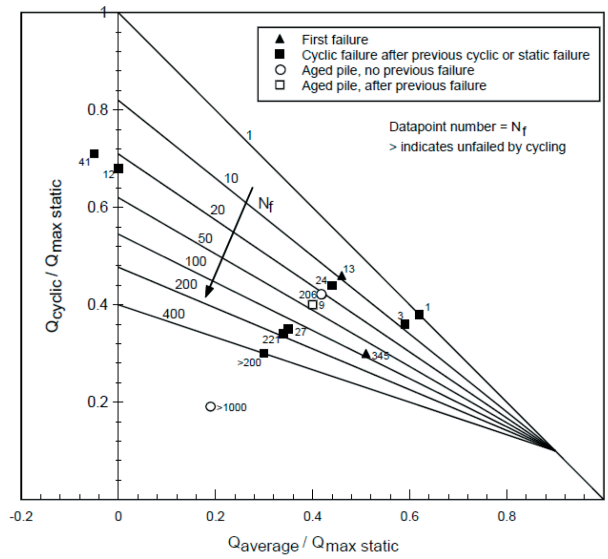

Figure 6.7: Summary interaction diagram from cyclic tests on steel tubular piles driven in dense sand at Dunkirk; after Jardine and Standing 2013. Piles loaded in tension

Field cyclic tests with highly instrumented piles (by Bond, 1989; Lehane, 1992 and Chow, 1997, supported in model tests by Tsuha et al., 2012) led Jardine et al. (2005a) to set out a simple method for predicting the potential reduction of local shaft resistance for piles subject to groups of uniform load cycles. Noting that shaft capacity reduces in both sands and clays in step with local radial effective stress changes that develop over the shaft they apply either Equation (3) for local analyses of cyclic shaft degradation or an equivalent global 'A, B, C' form to develop overall interaction diagrams (see Jardine and Standing, 2012). Highly instrumented pile tests and undrained DSS tests have shown that in cases where $\tau_{vh} / \sigma'_v < \tan \delta$, the relative loss in normal effective stress ($\Delta\sigma'_v / \sigma'_{vc}$) may be nearly independent of the average shear stresses applied and can be expressed with reasonable accuracy by either the simple function given below of normalised cyclic shear stress amplitude ($\tau_{cyc} / \tau_{max,stat}$) and number of cycles (N) such as the power law given below, or by an equivalent log (N) expression:

$$\frac{\Delta\sigma'_r}{\sigma'_{r0}} = A\left(B + \frac{\tau_{cy}}{\tau_{\max stat}}\right)N^C \qquad (3)$$

It may not always be appropriate to neglect the average shaft load component, as noted for example in the Drammen clay tests reported by Andersen (2004). More complex forms than Equation 3 can be developed and applied when this is proven by appropriate laboratory tests. Cyclic DSS, triaxial or HCA experiments may be undertaken to determine the material coefficients (such as the A, B and C terms in the equation given above) and define rates of radial effective stress reduction under cycling for both clays and sands; see for example the tests on Clair West of Shetland glacial tills described by Jardine et al. (2011). The approach requires laboratory test samples to be consolidated to the radial effective stresses predicted by the ICP methodology. It is very important to specify sufficiently long creep pause intervals in such tests. Pre-cycling should also be considered. As with shallow foundations, an accumulation procedure can be applied to consider irregular storm loading: see Jardine et al. (2011) and Merritt et al. (2012). The same principles can be applied in local beam column (T-Z) analyses of progressive cyclic failure (see Atkins, 2000).

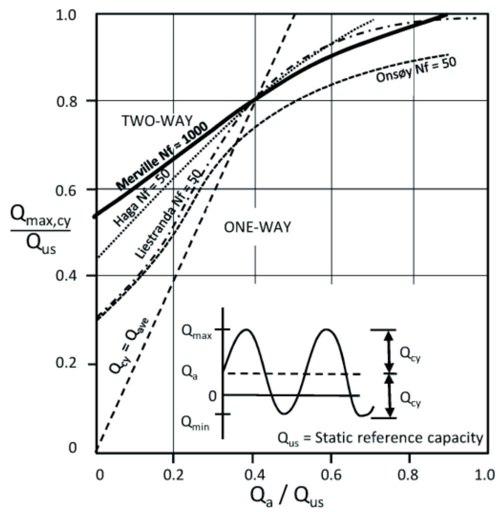

Figure 6.8: Comparison of Nf = 50 cyclic failure line for piles driven in several different clays

Some alternative procedures use 'global' purely empirical degradation laws calibrated to fit appropriate (good quality) experiments on model or field pile tests. Degradation laws have been proposed by, for example, Diyaljee and Raymond (1982) Poulos (1982) or Briaud and Felio (1986), the simplest of which are:

P(N)/P(1) = k•N-m (4)

or

P(N)/P(1) = 1- t•Ln(N) (5)

where P(N) is the value at cycle N of the property P being considered. P(1) is the reference value which can be the value for monotonic loading. The parameters m and t depend on the type of soil, the pile-soil system (rigidity) and the installation method. They are also expected to depend on the load characteristics although they have been found independent in some experiments. As illustrated by the interaction diagrams, it is imperative that the degradation laws are based on the relevant ratio between average and cyclic loads. The degradation laws can be applied (essentially to extrapolate and/or interpolate) any credible experimental observations regarding both capacity and stiffness trends.

6.2 *Lateral and moment capacity*

No screening tool equivalent to the axial cyclic loading interaction diagrams discussed above has been proposed to date for lateral or moment loading. Analogy with axial loading suggests that critical situations may perhaps be identified by developing equivalent iso-contours of relative pile head displacements y/B as functions of normalised average and cyclic load components based on experiments or analyses. Another approach is to develop purely empirical stiffness degradation laws, as outlined above for axial loading. Khemakhem et al. (2012) and Rosquoët et al. (2013) set out such treatments from their centrifuge lateral loading pile experiments on soft clays and sands respectively.

6.3 *Numerical analyses of pile response*

The simplified 'global' cyclic axial pile capacity approaches described above do not consider the effect of pile axial flexibility, which leads to progressive degradation along the shaft from the pile head downwards. For long and flexible piles this can give a greater cyclic effect than that estimated based on interaction diagrams if the diagrams are based on less flexible piles. The lateral loading response depends more critically on the relative slenderness and flexibility of the piles. Relatively slender jacket piles respond quite differently to low length-to-diameter (L/D) monopiles or anchors.

If 'global' approaches such as those outlined above for axial capacity indicate that pile capacity may be degraded significantly by cycling, more detailed site specific analysis may be considered. More detailed analyses may also be needed to check for any critical impacts of un-modelled features such as variable soil layering or pile flexibility. Such analyses are also necessary if it is important to determine cyclic and permanent displacements, as well as equivalent cyclic soil spring stiffnesses.

Numerical beam-column analyses and more advanced finite element analyses can be undertaken to meet these aims. Jardine et al. (2012) discuss the potential use of completely implicit numerical analyses involving cycle-by-cycle analysis and realistic constitutive laws to model the soil and the interface behaviour. They note, however, that such treatments do not appear to have been applied yet in mainstream offshore practice. Explicit finite element procedures, which rely on empirical or experimental accumulation laws, offer feasible practical application options: see Andersen and Høeg (1991), Saue et al. (2010) or Grimstad et al. (2013).

As mentioned above a key aim is to capture in axial analyses the progression of cyclic degradation from the pile head downwards. When lateral loading is applied one must also consider whether gapping may develop along the upper part of the pile and lead to subsequent erosion from water circulating in any soil-pile crack. Lateral cyclic loading is likely to degrade the shaft resistance available between the lowest depth where shaft friction is completely eliminated by gapping, down to the level where lateral straining is sufficiently low to cause no significant damage; Merritt et al. (2012). Approximate p-y analyses and small strain laboratory testing can provide guidance regarding the lower depth limit of this transitional range.

Any realistic numerical approach has to consider the effects of pile installation, which presents a considerable challenge. One key effect with displacement piles is the modification of soil properties around the pile. Extensive testing with highly instrumented piles (see Bond and Jardine, 1991 and 1995, Lehane et al., 1993, Lehane and Jardine, 1994a,b and Chow, 1997) demonstrated that local shaft shear resistance depends fundamentally on the effective radial stresses σ'_r applying at the interface. Soils, such as brittle plastic clays, that develop thin residual shear strength bands during displacement pile installation present low interface friction δ values that limit the τ_{rz} / σ'_r ratios and degree of cyclic damage that can be developed; Jardine (1991 and 1994). Piles driven in soils that develop high δ angles close to their $\varphi'_{\text{critical state}}$ angles experience large strain shearing which is considered within the NGI methodology as equivalent to remoulding. Examples of such soils include the Haga clay referred to earlier. Interface shear zones also develop around displacement piles driven in sands. Grain crushing takes place beneath the pile tip and a thin zone of finer and denser sand builds up over the pile shaft whose properties are distinctly different from those of the parent sand; see Yang et al. (2010).

The stress fields applying around pile shafts are modified considerably by pile installation. Total stresses increase sharply as the pile tip passes any given layer during installation and change with time after installation due to pore pressure redistribution and dissipation, creep and pre-shearing. All of these processes can change shaft capacity, although the trends vary with soil types. Jardine et al. (2006) showed that piles driven in sands can develop very significant gains in shaft capacity due to long term ageing processes. The latter are far clearer and more marked with piles that are not taken to failure during their ageing periods. These conclusions have been reinforced by Rimoy (2013). Monotonic and cyclic pre-shearing to failure can also add substantially to the capacity in high δ, low OCR, clays as illustrated in Figure 6.9. Thixotropy can cause similar increases in some cases. Andersen and Jostad (2002) consider that thixotropy can be as significant a factor as the radial effective stress development in some cases. They offer a procedure to allow for set-up effects in suction anchors design that might also be applied to driven piles. However, consideration must be given to potential brittleness when considering highly overconsolidated clays and dense sands. Full failure leads to sharp capacity losses through dilation and other processes in such soils: see Bond and Jardine (1995) and Jardine et al. (2006). In design the critical condition for capacity is normally that the design storm comes soon after installation, and one may then not be able to fully account for long term beneficial effects that are expected in clays with low OCR, particularly clays with low plasticity and sands. In overconsolidated clays and very dense sands, however, preshearing effects could be negative, and one should consider whether the long term situation can be critical. For fatigue, however, modelling of long term effects can be important.

The ICP effective stress methodology can be extended very naturally to consider cyclic capacity sands and clays. Shaft capacity reduces in step with the local radial effective stresses. Predictions of field behaviour rely on developing relationships between normal effective stress and cyclic loading parameters through field data or cyclic DSS, triaxial or hollow cylinder apparatus (HCA) laboratory tests. The approach is similar to that of Karlsrud and Nadim (1990), although the ICP approach requires laboratory test samples to be consolidated to the radial effective stresses predicted by the ICP methodology, which typically anticipates higher radial effective stresses than experiments by NGI (see Figure 6.10). The samples may be remoulded before testing when dealing with sensitive clays. It is important to allow suitable periods for creep and other ageing effects in such tests.

Karlsrud and Nadim (1990) proposed that monotonic (and cyclic) interface strength of should be calculated for clays on the basis of DSS tests on remoulded clay reconsolidated to normal (vertical) effective stresses matching the radial effective stress values σ'_{rc} interpreted as acting on the pile shaft after full pore pressure dissipation. The measured DSS shear strengths are corrected for the interpreted differences in the octahedral effective stresses developed in the DSS test and the pile 'disturbed' clay zone.

Karlsrud (2012) argues that the uncertainty in the effective stresses in the disturbed zone around the pile is a weakness in approaches that rely on effective stresses, and he preferred to retain empirical total stress approaches for defining monotonic and cyclic capacity in clays.

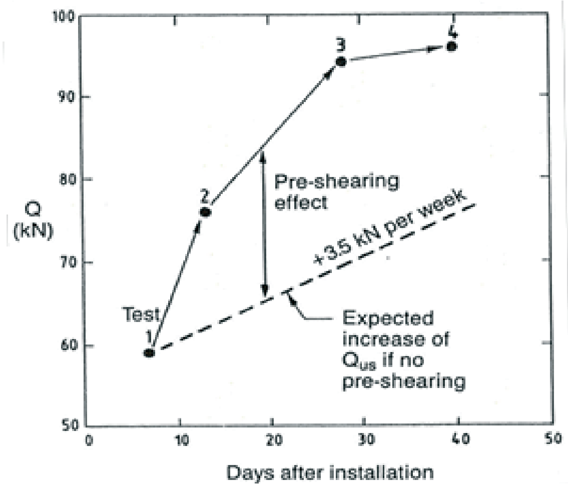

Figure 6.9: Influence of time and monotonic pre-shearing on monotonic axial pile capacity at Haga (Karlsrud and Haugen, 1985a

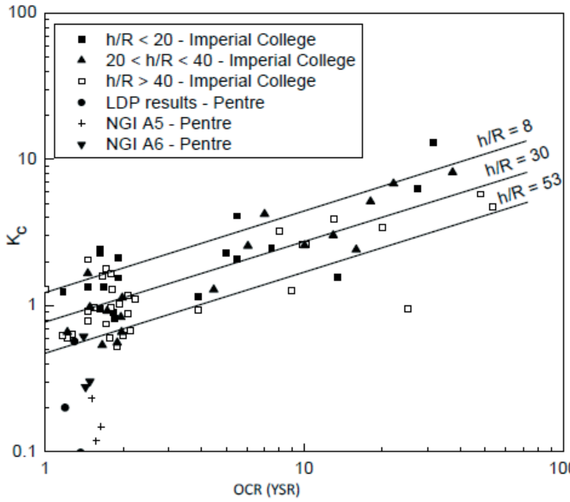

Figure 6.10: K_c trends with apparent OCR (YSR) and pile tip position (h/R) from Lehane (1992), adding measurements at Pentre by Imperial College by Chow (1997), Karlsrud et al. (1992) and McClelland Engineers (LDP)

The procedures based on laboratory tests are more uncertain for sands than for clays. Storm loading conditions will usually lead to a principally undrained response in clays. For sands, however, drainage may occur during a storm and volume changes can develop that provide scope for possible radial straining close to the pile shaft. If the response is dilative, as in the final stages of static loading to failure, the expanding interface shear zone reacts against the surrounding soil mass and generates radial effective stress increases. The reverse applies when the sand close to the shaft contracts under cyclic loading.

The effective stress changes observed in field and model pile tests (Lehane et al., 1993, Tsuha et al., 2012) are not modelled in standard laboratory tests but may be addressed in more sophisticated explicit finite element analyses as described later. Constant Normal Stiffness (CNS) tests reproduce the kinematic conditions that apply in any linearly elastic soil mass and indicate how radial effective stresses may fall under cycling along a pile shaft. A challenging aspect is to set fully appropriate CNS values during practical applications as they depend on (i) the sand's anisotropic, non-linear and pressure dependent stiffness and (ii) the inverse of the pile's outside diameters (see Jardine et al., 2005; Pra-ai, 2013). Tsuha et al. (2012) report local effective stress measurements made during pile cyclic loading and argue that constant volume (undrained) tests provide upper bound, infinite CNS, conditions and deliver safe design parameters for both sands and clays.

The soil parameters required to inform any numerical analyses depend on the approach that will be chosen. The ICP approach relies, for clays and sands, on constant volume DSS or HCA tests to predict rates of effective stress decay, combined with interface shear effective stress testing. The NGI's total stress clay approach relies on monotonic and cyclic shear tests on both intact and reconsolidated remoulded soil. The cyclic shear strength depends on ratio between cyclic and average shear stresses, applied stress path (TC, TE or DSS), and the number of cycles. Pore pressure generation due to cyclic loading and consolidation characteristics has to be tracked if a pore pressure accumulation procedure is to be applied, and in cases where partial drainage needs to be considered. The undrained shear strengths, thixotropy strength gain and virgin loading consolidation characteristics of the remoulded clay are required, along with the undrained shear strength of reconsolidated remoulded clay and unload-reload consolidation characteristics of both intact and remoulded clay samples, if site-specific set-up calculations are to be undertaken with the NGI approach.

Beam column analyses

There are several computer programs to calculate axial and lateral cyclic capacities based on beam column analyses. The soil can be represented by:

- Envelopes, such as the "cyclic" API p-y curves, (equivalent "cyclic" t-z curves have yet to be recommended by API or ISO), based on routine site investigation testing with UU laboratory tests.
- Cyclic p-y or t-z curves obtained by degrading static capacity using simple degradation laws
- Cyclic t-z curves generated by a more sophisticated algorithm, such as those described below.

The offshore Industry has developed codes for soil-structure interaction analysis such as SPLICE developed by Clausen (NGI 2006) that consider a (usually) linear superstructure supported by a simplified non-linear pile foundation system. The piles are represented by beam-column p-y, t-z and q-z curves that can be specified from several built-in procedures (as specified by API, ISO or DNV for example) or by direct manual input. The user may then take into account aspects that may not be covered by existing rules or recommendations. Pile group interaction is treated by a linear elastic procedure and a range of options exists for soil spring representation.

Current oil, gas and wind industry standards (G.L., 1999 or DNV, 2010) specify API/ISO p-y procedures for horizontal load-deformation analysis. As discussed by Jardine et al. (2012) these standard p-y procedures have limitations and imperfections that merit attention. Measurements on instrumented piled structures demonstrate that the standard beam-column curves and elastic interaction analyses can over-predict movements of single piles and groups (Jardine and Potts, 1988 and 1992) and hence structural natural frequencies; see for example Kühn and Watson (2000). Centrifuge tests performed by Aderlieste et al. (2011) in sands indicate that pile diameter increases have a greater effect on spring stiffness and static/cyclic lateral capacity than predicted by the API formulation. Advanced numerical analysis also questions the basis of the p-y methods to large diameter piles. Finite Element studies by Achmus et al. (2005, 2008 and 2010) and Augustesen et al. (2009), inter alia, also show that the API procedures may not be appropriate for large monopiles in sands under monotonic loading. Other cyclic finite element analyses by Saue et al. (2010) and Grimstad et al. (2012) of monopiles made with the previously described NGI clay accumulation model indicate lower displacements, rotations, bending moments and shear forces than standard p-y calculations.

Computer programs are available commercially that apply beam-column methods to assess axial pile response under cycling. The earlier cyclic t-z codes include RATZ (Randolph, 1994), PAXCY (Karlsrud et al., 1986) and PAX2 (Nadim and Dahlberg, 1996).

RATZ utilizes the load-transfer scheme illustrated in Figure 6.11. Under monotonic loading, the t-z curve consists of:

- A linear stage $\tau_o = k \cdot w / r_o$ that extends up to a fraction $\xi\tau_p$ of the peak shear stress (ξ is a parameter between 0 et 1)
- A parabolic stage with initial gradient k and final gradient of zero when $\tau = \tau_p$
- A softening stage, where the current value of shaft friction is related to the absolute pile displacement by :

$$\tau_o = \tau_p - 1.1\left(\tau_p - \tau_f\right)1 - \exp\left(-2.4(\Delta w/\Delta w_{res})^{\eta}\right) \quad (8)$$

where τ_f is the residual value of shaft friction, reached after an additional displacement of Δw_{res}, with Δw being the post-peak displacement. The parameter η controls the shape of the strain softening curve.

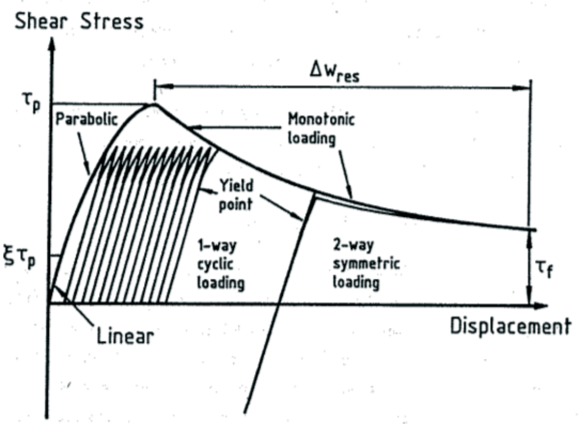

Figure 6.11: Load-transfer t-z curve used in RATZ

The accumulation of permanent displacement under cyclic loading is controlled by the parameter ξ which defines a yield point that is engaged on reloading. The post-yield plastic displacements are considered as equivalent to post-peak monotonic displacement. This leads to a gradual degradation of the shaft friction from peak to residual. An implicit assumption is that the load-transfer exhibits post-peak softening. The safe cyclic range can be varied in a way similar to that proposed by Goodman for metals. As noted above, many soil types that are susceptible to axial cyclic loading also show ductile static behaviour. Key input parameters in RATZ are the nominal linear shear modulus, G, the yield threshold, ξ , the peak shaft friction, τ_p, the residual shaft friction ratio, τ_r/τ_p, and the displacement to reach residual shear stress, Δw_{res}. For non-linear strain-softening, the shape factor, η, determines the exponential shape. For cyclic loading, the cyclic residual shaft friction ratio, τ_{cr}/τ_p and the absolute value of the yield ratio, ξ must be specified. Static parameters can be obtained from standard engineering practice. Cyclic parameters require calibration on series of fatigue curves from DSS, TX or CNS tests using the internal RATZ algorithm.

Erbrich et al. (2010) present methods for calculating cyclic behavior of axially loaded drilled and grouted piles in compressible cemented carbonate soils and laterally loaded drilled and grouted or driven piles in uncemented carbonate soils, implemented in software called CYCLOPS and pCyCOS, respectively. The programs are beam column approaches with t-z and p-y models. The t-z formulation in CYCLOPS is developed from RATZ, with the RATZ model enhanced by including a variable bias parameter and an initial softening parameter, and the shape of the t-z curve is modified within and immediately outside of a gap zone formed during cyclic loading. A significant number of CNS test is needed for the model to be used in practical design. The p-y curve in pCyCOS is established from finite element analyses of a horizontal disk around the pile with input in the form of a cyclic stress strain curve from monotonic and cyclic simple shear tests. The present version focuses on two-way cyclic loading. The procedures in both programs have a theoretical basis, but include a number of factors determined from empirical calibration. Both programs require a competent user with considerable skill and care. The programs were developed for carbonate soils, but have potential for more general applicability.

Alternative t-z procedures include the code PAXCY/PAX2 (Karlsrud et al., 1986; Nadim and Dahlberg, 1996) which incorporates key features of the NGI's laboratory based approach for clays. Here the t-z springs are established by integrating with respect to radius the shear strains γ_{rz} developed in the disk of soil surrounding the pile segment. The soil around the pile is divided into the three zones reflecting different degrees of disturbance during installation with a thin remoulded zone closest to the pile wall. The cyclic soil response is based on shear strain contour diagrams of the type presented in Figure 5.14, which show the average and cyclic shear strains as functions of average and cyclic shear stresses after a given number of cycles. Ideally, contour diagrams should be established for all the three zones around the pile. However, the inner reconsolidated "remoulded" zone is assumed to govern capacity and displacements. The DSS test results are corrected for octahedral effective normal stress conditions as proposed by Karlsrud and Nadim (1990) and mentioned previously.

It is assumed that the pile's cyclic loading history can be expressed by load parcels that each contains a fixed number of cycles with constant average and cyclic loads. The pile response is calculated at the beginning and end of each load parcel. Diagrams of the type shown in Figure 5.14 are used to establish relationships between average shear stress, τ_a, and average shear strain, γ_a, and between cyclic shear stress, τ_{cy}, and cyclic shear strain, γ_{cy}. The two relationships are not independent, however, and iterations are performed until acceptable convergence is obtained between the calculated τ_a and τ_{cy} distributions along the pile.

The effects of cyclic loading on capacity and displacements are taken into account by using strain contour diagrams of the type shown in Figure 5.11. The strain accumulation procedure described previously is followed over the cyclic load history, and the equivalent number of load cycles at the beginning and end of the specified load parcels is determined.

PAX2 is a simplified version of PAXCY that allows the NGI approach to be applied more easily and rapidly. PAX2 assumes that the cyclic shear strain is independent of τ_a, eliminating need to iterate the τ_a and τ_{cy}-γ_{cy} relationships. The programme contains a database of normalized stress-strain functions, and the equivalent number of cycles can either be specified or estimated automatically based on storm duration, soil type, platform type, and ratio between average and cyclic loads. Worked calculation examples in Karlsrud and Nadim (1990) demonstrated that PAXCY predicts pile displacements and stress redistribution well along the shafts of piles tested at Haga under various combinations of average and cyclic loads. Parallel analyses made with PAX2 and RATZ show at least reasonable agreement for the static and cyclic load cases.

Atkins (2000) report an alternative t-z formulation based on the simple 'A, B, C' effective stress ICP procedure (Jardine et al., 2005) that can be used in clays or sands, provided suitable cyclic laboratory (DSS, triaxial or HCA) tests are undertaken. In this approach pile slip was the sole source of permanent pile head deflection under cycling, although cyclic stiffness also fell proportionally with shaft capacity degradation. As with the NGI approach, a cyclic accumulation method was used to address storm loading with relative local radial effective stress (and hence shaft capacity) loss being carried forward as the memory parameter. Atkins (2000) were able to reproduce the load displacement behaviour of cyclic tests performed in dense sands at Dunkirk with reasonable accuracy and went on to apply the approach in full soil-structure interaction analyses of offshore jackets experiencing extreme storm events.

The t-z beam-column programmes provide predictions for cyclic axial displacements and allow, in principle, permanent axial displacements to be tracked under-cyclic loading. The same degree of development has not been achieved in lateral p-y beam-column analyses. The 'cyclic p-y' variants do not address the gradual evolution of displacements under specified cyclic loading conditions, but simply give softer envelope curves that take some account of the degradation that might be expected under 'typical Gulf of Mexico' storms.

Simplified boundary element formulation

Poulos (1989) took a different approach to axial cyclic analysis in developing the SCARP code. Here a simplified boundary element formulation is used in place of the t-z beam-column formulation. The soil mass is represented by an elastic continuum, but allowance is made for end-bearing failure and pile-soil slip along the interface by specifying limiting values of the pile-soil stress at each pile element. Strain-softening of the interface can also be considered (Figure 6.12). The program allows for three major effects of cyclic loading: (1) degradation of shaft and end-bearing resistances and soil modulus, (2) loading rate effects and (3) accumulation of permanent displacements under non-zero average loads. The "reverse plastic stress" model, proposed by Matlock and Foo (1979) is assumed in which degradation D develops progressively during cycling with:

$$D = (1 - \lambda)\,(D' - D_{min}) + D_{min} \qquad (9)$$

where:
D = Current value of degradation factor
D' = Degradation factor for previous cycle
D_{min} = Minimum possible degradation factor
λ = Degradation rate parameter

SCARP tracks three degradation factors: D_τ for shaft resistance, D_b for base resistance and D_E for soil modulus. Each expresses the ratio between the particular parameter and its corresponding value under static loading.

A loading factor D_R is applied in SCARP to the values of ultimate skin and base resistance and the soil modulus:

$$D_R = 1 = F_\rho \log_{10} (\zeta/\zeta_r) \quad (10)$$

where:
$F\rho$ = Rate coefficient (typically 0.1 to 0.25)
ζ = Loading rate
ζr = Reference loading rate (from static loading test)

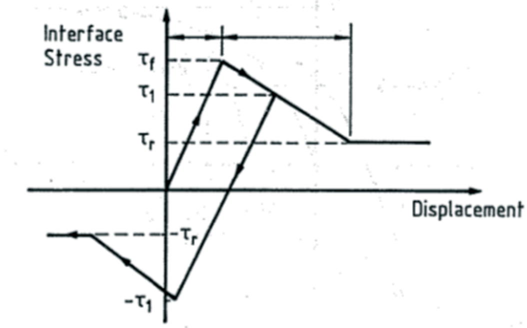

Figure 6.12: Strain-softening model curve used in SCARP

The incremental permanent soil displacements at the end of each cyclic parcel are computed from Diyaljee and Raymond's (1982) empirical expression:

$$\delta S_p = S_{pN}[n\delta X + (m\delta N/N)] \quad (11)$$

where:
δS_p =Increment in permanent soil displacement between cycle N and N+δN
δX = Change in stress level between cycle N and N+δN
S_{pN} = Permanent soil displacement at cycle N
m, n= Experimentally determined parameters, which are different for the shaft and base
$X = (P_o + 0.5P_c) / Q_c$
P_o = Mean load of loading parcel
P_c = Cyclic load amplitude of loading parcel
Q_c = Ultimate static capacity of the pile

Guidance is limited regarding input parameter selection for SCARP. Large ranges of values are proposed, based on laboratory and model tests with principally carbonate materials. One of the aims of the SOLCYP project (Puech et al, 2012) is to provide additional experimental data linking cyclic laboratory element and in-situ tests on clays and silica sands to trends from experiments on models of various scales and full scale piles.

Comparative studies by Chin and Poulos (1992) and others have shown that RATZ and SCARP lead to broadly comparable static load-displacement predictions, despite their fundamentally different approaches. However, the two codes' cyclic loading predictions can diverge considerably. Their use is most highly documented in relation to carbonate sediments. Further investigation and calibration over a wider range of geomaterial types is needed to increase confidence in quantitative predictions.

Explicit finite element procedures

Axial, lateral and rotational pile displacements are better considered by more advanced finite element analysis. Simplified, explicit, cyclic finite element procedures include those described for shallow foundations and suction anchors in Section 5.1 which are most suitable for monopiles with L/D ratios < 10. The calculations can also be used to establish p-y curves for monopiles (Saue et al., 2010 and Grimstad et al., 2013) to use in place of API guidance which may not be representative, as discussed above. Figure 6.13 shows the incremental displacements at failure of a 4.7m diameter, 16m long monopile for an offshore wind power structure in very dense sand. It was assumed here that conditions would be nearly undrained during storm loading due the pile's scale, so allowing the 'clay' procedures to be applied, although without the scope for high shear strengths to develop due to strong dilatancy.

The monopile is subjected to cyclic horizontal and moment loading at seabed level. The ratio between cyclic and average loads is high (2 to 10) and two-way loading was assumed. The ratio between overturning moment and horizontal load at seabed was 30m. The analysis involves 3D finite element analyses using cyclic laboratory data of the type described in Section 5.1, in this case assuming a fixed equivalent number of cycles of N_{eq}=10. The displacement pattern indicates a failure mode with active and passive zones in the upper part and a rotational failure in the lower part. The finite element analysis indicates a higher moment capacity than beam-column analysis using standard API p-y curves.

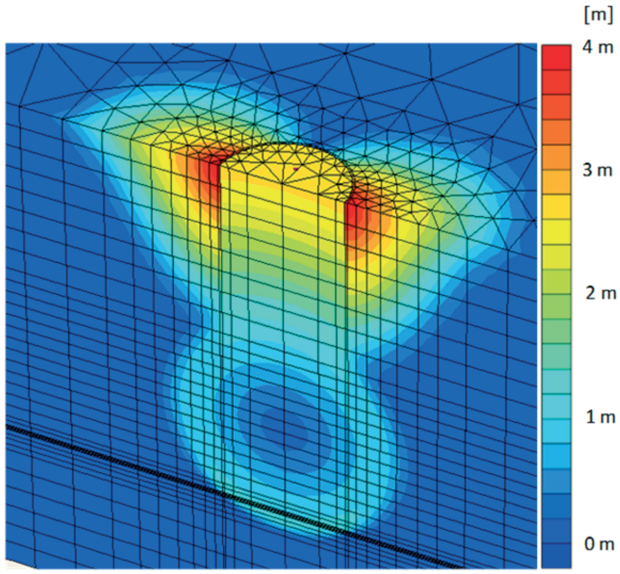

Figure 6.13: Incremental displacements at failure in a cross section of a PLAXIS 3D finite element analysis of a 4.7m diameter, 16 m long monopile in very dense sand (Saue et al., 2010)

6.4 *Equivalent cyclic soil spring stiffnesses*

Equivalent cyclic soil spring (axial, lateral or rotational) stiffnesses can be exported for dynamic soil-structure analyses that assess potential load amplification and fatigue trends by considering the cyclic loads and displacements given by the beam-column or finite element calculations. It is particularly important with wind-turbine structures to undertake fatigue calculations that address wind and wave loading throughout their working lifetimes. Very large numbers of small waves can be important in these assessments, and their impact depends on whether larger storms occur early or not in service and affect the stiffness under subsequent smaller cyclic loads.

The equivalent cyclic stiffnesses can be expressed as load-displacement curves defined at seabed level that are of course modified by the structure extending up from the sea bed.

7 CYCLIC SOIL PARAMETERS

Earlier sections have outlined the soil characteristics that need to be established to allow cyclic design assessments for shallow foundations, suction anchors, monopiles and piles. The necessary input parameters are re-summarized in Table 7.1 and in brief comments given below. The Table includes the parameters required to assess monotonic axial pile capacity because this step defines the key reference point for the cyclic axial interaction diagrams and degradation laws discussed in several parts of Section 6.

Shallow foundation assessment involves assessing drained frictional failure characteristics in cases involving sands when undrained conditions cannot be assumed to apply. Interface friction angles may also be needed to consider base sliding stability with low φ′ and δ soils, especially those with low sensitivity and potentially high OCRs.

Monotonic undrained shear strengths are crucial to the 'NGI' approach to cyclic characterisation in clays and undrained sands. The spread of tests required depends on the potential failure modes. If horizontal sliding is critical, for instance, compression and extension tests are less important than DSS experiments. Initial shear moduli are important to displacement and soil spring stiffness calculations, and may dominate the far-field response.

Cyclic testing is clearly crucial to cyclic shallow foundation assessments. Contour diagram reporting offers a convenient test data presentation format, independent of the calculation method eventually employed, as was illustrated in Section 5. Fatigue assessments require trends that may have been extended, potentially to hundreds of millions of cycles. Damping parameters are not always required, but may be called for with tall and slender structures.

Consolidation characteristics are needed to calculate dissipation and settlement rates stemming from cyclically induced pore pressures generated during storms. These processes are treated as being analogous to re-loading and are analysed with reloading moduli. The apparent pre-consolidation pressure is needed to determine the overconsolidation ratio, OCR (or Yield Stress Ratio – YSR), which is an important parameter in several respects, including cyclic behaviour.

Testing is undertaken on remoulded samples when site specific set-up analyses are performed in sensitive clays. The consolidation characteristics (modulus and permeability) contribute to analyses of set up times, while shear strength, sensitivity and thixotropy measurements are fed into analyses of the associated shear strength gains. Set-up factors may also be estimated as functions of plasticity and OCR following Andersen and Jostad (2002). Cyclic tests are not normally performed on remoulded clay as the skirt wall soils are assumed to have a similar cyclic response to the intact clay. But such tests can be considered in cases where the interface shear strength is likely to be crucial and/or significantly different to that of the intact soil.

The cyclic assessment of ***anchors*** requires a broadly similar range of input parameters to shallow foundations. However, noting that design is often dominated by overall holding capacity, deformation properties (e.g. shear modulus and damping) may not always be required. The emphasis on establishing shear strain and pore pressure trends can also generally be reduced, although knowing their relationships with cyclic shear stresses and numbers of cycles remains necessary to track the numbers of equivalent cycles and the cyclic strengths that determine cyclic holding capacity.

Monopiles may be designed following either the approaches set out for shallow foundations (requiring the parameter list discussed above) or those developed for longer (L/D > 10), which are reviewed below.

Deep, high L/D piles may be assessed by a range of alternative procedures, each of which involves a specific parameter assessment approach. Monotonic capacity prediction is the first step towards axial cyclic loading assessment. Depending on the methodology chosen, this may require CPT resistance, relative density, YSR, plasticity index, sensitivity, effective interface shear angles or monotonic UU/DSS undrained shear strengths. The interface friction angles required for effective stress methods should be determined through ring-shear tests, as described by Jardine et al. (2005a). Cyclic constant volume DSS or HCA experiments are needed to apply the simplified A,B,C ICP cyclic analysis method, while some cyclic procedures for sands call for drained cyclic CNS tests. In contrast, the NGI approach for clays requires intact DSS shear strength, sensitivity and thixotropy measurements. Tests on reconsolidated remoulded clay are also needed and cyclic DSS tests are called for if the PAXCY cyclic t-z approach is to be applied.

Explicit finite element cyclic analyses require similar parameter derivation approaches to shallow foundations or suction anchors, depending on the relative importance to design of predicting the foundations' load-displacement characteristics.

More advanced, fully implicit, finite element analyses involve a range of other procedures in which the constitutive modelling parameters are calibrated to fit specific static and cyclic tests. The scope for improving modelling through advanced testing is developing continuously. For example, Jardine (2013) sets out recent developments that can be applied to improve predictions for the monotonic and cyclic modelling of large displacement piles driven in sands by accounting for cyclic laboratory test behaviour as well as phenomena such as stiffness non-linearity and anisotropy, creep and time dependency, large displacement interface-shear characteristics, the stress regime imposed by installation, particle crushing beneath the pile tip and the development of an interface shear zone containing particle crushing products.

Table 7.1 Cyclic soil data for foundation design of shallow foundations, suction anchors, monopiles and piles

	Shallow foundations		Suction anchors		Monopiles		Piles	
Soil parameter	Clay	Sand	Clay	Sand	Clay	Sand	Clay	Sand
Frictional characteristics								
Peak drained friction angle, ϕ'		x		x		x		x[4,8]
Undrained friction angle, ϕ_u'		x		x		x		x[8]
Dilatancy angle, ψ		(x)		(x)		(x)		x[8]
Slope of DSS drained failure line, α'		x		x		x		x[8]
Slope of DSS undrained failure line, α_u		x		x		x		x[8]
Interface friction angle, δ_{peak} and $\delta_{residual}$	(x)[1]	(x)[1]	(x)[1]	(x)[1]	(x)[1]	(x)[1]	x[4,8,(1)]	x[4,8,(1)]
Monotonic data								
Monotonic undrained shear strength, s_u^C, s_u^{DSS}, s_u^E	x	x	x	x	x	x	x[2,7,8]	x[8]
Initial shear modulus, G_{max}	x	x			x	x	x[8]	x[9]
Cyclic data								
Cyclic undrained shear strength, $\tau_{f,cy} = f(\tau_a, \tau_{cy}, N)$, triaxial and DSS	x	x	x	x	x	x	x[2,8]	x[8]
Cyclically induced pore pressure, $u_p = f(\tau_a, \tau_{cy}, N)$, triaxial and DSS	x	x		x	x	x	x[9]	x[9]
$u_p = f(\tau_{cy}, \log N)$ for $\tau_a=\tau_0$, triaxial and DSS	x	x		x	x	x	x[9]	x[9]
Cyclic stress strain data, γ_a, γ_p & $\gamma_{cy} = f(\tau_a, \tau_{cy}, N)$, triaxial and DSS	x	x		x	x	x	x[2,9]	x[9]
$\gamma_{cy} = f(\tau_{cy}, \log N)$ for $\tau_a=\tau_0$, triaxial and DSS	x	x	x	x	x	x	x[2,8]	x[9]
Drop in radial effective stress along shaft $\sigma'_r = f(\tau_{cy}, N)$, DSS			x[10]		x[10]		x[10]	
Drop in radial effective stress along shaft $\sigma'_n = f(\tau_a, \tau_{cy}, N)$, CNS				x[11]		x[11]		x[11]
Damping	(x)	(x)			(x)	(x)	(x[9])	(x[9])
Consolidation characteristics, intact soil								
Preconsolidation stress (and OCR)	x	x	x	x	x	x	x	x[8]
Virgin, unloading and reloading constrained moduli	x	x	x[6]	x	x	x	x[6,9]	x[8]
Permeability	x	x	x[6]	x	x	x	x[6,9]	x[8]
Remoulded soil data								
Sensitivity, S_t	x[6]		x[6]		x[6]		x[6,7,8]	
Undrained shear strength of reconsolidated remoulded soil, DSS	x[6]		x[6]		x[6]		x[5,6,7,8]	
Cyclic undrained shear strength, $\tau_{f,cy} = f(\tau_a, \tau_{cy}, N)$, reconsol. DSS	(x)[6]		(x)[6]		(x)[6]		x[5,6,7,8]	
Virgin constrained modulus	x[6]		x[6]		x[6]		x[6,8]	
Permeability	x[6]		x[6]		x[6]		x[6,8]	
Thixotropy	x[6]		x[6]		x[6]		x[6,(7),8]	
Additional parameters for reference monotonic pile capacity								
Relative density, D_r								x[3]
CPT resistance							x[3]	x[3]
Plasticity index, I_p							x[3]	
Monotonic UU shear strength, s_u^{UU}							x[3]	
ε_{50}							x[3]	

(x): Generally not required

1) *May be required for low sensitive clay, high OCR clay and for low φ′ and δ soils*
2) *Input to PAXCY/PAX2 in clay. DSS only*
3) *To calculate reference monotonic capacity if using interaction diagrams or degradation laws*
4) *For design based on effective stress principles*
5) *If constructing interaction diagrams for piles based on DSS tests*
6) *In case of site specific set-up analyses*
7) *To calculate axial pile capacity in clay based on reconsolidated remoulded shear strength. DSS only.*
8) *In case of explicit finite element analyses*
9) *In case of explicit finite element analyses and where displacements are important*
10) *Simplified A,B,C method*
11) *In case of explicit finite element analyses where interface is modelled based on CNS tests*

8 LABORATORY TESTING

The cyclic soil parameters identified in the previous section can be determined by triaxial, DSS, oedometer, UU, bender element, resonant column, HCA, CNS and ring shear laboratory tests as indicated in Table 8.1. The last column in the table indicates papers that comprise database references for some key tests given in Table 10.1. A higher level guidance on planning and execution of geophysical and geotechnical ground investigations for offshore renewable energy projects is given in BSH (2008) and OSIG (2013).

Frictional characteristics. Drained effective-stress shear failure and dilatancy parameters can be determined from monotonic triaxial and DSS tests. As described in Section 4, HCA tests provide the best descriptions of the stress states developed in tests involving principal stress axis inclination (α) rotation, although sample preparation, apparatus control and data reduction are more complex and time consuming. Interface friction angles are best determined from ring-shear tests where the soil annulus is rotated against the required interface material. DSS or shear box tests where the sample is sheared back and forth have been used as alternatives, although the results are less satisfactory.

Monotonic shear tests. Undrained shear strength can be determined from monotonic triaxial compression, triaxial extension and DSS tests. The initial drained and undrained vertical Young's moduli and Poisson's ratios (E'_v, E_{Uv}, υ'_{hv} and υ_{Uhv}) can be determined by means of local strain transducers in triaxial testing. The vertical shear stiffness G_{vh} may also be assessed through bender element shear wave velocity measurements made in triaxial, DSS or even oedometer tests. Care is needed to address potentially marked small strain stiffness anisotropy. The full set of cross anisotropic elastic parameters can be measured statically in instrumented HCA tests, or by assuming rate independence and combining multi-axis bender tests with instrumented triaxial probing tests: see Kuwano and Jardine (2002 and 2007), Gasparre et al. (2006) or Jardine (2013). Bender element signals measured in DSS tests may experience less disturbance due to side boundary reflections, but the transducers are positioned close together and may give uncertainty to the effective wave travel path length. Initial values of shear modulus G_{hv} may also be measured in resonant column tests, although this may be less cost-effective in cases where information is not required regarding small strain damping. Bender element and locally instrumented triaxial tests have the advantage of measuring initial shear moduli and shear strengths on the same sample.

The strain ranges over which most soils show linearly elastic behaviour are very small and most practical field problems are dominated by non-linear behaviour; Andersen and Aas (1980), Jardine et al. (1986), Andersen (1991), Andersen and Høeg (1991), Jardine (1994). Locally instrumented triaxial tests allow high quality information to be recorded continuously from very small strains up to failure. Resonant column tests also allow the non-linear range to be explored to some extent, although under dynamic conditions that involve cycling at relatively high strain rates. Soil moduli are known to vary with the imposed stress regimes and be affected by the time allowed for ageing. Stiffness is therefore best measured in apparatus that allows the in-situ (often K_0) effective stresses to be applied and in tests that include suitable pause periods for samples to reach low creep rates before assessing stiffness; Jardine (2013).

Cyclic parameters. Undrained or drained cyclic triaxial and DSS testing is performed to aid offshore foundation design. Stress-controlled cyclic loading systems are usually adopted because the critical perturbations are predominantly imposed by wave and wind loads that are estimated from interactive fluid-structure analyses. Mixed-boundary cyclic CNS and HCA testing may also be considered. Damping parameters can be found from the stress-strain loops of cyclic triaxial and DSS tests. Small strain damping is best determined in resonant column tests or from locally instrumented triaxial experiments.

Consolidation characteristics of intact soil. The vertical yield stresses σ'_{vy} (or pre-consolidation stresses) and overconsolidation ratios (or YSRs) of lightly over consolidated deposits can often be determined directly from oedometer tests on clay samples. Such yield points cannot be seen in tests on sands and are usually harder to interpret in heavily overconsolidated clay samples. OCR (or YSR) may also be inferred from knowledge of the site's geological history, from shear strength profiles or from in-situ test profiles. A cross-checked, holistic, approach is recommended in cases where the OCR (or YSR) has an important bearing in design as with, for example, the ICP pile design method for clays.

The constrained (usually non-linear) moduli that apply over moderate strain ranges may be estimated from oedometer tests on intact clay and on sand specimens prepared to the most representative in situ condition. The oedometer tests should be performed with two unload/reload sequences. The first unloading should generally be performed from a vertical effective stress appreciably greater than the estimated preconsolidation stress, which also helps to clarify the latter's determination. The second unload/reload stage should be applied at the end of the tests. These two unload/reload loops help to establish the slopes of the 'swelling' curves and inform the interpolation/extrapolation of unload/reload moduli at different effective stress levels to those applied in the test.

Oedometer tests involve relatively thin samples that experience considerable bedding strain at their ends and friction over their side walls. These potential imperfections can be eliminated by undertaking drained stress path triaxial tests equipped with local strain transducers; see Jardine et al. (1984) or Tatusoka et al. (1997). Such triaxial tests are more demanding and require closer control than standard tests, especially if zero lateral strain or other mixed boundary conditions are required.

Permeability can be measured in the oedometer tests, but for clean sand it is necessary to check that the flow resistance of filters and other equipment is sufficiently small or correctable to have no significant influence on the measurements. Low-resistance triaxial permeability tests should be performed when necessary.

Remoulded soil testing. Clay sensitivity can be measured by fall cone, laboratory vane or UU tests on tests on intact and remoulded clay (e.g. De Groot et al., 2012). Undrained monotonic or cyclic DSS or triaxial tests may be performed on samples remoulded by hand before being set-up and consolidated to the desired testing stresses. Remoulded testing may also follow earlier testing of samples in an intact state where large strain undrained cyclic tests may be followed by final undrained shear stages. Oedometer tests on remoulded samples may provide constrained moduli and the permeability information.

Thixotropy may be investigated through tests on remoulded clay samples by fall cone or shear vane tests on specimens that are stored under constant water content conditions over a time series such as 1, 8 hours and 1, 2, 4, 8, 15, 30 and 60 days. It is important that the samples are well sealed and the remoulded strength and the water content of the multiple samples tested should also be measured to check that their basic properties are unchanged by storage or drying.

Sampling and specimen preparation. The load carrying capacity of foundations in sand is dominated by the sand's in-situ state, or relative density, which is usually assessed through CPT testing. The in-situ densities and water contents of high permeability samples are usually disturbed by standard tube sampling techniques which tend to loosen dense samples and densify loose deposits. Ground freezing techniques offer the only sure way of retaining the in-situ states of sands. While clays may usually be sampled without drainage affecting their water contents and unit weights, they suffer degrees of disturbance to their shear strengths, stiffnesses and YSRs that depend on the sampling technique adopted.

The difficulties of representative sampling pose questions regarding sand and silt test specimen preparation. It has been shown (e.g. Silver et al., 1976, Mulilis et al., 1977 and Hoeg et al., 2000) that sands' static and cyclic behaviour depends on the preparation method. In several cases, however, samples prepared by wet tamping (Andersen, 2009) or water pluviation (Vaid et al, 1999) have given similar cyclic shear strength as high quality frozen samples and NGI recommend adopting either technique, unless the sand has been deposited under dry conditions. Experience at Imperial College has also led to air or water pluviation being preferred; Kuwano and Jardine (2002). However, when fines are present even a few per cent of silt or clay makes reconstitution difficult, especially with clays. The properties of clay-sands (or 'dirty' sands) are highly dependent on their fines contents (Georgiannou and Hight, 1990). Use of "intact" clay-sand samples that are reconsolidated to in-situ stress conditions may then be preferable, even if such specimens have been disturbed. Whether the sampling disturbance leads to strengths and stiffnesses that are too high or too low depends on the in-situ state of the soil before sampling.

Laboratory test reconsolidation paths. The general recommendation is that reconstituted sand and silt samples should be taken through stress paths that re-trace their in-situ stress history, including any prior overconsolidation. For soft to very hard clays tests conducted after direct re-consolidation to in-situ stresses provide the best estimates of the in-situ response to loading: see Smith et al. (1992), Hight and Jardine (1993) or Lunne et al. (2006). High quality sampling techniques exist that can deliver good quality samples of most clay types.

While triaxial (and HCA) equipment offers full control over the consolidation effective stress paths, radial effective stresses cannot be controlled directly in DSS apparatus. NGI practice is to pre-load DSS samples to about 85% of the effective yield or pre-consolidation stress measured in 24 hour oedometer tests in order to generate an appropriate radial stress. However, this procedure may not be appropriate for DSS tests on stiff to hard clays which may have yield or pre-consolidation stress values of several MPa that are hard to establish in DSS tests.

Lean, low plasticity, low OCR clays suffer from tube sampling more than other types. Lunne et al. (2006) report difficulties encountered in testing disturbed samples of such deposits. Void ratio reductions sustained during reconsolidation can lead to a representatively dilative response on final shearing and shear strengths that over-predict those available in-situ. Lunne et al. (2006) recommend limiting the shear strengths to the shear stress values developed at 3% shear strain in such cases. Research at Imperial College has underlined the importance to stiffness measurements of partially re-tracing the recent stress history, choosing reconsolidation paths that lead to minimal shear and volume strains (see Jardine et al., 1991; Smith et al., 1992; Gasparre et al., 2007). The latter procedure history has less effect on the shear strength of most clays.

An awareness of sampling disturbance effects led Ladd and Foot (1964) to propose the SHANSEP re-consolidation procedure for samples with lower quality in which samples are K_0 consolidated to stresses 1.5 to 2 times yield or pre-consolidation stress and swelled back to a range of OCRs before being sheared. The normalised behaviour revealed by these tests is then assumed to apply in-situ. Research on natural clays led to this procedure being considered inappropriate for markedly 'structured' soils (see for example Leroueil and Vaughan, 1990; Le et al., 2008). However, SHANSEP approaches may be applicable to predicting properties that will be available in-situ after experiencing effective stresses far greater than those applying initially in-situ.

Monotonic consolidation and shear loading rates. Tests need to be consolidated and sheared at appropriate rates. Even clean sand can gain shear strength and stiffness significantly over time. Extended duration tests may be impractical in most projects and judgement has to be exercised: Andersen (2009). However, consolidation stresses should be held until pore pressures dissipate fully in all cases. The hold periods should extend for at least one overnight period, even with sands.

Most monotonic tests conducted at NGI and Imperial College on clays and sands are typically run with shear strain rates of about 2 to 4.5%/hr. These rates allow good rates of data collection and undrained pore pressure equalisation in most soils. Additional tests may be run at different rates to check time and rate dependency; care needs to be taken with pore pressure data in faster tests and mid-height pore pressure measurements are recommended when testing clays: see Hight (1982). Strain rates may also be varied during testing, which offers efficiency but may complicate shear strength determination. An example of such a test is presented in Figure 8.1 where the shear rate was varied by multiples of 10 in the pre-and post-peak domains. An approximately isotach response is seen in which the properties vary as functions of axial strain rate. Other patterns of behaviour are possible. Tatsuoka (2011) gives a comprehensive account of such time dependent behaviour in a wide range of geomaterials.

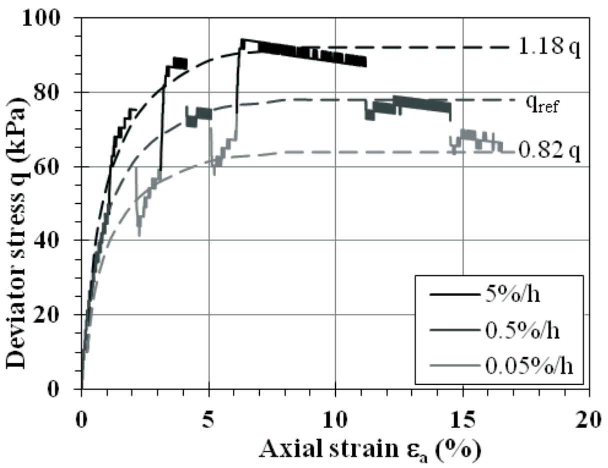

Figure 8.1: Example of rate effect measured on Gulf of Guinea clay (after Colliat et al., 2012)

Specimen pre-conditioning by cyclic pre-shearing. The cyclic response of soils, particularly sands, depends critically on whether they have experienced prior cycling. Samples may be pre-sheared in the laboratory to match the history of loading expected in-situ prior to the main design event. In this context, pre-shearing signifies conditioning the sample by cyclic loading with drainage applied either during or after the pre-shearing. The practice established by NGI for pre-shearing dense sand strata beneath large GBS platforms has been to apply ≈400 cycles at τ_{cy}/σ'_{vc} = 0.04 to model the build-up period of the design storm or the impact of earlier, less severe, storms.

A similar logic can be applied to driven piles foundations that experience extreme stress cycling during their installation (Jardine et al., 2013) and in earthquake engineering, where many sites will have experienced prior ground shaking. Pre-shearing generally increases cyclic shear strength in normally consolidated (even very dense) sand, provided it does not generate large shear strains that can break down the soil structure. It may also reduce the effects of sampling disturbance, preparation and re-consolidation methods (Andersen, 2009) although this requires more systematically study.

The lower permeability of clays and their lower cyclic susceptibility lead to pre-shearing being less appropriate in most GBS design cases. Consideration has to be given to the extended times available for dissipation of any pore pressures set up by earlier storms or storm build-ups. Pre-shearing usually leads to property improvements in low OCR clays, but the effects may be less positive or negative in high OCR deposits: Andersen (1988). In the latter case, the critical design situation could apply at a time well after installation when the clays may have been degraded by prior cyclic loading, swelling and drainage.

Cyclic loading tests. Suites of tests are needed for each critical soil unit that will affect the GBS, pile, anchor or other foundation under consideration. Tests may be eliminated from some units by considering the foundation's zones of loading influence and the potential importance of key layers in cyclic response. Noting that cyclic properties depend on degree of apparent overconsolidation, more than one suite of tests may be required within single units where OCR (or YSR) varies significantly with depth or when the soil beneath the foundation is consolidated under the weight of the structure to a higher consolidation stress than outside. Tests need to be run on samples taken as close to each other as possible to avoid variability affecting the patterns of behaviour.

Cyclic testing suites designed to provide input for the NGI's 'cyclic contour' methodology to construct cyclic contour diagrams such as those shown in Figures 5.10 to 5.11 and 5.14 to 5.17 are usually conducted undrained and stress controlled to match offshore storm loading. Each cyclic test applies one combination of average and cyclic shear stresses. Parallel monotonic 'control' tests are conducted under similar conditions (TC, DSS or TE) and on similar samples to the cyclic program and follow the same reconsolidation and pre-shearing paths. The monotonic tests define the zero cyclic load case and are used to normalize the shear stresses in tests conducted on clays.

The precise number of cyclic tests undertaken depends on whether full contour suites are needed. The degree of ambition in cyclic testing may reflect the project's stage of development (feasibility vs. detailed design) and the engineering consequences of significant uncertainty remaining in the cyclic response data. The testing strategy also depends on whether established sets of contour diagrams exist for soils comparable to those present at the site in question. One set that is often referred to is the complete suite undertaken for Drammen clay at OCRs of 1, 4 and 40; Andersen (2004).

The first step at a new site is to perform a limited programme involving perhaps three pairs of cyclic TC and DSS tests accompanied by monotonic TC, DSS and TE tests that may be compared with the library of existing cyclic data sets. If no reasonable contour diagram match is obtained, further suites of cyclic tests can be added until a reliable overall contour set is achieved. If a comprehensive definition of the contour diagrams is chosen, tests with high and low level cyclic shear stresses should be applied. The cyclic tests shall also be run with different combinations of average and cyclic shear stresses to fully define the contour diagrams. Referring to Figure 5.9, the average shear stress applied in cyclic triaxial tests, τ_a, is the sum of the initial shear stress prior to cyclic loading, τ_0, and the average shear stress, $\Delta\tau_a$, due to average environmental loads (from for instance waves, wind and current) and $\tau_a = \tau_0 + \Delta\tau_a$. The soil is consolidated under τ_0, but $\Delta\tau_a$ can be applied undrained or drained, depending on the design conditions. The impact of this choice can be significant, as shown for very dense Baskarp sand by Andersen and Berre (1999). Consolidation analyses are required to decide whether $\Delta\tau_a$ should be applied drained or undrained in sands and mixed strata. Dissipation times are usually long when considering storm loading on clays, leading to undrained conditions being adopted. When $\Delta\tau_a$ is applied under drained conditions the triaxial contour diagrams depend on whether $\Delta\tau_a$ is imposed by (i) increasing the vertical stress, or (ii) reducing the radial stress.

The higher level tests are usually run to failure, but tests involving low cyclic shear stresses may have to be stopped after perhaps 5000 cycles without any failure developing. Cyclic failure is usually defined at NGI as a point where either the average or the cyclic shear strain reaches 15%. Specimens that do not fail cyclically can be subjected to final monotonic shear to failure stages, or be consolidated back to their original consolidation stresses while recording the resulting volume changes.

The cyclic periods developed under storm wave loading generally vary between 10s and 20s. Test results are not expected to be affected significantly by cyclic periods varying between these limits and a 10s period has been adopted at NGI to reduce testing times and extend the numbers of cycles that can be applied in given periods. Shorter periods apply in earthquakes (1s or less) and under wind loading (where 3 to 4s may be typical), while periods can extend to 30s to 60s in the long duration swell conditions that can occur in some offshore areas. Cyclic testing rates should be varied to more appropriate values when considering such cases.

Alternative testing strategies may be adopted when considering other cyclic design procedures. For example, the simplified A, B, C effective stress cyclic axial pile design approach (Jardine et al., 2005a) calls for sufficient constant volume DSS or HCA testing to establish how normal effective stresses will reduce due to shaft shear stress cycling. Samples should be consolidated to the radial effective stresses acting on the pile wall at end of equalization as predicted by the ICP methodology. The main testing focus is on varying the ratio of τ_{cy} / σ'_{n0}; only limited testing is usually required with non-zero average initial shear stresses τ_a / σ'_{n0} (applied prior to cycling) to check whether this parameter is influential and needs to be considered. The testing suites are also designed considering that the ratio of τ_{rz} / σ'_r cannot exceed tan δ at the pile-soil interface. Cyclic stiffness may be assessed through a fully non-linear 'small strain' approach based on high quality, locally instrumented triaxial or HCA tests, as outlined by Jardine et al. (2005b) or Jardine (2013).

Emerging explicit finite element approaches for assessing cyclic pile response may well call for different mixes and types of triaxial, DSS or HCA tests, even if the contour diagrams network is likely to define the required data for most soil models. Drained CNS testing may be called for to calibrate model interface conditions. The difficulties of choosing single CNS values were reviewed earlier; further guidance on this point is given by Pra-ai (2013).

Table 8.1 Laboratory tests to determine required cyclic soil parameters

Parameter	Test Type														
	Triaxial			DSS											
	Drained mono	Undrained mono	Cyclic	Drained mono	Undrained mono	Cyclic	Drained cyclic CNS	Oedometer	Unconfined compr.	Bender element	Resonant column	Hollow cylinder	Ring shear interface	Comment	Ref. to data base (see Table 10.1)
Frictional characteristics															
Peak drained friction angle, ϕ'	x														a/b/c
Undrained friction angle, ϕ_u'		x													a/b/c
Dilatancy angle, ψ	x														a/b/c
Slope of DSS drained failure line, α'				x								x[1]			
Slope of DSS undrained failure line, α_u					x							x[1]			
Interface friction angle, δ_{peak} and $\delta_{residual}$													x		d/e
Monotonic data															
Monotonic undrained shear strength, s_u^C, s_u^{DSS}, s_u^E		x			x							x			f/g/h
Initial shear modulus, G_{max}										x[2]	x[3]				h
Cyclic data															
Cyclic undrained shear strength, $\tau_{f,cy} = f(\tau_a, \tau_{cy}, N)$,			x			x									g/i/j/ k/l/m
Cyclically induced pore pressure, $u_p = f(\tau_a, \tau_{cy}, N)$,			x			x									
$u_p = f(\tau_{cy}, \log N)$ for $\tau_a=\tau_0$,			x			x									
Cyclic stress strain data, γ_a, γ_p & $\gamma_{cy} = f(\tau_a, \tau_{cy}, N)$,			x			x									
$\gamma_{cy} = f(\tau_{cy}, \log N)$ for $\tau_a=\tau_0$,			x			x									
Drop in radial effective stress along shaft $\sigma'_r = f(\tau_{cy}, N)$, clay						x[12]									
Drop in radial effective stress along shaft $\sigma'_r = f(\tau_a, \tau_{cy}, N)$, sand							x[13]								
Damping			x			x					x				h/j/k
Consolidation characteristics, intact soil															
Preconsolidation stress (and OCR)								x							
Virgin, unloading and reloading constrained moduli	x[11]							x[4]							a
Permeability	x[11]							x[5]							a
Remoulded soil data															
Sensitivity, S_t									x[6]						q
Undrained shear strength of reconsolidated remoulded soil					x										h
Cyclic undrained shear strength, $\tau_{f,cy} = f(\tau_a, \tau_{cy}, N)$, reconsolidated soil						x									j/k
Virgin constrained modulus								x							
Permeability								x							
Thixotropy														x[7]	h
Parameters for reference monotonic pile capacity															
Relative density, D_r														x[8]	n/o/p
CPT resistance														x[9]	n
Plasticity index, I_p														x[10]	
Monotonic UU shear strength, s_u^{UU}									x						
ε_{50}									x						

1) *Alternative to DSS, but with more difficult sample preparation*
2) *Can be included as part of monotonic and/or cyclic tests*
3) *Bender element tests an alternative unless damping at small shear strain is needed,*
4) *Oedometer tests should be run with 2 unload/reload sequences*
5) *Consider triaxial set-up for clean sands where perm. may be high*
6) *Determined in UU tests, fall cone or lab vane on intact and remoulded clay.*
7) *Test aged remoulded clay samples stored at constant water content*
8) *Normally interpreted from in situ CPTU. Can also be based on in situ water content/unit weight, but these can be uncertain*
9) *From in situ CPTU*
10) *From routine index testing*
11) *Alternative to oedometer tests to eliminate testing imperfections*
12) *For simplified A, B, C method*
13) *In case of some explicit finite element analyses where drained CNS tests are used to model interface*

9 INTERPRETATION/PRESENTATION OF RESULTS

Some of the more important factors that should be considered in the interpretation and presentation of data from cyclic laboratory tests performed for principally offshore engineering applications are discussed briefly below.

Monotonic behaviour
Noting that all such programs have to start with retrieved soil samples and involve monotonic shear tests it is also important to consider the following issues in test interpretation:

- Sample disturbance must be assessed. Lunne et al. (2006), Berre et al. (2007), Lunne and Andersen (2007) and Andersen et al. (2008) discuss this issue and suggest ways of correcting for sample disturbance.
- Care is needed with oedometer tests. Andersen and Schjetne (2012) proposed a mathematical formulation to express virgin loading, unloading and reloading moduli that accounts for differences in stiffness and non-linearity on each of these branches. The formulation allows moduli to be defined for stress levels and stress increments different to those applied in the test.
- Remoulded and reconsolidated remoulded shear strengths should be related to the original intact shear strength.
- Tests that investigate thixotropy in shear strength data should be plotted against logarithmic time, together with the corresponding water content and remoulded shear strength measurements. Original intact shear strength should also be reported.
- It is important when assessing angles of shearing resistance φ′ from effective stress path plots to account for the differences between peak, critical and residual shear states. Peak monotonic shear strength corresponds to any peak in the stress strain curve or, if none is apparent, as the shear stress at a shear strain of 15%.
- DSS test interpretation should involve establishing the slopes of the horizontal shear stress against vertical effective normal stress plots, without making any a priori assumption regarding their possible relationship to φ′.
- Where interface shear tests are performed for driven pile analysis they should involve several metres of fast 'conditioning' pre-shear, which may be performed (when using the apparatus described by Bishop et al. 1971) with the gap between the interface and the upper confining ring closed. The principal output from the tests is the plot of τ/σ'_n against shear displacement obtained in slow 'open-gap' tests performed after fast shear and reconsolidation. These tests often show peak angles after small displacements and achieve their ultimate values within perhaps 30mm of travel; both angles should be recorded. Jardine et al. (2005) give full details of the test procedures.
- HCA experiments offer the capability of applying/measuring four dimensions of stress and strain and so following the foundation loading paths and soil responses more rigorously than conventional laboratory tests. Zdravkovic and Jardine (2000 and 2001) and Nishimura et al. (2007) provide examples of how the tests may be conducted and the results interpreted for a range of soil types.
- The initial Young's and shear moduli of soils are known to depend fundamentally on the applied effective stresses, and are often expressed as fractional power functions of these stresses that may include void ratio functions (see Jardine, 1994 or 2013). Initial stiffnesses can be presented in a range of normalised styles, including presentation as ratios of undrained shear strengths. But it must be made clear how normalisation has been undertaken and sufficient information provided for future users to express the data in the format required for their particular analytical approach.
- It is important to remain aware in test interpretation of the intense non-linearity and potential anisotropy of most soils, from small strains to large.

Cyclic data

- Earlier sections have emphasised the strong dependence of soils' cyclic response on: stress path (as seen in TC, TE and DSS tests); the ratio between average and cyclic shear stresses τ_a and τ_{cy}; the number of cycles N; and whether the average shear stress is applied under drained or undrained conditions. It is therefore convenient to provide separate diagrams for triaxial and DSS tests and group the cyclic results as set out in Section 5 where cyclic shear strength is related to τ_a and τ_{cy} and N; see Figure 5.10.
- Cyclic and average shear strains are related to τ_a and τ_{cy} and N; see Figures 5.14 and 5.15.
- Permanent 'excess pore pressure' are related to τ_a and τ_{cy} and N (Figures 5.16 and 5.17).
- In triaxial tests, the pore pressure increment related to the increase in mean normal stress ($p = \sigma_1 + \sigma_2 + \sigma_3)/3$, imposed when $\Delta\tau_a$ is applied, is subtracted to make the data more general (Figure 5.17).
- Cyclic shear strain and permanent pore pressures are expressed as functions of τ_{cy} and N for given values of τ_a (Figure 5.11).
- Damping parameters may also be plotted in contour diagrams, although this has not been general practice. .

As indicated in Section 8, full contour sets are not required for all design cases. Also, the testing strategy and interpretation can be optimised by making use of existing data sets obtained with potentially similar soils. References to such data libraries are given in the next section.

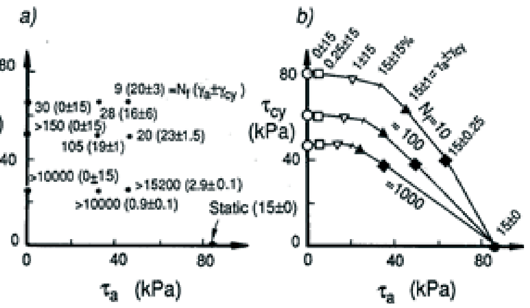

Figure 9.1: Example of data points and corresponding contours in τ_{cy} vs. τ_a type diagram showing number of cycles to failure and failure mode in DSS tests on normally consolidated Drammen Clay (Andersen, 2004)

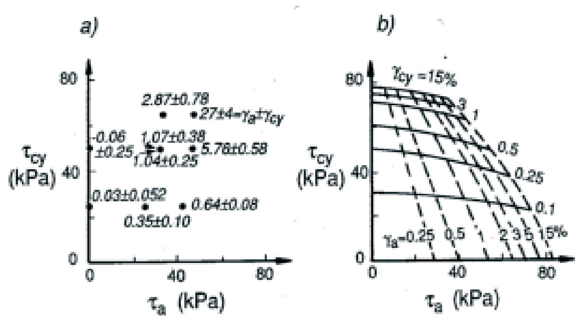

Figure 9.2: Example of data points and corresponding contours in τ_{cy} vs. log N type diagram showing average and cyclic shear strains after 10 cycles in DSS tests on normally consolidated Drammen Clay (Andersen, 2004)

The NGI contouring procedure starts with plotting the individual data outputs as illustrated by DSS test examples in Figures 9.1 and 9.2. The intersection with the horizontal axis in diagrams of the type in Figures 9.1 and 9.2 represents monotonic conditions and the companion static test data are plotted on this line. The contour diagrams can be used directly in the NGI's cyclic analysis toolset. They also form a basis that can be used as input to and to formulate or test other mathematical models.

10 CYCLIC AND STATIC ADVANCED GEOTECHNICAL TESTING DATA BASES

Advanced laboratory test data are often unavailable at the start of projects and it may indeed be unfeasible to conduct such tests at any stage in some settings. Lists of published high quality results can provide useful support in such circumstances. Table 10.1 offer a selection of references to such databases. The last column in Table 8.1 is linked to the further commentary and details given in Table 10.1. The main focus is on advanced static and cyclic laboratory testing.

This paper has concentrated on summarising contributions that are well known to the Authors and their colleagues and has not attempted to offer a full review of the large volume of relevant and significant work by others. This selectivity is maintained in the referencing made here and in the supporting data given in Table 10.1. Naturally, considerably more information, and many more references, are available in the broader literature.

Table 10.1 Literature with data on cyclic soil parameters in Tables 7.1 and 8.1

Reference	Description / Comment	Ref. param. in Table 8.1
Frictional characteristics		
Andersen & Schjetne 2013	Diagrams with frictional soil characteristics of sand as functions of relative density and effective normal stress from triaxial tests	a
Bolton 1986		b
Schmertman 1978		c
Jardine et al. 2005	Interface friction angles for clay	d
Ho et al 2011	Interface friction angles for sand	e
Monotonic data		
Lunne & Andersen 2007	Undrained shear strength of normally and lightly overconsolidated clays correlated to the preconsolidation stress. Shear strength anisotropy factors. Shows anisotropy is higher (smaller factors) the less disturbed the clay is. Reason; TC strength more affected by sample disturbance than TE and DSS	f
Andersen 2004	Normalised shear strength as function of OCR.	g
Jardine et al 1997, Zdravkovic & Jardine 2001, Nishimura et al 2007	HCA tests on range low OCR and high OCR soils showing anisotropic dependence of shear strength on parameters b and α	f/g
Andersen et al. 2008	Initial shear modulus of clay normalised both to vertical effective stress and to undrained shear strength as function of I_p and OCR.	h
Jardine et al 1984, Jardine 1994, Zdravkovic & Jardine 1997, Tatsuoka et al 1999, Kuwano & Jardine 2002, 2007, Gasparre et al 2007	Anisotropy and non-linearity of stiffness from very small strains to large, from dynamic and static tests in locally instrumented traixial and HCA apparatus	h
Cyclic data		
Andersen 2004	Complete set of cyclic contour diagrams for Drammen clay (I_p=27%). Triaxial and DSS tests with OCR= 1, 4 and 40. Most comprehensive contour set for clay. Also presents comparison of cyclic shear strength diagrams for 8 different clays with I_p ranging from 7% to 100%.	g
Jeanjean et al. 1998	Cyclic contour diagrams for triaxial and DSS tests on normally consolidated clays with I_p=30-70% from Marlin deepwater site in Gulf of Mexico.	i
Kleven & Andersen 1991 Andersen et al. 1991	Complete set of cyclic contour diagrams and damping ratio for the Great Belt Bridge clay till (I_p=7%-12%) for OCR=1 and 3. Triaxial and DSS tests. In addition, DSS contour diagrams for OCR=40 and for remoulded clay.	j k
Andersen & Berre 1999	Cyclic contour diagrams for very dense Baskarp sand with grain size similar to typical fine uniform North Sea sands (D_{50}=0.15mm and 3% fines. Because Baskarp sand is somewhat more angular than typical North Sea sands, one has been cautious to rely on the high strengths of Baskarp sand. However, more recent tests on actual North Sea sands seem to support Baskarp data.	l
Andersen 2009	Diagrams to establish cyclic shear strength of sand and silt as function of number of cycles, preshearing, OCR, D_r and water content. From published literature and NGI files. Refs. to other published papers on cyclic behaviour of sand. Some information on effect of load period for clay and sand.	m
Andersen et al. 2008	Damping from two-way stress controlled cyclic DSS tests on clay as function of cyclic shear strain and number of cycles.	h
Lunne & Andersen 2007	Effect of sample disturbance on cyclic parameters	f
Consolidation characteristics, intact soil		
Andersen & Schjetne 2013	c_v of clay as function of void ratio (or water content) and clay content. c_v of sand as function of void ratio (or water content) and D_{10}. Mathematical expressions and empirical constants for loading, unloading and reloading constrained moduli of sand and silt.	a
Remoulded soil data		
DeGroot et al. 2012	Discussion on ways to determine remoulded strength and S_t.	q
Andersen et al. 2008	Reconsolidated remoulded shear strength normalised by original intact shear strength as function of OCR for various clays. Diagram with thixotropy ratio as function of activity, time and sensitivity.	h
Parameters for reference monotonic pile capacity		
Lunne et al. 1997	Guidance on use and interpretation of CPT and CPTU. Determination of D_r.	n
Jamiolkowski et al. 2001	Updated determination of D_r from CPT (clean sand).	o
Jardine et al 2005	Lab and field procedures required to apply ICP-05 method in clays and sands	
Emerson et al 2008	Determination of D_r from CPT at shallow depth (clean sand).	p

11 APPLICATIONS TO OTHER TYPES OF STRUCTURES AND CYCLIC REGIMES

As outlined in the introduction, cyclic loading issues are considered carefully in some fields outside offshore engineering including: earthquake geotechnical design, pavement engineering, blast-resistant design, some harbour/marine works and machine foundation design. However, other types of mainstream civil engineering structures exist that are subjected to repeated loading patterns involving a degree of regularity in amplitude and period. These "cyclic" loads may be essentially environmental (seasonal, or induced by waves, wind, currents or tides) or operational in origin. Some examples of structures that may potentially be affected by cyclic loading that may not always be addressed in design include:

- Wind-turbines on land, which are submitted to wind and rotor/blade forces. The key geotechnical issue is to ensure that the foundation stiffness requirements match those required by the turbine manufacturer.
- Coastal structures including harbours, breakwaters and sea protection barriers.
- Energy transport pylons: winter storm events have demonstrated the inadequacy of some foundation concepts to resist extreme cyclic wind forces.
- High rise towers and chimneys are sensitive to wind cyclic loading.
- High speed train foundations and bridges, which transmit intense frequent and discontinuous traffic loads to the soil.
- Structures subject to variable industrial loading, such as static and travelling cranes and hydraulic turbines as well as vibrating machinery.
- Anchored rafts for coastal energy plants that are submitted to tidally varying ground water uplift pressures.
- Large storage tanks subject to regular loading and unloading cycles.

Load characterization

It is common in building works and civil engineering to consider applied loads as essentially static or quasi-static. In accordance with existing codes and standards, critical loads are defined by the maximum values expected under various load cases (operational - SLS, extreme - ULS, accidental- ALS). These approaches do not address fully the dependence emphasized throughout this paper of soils' cyclic response on mean stress and cyclic stress amplitude, loading frequency, number of cycles and cyclic stress path, which is well-established in offshore geotechnics. A greater awareness of these issues is urgently required in general civil engineering.

The cyclic loading conditions applied in the wider range of civil engineering needs to be characterised properly. Field measurement studies will provide critically needed new information. Figure 3.1 offers a provisional summary of some significant cyclic loading conditions by plotting representative periods against number of cycles.

Our present knowledge is concentrated in the zone defined by periods of typically less than 100s and N < 10,000 which corresponds to the current earthquake and offshore engineering demands. There is clearly a need to investigations to cover higher numbers of cycles to meet wind turbine and high-speed train challenges and also to consider longer loading period events. The latter deserves particular attention because of the strain rate dependence of shear strength in clay and the scope for partial or full drainage applying over large loading periods, even in low permeability soils.

In the same way, the accumulation of cyclic loading displacements and potential damage (or ageing benefits) need to be assessed over the whole lifetimes of facilities, rather than just one design storm. Low level cycling can be beneficial to capacity if accompanied by drainage and pre-shearing. However, negative effects are also possible in dilative low permeability soils, as discussed earlier.

Foundation types

The methodologies for cyclic design of offshore foundations set out in the preceding were divided into essentially two types: (i) monolithic rigid bodies with low depth to width L/D ratios and (ii) piles where L/D usually exceeds 10.

The first group, typically involving shallow foundations, were considered in the NGI framework by limit state or FEM analyses. Simplified approaches could be made in which cyclic shear strengths were applied around static critical failure surfaces. More advanced analyses considered the equilibrium of the average loads and average shear stresses along with strain compatibility along the potential failure surface (Andersen and Lauritzsen, 1988). Deep caissons such as offshore wind monopiles may be considered by similar approaches, or considered as piles (Jardine et al., 2012).

One critical aspect with deep caissons/monopiles is their sensitivity to lateral displacements and stiffness under a high number of cycles. This aspect has been addressed by deriving degradation laws from model pile tests (Peralta, 2010; Le Blanc et al., 2010), through simplified explicit FEM analyses (Andersen and Høeg, 1991; Saue et al., 2010 or Grimstad et al., 2013); the explicit procedure proposed by Wichtman (2005) can also be applied (see Abdel-Rahman and Achmus, 2005).

Well-designed deep piles tend to behave as flexible elastic bodies under cyclic loading. Their behaviour has been modelled traditionally by elastic continuum approaches or simplified t-z, p-y beam column approaches, although these conventional approaches suffer from a number of significant limitations, as emphasised by Jardine et al. (2012).

The range of foundation concepts used in building or civil engineering structures is much broader than that applied in offshore applications. Application of offshore shallow foundation procedures to strip footings and offshore pile techniques to deep onshore piles is relatively straightforward. However, new or modified approaches are needed for more complex piled raft, rigid inclusions, high pressure anchored, or reinforcement earth and other foundation techniques. The need to employ sophisticated physical modelling or FEM simulations can be envisaged for many such applications.

The SOLCYP project (Puech et al., 2012) is offering a significant contribution to making cyclic analysis feasible for conventional piled foundations. As shown in Figure 6.1, the SOLCYP cyclic assessment process starts with the use of cyclic axial stability diagrams. A key aim is to develop charts covering a wider variety of soil types and pile installation techniques, with an emphasis on better matching the range employed in mainstream building and civil engineering activities. Diagrams are being generated within SOLCYP from field tests involving:

- Closed-end (full-displacement) driven steel piles.
- Non-displacement augered, cast-in-place, bored reinforced concrete piles.
- Partial displacement screw piles formed by helical tool that penetrated by a combination of jacking and rotation with the concrete piles being cast in place and reinforced after concreting.

The diagrams were derived from tests on suites of similar piles installed at two French experimental sites. The first, at Merville, involved the stiff overconsolidated Flanders clay, which is from the same geological unit as the UK London clay. The second involved a dense to very dense sand at the Loon-Plage site which is located with about 1km of the Dunkirk test site utilised by Imperial College (Jardine et al., 2006; Rimoy et al., 2013) and involved similar strata. The piles were submitted to reference monotonic tests and suites of extensive one-way and more limited two-way cyclic tests. The SOLCYP programme integrated these field tests with other streams of centrifuge (e.g. Guefresh et al., 2012) and large calibration chamber tests that complemented and cross-checked the field results.

Examples of axial cyclic stability diagrams obtained for bored piles in dense sand and in one-way mode are presented in Figures 11.1 and 11.2, drawing on data from both field bored piles and centrifuge model simulations. The consistency between the two data sets is encouraging and highlights the marked sensitivity to cyclic loading of piles bored in sand under even one-way loading. The arguments advanced in this paper show that still more intensive effects can be expected under two-way loading conditions.

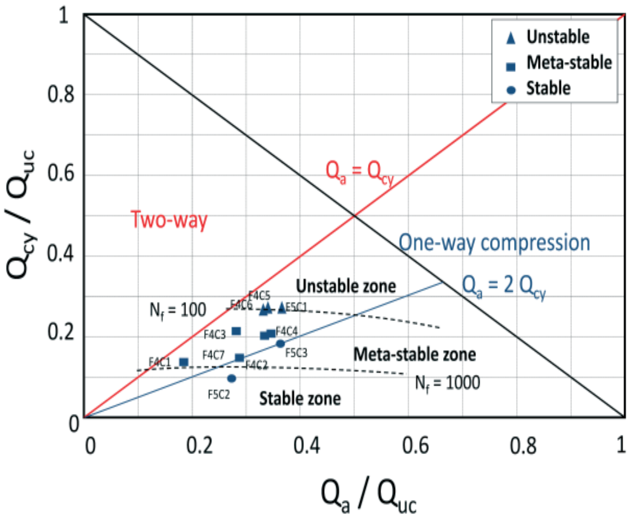

Figure 11.1 Cyclic stability diagrams for cast-in-place piles in dense sands: in situ tests, bored piles, Loon-Plage (Puech et al., 2013). Piles loaded in compression

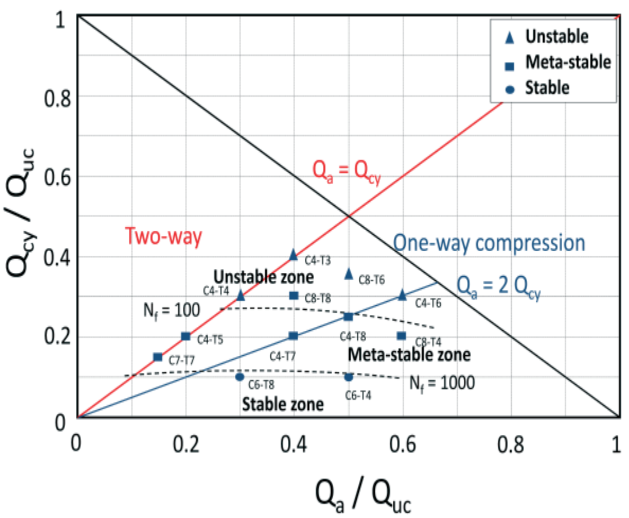

Figure 11.2 Cyclic stability diagrams for cast-in-place piles in dense sands: Centrifuge tests, Fontainebleau sand (Puech et al., 2013). Piles loaded in compression

12 CONCLUSIONS

- Cyclic loading generated by wind and wave loading is of crucial importance in offshore foundation engineering.
- Considering the cyclic loading induced by wind-turbine rotation is also a key concern in the offshore renewable energy sector.
- Offshore foundation designers often have to consider cyclic bearing capacity and stiffness, as well as permanent displacements due to cycling and potentially changing patterns of soil reaction stresses.
- These features have been illustrated first by examples drawn from offshore Gravity Base Structure (GBS) prototype observations as well as field and model test observations with piled foundations.
- The stress paths induced by foundations under static and cyclic loads and the corresponding responses seen in cyclic laboratory element tests have also been reviewed.
- Procedures have then been set out that can address the necessary design concerns for GBS, suction anchor, driven piles and other foundation types.
- A main objective of this paper has been to give guidance for obtaining the soil parameters for design of foundations under cyclic loading, and a review is offered of the ways in which the key soil parameters can be determined.
- While cyclic design is undertaken routinely for GBS foundations, it is often neglected in offshore pile design. The latter omission could have significant consequences in certain cases and closer attention is required especially in cases involving high ratios of cyclic to average axial pile-head loads.
- Offshore engineering cyclic design approaches may be applied across a wide range of applications where load cycling can be generated by seasonal changes, earthquakes, ice, traffic, machinery and other natural or anthropogenic processes.
- Important examples of other type of structures that must be designed to resist cyclic loading include sea protection barriers, wind turbines and road or rail pavements.
- Recent research into the response of traditional civil engineering foundation types, such as piles bored in sands has revealed a marked sensitivity to cyclic loading that clearly merits careful consideration in a wider range of design settings.

13 ACKNOWLEDGEMENTS

The Authors wish to acknowledge the many contributions made by their current and former colleagues at Norwegian Geotechnical Institute and Imperial College, in the SOLCYP project team and elsewhere for their extensive contributions made to the work described on the cyclic behaviour of soils and foundations. They also acknowledge gratefully the support provided over many years by multiple national and international governmental and industry sponsors.

14 REFERENCES

Abdel-Rahman K. and Achmus, M. 2005 Finite Element Modelling of horizontally loaded Monopile Foundations for Offshore Wind Energy Converters in Germany, *International Symposium, Frontiers in Offshore Geotechnics* (ISFOG), Perth, Australia, Sept. 2005.

Achmus M, Abdel-Rahman K and Peralta P. 2005. On the Design of Monopile Foundations with respect to Static and Quasi-Static Cyclic Loading. *Copenhagen Offshore Wind* 2005.

Achmus M, Abdel-Rahman K and Kuo YS. 2008. Design of monopile foundations for offshore wind energy plants. *11th Baltic Geotechnical Conference-Geotechnics in Maritime Engineering*, Gdansk, vol.1, 463–470.

Achmus M, Albiker J and Abdel-Rahman K. 2010. Investigations on the behaviour of large diameter piles under cyclic lateral loading, *Proc. International Symposium, Frontiers in Offshore Geotechnics*, ISFOG, Perth.

Aderlieste EA, Dijkstra J and van Tol AF. 2011. Experimental investigation into pile diameter effects of laterally loaded monopiles. *Proceedings of the 30th International Conference on Ocean, Offshore and Arctic Engineering,* OMAE 2011. Rotterdam, The Netherlands.

Andersen K.H. 1976. Behaviour of clay subjected to undrained cyclic loading*. Int. Conf. on Beh. of Offsh. Struct., BOSS'76*. Trondheim. Proc., Vol. 1, pp. 392 403. Also NGI Publ. 114, pp. 33 44.

Andersen K.H. and Aas P.M. 1980. Foundation performance. Shell Brent "B" Instrum. Project; Seminar. London. Proc., pp. 57 77. Org. by Soc. for Underwater Techn., London. Also NGI Publ. 137.

Andersen K.H. and Lauritzsen R. 1988. Bearing capacity for *foundations* with cyclic loads. *J. Geotech. Engrg.,* ASCE, 114 (5), 540 555.

Andersen K.H., Kleven A. and Heien D. 1988. Cyclic soil data for design of gravity structures. *J. Geotech. Engrg*., ASCE, 114 (5), 517 539.

Andersen, K.H. 1988. Properties of soft clay under static and cyclic loading. Invited lecture*. International Conf. on Eng. Problems of Regional Soils*, Proc., pp. 7 26, Beijing, China, 1988. Edited by Chinese Institution of Soil Mechanics and Foun¬da¬tion Engineering. Also in NGI Pub. 176.

Andersen K.H., Dyvik R., Lauritzsen R., Heien D., Hårvik L., Amundsen T. 1989. Model tests on gravity platforms. II: Interpretation. *J. Geotech. Engrg*., ASCE, 115, 1550-1568.

Andersen K.H. 1991. Foundation design of offshore gravity structures. Ch. 4 in *"Cyclic Loading of Soils. From Theory to Design"*. Ed. by M.P. O'Reilly and S.F. Brown. Publ. by Blackie and Son Ltd., Glasgow and London.

Andersen K.H. and Høeg K. 1991. Deformations of soils and displacements of structures subjected to combined static and cyclic loads. *X ECSMFE*, Firenze, Proc., Vol 4, pp. 1147-1158.

Andersen K.H., O.E. Hansteen and M. Gutierrez 1991. Bearing capacity, displacements, stiffness and hysteretic damping of Storebælt bridge piers under ice loading. *Seminar on Design of Exposed Bridge Piers*. Danish Society of Hydraulic Engineering. Copenhagen, Denmark, 22 January 1991. Also published in NGI Publ. 199.

Andersen K.H., Dyvik R., Kikuchi, Y. and Skomedal E. 1992. Clay behaviour under irregular cyclic loading. *Proc. Int. Conf. on Behaviour of Offsh. Structures*, London, Vol. 2, pp. 937-950.

Andersen K.H. and T. Berre 1999.Behaviour of a dense sand under monotonic and cyclic loading. Geotechnical Engineering for Transportation Infrastructure. *12th European Conference on Soil Mechanics and Geotechnical Engineering*. Amsterdam, The Netherlands. Proc. Vol.2, p. 667-676. Publ. by A.A. Balkema.

Andersen, K.H. and Jostad H.P. 1999. Foundation design of skirted foundations and anchors in clay. *Offsh. Techn. Conf*., Houston, Proc., Paper 10824.

Andersen K. H. and Jostad H. P. 2002. Shear strength along outside wall of suction anchors in clay after installation. *Proc. XII ISOPE Conf.*, Kyushu, Japan.

Andersen K.H. 2004. Cyclic clay data for foundation design of structures subjected to wave loading. Keynote Lecture; *Proc. Int. Conf. on Cyclic Behaviour of Soils and Liquefaction Phenomena*, CBS04, Bochum, Germany. Proc. p. 371-387, A.A. Balkema, Ed Th. Triantafyllidis.

Andersen, K.H., T. Lunne, T.J. Kvalstad and C.F. Forsberg 2008. Deep water geotechnical engineering. *XXIV Nat. Conf. of the Mexican Soc. of the Soil Mechanics*, Aguascalientes, 26-29. Nov. 2008. Proc. Vol IV. 57p. Also: Norwegian Geotechnical Institute, Oslo, Norway. Publ. No. 208.

Andersen K.H. 2009. Bearing capacity of structures under cyclic loading; offshore, along the coast and on land. *21st Bjerrum Lecture* presented in Oslo 23 Nov. 2007. Can. Geotech. J. 46: 513-535. Also: Norsk Geoteknisk Forening, Bjerrums Foredrag Nr. 21.

Andersen, K.H. and K. Schjetne 2012. Data base of friction angles of sand and consolidation characteristics of sand, silt and clay. ASCE *J. of Geotechnical and Environmental Engrg*. July 2013.

Andersen L.V., Hahdatirad M.J., Sichani M.T. and Sorensen J.D. 2012. Natural frequencies of wind turbines on monopole foundations in clayey soils – A probabilistic approach. *Computer and Geotechnics* 43 (2012) I-II.

Andresen L., Jostad H. P. and Andersen K. H. 2010. Finite Element Analyses Applied in Design of Foundations and Anchors for Offshore Structures. *Int. J. of Geomech*., ASCE.

Anh-Minh, N., Nishimura, S., Takahashi, A. and Jardine, R.J. 2011. On the control systems and instrumentation required to investigate the anisotropy of stiff clays and mudrocks through Hollow Cylinder Tests. *Deformation Characteristics of Geomaterials. Proc*. IS-Seoul, Pub. Hanrimwon, Seoul, Vol. 1, Eds. Chung et al, p 287-294.

Atkins Consultants Ltd 2000. Cyclic degradation of offshore piles*. HSE Offshore Technology Report OTO 2000 013*. Health and Safety Executive, London.

Augustesen AH, Brodbaeck KT, Moller M, Sorensen SPH, Ibsen LB, Pecersen TS and Andersen L. 2009. Numerical modelling of large-diameter steel piles at Horns Rev. *Proc. 12th Civil, Structural and Environmental Engineering Computing*, Topping-Costa Neves-Barros Edts, Civil-Comp Press, Stirlingshire, Scotland, Paper 239.

API 2000. Recommended practice for planning, designing and constructiong fixed offshore platforms – Working stress design. RP2A-WSD, American Petroleum Institute.

API RP2GEO. 2011. API Recommended Practice, Geotechnical and Foundation Design Considerations, First Edition, American Petroleum Institute, April 2011.

ASTM.1985. Standard practices for cycle counting in fatigue analysis. Designation E 1049-85, vol. 03. 01 of Metal Test Methods and Analytical Procedure. pp. 836-848.

Benzaria O. 2013. Contribution à l'étude du comportement des pieux isolés sous chargements cycliques axiaux. *Thèse*. Université de Paris-Est. A paraître.

Benzaria O., Puech A. and Le Kouby A. 2012. Cyclic axial load-tests on driven piles in overconsolidated clay, *7th Int. Conf. on Offshore Site Investigations and Geotechnics*, OSIG, London.

Benzaria A., Puech A. et Le Kouby A. 2013a. Essais cycliques axiaux sur des pieux forés dans l'argile surconsolidée des Flandres. *Proceedings 18th ICSMGE,* Paris.

Benzaria A., Puech A. et Le Kouby A. 2013b. Essais cycliques axiaux sur des pieux forés dans des sables denses. *Proceedings 18th ICSMGE*, Paris.

Berre, T., T. Lunne, K.H. Andersen, S. Strandvik, and M. Sjursen 2007. Potential improvements of design parameters by taking block samples of soft marine Norwegian clays. *Can. Geotech J.* 44: 698-716.

Bishop, A.W., Green, G.E., Garga,V.K., Andresen, A. and Brown, J.D. 1971. A new ring shear apparatus and its application to the measurement of residual strength. *Geotechnique*, 21, No 4, pp 273-328.

Bjerrum, L. 1973. Problems of soil mechanics and construction on soft clays. State-of-the-Art Report to Session IV, *8th International Conference on Soil Mechanics and Foundation Engineering*, Moscow. Proc., Vol. 3, p. 111-159.

Bolton, M.D. 1986. "The shear strength and dilatancy of sands". *Geotechnique,* Vol. 36, No. 1, pp. 65-78.

Bond, A. J. and Jardine, R. J. 1991. The effects of installing displacement piles in a high OCR clay. *Geotechnique*, Vol 41, No. 3, pp 341-363.

Bond, A J and Jardine R J 1995. Shaft capacity of displacement piles a high OCR clay. *Geotechnique*, 45, No 1, pp3-23.

Boukovalas G., Whitman R.V. and Marr W.A. 1984. Permanent displacement of sand with cyclic loading. *J. Geotech. Engrg*., ASCE 110: 1606–1623.

Briaud J.L. and Felio G.Y. 1986. Cyclic axial loads on piles: analysis of existing data. *Canadian Geotechnical Journal*, 23,362-371.

BSH - a) Standard: Design of Offshore Wind Turbines 2007, b) Guidance for use of the BSH standard „Design of Offshore Wind Turbines“ 2011, c) Ground investigations for offshore wind farms 2008, Federal Maritime and Hydrographic Agency (BSH), Hamburg and Rostock.

Chaboche J.L. 1994. Modeling of ratchetting: evaluation of various approaches. *Eur. J. Mech. A/Solids* 13: 501–518.

Chin JT and Poulos HG. 1992. Cyclic axial loading analyses: a comparative study. *Computers and Geotechnics* 13: 137–158.

Chow FC. 1997. Investigations into displacement pile behaviour for offshore foundations*. PhD thesis*, Univ. London (Imperial College)

Clausen C.J.F., DiBiagio E., Duncan J.M and Andersen K.H. 1975. Observed behaviour of the Ekofisk oil storage tank foundation*. 7th Offsh. Techn. Conf.*, Houston 1975. Proc., Vol. 3, pp. 399 413. Also NGI Publ. 108.

Clausen CJF, Aas PM and Karlsrud K. 2005. Bearing capacity of driven piles in sand: the NGI approach. *Proc. ISFOG'05*, Perth, WA, 677–681.

Clukey, E., Gilbert, R.B., Andersen K.H. and Dahlberg, R. 2013. Reliability of Suction Caissons for Deep Water Floating Facilities. *ASCE Geotechnical Special Publication* No. 229; Foundation Engineering in the Face of uncertainty.

Colliat, J.L., Dendani, H., Puech, A. and Nauroy, J.F. 2010. Gulf of Guinea deepwater sediments: geotechnical properties, design issues and installation experiences. *Proc. 2nd Int. Symposium on Frontiers in Offshore Geotechnics, ISFOG 2010*, Perth, Australia.

DeGroot, D.J., T. Lunne, K.H. Andersen and A.G. Boscardin 2012. Laboratory measurement of the remoulded shear strength of clays with application to design of offshore infrastructure. *7th Intern. Offshore Site Investigation and Geotechnics Conference*; Sept. 2012, London, UK, Proc. p. 355 366.

Diyaljee V.A. and Raymond G.P. 1982. Repetitive load deformation of cohesionless soil. *J. of Soil Mech. and Found. Engrg.* 10: 1215–1229.

DNV 1979. Rules for the design, construction and inspection of offshore structures. Det Norske Veritas, Høvik, Norway. 67p.

DNV. 1992. Classification Note 30-4, Foundations. Det Norske Veritas, Oslo.

DNV-OS-J101. 2010. Design of Offshore Wind Turbines Structures, DnV Offshore Standards, Det Norske Veritas, Oslo.

Dyvik R., Andersen K.H., Madshus C. and Amundsen T. 1989. Model tests of gravity platforms. I. Description. *J. Geotech. Engrg*., ASCE 115 (11) 1532-1549.

Emerson, M., Foray, P., Puech, A. and Palix, E. 2008. A global model for accurately interpreting CPT data in sands from shallow to greater depth.Proceedings of the *3rd International Conference on Site Characterization ISC'3*, Taipei, Taiwan. Pages 687-694.

Erbrich C.T., O'Neill M.P., Clancy P. and Randolph M.F. 2010. Axial and lateral pile design in carbonate soils. *Frontiers in Offshore Geotechnics II. Proc.,* Gourvenec & White (eds). 2011 Taylor & Francis Group, London, ISBN 978-0-415-58480-7, p. 125-154.

GL Rules and Guidelines. 2005. IV Industrial Services. Part 2- Guidelines for the Certification of Offshore Wind Turbines, Germanischer Lloyd, Reprint 2007.

Gasparre, A., Nishimura, S., Anh-Minh, N., Coop, M.R. & Jardine, R.J. 2007. The stiffness of natural London clay." Symposium in Print on Stiff Clays. *Géotechnique,* 57(1), pp 33-48.

Georgiannou V N , Burland, J B and Hight, D W 1990. The undrained behaviour of clayey sands in triaxial extension and compression. *Geotechnique,* Vol 40, No 3, pp 431-450.

Gibson R E 1963. An analysis of system flexibility and its effect on tire lag in pore water measurements. *Géotechnique,* Vol 13, No 1, pp 1-11.

Gotschol A. 2002. Veränderlich elastisches und plastisches Verhalten nichtbindiger Böden und Schotter unter zyklisch-dynamischer Beanspruchung, *Schriftenreihe Geotech.,* Univ. Gh Kassel, Heft 12.

Grimstad G., Andersen K.H., Saue M., Jostad H.P., Shin Y.S. and You D.Y. 2013. An undrained cyclic accumulation model used in monopile design. Submitted for publication.

Gudehus G. 1996. A comprehensive constitutive equation for granular materials. *Soils and Foundations* 36: 1–12.

Guefrech A., Rault G, Chenaf N., Thorel L., Garnier J., Puech A. 2012. Stability of cast in place piles in sand under axial cyclic loading . *Proc. 7th Int. Conf. Offshore Site investigation and Geotechnics*. OSIG, London. pp.329-334.

Hansteen O.E. 1980. Dynamic performance. Shell Brent "B" Instrum. Project; Seminar. London 1979. Proc., pp. 57 77. Org. by the Soc. for Underwater Techn., London. Also NGI Publ. 137.

Hansteen, O.E. 1991. Description of INFIDEL – a non-linear 3D finite element program. NGI Report 514090-3, rev. 1.

Hight, D W 1982. A simple piezometer probe for the routine measurement of pore pressures in triaxial tests on saturated soils. *Geotechnique,* Vol.32, No.4, pp 396-402.

Hight, D W and Jardine, R J 1993. Small strain stiffness and strength characteristics of hard London Tertiary clays. *Proc. Int. Symp. on Hard Soils - Soft Rocks,* Athens, Greece, Vol 1, Balkema, Rotterdam, pp 533-522.

Ho, Y.K., Jardine, R.J. and Anh-Minh, N. 2010. Large displacement interface shear between steel and granular media. *Geotechnique*, Vol. 61, No. 3, pp 221.234.

Høeg, K., Dyvik, R. and Sandbækken, G. 2000. Strength of undisturbed versus reconstituted silt and silty sand specimens. ASCE, *J. Geotech. and Geoenv. Engrg*. 126(7): 606-617.

ISO 19 902. 2007. International standard for the design of fixed steel offshore platforms, International Standards Office, British Standards Institute, London.

Jamiolkowski, M., Lo Presti, D.C.F and Manassero, M. 2001. Evaluation of Relative Density and Shear Strength of Sands from CPT and DMT. In *Proceedings of Conference on Soft Ground Construction*: pp. 201-238. ASCE.

Jardine, R J, Symes, M J and Burland, J B 1984. The measurement of soil stiffness in the triaxial apparatus. *Geotechnique* 34, No.3, pp 323-340.

Jardine R J, Potts D M, Fourie A B, and Burland J B 1986. Studies of the influence of non-linear stress-strain characteristics in soil-structure interaction. *Géotechnique*, 36, No 3, pp377-396.

Jardine, R. J. and Potts, D. M. 1988. Hutton Tension Leg Platform Foundations: an approach to the prediction of pile behaviour. *Geotechnique*, Vol.38, No.2, pp 231-252.

Jardine R. J., St John, H. D., Hight, D. W. and Potts, D. M. 1991. Some practical applications of a non-linear ground model. *Proc. Xth ECSMFE*, Florence, Vol. 1, pp 223-228.

Jardine, R.J. 1991. The cyclic behaviour of large piles. Chapter in *'The Cyclic Loading of Soils*', Eds. Brown & O'Reilly, Blackie & Son, Glasgow, pp 174-248.

Jardine R J and Potts D M 1993. Magnus foundations: Soil properties and predictions of field behaviour. *Proc. Conf. Large scale pile tests in clay*. Thomas Telford, London, pp 69-83.

Jardine, R.J. 1994. Review of offshore pile design for cyclic loading: North Sea clays. HSE Offshore Techn. Report, OTN 94 157.85.

Jardine, R J 1994b. One perspective on the pre-failure deformation characteristics of some geomaterials. Keynote lecture. *Proc. International Symposium on pre-failure deformation characteristics of geomaterials*. Hokkaido, Japan, Balkema, Vol. II, pp 855-886.

Jardine, R. J., Zdravkovic, L., and Porovic, E. 1997. Anisotropic consolidation including principal stress axis rotation: experiments, results and practical implications. Invited panel contribution, *Proc XIVth ICSMFE*, Hamburg, Balkema, Volume 4, pp2165-2168

Jardine, R. J. and Menkiti, C. O. M. 1999. The undrained anisotropy of K_0 consolidated sediments. *Proc. 12th ECSMGE*, Amsterdam. Balkema, Vol 2, pp1101-1108.

Jardine, R.J. and Standing, R.J. 2000.Pile load testing performed for HSE cyclic loading study at Dunkirk, France. Offshore Technology Report OTO 2000 007; Health and Safety Executive, London. Vol, 1, 160.p., Vol, 2, 200p.

Jardine, R.J., Chow, F.C., Overy, R. and Standing, J. 2005a. ICP design methods for driven piles in sands and clays. Thomas Telford Ltd, London, p 105.

Jardine, R.J., Standing, J.R.and Kovacevic, N. 2005b. Lessons learned from full-scale observations and the practical application of advanced testing and modelling. Keynote paper, *Proc International Symposium on Deformation Characteristics of Geomaterials*, Lyon, Vol 2, pub Balkema, Lisse, Vol. 2, pp 210-245.

Jardine, R.J, Standing, J.R and Chow, F.C. 2006. Some observations of the effects of time on the capacity of piles driven in sand. *Geotechnique* Vol 55, No. 4, pp 227-244.

Jardine, R.J., Aldridge, T. and Evans, T.G. 2011. Offshore foundation engineering in extremely dense glacial tills West of the Shetland Islands. *Proc. 15th ECSMGE*, Athens, Millpress, pp 879-884.

Jardine, R.J., Andersen, K. and Puech, A. 2012. Cyclic loading of offshore piles: potential effects and practical design. Keynote Paper. *Proc 7th Int. Conf. on Offshore Site Investigations and Geotechnics*, SUT London, pp 59-100.

Jardine R.J. and Standing, J.R. 2012. Field axial cyclic loading experiments on piles driven in sand. *Soils and Foundations*. Vol. 52, No 4, pp 723-737.

Jardine R.J, Zhu, B.T., Foray, P. and Yang, Z.X. 2013. Measurement of Stresses around Closed-Ended Displacement Piles in Sand. *Geotechnique* 63, No. 1, 1–17.

Jardine R. J. 2013. Advanced laboratory testing in research and practice: the Second Bishop Lecture. *Proc 18th ICSMGE*, Paris, 20p.

Jeanjean P., Andersen K.H. and Kalsnes B. 1998. Soil parameters for design of suction caissons for Gulf of Mexico deepwater clays. *Offshore Technology Conf.*, Houston, Proc., Paper 8830 (1998).

Jostad H.P and Andresen L. 2009. A FE procedure for calculation of displacements and Capacity of foundations subjected to cyclic loading. *Proc. COMGEO I*, Juan-les-Pins, France.

Kaggwa W.S., Booker J.R. and Carter J.P. 1991. Residual strains in calcareous sand due to irregular cyclic loading. *J. Geotech. Engrg.*, ASCE 117: 201–218.

Karlsrud K and Haugen T. 1985a. Axial static capacity of steel models piles in overconsolidated clay, *Proc. 11th Int. Conf. on Soil Mech. and Found. Eng.*, San Francisco.

Karlsrud K and Haugen T. 1985b. Behaviour of Piles in clay under cyclic axial loading-results of field model tests. *Proc. Behaviour of Offshore Structures*, BOSS'85, 589–600.

Karlsrud K. Nadim F and Haugen T. 1986. Piles in clay under cyclic loading: Field tests and computational modelling. Proc. 3rd Int. *Conf. on Numerical Methods in offshore Piling*. Nantes, France, May 1986, 165–190.

Karlsrud K. and Nadim F. 1990. Axial pile capacity of offshore piles in clay. *Proc. Offshore Technology Conference*. OTC 6245. Houston, USA.

Karlsrud K, Hansen S.B, Dyvik R and Kalsnes B. 1992a. NGI's pile tests at Tilbrook and Pentre – Review of testing procedures and results. *Proceedings of the Conference on Recent large-scale fully instrumented pile tests in clay*, London, 405–429.

Karlsrud K., Kalsnes B., and Nowacki F. 1992b. Response of piles in soft clay and silt deposits to static and cyclic axial loading based on recent instrumented pile load tests. *Proc. Offshore Site Investigation and Foundation Behaviour*. London, 549–583.

Karlsrud K, Clausen CJF and Aas PM. 2005. Bearing capacity of driven piles in clay: the NGI approach. *Proc. ISFOG'05*, Perth, WA, 775–782.

Karlsrud K. 2012. Prediction of load-displacement behaviour and capacity of axially loaded piles in clay based on analyses and interpretation of pile load test results. *PhD thesis*, NTNU, Trondheim, Norway.

Khemakhem M. 2012. Etude expérimentale de la réponse aux charges laterales monotones et cycliques d'un pieu foré dans l'argile, *Thèse*, Ecole Centrale de Nantes, 314pp.

Khemakhem M., Chenaf N., Garnier,J., Favraud C and Gaudicheau P. 2012. Development of degradation laws for describing the cyclic lateral response of piles in clays. *7th Int. Conf. Offshore Site Investigation and Geotechnics,* SUT, London.

Kleven A. and K.H. Andersen 1991. Cyclic laboratory tests on Storebælt clay till. Seminar on *Design of Exposed Bridge Piers*. Danish Society of Hydraulic Engineering. Copenhagen, Denmark, 22 January 1991. Also published in NGI Publ. 199.

Kraft, L.M., Ray R.P. and Kagawa.T. 1981. Theoretical t z curves. *J. Geotech. Engrg*., ASCE, 107, GT11: 1543 1561.

Kühn M. 2000. Dynamics of offshore wind energy converters on monopile foundations – experience from the Lely offshore wind farm. Oral contribution reported in EPSRC Offshore Wind Energy Network. *Workshop on Structure and Foundation Design of Offshore Wind Installations*. CLRC Rutherford Appleton Laboratory (1 March 2000).

Kuwano, R. and Jardine R.J. 2002. On the applicability of cross anisotropic elasticity to granular materials at very small strains. *Geotechnique*, Vol 52, No 10, pp 727-750.

Kuwano, R. and Jardine, R.J. 2007. A triaxial investigation of kinematic yielding in sand. *Géotechnique*, 57., No. 7, p. 563-580.

Ladd C.C. and Foott R. 1974. New design procedure for stability of soft clays. *J. Geotech. Engrg*., ASCE, 100, GT7: 763 786.

Lauritzsen R. and Schjetne K. 1976. Stability calculations for offshore gravity structures. *Proc., 8. Offsh. Tech. Conf.*, Houston, Tex., 75-82.

Le, M.H., Nauroy, J.F., De Gennaro, V., Delage, P., Thanh, N., Flavigny, E., Colliat, J.L., Puech, A. and Meunier, J. 2008. Characterization of soft deepwater West Africa clays: SHANSEP testing is not recommended for sensitive structured clays. *Proc. Offshore Technology Conference*, OTC paper 19193, Houston.

LeBlanc C., Houlsby G. T.and Byrne B. W. 2010. Response of stiff piles in sand to long-term cyclic lateral loading, *Geotechnique* 60, No. 2, 79–90

Lehane BM. 1992. Experimental investigations of pile behaviour using instrumented field piles. *PhD thesis*, University of London (Imperial College).

Lehane, B.M., Jardine, R.J., Bond, A.J. and Frank, R. 1993. Mechanisms of shaft friction in sand from instrumented pile tests. *ASCE Geot. Journal*. Vol 119, No 1, pp 19-35.

Lehane, B M and Jardine, R J 1994a. Displacement pile in glacial. *Canadian Geotechnical Journal*, Vol. 31, 1, pp 79-90.

Lehane, B M and Jardine, R J 1994b. Displacement pile in soft marine clay. *Canadian Geotechnical Journal*, Vol. 31, 2, pp 181-191.

Lehane, B.M., Jardine, R.J. and McCabe, B.A. 2003. Pile Group Tension Cyclic Loading: Field test programme at Kinnegar, N.Ireland. HSE Research Report 101; HSE Books, p42.

Leroueil, S and Vaughan, P R 1990. The general and congruent effects of structure in natural soils and weak rocks. *Geotechnique*, Vol 50, No 3, pp 467-488.

Lunne, T., Robertson, P.K., Powell, J. 1997. CPT and piezocone testing in geotechnical practice. Textbook: Spon Press, Taylor and Francis Company, London.

Lunne T., Berre T., Andersen K.H., Strandvik S. and Sjursen M. 2006. Effects of sample disturbance and consolidation procedures on measured shear strength of soft marine Norwegian clays. *Can. Geotech. J.* 43: 726-750.

Lunne, T. and K.H. Andersen 2007. Soft clay shear strength parameters for deepwater geotechnical design. Keynote Address; *Proc., 6th International Offshore Site Investigation and Geotechnics Conference*; Confronting New Challenges and Sharing Knowledge, p. 151-176, 11-13 September 2007, London, UK.

OSIG 2013. Guidance notes for the planning and execution of geophysical and geotechnical ground investigations for offshore renewable energy developments (Draft 02/05/13). Society for Underwater Technology, London.

Menkiti, C O 1995. Behaviour of clay and claey-sand, with particular reference to principal stress rotation. *PhD Thesis*, University of London.

Merritt, A., Schroeder, F., Jardine, R., Stuyts, B., Cathie, D., Cleverly, W. 2012. Development of pile design methodology for an offshore wind farm in the North Sea. Proc 7th Int. Conf. on Offshore Site Investigations and Geotechnics, SUT London, pp 439-448.

Mroz Z., Norris V.A. and Zienkiewicz. 1978. Simulation of soil behavior under cyclic loading by using a more general hardening rule. Univ. College Swansea, Dept. of Civil Engrg., Institute for Numerical Methods in Engineering.

Mulilis, J.P., Seed, H.B., Chan, C.K., Mitchell, J.K. and Arulanandan, K. 1977a. Effects of sample preparation on sand liquefaction. *ASCE, J. Geotech. Engrg*. 103(2): 91-108.

Mulilis, J.P., Mori, K., Seed, H.B. and Chan, C.K. 1977b. Resistance to liquefaction due to sustained pressure. *ASCE, J. Geotech. Engrg.*, 103(7): 793-797.

Nadim F and Dahlberg R. 1996. Numerical modeling of cyclic pile capacity in clay. *Proc. Offshore Technology Conference*, OTC paper 7994, Houston, USA.

Niemunis A. and Herle I. 1997. Hypoplastic model for cohesionless soils with elastic strain range. Mech. of Cohesive-Frictional Materials 2: 279–299.

Nishimura, S., Minh, N.A. and Jardine, R.J. 2007. Shear strength anisotropy of natural London clay. Symposium in Print on Stiff Clays. *Géotechnique*, 57(2), pp 49-62.

NGI 2006. SPLICE

Nowacki F, Karlsrud K and Sparrevik P. 1992. Comparison of recent tests on OC clay and implications for design. *Proceedings of the Conference on Recent large-scale fully instrumented pile tests in clay*. London, 511–537.

Peralta P. 2010. Investigations on the behaviour of large diameter piles under long-term lateral cyclic loading in cohesionless soil, *PhD Thesis*, Leibnitz University, Hannover, pp 201.

Poulos HG. 1982. Single pile response to cyclic lateral load. *Journal of the Geotechnical Engineering Division* 108: 355–375.

Poulos HG. 1989. SCARP USERS'S MANUAL. Centre for Geotechnical Research, The University of Sydney, Australia.

Pra-ai, S. 2013. Essais et modélisation du cisaillement cyclique sol-structure à grand nombre de cycles. Application aux pieux, *Thèse de Doctorat*, IMEP2, Université de Grenoble (to be published).

Prevost J.-H. 1977. Mathematical modeling of monotonic and cyclic undrained clay behaviour. *Int. J. for Num. Methods in Geomech.* 1: 195–216.

Puech A., Canou J., Bernardini C., Pecker A., Jardine R., and Holeyman A. 2012. SOLCYP: a four year JIP on the behavior of piles under cyclic loading. *Offshore Site Investigation and Geotechnics*, SUT, London.

Puech A., Benzaria O., Thorel L., Garnier J., Foray P. et Jardine R. 2013. Diagrammes de stabilité cyclique de pieux dans les sables. *Proceedings 18th ICSMGE, Paris.*

Rakotonindriana M.J. 2009. Comportement des pieux et des groupes de pieux sous chargement latéral cyclique, *Thèse de Doctorat* ENPC / LCPC.

Randolph MF. 1994. RATZ program manual: Load transfer analysis of axially loaded piles. Dept. of Civil and Resource Engineering, University of Western Australia.

Rimoy SP, Jardine RJ, Silva M, Foray PY, Tsuha CHC and Yang Z. 2012. Local and global behaviour of cyclically loaded instrumented model displacement piles in sand. *In: Proc. 7th Offshore Site Investigation and Geotechnics: Integrated Geotechnologies – Present and Future*. London: SUT.

Rimoy, S., Jardine, R.J and Standing, J.R. 2013. Displacement response to axial cycling of piles driven in sand. *Geotechnical Engineering*, 116 (2): 131-146.

Rimoy, S.P. 2013. Ageing and axial cyclic loading studies of displacement piles in sands. *PhD Thesis*, Imperial College London.

Rosquoët F., Thorel L., Garnier J. and Chenaf N. 2013. Pieu sous charge latérale dans les sables: développement de lois de dégradation pour prendre en compte l'effet des cycles. *Proceedings 18th ICSMGE, Paris*

Saue M., Langford T. and Mortensen N. 2010. Design of monopile Foundations in Sand for Offshore Windfarms. *Intern. Symp.on Frontiers in Offsh. Geotechnics (ISFOG)*. Nov. 2010, Perth, Australia.

Schmertmann, J. H. 1978. Guidelines for cone penetration tests, Performance and Design, Report 446 FHWA-TS-78-209, US Department of Transportation.

Silver, M.L., Chan, C.K., Ladd, R.S., Lee, K.L., Tiedemann, D.A., Townsend, F.C., Valera, J.E. and Wilson, J.H. 1976. Cyclic triaxial strength of standard test sand. *ASCE, J. Geotech. Eng.*, 102(5): 511-524.

Sim, W.W., Aghakouchak, A. and Jardine, R.J. 2013. Effects of duration and amplitude on cyclic behaviour of over-consolidated sands under constant volume conditions. *Geotechnical Engineering,* 116 (2): 111-121.

Smith P.R., Jardine R.J. and Hight, D.W. 1992. On the yielding of Bothkennar clay. *Geotechnique,* Vol 41, No 2, pp 257-274.

Tatsuoka, F., Jardine, R. J., Lo Presti, D., Di Benedetto, H. and Kodaka, T. 1997. Characterising the pre-failure deformation properties of geomaterials. Theme Lecture, *Proc XIVth ICSMFE*, Hamburg, Volume 4, Balkema, Rotterdam, 1999, pp 2129-2164

Tatsuoka, F. 2011. Laboratory stress-strain tests for developments in geotechnical engineering. 1st Bishop Lecture, *Deformation Characteristics of Geomaterials. Proc.* IS-Seoul, Hanrimwon, Vol. 1, p 3-53.

Tsuha, C.H.C, Foray, P.Y., Jardine, R.J., Yang, Z.X., Silva, M. and Rimoy, S.P. 2012. Behaviour of displacement piles in sand under cyclic axial loading. *Soils and Foundations*, Vol. 52, No 3, pp 393-410.

Vaid, Y.P., Sivathayalan, S. and Stedman, D. 1999. Influence of specimen reconstitution method on the undrained response of sand. *ASTM Geotech. Testing J.* 22(3): 187-195.

Valanis K.C. and Lee C.F. 1984. Endochronic theory of cyclic plasticity with applications. *J. of Applied Mechanics* 51: 367–374.

Wichtmann T. 2005. Explicit accumulation model for non-cohesive soils under cyclic loading. In: Triantafyllidis Th. (ed.). *Schriftenreihe des Institutes für Grundbau und Bodenmechanik der Ruhr-Universität* Bochum, Heft 38.

Wichtmann T., Niemunis A. and Triantafyllidis Th. 2004. Strain accumulation in sand due to drained uniaxial cyclic loading. In: Triantafyllidis Th. (ed.). *Cyclic Beh. of Soils and Liquefaction Phenomena*. London: Taylor & Francis Group.

Yang, Z.X., Jardine, R.J., Zhu B.T., Foray, P. and Tsuha, C.H.C.. 2010. Sand grain crushing and interface shearing during displacement pile installation in sand, *Géotechnique*, Vol 60, No 6, pp 469-482.

Zdravkovic L. and Jardine, R.J. 1997. Some anisotropic stiffness characteristics of a silt under general stress conditions. *Geotechnique*, 47, No 3, 407-438.

Zdravkovic, L. and Jardine, R.J. 2000. Undrained anisotropy of K_0 consolidated silt. *Canadian Geotechnical Journal*, Vol 37, No.1, pp 178-200.

Zdravkovic, L. and Jardine, R.J. 2001. The effect on anisotropy of rotating the principal stress axes during consolidation. *Geotechnique*, 51, 1, pp 69-83

Zdravkovic, L., Potts, D.M. and Jardine, R.J. 2001. A parametric study of the pull-out capacity of bucket foundations in soft clay. *Geotechnique*, 51, 1 pp 55 -67.

Advances in axial cyclic pile design: Contribution of the SOLCYP project

Avancées dans le dimensionnement des pieux sous chargement cyclique axial : contribution du projet SOLCYP

A. Puech
FugroGeoConsulting, France

ABSTRACT: The SOLCYP joint industry project is aimed at developing improved methodologies for designing piles submitted to axial or lateral cyclic loading. This paper outlines the objectives and technical content of the project and highlights how the experimental data gathered throughout the past four years can be used to develop advanced procedures for designing piles under axial cyclic loading. A companion paper addresses SOLCYP's contribution to the design of piles under cyclic lateral loading.

RÉSUMÉ : Le projet de recherche collaborative SOLCYP a pour objet de développer des méthodologies innovantes pour dimensionner les pieux soumis à des chargements cycliques axiaux ou latéraux. Cette communication rappelle les objectifs et le contenu technique du projet et montre comment les données expérimentales obtenues durant les quatre dernières années peuvent contribuer à l'élaboration de procédures avancées pour le calcul des pieux soumis à des charges cycliques axiales. Un papier séparé s'intéresse à l'apport de SOLCYP pour le dimensionnement des pieux sous charges cycliques latérales.

KEYWORDS: pile, axial load, cyclic loading, SOLCYP

MOTS-CLES: pieu, charge axiale, chargement cyclique, SOLCYP

1 INTRODUCTION

The oil and gas industry has developed procedures for considering the effects of large wave cyclic loads on foundations for offshore structures. Design guidelines include API RP 2GEO (2011); DnV Foundations (1992) and ISO 19902 (2007). The offshore turbines industry is progressively adapting such methodologies in e.g. DnV-OS-J101 (2010); GL (2007); BSH (2007).

Surprisingly the effects of cyclic loading on foundations are largely ignored in most civil engineering and building activities. French codes and Eurocode 7 reflect this poor level of consideration. A committee working under the umbrella of the French National Agency IREX called for a national engagement in an ambitious research and development project to address the present lack of guidance regarding piles under cyclic loading. A wide range of applications are considered including offshore and onshore wind farms, coastal structures, onshore foundations such as bridges submitted to intense traffic loads, high rise towers and chimneys, energy transport pylons and crane foundations.

This paper summarises the objectives and overall technical content of the project, already described in more detail in Puech et al. (2012). The most significant experimental data currently available are discussed and it is shown how they can be used to develop improved design methodologies for designing piles under cyclic axial loading. A companion paper (Garnier 2013) focuses on SOLCYP's contribution to the design of piles under cyclic lateral loading.

2 THE SOLCYP PROJECT

The SOLCYP project (French acronym for Piles under CYclic SOLicitations) was launched in 2008 with the objectives of i) understanding the physical phenomena which affect the response of piles to vertical and horizontal cyclic loads, (ii) developing advanced design methods and (iii) initiating pre-normative development of methodologies that may subsequently be included in national and international codes or professional standards.

The project has a total budget approaching 4.5 millions €, financed by Agence Nationale de la Recherche (ANR), Ministère de l'Ecologie, du Développement Durable et de l'Energie (MEDDE), Fédération Nationale des Travaux Publics (FNTP) and 14 private companies of the civil engineering and energy sectors.

The behaviour of bored and driven piles under cyclic loading in sands and clays is investigated through a range of laboratory, field and theoretical approaches. A detailed description of the scope of work can be found in Puech et al. (2012). Most the test programme is complete at the time of issue of this paper. However, detailed interpretations of observed phenomena are yet to be combined with results of advanced laboratory tests. This section only discusses the most significant tests.

2.1 Field tests

In situ axial pile tests were conducted at two test sites. The first site is Merville, in northern France where stiff to very stiff overconsolidated (OCR of about 10) plastic Eocene Flanders clay is encountered below 3 m depth. Ten test piles were installed in March 2011 (Figure 1), including four driven closed-ended tubular steel piles, four bored piles and two screwed piles. The piles were 13.5 m long with diameters of 406 mm (driven piles) or 420 mm (bored and screwed piles). All piles were instrumented. Load tests were conducted from May to June 2011, including conventional incremental static tests, rapid load tests and cyclic load tests. The latter covered both tests that failed after relatively small numbers of large cycles and those that extended to very large numbers (> 10 000) of relatively low amplitude cycles. All loading modes were investigated: tension, compression, one-way and two-way. The main results for driven piles were presented in Benzaria et al. (2012). Partial results for bored piles are presented in Benzaria et al. (2013a) and Benzaria et al. (2013c).

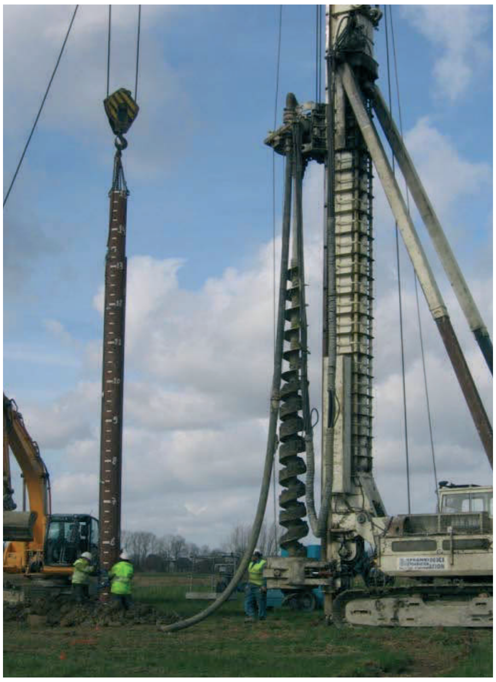

Figure 1: Installing driven and bored piles at MERVILLE

The second site is at Loon-Plage near Dunkirk where post-glacial Flandrian dense to very dense fine sands are encountered. Given the availability of previous cyclic pile testing by Imperial College in the same sands at a neighbouring site (see Jardine and Standing 2000 and 2012 and Rimoy et al. 2013) only two steel piles (13.5 m long, 406 mm diameter) were driven and tests conducted to complement and extend the existing data set. Five bored piles (420 mm diameter, 8 m or 10.5 m long) were installed in November 2011and submitted in March 2012 to a very similar load testing programme to the Merville piles. Initial results are presented in Benzaria et al. (2013b) and Benzaria et al. (2013d).

Figure 2: Set-up for SOLCYP two-way cyclic pile tests

2.2 *Model tests*

Extensive centrifuge tests on model piles have been and are still being performed in Fontainebleau sand and Speswhite clay using the large centrifuge of IFSTTAR (formerly LCPC) in Nantes. The main objective is to derive cyclic stability diagrams for different soil conditions (medium dense or dense sands and soft clays), installation modes (cast in place or driven), and loading modes (tension or compression, one-way and two-way). Preliminary results are given in Guefresh et al. (2012); Puech et al. (2013a and b).

Highly instrumented displacement pile tests are also being performed in the large calibration chamber of the 3S-R Laboratory in Grenoble. These tests, carried out in collaboration with Imperial College London, are providing very valuable data on the mobilisation of the interface pile-sand friction and its evolution with number of cycles (e.g. Tsuha et al. 2012; Rimoy et al. 2012).

3 STATIC AND CYCLIC PILE RESPONSES IN HIGH OCR FLANDERS CLAY (MERVILLE PILE TESTS)

3.1 *Flanders clays*

The geological history and geotechnical properties of the Flanders clays can be found in Benzaria et al. (2013a and c).

3.2 *Response of piles under static loading*

Only the results of the conventional static tests in compression are discussed in this section, which focuses in particular on the installation method's effect on the static capacity of the piles.

3.2.1 Installation and loading modes

The four tubular metallic piles (OD = 406 mm, w.t. = 14 mm) were installed in a 4 m prebored hole, then driven to 13 m blow ground level (BGL) using a hydraulic IHC 30 hammer. The piles were closed-ended and the soil around the pile was fully displaced.

The bored piles (OD = 420 mm) were of the Continuous Flight Augering (CFA) type i.e. drilled using a hollow auger screwed into the soil, then removed without rotation while grout was poured through the hollow stem. A telescopic nose was used to improve grouting conditions at the base. The reinforcement cage was lowered into the fresh grout. For this type of pile, the soil is entirely removed (non-displacement piles).

Two piles (OD = 420 mm) were screwed and cast in place: a conical tool is inserted into the soil by a combined action of rotation and jacking. Grouting is through a hollow stem as for CFA piles. The soil is significantly displaced (approximately 15 to 20% of the soil is extracted).

The piles were instrumented using removable extensometers. This technique developed by LCPC gives access to load distribution along the pile and to local shear transfer mobilization (1 m long sections). For metallic piles, two sets of extensometers were introduced after driving in reservation tubes welded on the outside the pile wall. For bored piles, one single set was installed in a reservation tube welded to the reinforcement cage.

Conventional static tests were of the incremental type with load increments maintained 1 hour (ISSMGE, 1985; AFNOR NF P 94-150-2)

3.2.2 Global response

A conventional static test in compression was performed on a virgin pile of each type. Pile head displacement curves are compared on Figure 3. Given the high degree of lateral homogeneity of the clay at Merville, any differences observed can be attributed to the different installation methods.

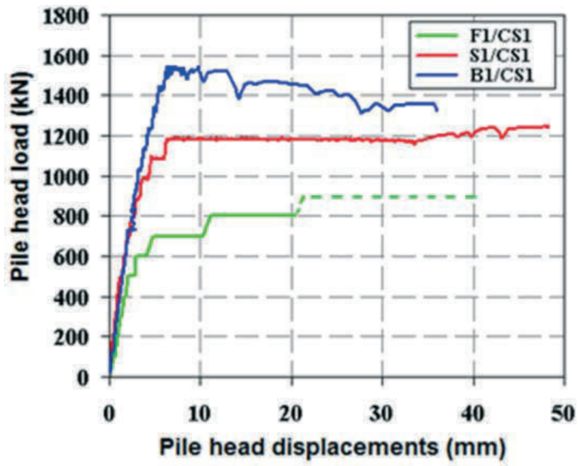

Figure 3: MERVILLE field test. Pile head load-displacement curves for conventional static tests on piles B1 (driven), S1 (screwed) and F1 (bored)

The ultimate pile capacity is respectively 1530 kN, 1230 kN and 900 kN for the driven pile B1, the screwed pile S1 and the bored pile F1. The difference is even higher if one considers that the frictional capacity of the driven pile is nil on the upper 4 m (predrilled hole). Obviously, the higher the amount of soil displacement at installation, the higher the ultimate pile capacity.

The pile head displacement at failure is lower for the displacement piles (6 to 7 mm or 1.5% of pile diameter for B1 and S1) than for the non-displacement pile (at least 12 mm or 3% of pile diameter for pile F1).

Failure is fragile for the driven pile B1: significant strain softening is observed after a clear peak in capacity. Tension tests on pile B4 (Benzaria et al. 2012) showed that strain softening continues to develop up to 80 mm to 100 mm of displacement. Failure is ductile on the two bored piles (S1 and F1).

3.2.3 Local response

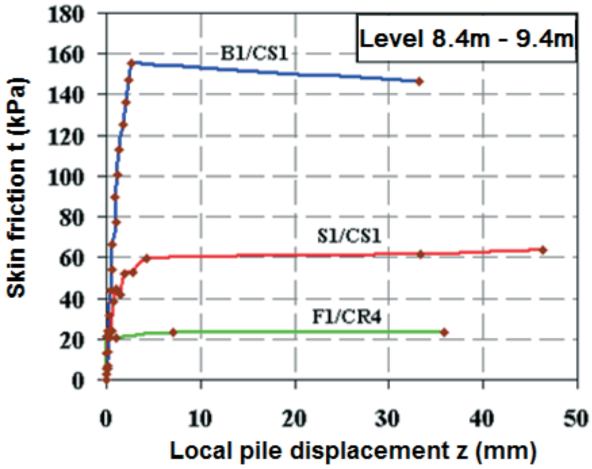

Figure 4: MERVILLE field tests. Typical shear strength transfer curves at a given depth interval (8.4-9.4m) for pile B1 (driven), pile S1 (screwed) and pile F1 (bored)

The global behaviour is confirmed by local friction analysis. Figure 4 shows typical curves of friction mobilization at a selected level (between 8.4 m and 9.4 m) for each pile. In the lower part of the piles, ultimate friction values are typically of the order of 40 kPa for the bored pile F1, 60 kPa for the screwed pile S1 and 160 kPa for the driven pile B1. More details on the skin friction distribution and comparison with various prediction methods can be found in Puech and Benzaria (2013a and b)

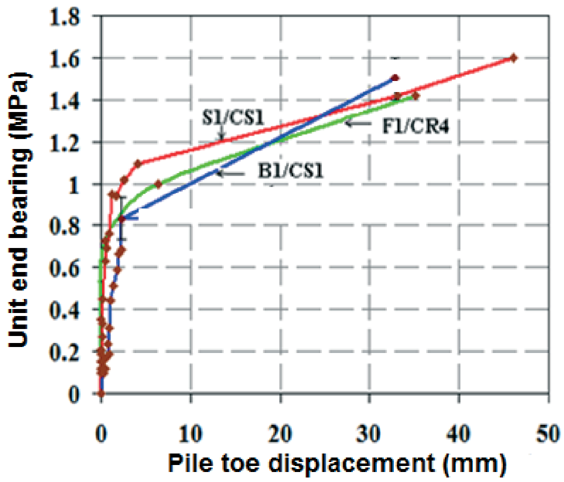

Figure 5: MERVILLE field tests. End bearing mobilisation curves for piles B1 (driven), S1 (screwed) and F1 (bored)

Mobilisation of the end bearing for each pile is shown on Figure 5. Responses are very similar with a rapid reaction of the toe, which indicates a careful execution of the base grouting for the bored pile F1. At Zp = 0,1 D, the bearing resistance under the three piles is close to 1.5 MPa in good agreement with the theoretical end bearing pressure $q_p = 9.Cu$.

3.3 Response of piles under cyclic loading

3.3.1 Cyclic loading modes

The complete characterisation of cyclic loading requires the definition of the following parameters:

Q_a = mean value of the load during cycling (may also be noted Q_m or Q_{ave})

Q_{cy} = half-amplitude of the cyclic load (may also be noted Q_c)

Q_{max} = maximal cyclic load ($Q_{max} = Q_a + Q_{cy}$)

N = number of cycles (tests were conducted to failure after N_f cycles or to a great number of cycles N > 1000)

F = frequency of cycles (normally 0.5 Hz)

Q_{us} = ultimate static capacity for the mode considered (tension Q_{ut} or compression Q_{uc}).

Loading is in one-way mode when $Q_{cy} < Q_a$ and two-way mode when $Q_{cy} > Q_a$.

3.3.2 Typical results for bored piles in compression

Pile head load-displacements relationships observed on Pile F2 are shown in Figure 6. This pile was tested in compression only and submitted to:

- three batches of cyclic loads CC1 to CC3
- one rapid load test CR1 in compression
- seven batches of cyclic loads CC4 to CC10
- one rapid test CR2 including two loading/unloading paths.

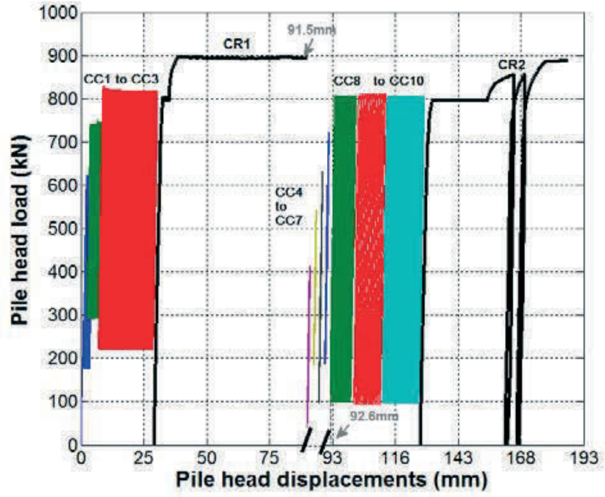

CC1-2: N>3000; CC3: N=2000, CC4 to7: N~1000; CC8-10: N<100

Figure 6: MERVILLE field tests. Pile head load-displacement relationships on bored pile F2. One-way compression loading

The reference static capacity Q_{uc} measured on Pile F1 is estimated at 900 kN (Figure 3). Detailed loading characteristics can be found in Benzaria et al. (2013a and c).

The main observations are as follows:

- For maximum cyclic loads below 800 kN, pile head displacements remain negligible even for high numbers of cycles (several thousand);
- Significant pile head displacements are generated as soon as the maximum cyclic load reaches or slightly exceeds 800 kN;
- The post-cyclic capacity is not affected by previous cyclic loading.

Pile F4 was tested in two-way mode with a positive (compressive) value of Q_a. Nine cyclic tests were performed with number of cycles between 400 and 2000. Due to limitations in the cyclic jack (the maximum amplitude was 1000 kN), the unstable domain could not be explored. All tests were in the stable domain (no significant permanent pile head displacements were observed) and closed hysteresis loops were recorded (Benzaria et al. 2013a and c)

3.3.3 Typical results for screwed piles

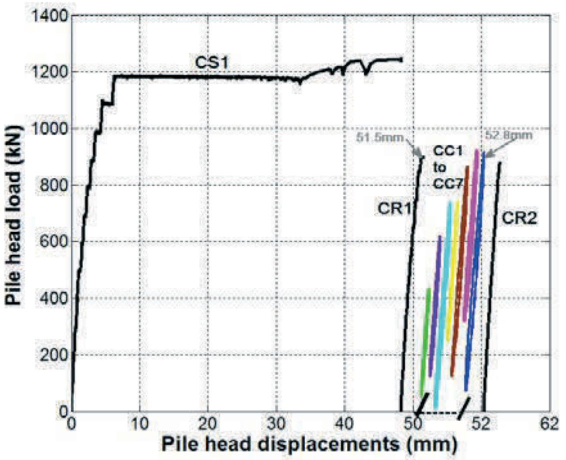

Figure 7: MERVILLE field tests. Pile head load-displacement relationships on screwed pile S1. One-way compression loading

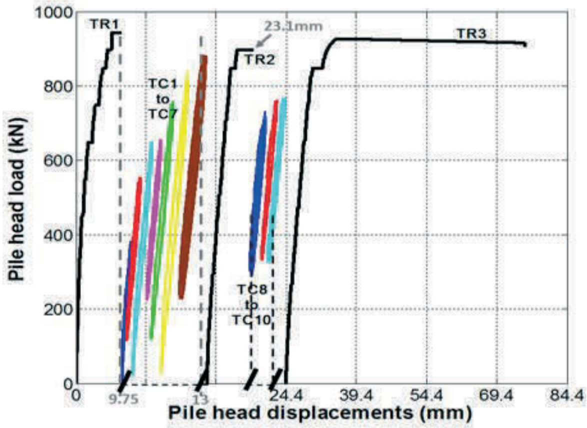

Figure 8: MERVILLE field tests. Pile head load-displacement relationships on screwed pile S2. One-way tension loading

The screwed piles S1 and S2 were tested in compression and in tension respectively.

The static reference test CS1 on pile S1 indicates an ultimate compressive capacity Q_{uc} = 1230 kN. From the load distribution in the pile measured with the extensometers, the end bearing capacity can be evaluated with confidence at 220 kN. It may therefore be anticipated that the ultimate capacity in tension of pile S2 is close to1000 kN.

Following the static reference test, series of rapid load tests and cyclic tests were applied to pile S1. Batches CC1 and CC2 are characterized by 5000 cycles of relatively small amplitude whereas batches CC3 to CC7 include 1000 cycles of increasing severity up to a maximum cyclic load of 900 kN representing about 75% of Q_{uc}. Pile head displacements were always negligible.

Pile S2 was first submitted to a rapid load test. Under the 950 kN increment, significant creep was observed confirming an ultimate capacity close to 1000 kN. The test was stopped to preserve the pile from large displacements and friction degradation due to strain softening. The testing sequence was then similar to pile S1 (5000 cycles for batches TC1 and TC2 and 1000 cycles for all subsequent batches). In total, the pile withstood some 18 000 cycles including 1000 cycles with a maximum load at 880 kN without any significant generation of permanent pile head displacements. Test CR3 may suggest a slight decrease of the post-cyclic ultimate pile capacity in tension.

3.3.4 Typical results for driven piles

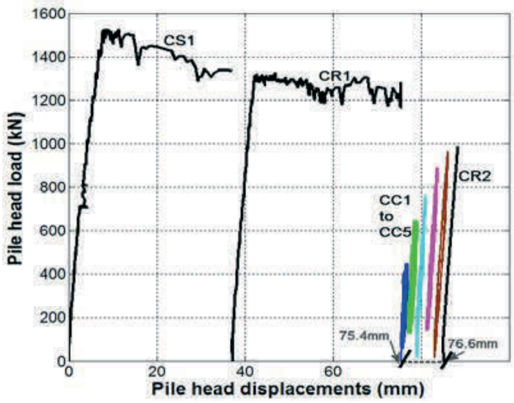

Figure 9: MERVILLE field tests. Pile head load-displacement relationships on driven pile B1. One-way compression

Pile B1 was used to determine the reference static capacity in compression. The pile capacity peaked at 1530 kN for some 6 to 7 mm of pile head displacement then decreased continuously to 9% to 10% of relative displacement. A second (rapid) static test confirmed the strain softening behaviour to about 80 mm of cumulated pile head displacement. At the end of CR1 the ultimate capacity of the pile was only 1250 kN.

The pile was then submitted to 10 000 cycles of small amplitude (CC1) followed by four series of 1000 cycles with increasing severity. The maximum load applied was close to 980 kN, i.e. approximately 78% of the ultimate capacity of the pile just before starting the cyclic tests. No significant permanent displacements were generated.

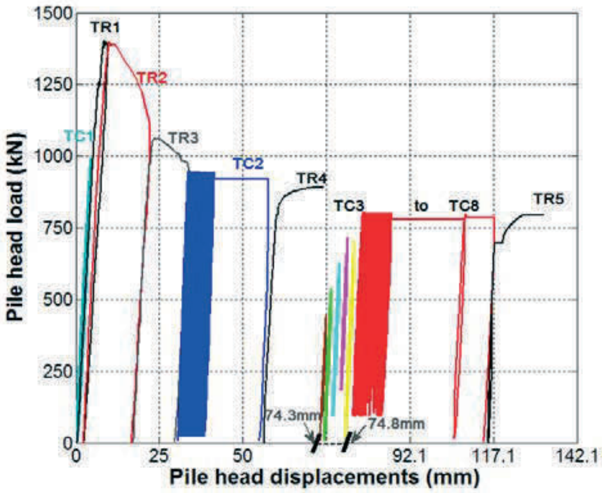

Figure 10: MERVILLE field tests. Pile head load-displacement relationships on driven pile B4. One-way tension loading

The response of Pile B4 is described in detail in Benzaria et al. 2012. Particular points of interest are as follows:

- The first batch of cyclic tests was applied on the virgin pile: 3000 cycles with a maximum load of 980 kN caused negligible permanent displacements;
- Rapid load test CR1 showed a peak ultimate capacity in tension of approximately 1400 kN fully compatible with the compressive capacity measured on Pile B1.
- Two subsequent rapid load tests generated strain softening
- and a decrease of the ultimate capacity to about 980 kN;
- A second batch of cyclic loads similar to the first one with a maximal load of 980 kN was applied which generated a cyclic failure of the pile after only 94 cycles. This confirms that the cyclic response is governed by the ratio of the maximum load to the ultimate static capacity just before cycling.

3.3.5 Cyclic interaction diagrams

The cyclic response of piles in Flanders clays can be summarised as follows:

- The cyclic response is controlled by the ratio of the maximum cyclic load Q_{max} to the ultimate static capacity Q_{us} just before applying the cyclic sequence. For compressive loading Q_{us} refers to Q_{uc}, the ultimate capacity in compression and for tension loading Q_{us} refers to Q_{ut}, the ultimate capacity in tension.
- The existence a threshold value of Q_{max}/Q_{us} for explaining the response of the piles is supported by the full set of data collected.
- For values of Q_{max}/Q_{us} below the threshold, piles are stable even for a large number of cycles (N > 1000): they do not accumulate significant pile head displacements, hysteresis loops are closed and pile head stiffness remains constant for given loading characteristics.
- For values of Q_{max}/Q_{us} reaching or in excess of the threshold, permanent pile head displacements are rapidly generated and cyclic failure occurs in a small number of cycles. The cyclic pile head stiffness remains constant even in the near-failure stage (Benzaria et al. 2012).
- In the near-failure domain, loading frequency may affect the rate of evolution to failure (reducing the frequency increases the rate of displacement).
- The post-cyclic capacity is not (or only marginally) affected even for severe loading histories.

The threshold is expected to be dependent on the loading characteristics (average cyclic load Q_a, cyclic load amplitude Q_c). Interaction diagrams are useful tools for representing the response of piles to cyclic loading. The number of cycles to failure (N_f) or the number of cycles (N) applied to the piles without causing failure is plotted as a function of the normalised average (Q_a/Q_{us}) and cyclic (Q_{cy}/Q_{us}) load components. The $Q_{max} = Q_{us}$ diagonal line corresponds to the static capacity, whereas the second diagonal delineates the separation between one-way ($Q_{cy} < Q_a$) and two-way ($Q_{cy} > Q_a$) loading.

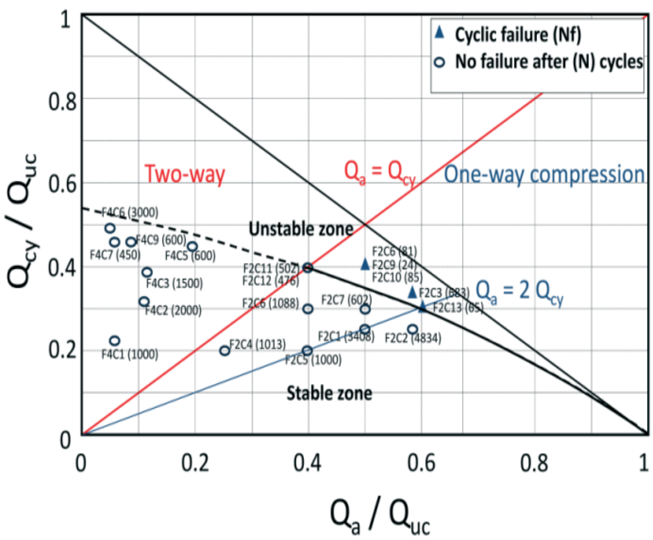

Figure 11: MERVILLE field tests. Cyclic interaction diagram for bored piles in compression. One-way and two-way loading modes

The interaction diagram for bored piles in compression is presented on Figure 11. It is observed that in the one-way domain, the separation between the stable zone and the unstable zone is thin and can be delineated with the continuous line. Threshold values in the one-way domain investigated are in the range 0.8 to 0.9. As explained above, the two-way domain could not be fully explored. Only stable pile configurations were demonstrated. In this domain, the dotted line should be considered as a conservative envelope of the stable zone.

The interaction diagram for the screwed piles is presented on Figure 12. Only stable configurations in the compressive and tensile one-way domains could be tested. The dotted lines inferred from the lines proposed for bored piles in one-way compression appear as realistic envelopes for defining the proved stable zones in compression and tension.

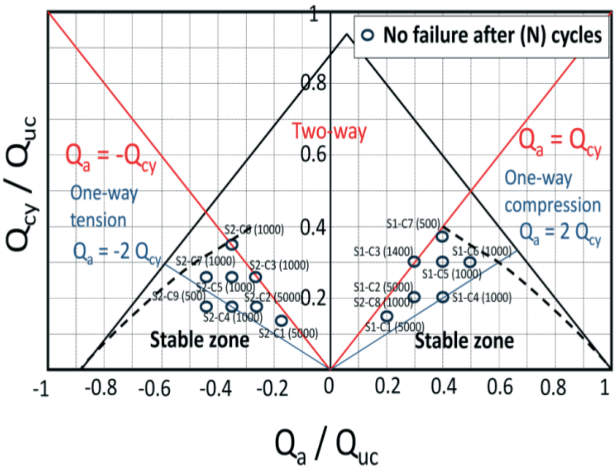

Figure 12: MERVILLE field tests. Cyclic interaction diagram for screwed piles in one-way compression and one-way tension

The interaction diagram for driven piles in tension is presented on Figure 13. Here again the line proposed for the bored piles delineates correctly the separation between stable and unstable piles in the one-way domain. The same line provides a realistic envelope for the stable zone in one-way compression (not shown here).

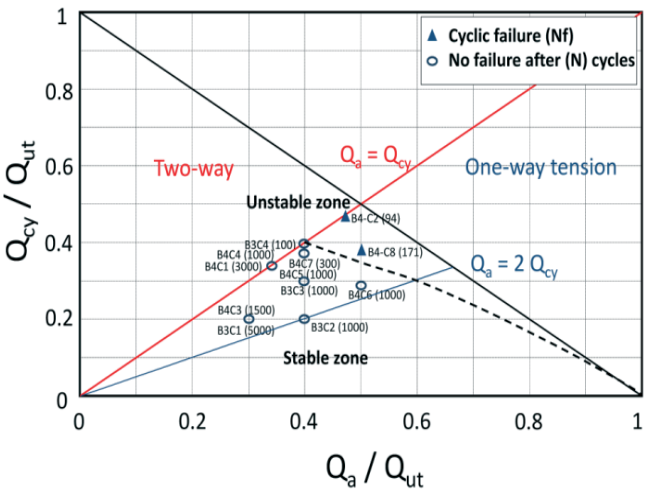

Figure 13: MERVILLE field tests. Cyclic interaction diagram for driven piles in one-way tension

The results suggest that in Flanders clay a common "threshold line" can be proposed for the three types of piles (bored, screwed and driven) and all loading modes (one-way compression, one-way tension and two-way) provided the reference ultimate capacity used to normalise the load components (Q_{uc} or Q_{ut}) is the capacity of the pile just before the cyclic loading sequence considered is applied.

Two main differences with existing data in clays can be highlighted. In the interaction diagram proposed by Karlsrud and Haugen (1985) for the Haga pile tests (reproduced in Andersen et al. 2013), the authors were able to define isocontour lines of number of cycles (N_f) required to cause cyclic failure of the piles. In the Flanders clay such isocontour lines cannot be defined. The transition between the stable zone and the unstable zone is not progressive: when the pile is stable, the pile can sustain more than 1000 cycles without cumulating permanent displacements, whereas when the pile enters the instable domain, cyclic failure occurs in a relative small but unpredictable number of cycles. This is why the concept of threshold is appropriate for Flanders clay.

The second difference is shown in the diagram presented in Figure 14. This diagram is equivalent to an interaction diagram but with the normalised maximum cyclic load in place of the normalised cyclic load. Available data from pile tests in clays are plotted together with the isocontour lines for $N_f = 50$ of the Haga, Lierstranda and Onsøy clays. The threshold line of the Merville tests can be approximately considered as a $N_f = 1000$ contour line for Flanders clay. This line is roughly compatible with all other data in the one-way domain but plots above the other clays in the two-way domain which indicates less sensitivity to alternate loading.

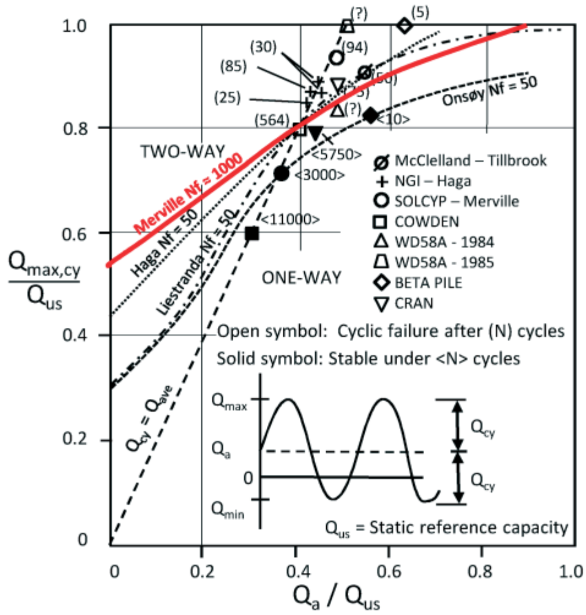

Figure 14: Comparison of existing cyclic interaction diagrams in clays

4 STATIC AND CYCLIC PILE RESPONSES IN DENSE SAND (LOON-PLAGE TESTS)

This section discusses the results obtained with bored CFA piles. The results with driven piles are being analysed with reference to results obtained by Jardine and Standing (2000) at Dunkirk and are expected to be published at a later stage.

1.1 *Dunkirk sand*

The sand encountered at the Loon-Plage test site belongs to the Flanders sand formation and is similar (although a slightly finer) than the sand encountered at Dunkirk where previous pile tests were performed (CLAROM tests by Brucy et al., 1991; Imperial College tests by Jardine et al., 2005; GOPAL tests by Jardine and Standing, 2000). The geotechnical properties of the Dunkirk sand are discussed in Benzaria et al. 2013b and 2013d.

1.2 *Characteristics of bored piles*

As mentioned previously, five bored piles were installed at Loon-Plage. The piles were CFA piles with a common diameter of 420 mm. Further details can be found in Benzaria et al. 2013b and 2013d.

Due to the presence of a cohesive layer of poor geotechnical properties below 12 m depth and the limitations of the cyclic jack (maximum cyclic amplitude of 1000 kN) the length of the piles was limited to:

- 10.5 m for piles tested in tension
- 8 m for piles tested in compression.

1.3 *Response of bored piles under static loading*

The response of Pile F4 under the static reference test in compression is described in Benzaria et al. 2013b and 2013d. Typical t-z curves in Dunkirk sand derived from extensometer measurements are shown in Figure 15. Ultimate skin frictions are low (in the range 20 kPa to 45 kPa) with regard to the high values of cone resistances (10 MPa to 30 MPa) and relative density ($I_D \sim 80\%$). Mobilisation of friction is slow and requires about 3% of local relative displacement.

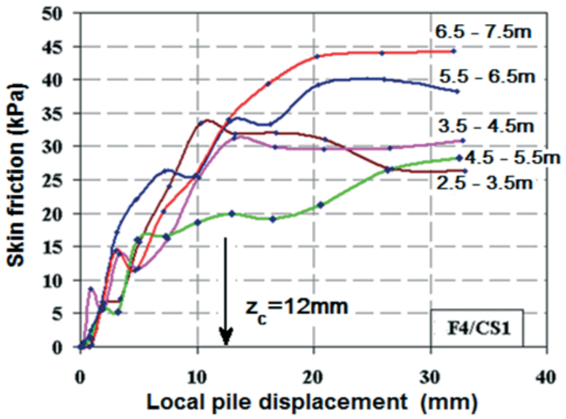

Figure 15: LOON-PLAGE field tests. Static shear strength transfer curves in Flanders sand for bored pile F4

The reference ultimate capacity of the bored piles is:

- 1 100 kN for the 8 m long piles in compression (test F4S1)
- 820 kN for the 10.5 m piles in tension (test F1S1)

1.4 *Response of bored piles under cyclic loading*

4.1.1 *Cyclic tests on virgin piles*

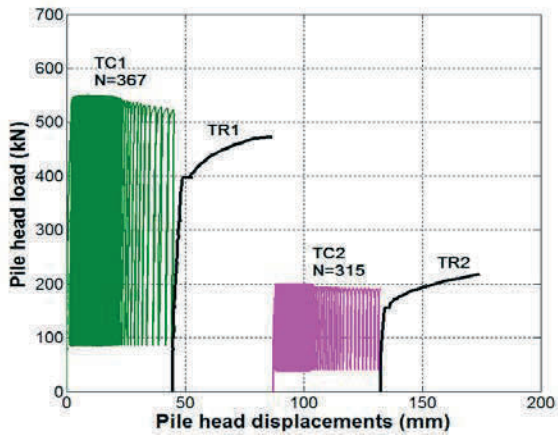

Figure 16: LOON-PLAGE field tests. Pile head load-displacement relationships on bored pile F2. One-way tension loading

Two cyclic tests were performed respectively on Pile F2 (tension TC1) and Pile F5 (compression CC1) before these piles were submitted to any other loading. The loading characteristics were very similar (Q_a / Q_{us} ~ 0.36; Q_{cy} / Q_{us} ~ 0.27; Q_{max} / Q_{us} ~ 0.63).

Pile F2 (Figure 16) rapidly cumulated permanent displacements under TC1. The rate of pile head displacements accelerated constantly and the test was stopped after 387 cycles when the pile had reached a total relative displacement of 10% (42 mm). A subsequent rapid load test TR1 indicated that the post cyclic capacity had dropped to 480 kN (58% of reference static capacity). A second cyclic test was applied at a ratio Qmax/Qut = 0.42, Qut being the ultimate capacity measured in TR1. The pile reached failure after 315 cycles and the rapid load test TR2 showed that the post-cyclic capacity was reduced to 220 kN.

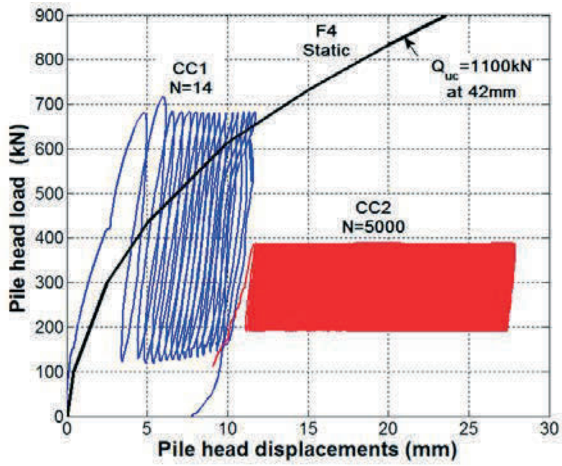

Figure 17: LOON-PLAGE field tests. Pile head load-displacement relationships on bored pile F5. One-way compression

Pile F5 (Figure 17) also rapidly cumulated large permanent displacements under CC1. The test had to be stopped after 14 cycles and 3% of relative displacement (instability of a reaction pile). A drastic reduction of the maximum cyclic load to 390 kN was insufficient to stabilise the pile: 5000 cycles at this level generated more than 15 mm of additional displacement.

4.1.2 *Cyclic tests on prefailed piles*

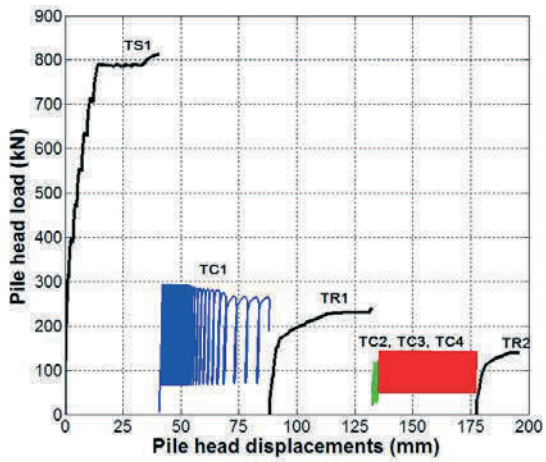

Figure 18: LOON-PLAGE field tests. Pile head load-displacement relationships on bored pile F1. One-way tension loading

Figure 18 illustrates the loading in tension applied on Pile F1. The cyclic test TC1 carried out after the static reference test TS1, despite a very low load ratio ($Q_{max}/Q_{ut} = 0.36$), led the pile to failure after only 126 cycles. The post cyclic capacity dropped to 240 kN. Further testing continued to reduce the capacity.

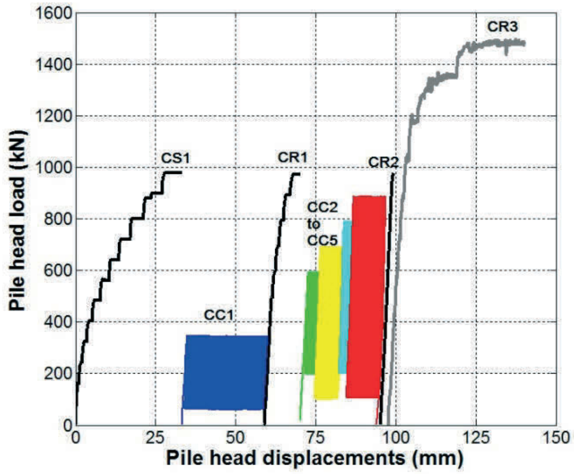

Figure 19: LOON-PLAGE field tests. Pile head load-displacement relationships on bored pile F4. One-way compression loading

The loading in compression applied on Pile F4 is shown on Figure 19. A low cyclic ratio (Q_{max}/Q_{uc} = 0.32) was selected for the first cyclic test CC1 applied after the static reference test CS1. The pile had more than 3% (12 mm) of relative pile head displacement after a batch of 2000 cycles. At the end of this loading sequence the post-cyclic capacity determined by test CR1, stopped at 1000 kN, was not reduced and the pile stiffness had increased. Four batches of 100 or 200 cycles with increasing load characteristics were then applied. They generated significant additional pile head displacements but simultaneously the pile stiffness increased as evidenced by test CR2. Test CR3 was conducted to failure (10% of additional pile displacement) and demonstrated that the post-cyclic capacity of the pile was 35% higher than the initial reference static capacity.

4.1.3 *Failure criterion*

The cyclic response of bored piles in Dunkirk sand can be summarised as follows:

- Bored piles in the dense Flanders sands were found to be very sensitive to cyclic loading;
- The response of the piles to cyclic loading is highly dependent of the loading history;
- Tests on prefailed piles cause cyclic failure of the piles for dramatically low Q_{max}/Q_{us} ratios;
- Tests on virgin piles indicate a better resistance to cyclic loading but moderate ratios of Q_{max}/Q_{us} generate significant pile head displacements which cumulate with number of cycles. Similar responses are observed in tension and compression.
- For piles in tension, failure could be defined in a conventional manner (i.e. 10% of relative pile head displacement)
- For piles in compression, the conventional definition is insufficient to describe the complexity of the phenomena. As explained in Benzaria et al. 2013, cyclic loads generate first a reduction in skin friction accompanied by permanent pile head displacements. After significant displacement of the pile toe, the end bearing mobilisation compensates the loss in frictional capacity. Cyclic loading may simultaneously induce progressive compaction of the sand below the toe and increase the end bearing resistance of the pile, resulting in an increase of the total pile capacity. Strictly speaking, no failure of the pile can be observed for maximum cyclic loads remaining below the initial reference static capacity. However cumulated pile head displacements can rapidly reach values well in excess of those tolerated for the in-service conditions of the pile.

When interpreting the Loon-Plage tests, the criterion for cyclic failure was set to 12 mm i.e. 3% of relative pile head displacement. This value corresponds to the initiation of large (plastic) displacements in the static tests and also to the local displacement required for full mobilisation of the skin friction. This criterion was applied for both tension and compression loading.

4.1.4 *Cyclic interaction diagrams*

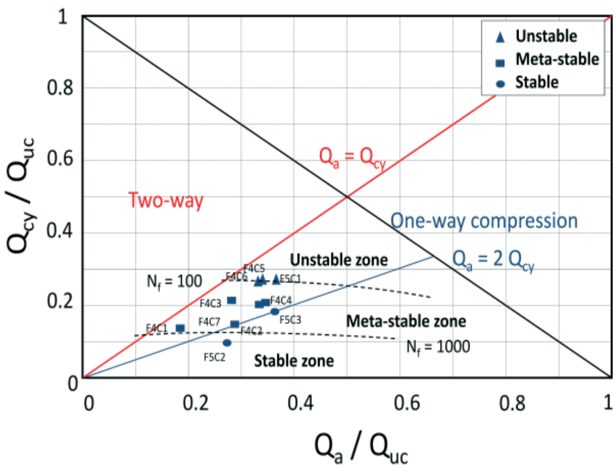

Figure 20: LOON-PLAGE field tests. Cyclic interaction diagram for bored piles in one-way compression

An interaction diagram for bored piles in one-way compression was developed for the Loon-Plage tests (Figure 20). This diagram is based on the following assumptions:

- Cyclic loads Q_{ave} and Q_c are normalised by the value of the static capacity Q_{uc} measured just before the cycling sequence is applied;
- The criteria for defining cyclic failure is set at 3% relative pile head displacement (0.03D = 12 mm)

Three zones can be defined:

- In the *unstable* zone, cyclic failure is reached for a small number cycles ($N_f < 100$)
- The *stable* zone corresponds to small amplitude cyclic load tests where piles did not reach the criterion and the rate of displacement was very low. For more details, please see Puech et al. 2013a and 2013b.
- In the intermediate *metastable* zone the piles reached failure for a number of cycles between 100 and 1000.

One important observation is the very limited extent of the stable zone. It may be argued that results are biased because most of the plots in the graph are derived from cyclic tests performed on the same piles.

Cyclic tests were performed in the IFSTTAR centrifuge under the following conditions:

- Fontainebleau sand, density index ID = 0.70,
- Model piles at 1/23 scale, simulating the in situ piles,
- Piles preinstalled in container and sand poured around piles by pluviation: this is representative of precast piles;
- Eight piles per container; one reference static test per container; all cyclic tests performed on virgin piles and compared to the reference static test.

The interaction diagram for the model tests is given on Figure 21 (refer to Guefresh et al. 2012 and Puech et al. 2013 for more details). Both in situ and model test diagrams are very close, which supports the validity of the findings.

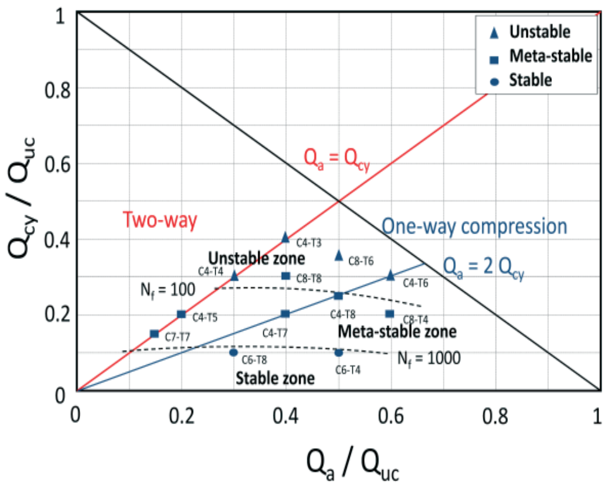

Figure 21: Centrifuge model tests in dense Fontainebleau sand. Cyclic interaction diagram for cast-in-place piles in one-way compression

5 SOLCYP METHODOLOGY FOR CYCLIC PILE DESIGN

The full design of a pile subject to cyclic loads may call for relatively complex procedures which may not be justified in every day's practice. The relative success of standard engineering approaches (which basically ignore potential effects of cyclic loads) suggests that in most cases cyclic loads can be accommodated by expert engineering judgement and reasonably conservative assumptions. However this is not always the case. Graduated approaches are proposed corresponding to increasing complexity and criteria are being developed to determine which level of analysis is appropriate to the case considered.

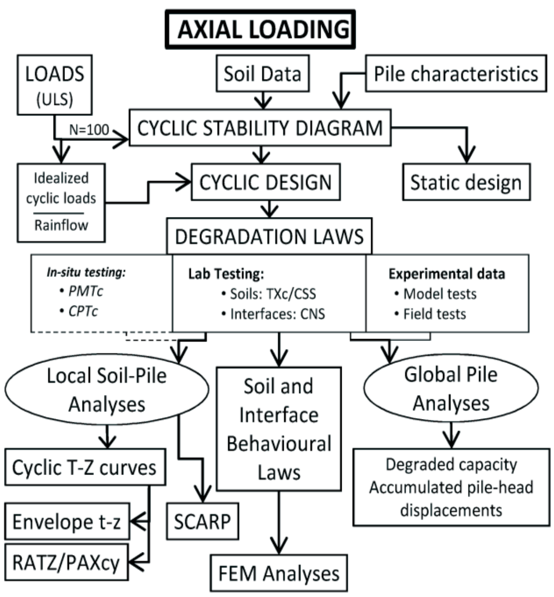

Figure 22: SOLCYP flow chart for designing piles under axial cyclic loading

Criteria should integrate the following:

- Sensitivity of the structure to foundation displacements and rigidity;
- Relative importance of the cyclic load component (characterised by the ratio Q_{cy} / Q_a of the cyclic amplitude to the average load)
- The nature of the soil and its more or less degradation potential to cycles;
- Potential human, environmental or economical consequences of a poor foundation response.

The proposed design philosophy is illustrated by the flow chart in Figure 22. The methodology is discussed briefly below. At this stage SOLCYP's efforts have mainly concentrated on acquiring high quality test data. In-depth interpretation of these data will require additional time and human investment. The aim of section 5 is to show where and how SOLCYP data can contribute to make significant advances.

1.5 *Cyclic stability diagrams*

Axial loading interaction diagrams may offer useful guidance to assess whether cyclic loading could be critical for a given soil-pile configuration.

Pile characteristics and soil data required for a reliable static design and loads are assumed available. It is recognised that loading is often only characterised by the ULS load (maximum load under extreme environmental conditions). The composition of the average and the cyclic components in the ULS design storm must also be known to make even a screening assessment.

As a first estimate, a pile's potential sensitivity to cyclic loading can be gauged by comparing the ULS event, as defined by the (Q_{cy} / Q_{us}; Q_a / Q_{us}) load point, with the zero damage contour and other contours (for example that for N_f = 100) at which significant damage is likely.

An example of such a screening analysis for several offshore jacket platforms with different operational and environmental conditions is given in Jardine at al. (2012).

Cyclic stability diagrams must be established from high quality model or field tests performed in various soil conditions and involving different pile installation methods and cyclic loading modes. Until recently, a very few diagrams were available. These included:

- Poulos (1988) diagrams, obtained from small laboratory model tests in carbonate materials and which are more conceptual than quantitative;
- Interaction diagrams from NGI (Karlsrud and Haugen, 1985) in clays of various plasticity indices and degrees of consolidation but only for driven metallic piles;
- The stability diagram for driven piles in Dunkirk sand by Jardine and Standing (2000);
- Approximate equations for deriving interaction diagrams based on analyses of existing data by Mittag and Richter (2005).

A major contribution of the SOLCYP project is the development of cyclic stability diagrams for different soil conditions (highly consolidated clay, sands at various relative densities), pile types (driven, bored, screwed) and loading modes (tension, compression, one-way and two-way).

1.6 *Parameters for cyclic design*

If the preliminary assessment suggests that the pile configuration may be critical and requires further attention, a detailed site-specific analysis should be undertaken.

For this type of analysis, as discussed in Puech et al. (2012), loads should be provided as series of cycles of regular amplitude. Procedures for transforming actual load histories can be found in e.g. BSH (2011). Dedicated software called

Cascade based on 'rainflow' analysis (ASTM E 1049-85) has been developed as part of the SOLCYP project.

The detrimental effect of cycles on soils or soil-pile interfaces can be determined by using (or combining) information from different sources.

Standard practice for the offshore industry is to determine the degradation of the soil properties (strength, stiffness, effective stress) in the laboratory by performing cyclic triaxial (TXc), direct simple shear (CSS) or hollow cylinder apparatus (HCA) tests. Degradation of soil-pile interfaces is also investigated by means of cyclic direct shear or constant normal stiffness (CNS) tests on steel-pile interfaces with appropriate roughness. "Guidelines for obtaining soil parameters for cyclic design" (Andersen et al. 2013) have been established under the umbrella of the TC 209 of the ISSMGE. They form part of these proceedings.

A significant contribution of the SOLCYP project is the creation of a database of cyclic CNS tests on Fontainebleau sand-steel interfaces (Pra-ai, 2013). Figure 23 illustrates the drop in normal effective stress as a function of the cyclic load characteristics and number of cycles for a high stiffness value.

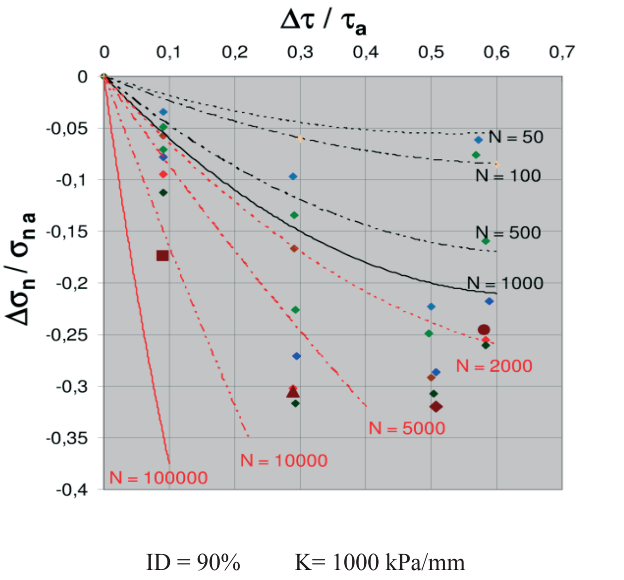

Figure 23: Cyclic Constant Normal Stiffness (CNS) interface tests on Fontainebleau sand. Evolution of normal effective stress with shearing amplitude and number of cycles (Pra-ai, 2013)

It is anticipated that degradation of soil properties might also be obtained from specifically devised in situ tests. This is being investigated with cyclic pressuremeter (PMTc) tests (Reiffsteck et al. 2013). Procedures have still to be developed and calibrated and these will be considered in the next French National project ARSCOP (see TC 101 proceedings).

The detrimental effect of cycles can also be captured from good quality experiments on model or field pile tests. Degradation laws are proposed by, for example, Poulos (1982) in various forms, the simplest of which is:

$$P_{(N)}/P_{(1)} = k.N^{-m} \qquad (4)$$

or

$$P_{(N)}/P_{(1)} = 1- t.Ln(N) \qquad (5)$$

where $P_{(N)}$ and $P_{(1)}$ are the value of the property P being considered (which can be undrained shear strength or radial effective stress) at cycle N and 1 respectively; m is an exponent depending on the type of soil; and k or t are factors depending on the average load and cyclic amplitude.

1.7 *Global pile analyses*

In global pile analyses, the axial capacity and the response of the pile head are first calculated under monotonic conditions. These results are then modified by applying degradation laws.

Jardine and Standing (2000) and Jardine et al. (2005) consider that in sands and clays shaft capacity reduces in step with the local effective stress changes and they set out a simple method for predicting the potential reduction of local shaft resistance for piles subject to groups of uniform load cycles.

Undrained DSS tests have shown that in cases where τ_{vh}/σ'_v < tan δ the relative losses in normal effective stress ($\Delta\sigma'_v/\sigma'_{vc}$) were nearly independent of the average shear stresses applied and could be expressed with reasonable accuracy as simple functions of the normalised cyclic shear stress amplitude ($\tau_{cyc}/\tau_{max,stat}$) and number of cycles (N) such as:

$$\frac{\Delta\sigma'_r}{\sigma'_{r0}} = A\left(B + \frac{\tau_{cy}}{\tau_{\max stat}}\right)N^C$$

Suitable laboratory tests (DSS, TX or HCA) may be undertaken to determine the material coefficients (A, B and C) and define rates of radial effective stress reduction under cycling for both clays and sands; see for example Jardine et al. (2011). This approach requires laboratory test samples to be consolidated to the radial effective stresses predicted by the ICP methodology. Noting that the average loss of radial effective stress broadly determines the loss of static shaft resistance (ΔQ_{stat}), the relative loss of shaft resistance (ΔQ_{stat} / $Q_{max,\ stat}$) can be expressed as a similar function of the normalised cyclic load amplitude (Q_{cy} / $Q_{max,\ stat}$) as follows:

$$\frac{\Delta Q_{stat}}{Q_{\max stat}} = A\left(B + \frac{Q_{cy}}{Q_{\max stat}}\right)N^C$$

This expression can be manipulated to make explicit predictions for cyclic losses during specified storms by adjusting between packages of cycles following an 'equivalent number of cycles procedure'. This procedure has been applied for oil and gas platform piles (Atkins, 2000; Jardine et al., 2011; Jardine et al., 2012).

Jardine et al. (2005) recommend that laboratory tests to determine the A, B, C coefficients are performed at constant volume (assuming infinite radial pile stiffness). DSS constant volume cyclic tests are being performed on the Merville clay with the aim of comparing predicted and observed losses in shaft resistance. Constant volume DSS tests and also constant normal stiffness (CNS) tests are being performed on Fontainebleau and Loon-Plage sands.

Typical evolutions of permanent pile head displacements under maximum cyclic load Z_{max} are shown on Figure 24 for Loon-Plage tests. Similar trends have been obtained in centrifuge model tests (Guefresh et al., 2012). Three types of behaviour are observed:

- Under severe cyclic loading, displacements increase rapidly until failure occurs;
- Under low cyclic loading, displacements tend to stabilise at high number of cycles (rate of displacement decreases);
- For intermediate loading cases, an acceleration of the rate of displacements can follow a phase of pseudo-stabilisation.

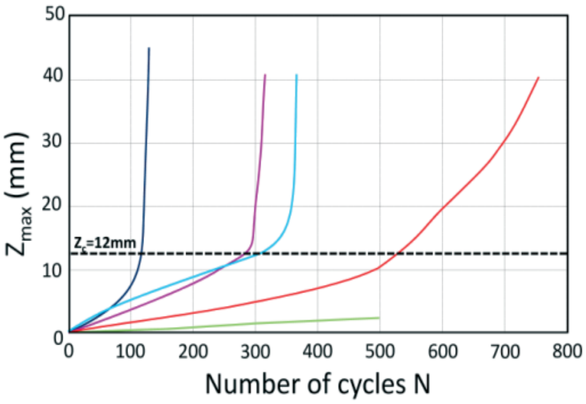

Figure 24: Typical evolution of permanent pile head displacement under maximum cyclic load for bored piles at LOON-PLAGE

In the stabilisation or pseudo-stabilisation phases the evolution of permanent displacements can be described by degradation laws of the type:

$$Z(N)/Z(1) = k.N^m \quad \text{or} \quad Z(N)/Z(1) = 1+t.\text{Ln}(N)$$

with: m = exponent depending on soil nature, k and t = functions of loading characteristics (Q_a and Q_{cy}), rigidity of pile-soil system and mode of installation.

Determination of sets of m, k and t coefficients from SOLCYP field and model tests is currently in progress.

Global approaches do not take into account the natural variability of soils along the pile shaft and ignore a fundamental mechanism which is the progressive degradation of the shaft friction from the pile head to the pile toe as a result of pile flexibility. These methods should be limited to the analysis of relatively short (rigid) piles and for cases where the soil conditions are relative homogeneous over the upper half-length of the pile.

1.8 *Local beam column analyses*

For long flexible piles or where soil conditions vary significantly along the pile shaft, local beam column analyses are more appropriate. The local relationship between pile displacement and skin friction resistance at the pile soil interface is modelled by transfer curves commonly called t-z curves. Monotonic t-z curves for standard soil conditions (clays and sands) are recommended in e.g. API RP2GEO (2011) and are commonly used in the offshore oil and gas industry.

Three types of approaches might be considered for taking into account the effect of cyclic loading:

- Using t-z cyclic envelope curves aimed at describing the quasi-static pile response of a pile at the end of a major cyclic event (e.g. a centennial storm). This approach is used for lateral cyclic loading where "cyclic" envelope curves are proposed. However the method has a number of limitations (Jardine et al., 2012). Envelope t-z curves are not proposed in standards;

- Using « degraded » t-z curves: monotonic curves are modified using degradation laws (of the type described in section 1.7) which account for load characteristics and number of cycles. High quality model or field test data, where local measurements of unit skin friction are available, are needed to derive the degradation parameters. SOLCYP data are presently analysed in this respect;

- Using "true cyclic" t-z curves, i.e. cyclic curves describing the behaviour of the interface cycle by cycle. Algorithms for generating such curves are proposed by several authors and are included in specialised software.

Three examples of simplified computer codes that can be potentially applied in practical cyclic analyses are outlined in Jardine et al., 2012: RATZ (Randolph, 1994), SCARP (Poulos, 1989) and PAXCY/PAX2 (Karlsrud et al., 1986). It has been observed from simulation of reference cases that these computer codes:

- Are able to describe satisfactorily the monotonic response of the piles,
- Have good potential to describe qualitatively the cyclic response of the piles.

However their use for industrial cases is very limited. This can be explained by the following reasons:

- RATZ and SCARP are calibrated for carbonate sediments. Data are missing for standard materials,
- PAXCY/PAX2 are only applicable in clays and extensive require series of cyclic laboratory tests.

Before reliable quantitative predictions can be expected, it is essential that i) each programme can be tested and validated under different situations (soil conditions and pile types) and ii) calibration parameters can be supplied for usual soil and pile conditions. SOLCYP experimental data are expected to provide a sound basis to support such work.

1.9 *FEM analyses*

In the implicit, time domain, procedure, each cycle is calculated with an appropriate constitutive model and iterated over many small strain increments. This procedure becomes difficult as soon as the number of cycles becomes significant (say 50) because (i) computational resource costs become high and (ii) errors can accumulate with the constitutive models and integration algorithms that may be employed. Completely implicit numerical analyses appear to be principally of academic interest at present (Jardine et al. 2012).

When considering large numbers of cycles, the explicit procedure in the sense of Wichtman (2005) appears more appropriate. The accumulation of residual strains developing under cycling is treated in a similar way to the problem of creep under constant load.

Modelling approaches are being investigated within the SOLCYP project. As described by Papon (2010), Cao et al. (2012) and Bagigli (2011), these include:

- Implementation and comparison of constitutive models including bounding surface and multiple kinematic bubble yield surface approaches;
- Implementation of constitutive laws for soil-structure interfaces;
- Treatment of large number of cycles using the skipped cycle and time-homogenisation schemes.

Pra-ai (2013) proposes a promising approach of the explicit type where interface cyclic pseudo-creep functions are derived from results of CNS tests devised to simulate the evolution of the normal effective stress with number of cycles. The procedure needs further improvement and calibration but appears feasible for practical applications.

6 CONCLUSION

The joint industry project SOLCYP is aimed at providing better understanding of the physical phenomena which condition the response of piles to vertical and horizontal cyclic loads and at developing advanced methods for designing piles under cyclic loading.

The behaviour of bored and driven piles under axial cyclic loading in sands and clays has been investigated through a range of laboratory, field and theoretical approaches. A large part of the experimental programme is complete at the time of issue of this paper. The most significant test data presently available are discribed with a particular focus on field data. The response of piles installed in overconsolidated Flanders clay (MERVILLE site) and dense sands (LOON-PLAGE site) is discussed.

In the second part of the paper, it is shown how the high quality data obtained can be used to develop improved design methodologies for piles under cyclic axial loading. The SOLCYP design philosophy is based on a gradual approach. The necessity to proceed to a detailed cyclic design is first assessed by comparing the characteristics of the cyclic loads to a relevant cyclic pile stability diagram. A major contribution of SOLCYP is the provision of cyclic stability diagrams for bored and driven piles, in sands and overconsolidated clays, for all loading modes (tension, compression, two-way). Further interpretation work is required but it is expected that significant advances for cyclic pile design will be possible in three directions: i) *global* pile analyses (proposing degradation laws for describing accumulation of pile head displacements and degradation of pile capacity) ii) *local* beam column analyses (developing or calibrating algorithms for generating appropriate transfer curves) and iii) simulating cyclic axial pile responses by *finite element*s using explicit procedures.

A companion paper (Garnier 2013) focuses on SOLCYP's contribution to the design of piles under cyclic lateral loading.

7 ACKNOWLEDGEMENTS

The author wishes to acknowledge the many contributions made by his colleagues at CERMES, Ecole Centrale de Lyon, Ecole Centrale de Nantes, IFSTTAR, 3SR Grenoble, Polytech' Lille and Fugro GeoConsulting.

The experimental work reported in this paper was directed by Dr J. Garnier, Dr A. Le Kouby, Dr L. Thorel at IFSTTAR and Prof. P. Foray at 3SR. Special thanks to O. Benzaria and A. le Kouby who conducted the in situ pile tests at Merville and Loon-Plage. The high level of quality and reliability of SOLCYP's experiments is acknowledged.

The expertise and advice provided throughout the project by Professor R. Jardine (Imperial College of London, UK) and Professor A. Holeyman (Université Catholique de Louvain, Belgium) are highly appreciated.

The author is pleased to acknowledge the significant contributions to the project of: Y. Bagagli, M. Boulon, S. Burlon, J. Canou, J. Cao, N. Chenaf, C. Dano, A. Guefresh, M. Khemakhem, H. Mroueh, A. Papon, S. Pra-ai, G. Rault, J. Rakotonindriana, P. Rimoy, F. Rocher-Lacoste, F. Rosquoët, M. Silva, B. Tali, C. Tsuha, E. Vincens.

The author gratefully acknowledges the technical support provided by IREX and the financial support provided by Agence Nationale de la Recherche (ANR), Ministère de l'Ecologie, du Développement Durable et de l'Energie (MEDDE), Fédération Nationale des Travaux Publics (FNTP) and the fourteen sponsors of the SOLCYP project.

8 REFERENCES

AFNOR.1999. NF P 94-150-2 Norme Française. Sols: Reconnaissance et Essais – Essai statique de pieu sous effort axial – Partie 1: en compression et Partie 2: en traction.

Andersen K., Puech A. and Jardine R. 2013. Guidance for obtaining soil parameters for design of foundations under cyclic loading. *Proceedings TC 209 Workshop, 18 ICSMGE*, Paris, 2-5 September 2013

API RP2GEO. 2011. API Recommended Practice, Geotechnical and Foundation Design Considerations, First Edition, April 2011.

Atkins Consultants Ltd. 2000. Cyclic degradation of offshore piles. HSE Offshore Technology Report OTO 2000 013. Health and Safety Executive, London.

Bagigli Y. 2011. Modélisation du comportement cyclique des sols et des interfaces sol-structure, *Thèse*, Ecole Centrale de Lyon

Benzaria O. 2013. Contribution à l'étude du comportement des pieux isolés sous chargements cycliques axiaux. *Thèse.* Université de Paris-Est, A paraître.

Benzaria O., Puech A. and Le Kouby A. 2012. Cyclic axial load-tests on driven and bored piles in overconsolidated clay, *Offshore Site Investigation and Geotechnics*, SUT, London.

Benzaria O., Puech A. et Le Kouby A. 2013a. Essais cycliques axiaux sur des pieux forés dans l'argile des Flandres. *Proceedings 18th ICSMGE, Paris,* 2-5 September 2013

Benzaria O., Puech A. et Le Kouby A. 2013b. Essais cycliques axiaux sur des pieux forés dans des sables denses. *Proceedings 18th ICSMGE,* Paris, 2-5 September 2013

Benzaria O., Puech A. and Le Kouby A. 2013c. Cyclic axial load tests on bored piles in overconsolidated Flanders clay. *Proceedings TC 209 Workshop, 18 ICSMGE*, Paris, 2-5 September 2013

Benzaria O., Puech A. and Le Kouby A. 2013d. Cyclic axial load tests on bored piles in dense sands. *Proceedings TC209 Workshop, 18 ICSMGE*, Paris 2-5 September 2013

Bond A.J. and Jardine R.J. 1991. Effects of installing displacement piles in a high OCR clay. *Géotechnique*, 41(3) 341-363.

Brucy F., Meunier J. and Nauroy J.F. 1991. Behaviour of a pile plug in sandy soils during and after driving. *Proc. 23rd Offshore Technology Conference,* OTC paper 6514, Houston, Tx

BSH - a) Standard: Design of Offshore Wind Turbines. 2007. and b) Guidance for use of the BSH standard „Design of Offshore Wind Turbines" 2011, Federal Maritime and Hydrographic Agency (BSH), Hamburg and Rostock

Cao J., Mroueh H. and Burlon, S. 2012. Skipped cycles method for geotechnical structures under large number of cycle loads, *Offshore Site investigation and Geotechnics*, SUT, London

DnV. 1992. Classification Note 30-4, Foundations. Det Norske Veritas, Oslo

DnV-OS-J101. 2010. Design of Offshore Wind Turbines Structures, DnV Offshore Standards, Det Norske Veritas, Oslo.

Garnier J. 2013. Advances in lateral cyclic design: contribution of the SOLCYP project. *Proceedings TC209 Workshop, 18 ICSMGE*, Paris 2-5 September 2013

GL Rules and Guidelines. 2007. IV Industrial Services. Part 6 - Offshore Technology, Germanischer Lloyd, 2007.

Guefrech A., Rault G, Chenaf N., Thorel L., Garnier J., Puech A. 2012 Stability of cast in place piles in sand under axial cyclic loading . *Proc. 7th Int. Conf. Offshore Site investigation and Geotechnics*. London. 12-14 Sept. pp.329-334.

International Society for Soil Mechanics and Geotechnical Engineering (ISSMGE). 1985. Axial pile loading test – part 1: static loading. Geotechnical Testing Journal 8.

ISO 19 902. 2007. International Standard – Petroleum and natural gas industries – Fixed steel offshore structures.

Jardine R.J. and Standing J.R. 2000. Offshore Technology Report, OTO 2000 008, Pile load testing for HSE cyclic loading study at Dunkirk, France, Vol.1 and 2, HSE Books, UK.

Jardine R.J., Chow FC, Overy RF and Standing J.R. 2005. ICP design methods for driven piles in sands and clays". Thomas Telford Ltd, London p. 105.

Jardine R.J., Standing J.R. and Chow F.C. 2006. Some observations of the effects of time on the capacity of piles driven in sand. Geotechnique, 56 (4), 227-244.

Jardine R.J. and Chow F.C. 2007. Some developments in the design of offshore piles. Keynote Paper. Proc. 6th Int. Conf. on Offshore Site Investigations and Geotechnics, SUT London, p. 303-332.

Jardine R., Bitang Z., Foray P., and Dalton C. 2009. Experimental Arrangements for Investigation of Soil Stresses Developed around a Displacement Pile. Soils and Foundations, 49(5), 661–673.

Jardine R.J., Aldridge T. and Evans T.G. 2011. Offshore foundation engineering in extremely dense glacial tills west of the Shetland Islands. Proc. ECSMGE, Athens.

Jardine R.J. and Standing. 2012. Field axial cyclic loading experiments on piles driven in sand. *Soils and Foundations*, 52(4), 723–736.

Jardine R, Puech A and Andersen K. 2012. Cyclic loading of offshore piles: potential effects and practical design. *Proc.7th Int. Conf. on Offshore Site Investigations and Geotechnics,* SUT, London, 59-100

Karlsrud K. and Haugen T. 1985. Behaviour of Piles in clay under cyclic axial loading-results of field model tests, *Proc. Behaviour of Offshore Structures, BOSS'85,* pp. 589-600.

Karlsrud K., Nadim F. and Haugen T. 1986. Piles in clay under cyclic loading: Field tests and computational modelling. *Proc. 3rd Int. Conf. on Num. Meth. in Offshore Piling,* 165-190, Nantes, France, May 1986.

Mittag J. and Richter T. 2005. Beitrag zur Bemessung von vertikal zyklisch belasteten Pfählen. In: *Festschrift zum 60. Geburtstag von Prof. Dr.-Ing. H.-G. Kempfert,* Heft 18 der Schriftenreihe Geotechnik Universität Kassel.

Papon A. 2010. Modélisation numérique du comportement des sols sous très grand nombre de cycles. Homogénéisation temporelle et identification des paramètres, *Thèse*, Ecole Centrale de Nantes, 152pp.

Poulos H. G. 1982. Single Pile Response to Cyclic Lateral Load, *Journal of the Geotechnical Engineering Division*, Proceedings ASCE, Vol.108, No.GT3, 355-375.

Poulos H.G. 1988. Cyclic stability diagram for axially loaded piles. *Journal of Geotechnical and Geoenvironmental Engineering*. 114 (8): 877-895

Poulos H.G. 1989. SCARP USERS'S MANUAL, Centre for Geotechnical Research, The University of Sydney, Australia

Puech A., Canou J., Bernardini C., Pecker A., Jardine R., and Holeyman A. 2012. SOLCYP: a four year JIP on the behaviour of piles under cyclic loading. *Offshore Site Investigation and Geotechnics*, SUT, London.

Puech A. 2013. Advances in axial cyclic pile design: contribution of the SOLCYP project. *Proceedings TC 209 Workshop, 18 ICSMGE*, Paris, 2-5 September 2013

Puech A. et Benzaria O. 2013a. Effet du mode de mise en place sur la réponse statique et cyclique de pieux dans l'argile surconsolidée des Flandres. *Proceedings 18th ICSMGE, Paris,* 2-5 Septembre 2013

Puech A. and Benzaria O. 2013b. Effect of installation mode on the static and cyclic response of piles in overconsolidated Flanders clay. *Proceedings TC 209 Workshop, 18 ICSMGE*, Paris, 2-5 September 2013

Puech A., Benzaria O., Thorel L., Garnier J., Foray P. et Jardine R. 2013a. Diagrammes de stabilité cyclique de pieux dans les sables. *Proceedings 18th ICSMGE, Paris,* 2-5 Septembre 2013

Puech A., Benzaria O., Thorel L., Garnier J., Foray P. et Jardine R. 2013b. Cyclic stability diagrams of piles in sands. *Proceedings TC 209 Workshop, 18 ICSMGE*, Paris, 2-5 September 2013

Pra-ai S. 2013. Behaviour of soil-structure interfaces subjected to a large number of cycles. Application to piles. *Thesis*, University of Grenoble, 353p.

Randolph M.F. 1994. RATZ program manual: Load transfer analysis of axially loaded piles. Dept. of Civil & Resource Engineering, University of Western Australia

Reiffsteck P., Fanelli S., Tacita J.L., Dupla J.C. and Desanneaux G. 2013. Utilisation des essais d'expansion cyclique pour définir des modules élastiques en petites déformations. *Proceedings 18th ICSMGE,* Paris, 2-5 Septembre 2013

Rimoy S.P., Jardine R.J., Silva M., Foray P.Y., Tsuha C.H.C and Yang, Z. 2012. Local and global behaviour of cyclically loaded instrumented model displacement piles in sand. *Proc 7th Int. Conf. on Offshore Site Investigations and Geotechnics,* SUT London.

Rimoy S., Jardine R. and Standing J. 2013. Displacement response to axial cyclic loading of driven piles in sand. *Proceedings 18th ICSMGE,* Paris, 2-5 September 2013

Tsuha C., Foray P., Jardine R., Yang Z., Silva M., Rimoy S. 2012. Behaviour of displacement piles in sand under cyclic axial loading. *Soils and Foundations 52(3), June 2012, 393–410,*

Wichtmann T. 2005. Explicit Accumulation Model for Non-Cohesive Soils under Cyclic Loading, In Th. Triantafyllidis (Ed.), Schriftenreihe des Institutes für Grundbau und Bodenmechanik der Ruhr-Universität Bochum, Heft 38.

Advances in lateral cyclic pile design: Contribution of the SOLCYP project

Avancées dans le dimensionnement des pieux sous chargement cyclique latéral : contribution du projet SOLCYP

J. Garnier
LUNAM University – IFSTTAR Nantes

ABSTRACT: The SOLCYP joint industry project aims to develop improved design methodologies for piles submitted to axial or lateral cyclic loading. This paper presents the results of several centrifuge model test programs carried out as part of SOLCYP on the response of single piles to lateral loads in sand and in clay. Based on these test data and results of other published studies, two methods are proposed to take into account the cyclic load effects in lateral pile design.

RÉSUMÉ : Le projet de recherche SOLCYP a pour objectif d'améliorer les méthodes de dimensionnement des pieux sous charges cycliques, axiales ou latérales. L'article présente les résultats de plusieurs programmes d'essais, conduits dans le cadre de SOLCYP, sur des pieux sur pieux modèles centrifugés soumis à des charges latérales monotones et cycliques, dans des sables et des argiles. A partir des données expérimentales recueillies et des résultats d'autres études publiées, deux méthodes ont été développées et sont proposées pour prendre en compte les effets de charges cycliques lors du dimensionnement des pieux.

KEYWORDS: Pile, design, cyclic lateral load, sand, clay.

1 INTRODUCTION

Efficient methods based on P-y reaction curves are used to design piles under lateral loads but, except for the offshore structures adhering to API RP 2GEO (2011), DnV Foundations (1992) or ISO 19902 (2007) rules, these methods are limited to static loads. For example, the Eurocode 7 and the French new code on piles being published soon (NF P 94 262) mention the probable effects of cycles but do not advise how to take them into account. To address the present lack of guidance regarding piles under cyclic loading, a committee working under the umbrella of the French National Agency IREX (Institute for experimental research) called for a national engagement in an ambitious research and development project. The objectives and overall technical content of the SOLCYP project are described in more details in Puech et al. (2012). The project aims to develop several approaches for designing piles under cyclic axial or lateral loads. A companion paper (Puech, 2013) summarises the findings of the SOLCYP project for cyclic axial loading. This paper is devoted to findings for lateral cyclic loading.

Two approaches were investigated for lateral cyclic pile design:

- **global** pile analyses: the pile head displacements and the maximum pile moment are first calculated under static conditions at the maximum applied load. Results are then modified to take into account the effect of cycles by applying so called degradation laws;
- **local** beam column analyses: soil-pile interactions are described by local transfer curves called P-y curves. Whereas static transfer curves are proposed in standards for usual soil types, cyclic transfer curves capturing the effect of the cyclic loading amplitude and of the number of cycles are not available. New approaches are proposed to derive these cyclic transfer curves from the static curves.

A large amount of new test data was needed for developing these different approaches. To investigate the response of piles to cyclic lateral loading, extensive centrifuge tests were performed on model piles using the IFSTTAR (formerly LCPC) geotechnical centrifuge in Nantes.

One-way and two-way cyclic tests were performed on instrumented model piles cast-in-place in medium dense and dense Fontainebleau sand and soft normally consolidated and stiff overconsolidated Speswhite clay. Typical results can be found in Khemakhem (2012), Khemakhem et al. (2012), Rakotonindriana (2009), Rosquoët (2004) and Rosquoët et al. (2013). The main objective was to derive degradation laws of pile displacement and bending moment for global pile analyses or degraded p-y curves for local pile analyses as mentioned above.

2 EXPERIMENTAL METHODOLOGY

Centrifuge modelling was used since this technique is suitable for parametric studies where large amounts of data are obtained from controlled repeated tests. In total, 62 cyclic lateral loading tests were performed in sands (some up to 75 000 cycles) and 36 tests in clay. The cyclic lateral loads are defined by the parameters shown in Figure 1.

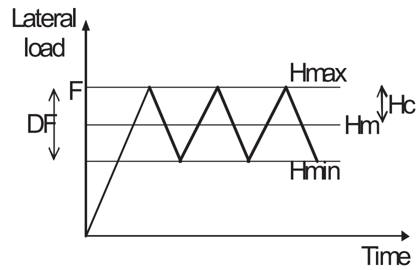

Figure 1: Definition of cyclic load sequences

The amplitude of the cycles may be given by the ratio DF / F or H_c /H_{max} or by the cyclic load ratio $R_H = H_{min} / H_{max}$. One-way loading corresponds to DF / F < 1 (and $R_H > 0$).

It must be noted that, in this study, only in-service conditions were investigated with the maximum lateral load H_{max} applied during the tests being limited to about one third the lateral ultimate capacity H_u. It is assumed that, from a practical point of view, before being designed under any cyclic load sequence, a pile must first and foremost be able to statically withstand the maximum applied load H_{max} with a sufficient safety margin.

The lateral bearing capacity H_u was determined by static load tests. No peak load was observed during these static tests but the load-displacement curves show two nearly linear branches separated by a clear inflexion point (Figure 2). Results showed that the change in curvature occurs at a displacement of the pile head between 20% and 25% its diameter, in both sand and clay.

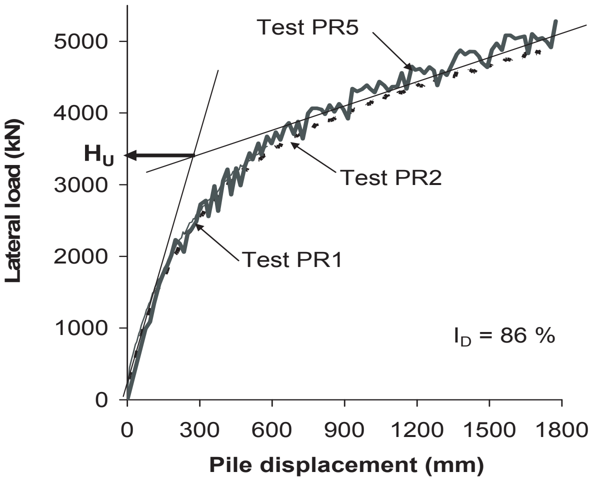

Figure 2: Example of estimation of the ultimate lateral resistance H_u from three static load tests in dense sand (from Rosquoet, 2004)

2.1 Model piles and instrumentation

Model piles at a scale of 1/40 in sand and 1/50 in clay were tested respectively under 40-g and 50-g accelerations. Table 1 shows the geometrical and mechanical properties of prototypes (true scale) piles simulated by these centrifuge models. In respect of the soil characteristics, these piles may be considered flexible. The piles were instrumented with 20 pairs of strain gauges for determining the bending moment profiles during the load tests.

Table 1: Properties of the true scale simulated piles

Parameters	Tests in sand	Tests in clay
Material	Steel	Steel
Penetration depth D (m)	12	16
Pile diameter B (m)	0.72	0.9
Wall thickness e (mm)	17.5	15
Bending stiffness EI ($MN.m^2$)	476	895

Monotonic and cyclic loads were applied using servo-jacks that were load controlled for the cyclic loading tests. In addition, the pile displacements and rotation were recorded by several horizontal and vertical transducers (Figures 3a and 3b).

Cyclic sequences are defined by number of cycles N (or n), frequency f, mean applied load H_m and cyclic load half amplitude H_c. During a cycle, the load varies between $H_{max} = H_m + H_c$ and $H_{min} = H_m - H_c$. Both one-way and two-way load tests were carried out.

In dry sand, preliminary tests showed that the cyclic load frequency has no influence on the pile response in the range tested (0.1 Hz to 1 Hz). In soft saturated clay, the loading rate was kept in the undrained range as determined by House et al. (2001) from T-bar tests carried out in the UWA centrifuge.

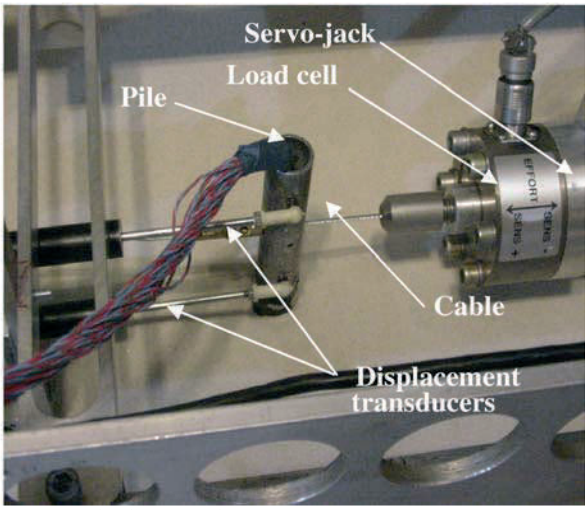

a – One-way loading (H_{min} / $H_{max} > 0$)

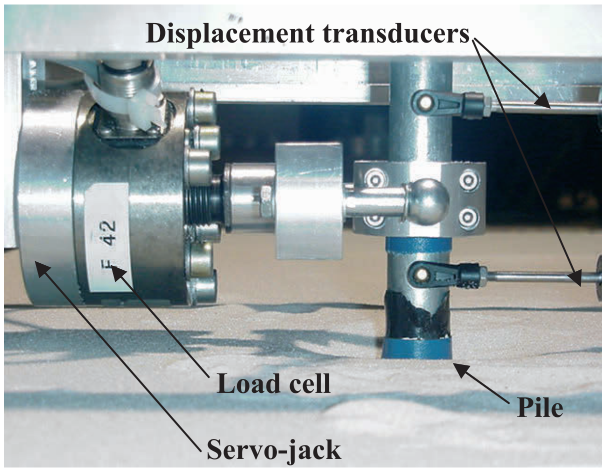

b – Two-way loading (H_{min} / $H_{max} < 0$)

Figure 3: Experimental equipment used for the pile lateral load tests

2.2 Soil samples

Dry Fontainebleau sand samples ($d_{50} = 0.2$ mm) were prepared at two densities ($I_D = 53\%$ and 86%) by a raining technique using the IFSTTAR automatic hopper. The Speswhite clay samples were first statically consolidated in containers from a saturated slurry. They were then consolidated again in-flight under self-weight before starting the pile loading tests. Two types of clay beds were used:

- A saturated clay, slightly overconsolidated to simulate a soft compressible clay (that may for example be found in offshore conditions);
- A non-saturated overconsolidated clay (OCR ~ 4) to simulate a much stronger soil more typical of onshore projects.

The soil sample characteristics were determined from in-flight cone penetration tests (CPTs) performed in all soil samples just before and after the pile load tests, using the onboard movable CPT device. An example of profile of tip resistance versus depth recorded in a sand at $I_D = 53\%$ is presented in Figure 4. The data show that the tip resistance of the sand samples may be estimated by Equations (1):

$q_c = 1{,}1z$ for medium dense sand ($I_D = 53\%$)

$q_c = 3{,}1z$ for dense sand ($I_D = 86\%$) (1)

where cone resistance q_c is given in MPa and depth z in metres.

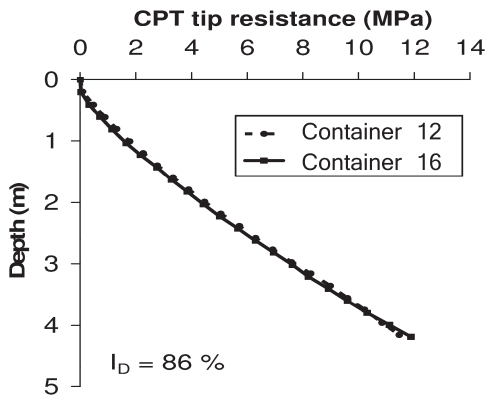

Figure 4: Tip resistance versus depth in two medium dense sand samples at ID = 86% (Rosquoët 2004)

In Speswhite clay, the correlation given in equation (2) between CPT tip resistance q_c and undrained shear strength c_u was obtained by comparing in-flight CPT and vane test results:

$$c_u = 18.5\, q_c \tag{2}$$

The data recorded during the CPTs carried out in soft clay are presented in Figure 5. The undrained shear strength increases linearly with depth with a gradient of about 1.25 kPa/m.

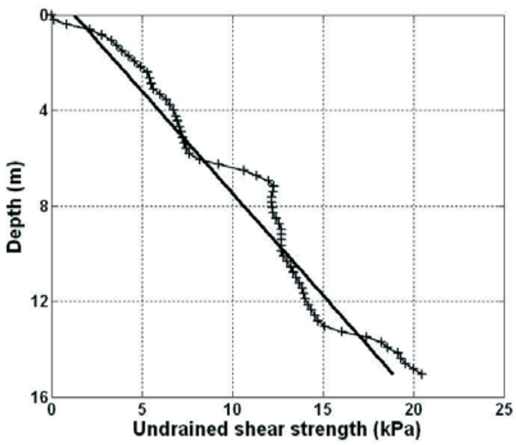

Figure 5: Undrained shear strength versus depth in soft clay (Khemakhem 2011)

3 GLOBAL PILE ANALYSES

3.1 Piles in sands

Only cyclic tests in one-way mode were considered for the interpretation. Preliminary tests had shown that this mode of loading was more detrimental in sands than two-way loading as also observed by other authors (Long and Vanneste 1994; Lin and Liao 1999; Peralta 2010). For example, according to Lin and Liao, two-way loads ($H_{min} = -\ H_{max}$) produce pile displacements ten times less than on-way loads ($H_{min} = H_{max}$).

In the Rosquoët (2004) tests, the effect of cyclic load ratio was investigated in detail but for a relatively small number of cycles (N < 50). The results were then extended to a much larger number of cycles (N up to 75 000) in Rakotonindriana (2009).

3.1.1 Pile head displacement

The effect of cycles on the normalised displacement y_N/y_1 at the load application point (Figure 6) is strongly dependent on both the amplitude of the cycles (H_c) and the maximum load (H_{max}). The effect of sand density (between $I_D = 53\%$ and 100%) is rather small.

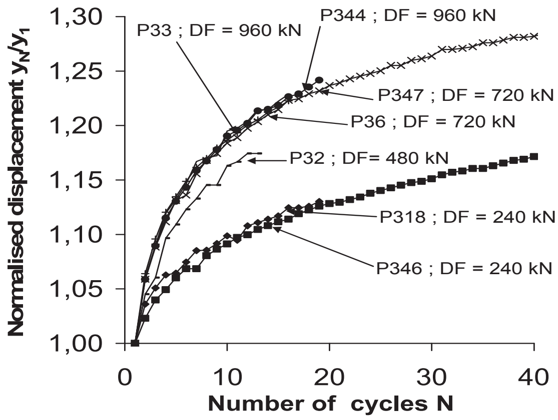

Figure 6. Plot of normalised displacements under maximum load (H_{max} = 960 kN for various cycle amplitudes DF (from Rosquoët et al. 2013)

A logarithmic law (Equation (3) describes correctly the relationship between relative displacement and number of cycles:

$$y_N / y_1 = 1 + b \ln(N) \tag{3}$$

where y_N = displacement at cycle N
y_1 = displacement at end of static loading phase
b = degradation parameter.

The degradation parameter b increases with the ratio H_c/H_{max}. A regression analysis on Rosquoët data base (N < 50) yields:

$$b = 0.10\ (H_c/H_{max})^{0.35} \tag{4}$$

whereas:

$$b = 0.15\ (H_c/H_{max})^{0.35} \tag{5}$$

fits better with Rakotonindriana (2009) database compiled of tests with a much larger number of cycles (up to 75 000).

Logarithmic formulas for describing the effect of cycles on pile head displacement were proposed by several authors (Hettler 1981; Hadjadji et al. 2002; Li et al. 2010; Peralta 2010). The most complete study was carried out by Long and Vanneste (1994) and extended by Lin and Liao (1999). They both are based on the results of 34 full-scale tests from different sites of sandy soils. They showed how the degradation parameter b of Equation (3) depends on cyclic load characteristics (parameter φ) but also on pile-soil relative stiffness, installation procedure (parameter ξ) and to some extent on soil density (parameter β) as shown by equation (6) for flexible piles :

$$b = 0.16\beta\xi\varphi \tag{6}$$

Values for β, ξ and φ given by the authors are always around 1. The proposed logarithmic formulae all show the same trend of pile head displacement increasing with the number of cycles.

However they differ in the way that they introduce the effects of the cyclic load characteristics (H_c and H_m or H_{max}).

The easiest way to compare these expressions is to look at the predicted values of y_N / y_1 for a given number of cycles. For example Figure 7 shows the effects of the relative cyclic load amplitude H_c / H_{max} on the pile head displacement at 500 cycles (y_{500} / y_1), calculated by the Lin and Liao (1999) relationship (6) and by the SOLCYP equation (5).

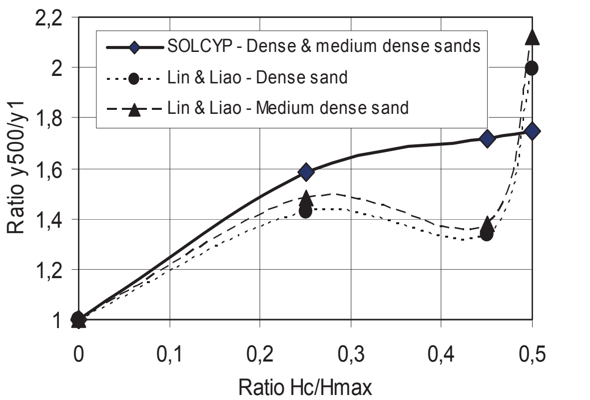

Figure 7:. Effects of the relative cyclic load amplitude H_c / H_{max} on the pile head displacement at 500 cycles (y_{500} / y_1)

At 500 cycles, for the most severe cyclic amplitude (H_c / H_{max} = 0), the ratio y_{500} / y_1 given by Lin and Liao (1999) is 2.12 in dense sand and 1.99 in medium dense sand, i.e. slightly larger than the unique value proposed for both sands by SOLCYP (y_{500} / y_1 = 1.75). Lin and Liao (1999) gave parameter values φ (see Equation (6)) for only three values of H_c / H_{max} (0.25, 0.45 and 0.5) and these values are based on an extremely small number of tests. This most likely explains the anomalous result in Figure 7 for H_c / H_{max} varying from 0.25 to 0.5 when compared to the results from the SOLCYP equation, which is based on a much larger number of loading tests.

3.1.2 Bending moment

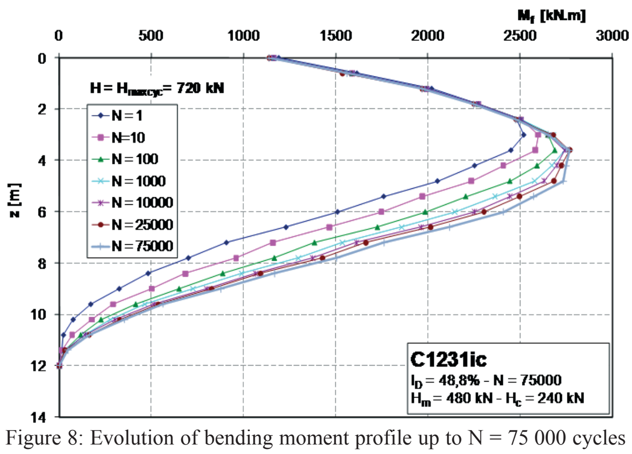

Figure 8: Evolution of bending moment profile up to N = 75 000 cycles (H_m = 480kN and H_c = 240kN) in dense Fontainebleau sand (Rakotonindriana 2009)

As illustrated in Figure 8, the effect of cycles on the maximum bending moment is moderate in sands: lower than 8% over the first 15 cycles (Rosquoët 2004) and lower than 12% after 75 000 cycles (Rakotonindriana 2009).

3.2 Piles in clay

3.2.1 Pile head displacement

An example of pile head displacements with the number of cycles is shown in Figure 9 for a one-way test. The permanent displacement increases whereas the cyclic rigidity basically remains stable.

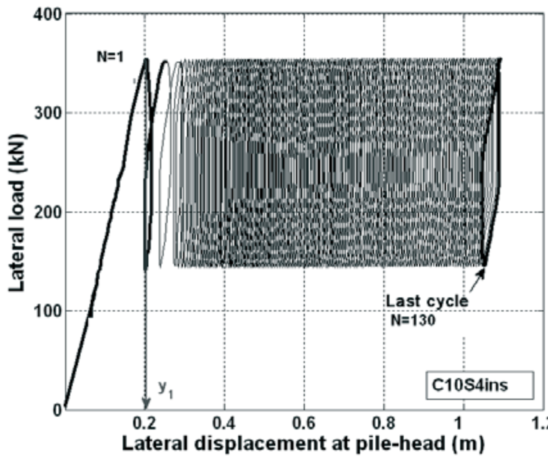

Figure 9: Typical evolution of pile head displacements with cycles in a one-way test up to N = 130 (Khemakhem et al. 2012)

Figure 10 illustrates different responses to the number of cycles according to the severity of the applied cyclic regime. One can clearly distinguish two categories: piles where pile head displacements tend to stabilise and piles where pile head displacements accelerate. Tests have been stopped at a predetermined relative displacement to protect the strain gauges. There is no generalised soil failure but the pile structure would rapidly plastify. Only cases leading to quasi stabilisation are considered hereafter.

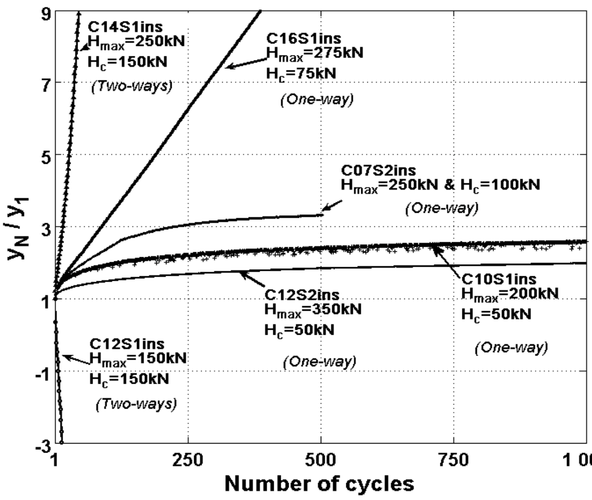

Figure 10: Evolution of normalised pile head displacements y_N/y_1 with number of cycles for various load cases (Khemakhem et al. 2012)

Figure 11 shows that normalised pile head displacements y_N / y_1 can be correctly described by:

$$\frac{y_N}{y_1} = k \cdot N^{\alpha} \tag{7}$$

where k and α are empirical parameters. The analysis of the full data base indicates that k and α are moderately dependent on the ratio H_c / H_{max}, with:

- k always close to 1
- α in the range 0.1 to 0.2.

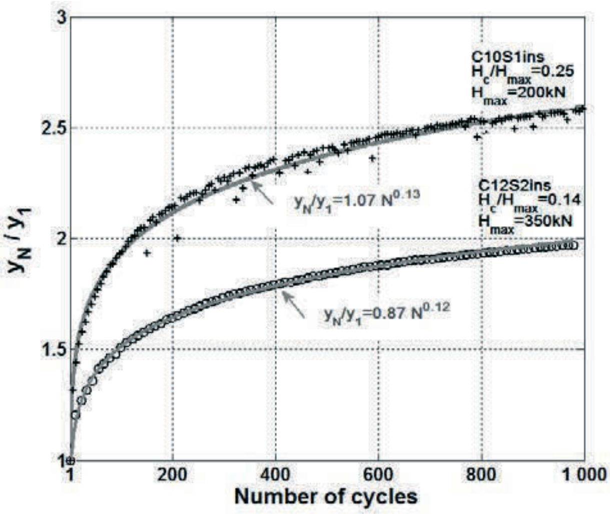

Figure 11: Comparison of calculated and measured normalised pile head displacements y_N / y_1 (Khemakhem et al. 2012)

3.2.2 *Bending moment*

Figure 12 illustrates the evolution of bending moments in the pile. Contrary to sands, in soft clay the maximum bending moment significantly increases over the first cycles while simultaneously the position of the maximum moves downward. Phenomena tend to stabilise with number of cycles.

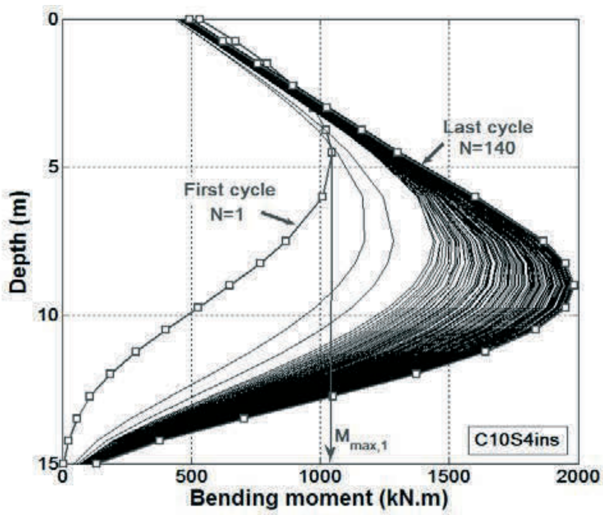

Figure 12: Typical evolution of bending moments in pile (Khemakhem et al. 2012)

As shown on Figure 13, the evolution of the normalised maximum bending moment $M_{max,N} / M_{max,1}$ can be approached by the following equation:

$$\frac{M_{max,N}}{M_{max,1}} = \mu . N^{\alpha} \tag{8}$$

where μ and α are empirical coefficients:

- μ is always close to 1
- α is a function of the ration H_c/H_{max}. A regression analysis on Khemakhem database yields:

$$\alpha = 0.25 \frac{H_c}{H_{max}} \tag{9}$$

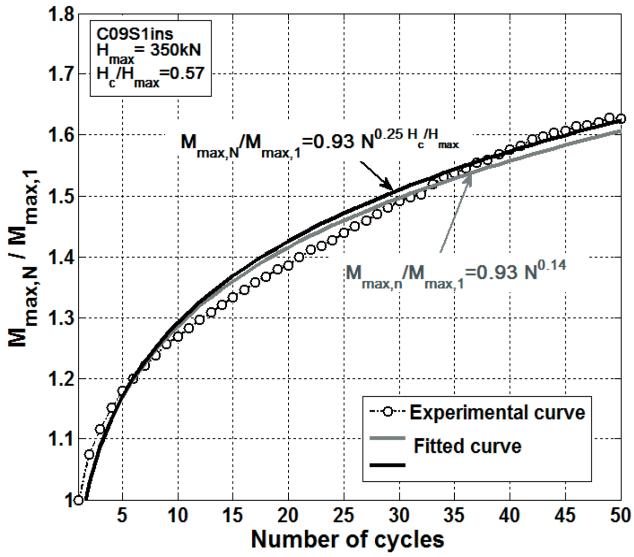

Figure 13: Comparison of calculated and measured normalised bending moments $M_{max,N} / M_{max,1}$ (Khemakhem et al. 2012)

3.3 *Proposal for global pile design*

At this stage, the following proposals may be made for global analysis of laterally cyclic piles. It should be repeated that these relationships apply to pile in-service conditions, where the maximum applied cyclic load H_{max} is less than one third of the ultimate lateral capacity H_u. If no other data are available, the static load producing a pile head displacement of about 30% of the pile diameter may be accepted as value of H_u.

- **Effect of cycles on the pile head displacement**

The increase in pile displacement y_N / y_1 between the first loading at H_{max} and the loading at H_{max} at cycle N may be estimated by (for N >1):

$$\frac{y_N}{y_1} = 1 + 0.15 \ln(N) \left(\frac{H_c}{H_{max}} \right)^{0.35} \tag{10}$$

Dense to medium dense sand

$$\frac{y_N}{y_1} = 1.1 N^{0,2} \tag{11}$$

Normally consolidated soft saturated clay
(this relationship is rather conservative)

- **Effect of cycles on the maximum bending moment**

The increase in maximum bending moment $M_{max,N} / M_{max,1}$ between the first loading at H_{max} and the loading at H_{max} at cycle n may be estimated by (for N >1):

$$\frac{M_{\max,N}}{M_{\max,1}} = 1 + 0.035\left(1 - \frac{2H_c}{H_{\max}}\right)\ln(N) \qquad (12)$$

Dense to medium dense sand;

$$\frac{M_{\max,N}}{M_{\max,1}} = 1.2N^{0.35\frac{H_c}{H_{\max}}} \qquad (13)$$

Normally consolidated soft saturated clay

In clay, the depth where the bending moment is maximum can be calculated by:

$$\frac{Z_{M\max,N}}{Z_{M\max,1}} = 1.2N^{0.35\frac{H_c}{H_{\max}}} \qquad (14)$$

Normally consolidated soft saturated clay

4 LOCAL PILE ANALYSES

Beam column analysis coupled with P-y transfer curves is the most commonly used method to analyse the response of long (flexible) piles to lateral loads. In many countries, rules have been developed to build the static P-y curves from results of laboratory or in-situ soil tests but no methods are proposed for cyclic loading, except for offshore applications.

Offshore standards (e.g. ISO 19902, DnV, API RP2GEO) recommend procedures to develop static P-y curves for normal soils (silica sands, soft and stiff clays) and also so-called cyclic P-y curves which were initially proposed for soft clays (Matlock 1970), stiff clays (Reese and Cox 1975) and sands (Cox et al. 1974; Reese et al. 1974).

These initial methods were based on test data obtained on small diameter piles (32 cm to 61 cm) on which cycle batches representative of loads imposed on a platform foundation pile during a Gulf of Mexico storm were applied. The objective was to produce envelope curves aimed at modelling the (degraded) response of a pile under a static load applied at the end of the centennial storm. This approach is difficult to extrapolate to other loading conditions and is limited in that it is impossible to take into account the effects of load characteristics (severity of loading) and of the number of cycles.

More advanced studies have been carried out on static and cyclic P-y curves from the centrifuge experimental data collected in the SOLCYP project. The technique developed in LCPC was used for deriving both the pile displacement profiles y(z) and soil reaction profiles P(z) from the bending moment data M(z). Displacements y(z) are calculated by double-integrating the moment using two integration constants achieved from the boundary conditions at the pile cap. The solution for P(z) is obtained through double derivation of the moment data after being interpolated by quintic Splines (Garnier 2001).

4.1 *Piles in sand*

4.1.1 *Static P-y curves in sands*

Figure 14 shows an example of experimental static P-y curves obtained in medium dense sand (I_D = 50%).

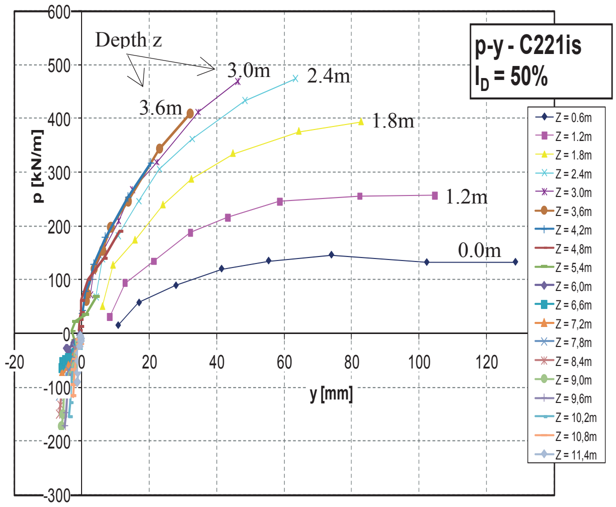

Figure 14: Example of static P-y curves in medium dense sand at different depths from 0.6 m to 11.4 m (Rakotonindriana 2009)

These static transfer curves in sands can be modelled by equations such as (Figure 15):

$$P = a.y^b$$

In dense sand, Rosquoët (2004) proposes the following expressions for coefficients a and b:

- a = 26z + 15 (with z in metres)
- 0.48 < b < 0.56

It can be noted that Japanese PHRI rules recommend b = 0.5.

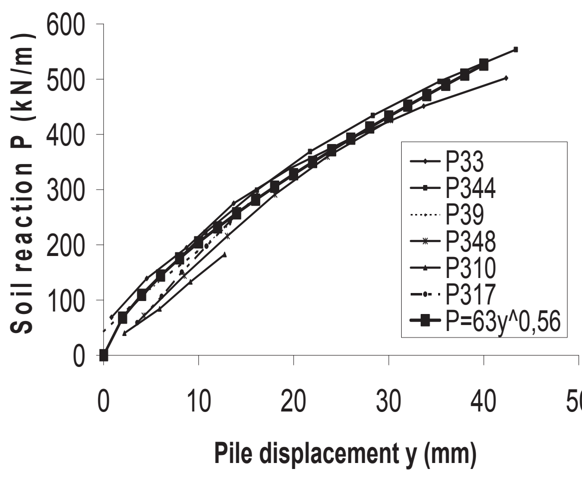

Figure 15: Comparison of experimental (six different tests) and modeled P-y static curves in dense sand at depth z =1.8 m (from Rosquoet 2004)

4.1.2 *Cyclic P-y curves in sands*

Typical cyclic P-y relationships obtained at different depth intervals during a one-way test ($H_c / H_{max} = 0.25$) are shown in Figure 16. The first phase corresponds to the application of the monotonic load, up to the maximum load H_{max}. Cycles between H_{max} and H_{min} are accompanied in the upper part of the pile (depth up to about 5 B) by a continuous decrease of P_{max} and an increase of the permanent displacement y.

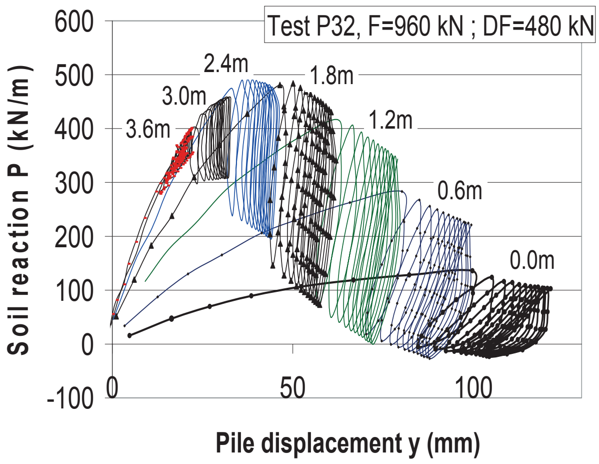

Figure 16: P-y relationships obtained at different depths during a one-way cyclic test with $H_c / H_{max} = 0.25$ (Rosquoet 2004)

Assuming that sufficient data are available (several cyclic tests at different load levels), it is possible to define at each depth a set of P-y curves corresponding to a given number of cycles.

An example is provided in Figure 17 by Rakotononindriana (2009). These curves called cyclic P-y curves are capable of restoring the global response of the pile after N cycles (and for given loading characteristics).

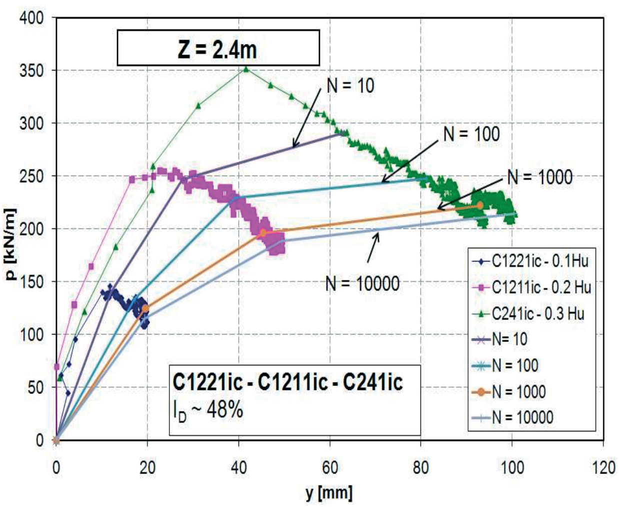

Figure 17: Example of experimental cyclic P-y curves at a given depth z = 2.4 m (Rakotonindriana 2009)

As for clays, cyclic P-y curves for sands can be derived from the static curves by introducing a degradation coefficient r_c (sometimes also called P-multiplier). Work is presently ongoing and preliminary results can be found in Rosquoët et al. (2013). At this stage, the proposed values of the degradation coefficient r_c are given in Table 2.

Table 2: Proposed degradation coefficients r_c.

Relative depth z/B	Degradation coefficient $r_c = f(N, H_c / H_{max})$
0 < z/B < 1.5	$r_c = 1 - \left(0.034 \ln(N) + 0.24 \, {H_c}/{H_{max}}\right)$
1.5 < z/B < 3	$r_c = 1 - \left(0.017 \ln(N) + 0.12 \, {H_c}/{H_{max}}\right)$
3 < z/B < 5	$r_c = 1 - \left(0.008 \ln(N) + 0.06 \, {H_c}/{H_{max}}\right)$
z/B > 5	$r_c = 1$

4.2 *Piles in clay*

4.2.1 *Static P-y curves in clays*

Typical monotonic P-y curves obtained in normally consolidated clays by Khemakhem (2012) are shown in Figure 18. The maximum soil reaction P_u is reached for a displacement y_u (close to 0.05 B). Moderate strain softening is observed afterwards. In the pre-peak phase the P-y relationship can be described by a law of the type $P = k.y^a$, also illustrated in Figure 18.

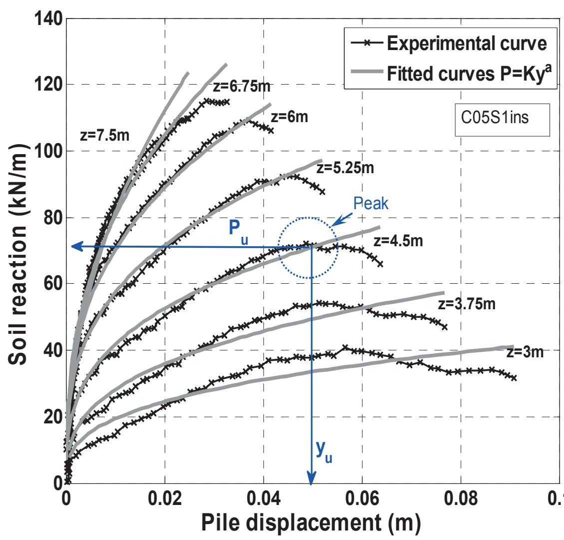

Figure 18: Modelling static P-y curves in soft clay using $P = k.y^a$ (Khemakhem 2012)

After normalisation by P_u and y_u (Figure 18), a convergence of curves is obtained which can be reasonably modelled by (as shown on Figure 19):

$$\frac{P}{P_u} = 1.03\left(\frac{y}{y_u}\right)^{0.42} \tag{15}$$

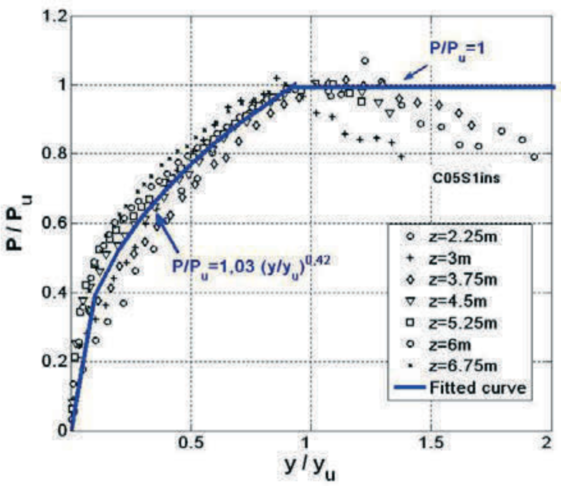

Figure 19: Modelling normalised monotonic P-y curves in soft clay (Khemakhem 2012)

The ultimate soil reaction P_u is strongly dependent on the undrained shear strength c_u. As also observed by Jeanjean (2009), in soft clay the ratio $P_u / B.c_u$ is found ranging from 6 to 13 and tends to increase with depth. The exponent $a = 0.42$ in Equation (15) derived from the data collected by Khemakhem (2012) is closer to the value 0.5 obtained by Jeanjean than to the value 0.33 proposed by API RP2GE0 (2011).

4.2.2 *Cyclic P-y curves in clays*

Figure 20 illustrates a typical P-y curve obtained in the upper part of the pile (z/B < 5) under cyclic loading (in this particular two-way mode case H_c / H_{max} = 0.57). The first phase corresponds to the static curve until application of H_{max}. Then, cycles between H_{max} and H_{min} are accompanied by a continuous decrease in P_{max} and an accumulation of permanent displacement y.

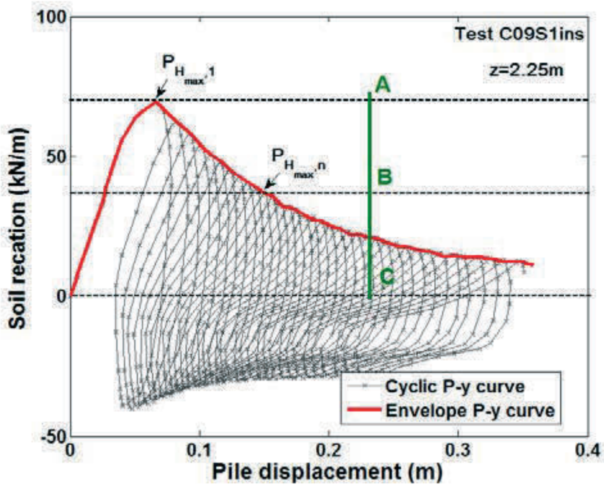

Figure 20: Typical P-y relationships obtained at depth z = 2.25 m during a two-way (H_c / H_{max} = 0.57) cyclic test (Khemakhem 2012)

The decrease of the soil resistance during cycling may be quantified by introducing a degradation coefficient r_c which is expected to be a function of depth z, pile displacement y, number of cycles n, maximum applied load H_{max} and amplitude of cycles H_c.

A first estimation of the degradation coefficient r_c at cycle n can be obtained by the ratio BC/AC in Figure 20. However, the study showed that these preliminary values of coefficients r_c cannot be directly used to derive cyclic P-y curves from the static curves. A more complex procedure that includes several validation stages can be found in Khemakhem (2012) and this was followed for determining efficient values of r_c. A best fit of the database was found for (Equation (16)):

$$r_c\left(N, \frac{z}{B}, \frac{H_c}{H_{max}}\right) = 1 - \frac{H_c}{H_{max}}\left[0.005\frac{z}{B} - \log(N)\left(0.25\frac{z}{B} - 2.16\right) - 0.68\right] \qquad (16)$$

This expression (16) is valid in the domain:

$z/B < 6$; $0 < H_c / H_{max} < 0.6$; $n < 100$.

Figures 21 and 22 present a comparison of measured and calculated pile head displacements (Figure 21) and moments (Figure 22) using the degradation coefficient r_c. The comparison is made on a pile correctly designed to sustain the static loads and submitted to relatively severe cyclic loads (H_c / H_{max} = 0.25).

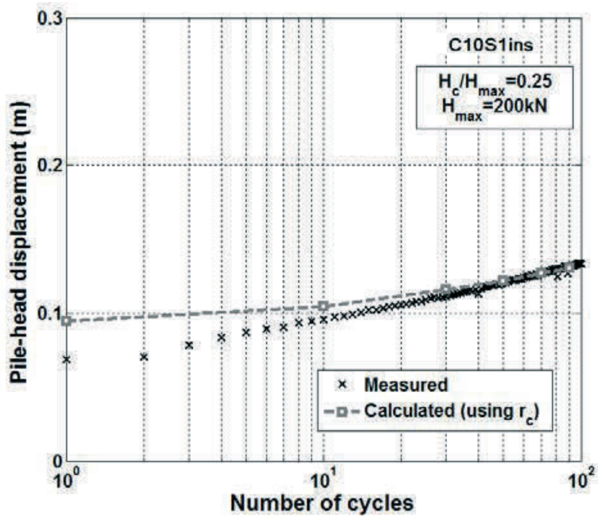

Figure 21: Comparison of pile displacements measured and calculated using the degradation coefficient procedure (Khemakhem 2012)

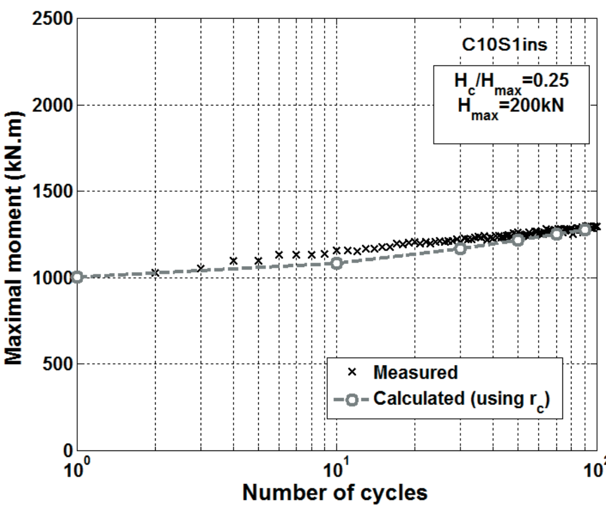

Figure 22: Comparison of maximum moments measured and calculated using the degradation coefficient procedure (Khemakhem 2012)

P-y curves defined above by applying the degradation coefficients to static P-y curves are not true cyclic P-y curves in the sense that they do not describe the behaviour of the soil-pile interface cycle by cycle. They can be qualified as envelope curves in the sense that they describe the soil-pile response only under the maximum load H_{max}. However, unlike the API RP2GEO (2011) curves, they take into account the load characteristics and the number of cycles.

It is interesting to compare both approaches. Figure 23 presents, for a prototype pile, a set of cyclic P-y curves for a loading case characterised by a ratio H_c / H_{max} = 0.14 and a number of cycles of 10 and 100. These curves are compared to API RP2GEO (2011) cyclic curves for N = 1 (API static curve) and at end of storm (API envelope curve).

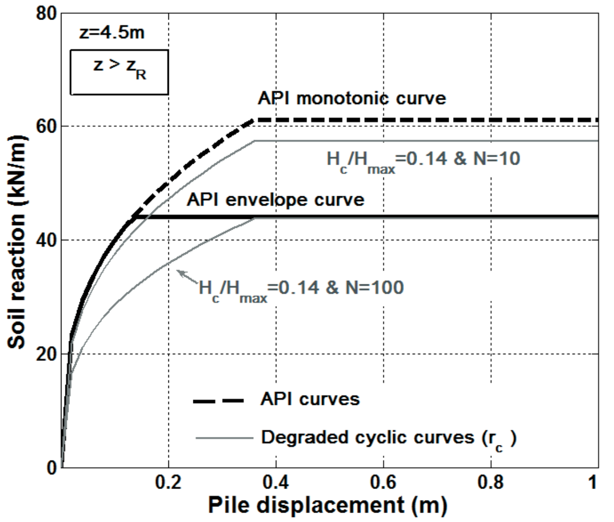

Figure 23: Comparison of degraded cyclic curves (r_c = f [H_c/H_{max}, N]) and API RP2GEO (2011) envelope curves (Khemakhem 2012)

Pile head displacements and bending moments calculated by integration of both sets of P-y curves are compared in Figures 24a and 24b. Agreement between API and proposed cyclic P-y curves is found for a given number of cycles (N#10 in this case). Proposed cyclic P-y curves provide a useful and simple tool to analyse the effect of batches of constant average load and cyclic amplitude. Making explicit predictions for actual load cases will require the implementation of an equivalent number of cycles procedure.

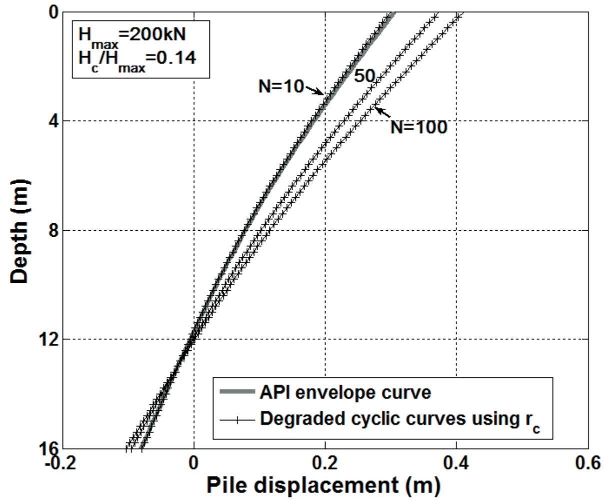

a – Pile displacement vs depth

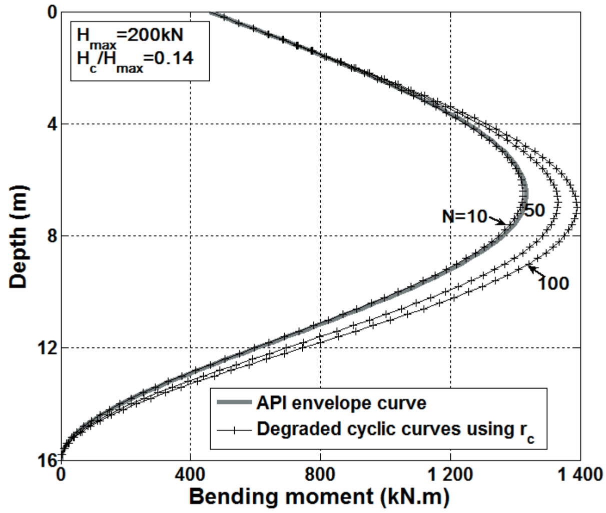

b – Bending moment

Figure 24: Comparison of displacements and moments obtained by integration of static curves degraded by r_c = f [H_c/H_{max}; n] and by API RP2GEO envelope curves (Khemakhem 2012)

5 CONCLUSION

Extensive centrifuge tests were conducted in sand and clay to investigate the response of single piles to lateral cyclic loads up to 75 000 cycles. The effects of cycles on the pile head displacement, bending moment profile and soil reaction were quantified for different cyclic load characteristics (maximum load and cyclic amplitude).

From the collected data, degradation laws have been obtained and the degradation factors are functions of the average and cyclic load components and of the number of cycles.

Degradation laws can be used in global analyses to modify the pile displacements and bending moments calculated from static conditions. Degradation factors may also be used in local analysis to derive cyclic P-y curves for beam column analyses. These transfer curves, unlike the so called cyclic envelope curves provided in API RP2GEO (2011), capture the effect of the cyclic load components and of the number of cycles.

6 ACKNOWLEDGEMENTS

The author would like to acknowledge the PhD students for their essential contribution to this work (F. Rosquoët, J. Rakotonindriana, M. Khemakhem) and the researchers who participated in the direction of these studies (Dr L. Thorel, Dr A. Le Kouby and Dr. N. Chenaf). The author acknowledges the Région des Pays de la Loire and the Agence Nationale de la Recherche (ANR) for their financial support.

7 REFERENCES

API RP2GEO 2011. API Recommended Practice, Geotechnical and Foundation Design Considerations, First Edition, April 2011

Cox W.R., Reese L.C. and Gubbs B.R. 1974. Field testing of laterally loaded piles in sand, *Proc. Offshore Technology Conference*, OTC 2009, Houston, Tx

DnV 1992. Classification Note 30-4, Foundations. Det Norske Veritas, Oslo

Garnier J. 2001. Physical models in geotechnics: State of the art and recent advances. *First Coulomb Lecture*, Caquot Conference, 3-5 Oct. 2001, Paris, 1-59.

Hettler A. 1981. Verschiebungen starrer und elastischer Gründungs körper in Sand bei monotoner und zyklischer Belastung. In A. Blinde, G. Gudehus, O. Natau (Ed.), *Veröffentlichungen des Institutes für Bodenmechanik und Felsmechanik der Universität Fridericiana in Karlsruhe*, Heft 90, Karlsruhe.

Hadjadji T., Frank R. and Degny E. 2002. Analyse du comportement expérimental de pieux sous chargements horizontaux, Rapport LCPC GT 74, Collection Etudes et Recherches des Laboratoires des Ponts et Chaussées, 301 p.

House, A. R., Oliveira, J. R. and Randolph, M. F. 2001. Evaluating the coefficient of consolidation using penetration tests. *International Journal of Physical Modelling in Geotechnics*, Vol 3, 17-26

ISO 19 902 2007. International standard for the design of fixed steel offshore platforms, International Standards Office, British Standards Institute, London.

Jeanjean Ph. 2009. Re-Assessement of P-y curves for soft clays from centrifuge testing and finite element modeling, *Proc. Offshore Technology Conference*, OTC Paper 20158, Houston, Texas, 23 p.

Khemakhem M. 2012. Etude expérimentale de la réponse aux charges latérales monotones et cycliques d'un pieu foré dans l'argile, *Thèse,* Ecole Centrale de Nantes, 314 p.

Khemakhem M., Chenaf N. and Garnier, J. 2012. Centrifuge modelling of piles in clay under cyclic lateral loads, *7th Int. Conf. Offshore Site Investigation and Geotechnics*, OSIG, London.

Li Z., Haigh S.K and Bolton M. 2010. Centrifuge modelling of mono-pile under cyclic lateral loads, *Int. Conf. Physical Modelling in Geotechnics,* IJPMG 2010, Zurich, Springman, Laue & Seward (Ed.), Taylor & Francis, Vol. 2, 965-970.

Lin S. S. and Liao J. C. 1999. Permanent strains of piles in sand due to cyclic lateral loads. *Journal of Geotechnical and Geoenvironmental Eng.* 125, No. 9, 798–802

Long J. and Vanneste G. 1994. Effects of cyclic lateral loads on piles in sand, *J. of Geotechnical Engineering* 120, No. 1, 225–244

Matlock H. 1970. Correlations for design of laterally loaded piles in soft clay, *Proc. Offshore Technology Conference*, OTC Paper 1204, Houston, Texas.

Peralta P. 2010. Investigations on the behaviour of large diameter piles under long-term lateral cyclic loading in cohesionless soil, *PhD Thesis*, Leibnitz University, Hannover, 201 p.

Puech A., Canou J., Bernardini C., Pecker A., Jardine R. and Holeyman A. 2012. SOLCYP: a four-year JIP on the behaviour of piles under cyclic loading, *7th Int. Conf. on Offshore Site Investigations and Geotechnics*, OSIG, London.

Rakotonindriana M.J. 2009. Comportement des pieux et des groupes de pieux sous chargement latéral cyclique, *Thèse* de Doctorat ENPC / LCPC.

Reese L. C., Cox W. R. and Koop F. D. 1974. Analysis of Laterally Loaded Piles in Sand*, Proc. 6th Annual Offshore Technology Conference,* OTC Paper 2080, 473-483, Houston, Texas

Reese L.C. and Cox W.R. 1975. Field testing and analysis of laterally loaded piles in stiff clay, , *Proc. Offshore Technology Conference*, OTC Paper 2312, Houston, Texas.

Rosquoët F. 2004. Pieux sous charge latérale cyclique, *Thèse*, Ecole Centrale de Nantes, 305 p.

Rosquoët F., Thorel L., Garnier J. and Chenaf, N. 2013. Pieu sous charge latérale dans les sables : développement de lois de dégradation pour prendre en compte l'effet des cycles. *Proceedings 18th ICSMGE*, Paris

Effects of installation method on the static behaviour of piles in highly overconsolidated Flanders clay

Effet du mode de mise en place sur le comportement statique de pieux dans l'argile fortement surconsolidée des Flandres

A. Puech
Fugro GeoConsulting, Nanterre, France

O. Benzaria
Fugro GeoConsulting, Nanterre, France

ABSTRACT: As part of the French national project SOLCYP, driven, bored and screwed instrumented piles were installed in the overconsolidated Flanders clay. Piles were submitted to series of static and cyclic load tests to failure. This paper focuses on a comparison of the ultimate capacities and local skin frictions measured on the three types of piles under static loading. The effects of the installation method and of the particular soil properties on the behaviour of the piles are discussed. Results are compared to prediction methods.

RÉSUMÉ : Dans le cadre du projet national SOLCYP, des pieux instrumentés ont été installés par battage, forage et vissage dans l'argile surconsolidée des Flandres. Ils ont été soumis à des séries d'essais de chargements statiques et cycliques jusqu'à la rupture. Cette communication est centrée sur la comparaison des capacités ultimes et des frottements locaux obtenus sur les trois types de pieux sous chargements statiques. On s'est particulièrement attaché à montrer l'effet du mode de mise en place et de la nature du matériau sur le comportement des pieux. Les résultats sont comparés aux méthodes prévisionnelles.

KEYWORDS : SOLCYP, driven pile, bored pile, screwed pile, static capacity, overconsolidated clay, Flanders clay.

MOTS-CLES: SOLCYP, pieu battu, pieu foré, pieu vissé, capacité statique, argile surconsolidée, argile des Flandres.

1 INTRODUCTION.

The main objective of the French National Project SOLCYP (Puech et al. 2012) is to develop a methodology for designing cyclically loaded piles. As part of the project instrumented piles have been installed in overconsolidated Flanders clay. Three installation methods were used: driving, boring and screwing. Piles were then submitted to a series of conventional static tests and cyclic tests with various average loads and cyclic amplitudes. Tests were conducted to failure.

The ultimate pile capacity and mobilised skin frictions observed under static loading were found to be highly dependent on the installation method. The results are examined in relation to the mechanical response of the Flanders clay and evaluated by reference to available design methods.

2 FLANDERS CLAY

The site is located at Merville in northern France. The stratigraphy consists of a top cover of 3.5 m of sandy to clayey silts, below which is the Flanders clay formation, very homogeneous across the site and extending to at least 40 m below ground level (BGL). The water table fluctuates within the upper silt according to the seasons but was approximately 2 m BGL during the testing period.

The Flanders clay, geologically similar to the London clay and to the Boom clay, was deposited 50 million years ago (Eocene) in a marine gulf extending over northern France, Belgium and south-east of England. The clay was covered by tertiary formations. Sedimentation continued until the Upper Pleistocene period and the ground level was probably some 200 m higher than today. The underlying formations were eroded and Flandrian alluvions were deposited during the Quaternary period. The sediment was submitted to loading/unloading cycles and periglacial processes associated with chemical cementation and ageing phenomena which significantly contributed to the apparent degree of overconsolidation (Josseaume, 1998)

Physical characteristics of the Flanders clay are similar to those of the London and Boom clays (Borel and Reiffsteck, 2005):

- low water content (about 30%)
- high plasticity (plasticity index PI close to 50)
- significant degree of fissuring particularly below 5 m depth

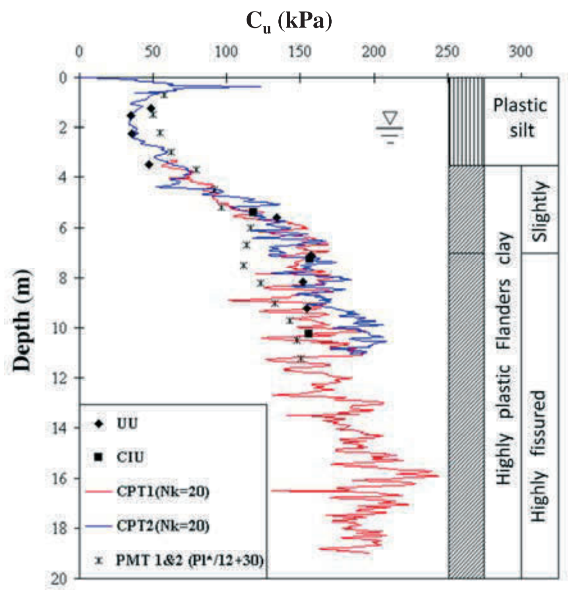

Figure 1: Soil conditions at the Merville pile test location

A dedicated geotechnical investigation was carried out at the pile testing site including piezocone tests (CPTUs), Ménard pressuremeter tests (PMTs), continuous high quality sampling and a series of standard and advanced laboratory tests on recovered samples. The results are summarised on Figures 1 and 2 and the characteristic parameters used for capacity evaluations are indicated in Table 1.

Table 1: Characteristic geotechnical parameters of the Merville clay

z (m)	γ (kN/m^3)	Cu (kPa)	OCR	Pl* (MPa)	q_{net} (MPa)
0-0,6	20	60		0,4	1,2
0,6-2,0	18	40		0,3	0,8
2,0-3,5	7	50		0,4	1,0
3,5-6,0	8	50/140	10/16	0,5/1,0	1,0/2,8
6,0-7,5	10	140/150	16	1,0	2,8/3,0
7,5-9,5	10	150/155	14	1,0/1,3	3,0/3,1
9,5- 13	10	155/165	12	1,3/1,5	3,1/3,3

Note: Water table at 2 m BGL; sandy to clayey silts from 0 m to 3.5 m; fissured Flanders clay from 3.5 m to 5 m, highly fissured beyond 5 m.

The clay is highly overconsolidated but limited reliable information is available in the technical literature. The overconsolidation ratio (OCR) was estimated from CPT data using the relationship proposed by Mayne (1991): OCR = k. $(qt-\sigma_{v0})/\sigma'_{v0}$ with k = 0.5. The factor k depends on the type of soil. A value of 0.5 was selected, giving OCR values compatible with both the supposed past overburden and the gradient of the cone resistance $q_n = qt-\sigma_{v0}$ in the deep clay (beyond 8 m BGL). In the London clay Powell et al. (1988) suggest that k values may be higher than 1.

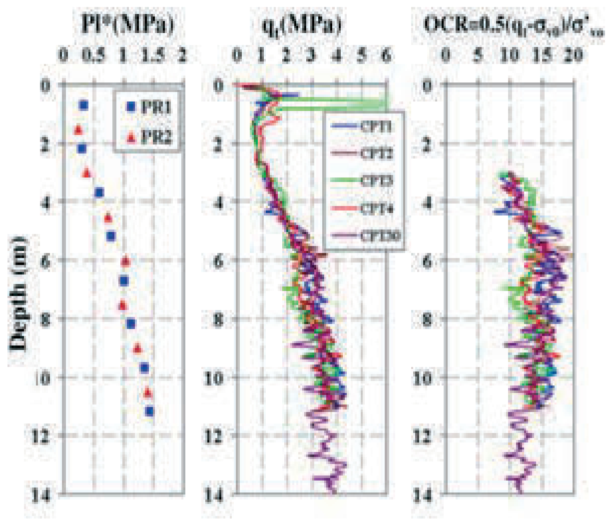

Figure 2: Net limit pressure pl*, cone resistance q_t and OCR profiles at Merville

Unconsolidated undrained (UU) and isotropically consolidated, undrained (CIU) triaxial tests show fragile premature failures of the samples as frequently observed in this type of fissured and highly overconsolidated plastic clays. Failure is characterised by the formation of shear planes containing reoriented particles as noted by Bond and Jardine (1991) in the London clay. Undrained shear strength C_u values correlate with cone resistance values using a high cone factor N_{kt} , $[N_{kt} = (q_t - \sigma_{vo}) /C_u =20]$, compatible with the fissured high OCR soil. The ratio C_u/σ'_{vo} is high ($1.2 < S_u/\sigma'_{vo} <1.8$). Net limit pressure values pl* are relatively well linked to C_u using the relationship proposed by Amar and Jezequel (1998): C_u = pl*/12+30, with C_u in kPa and pl* in MPa.

3 TEST PILES AND LOADING MODES

Ten 13 m piles were installed at the beginning of March 2011 by Franki Fondation on the Merville site:

- four tubular metallic piles (OD = 406 mm, w.t.=14 mm) were placed in a 4 m prebored hole, then driven to 13 m BGL using a hydraulic IHC 30 hammer. The piles were closed ended and the soil around the pile was fully displaced ;
- four bored piles Continuous Flight Augering (CFA) piles (OD = 420 mm) were drilled using a hollow auger screwed into the soil, then removed without rotation while grout was poured through the hollow stem. A telescopic nose was used to improve grouting conditions at the base. The reinforcement cage was lowered into the fresh grout. For this type of pile, the soil is completely removed (non-displacement piles)
- two piles (OD = 420 mm) were screwed and cast in place: a conical tool is inserted into the soil by a combined action of rotation and jacking. Grouting is done through a hollow stem as for the CFA piles. The soil is significantly displaced (it is estimated that about 15% to 20% of the soil is extracted).

The piles were instrumented using removable extensometers. This technique developed by LCPC gives access to load distribution along the pile and to local shear transfer mobilisation (1 m long sections).

Load tests started at the end of May and included conventional static tests with one-hour load increments (ISSMGE; AFNOR NF P 94-150-2), rapid static tests, and series' of cyclic tests. Cyclic tests were either of one way or two way mode. Results have been partially published (Benzaria et al., 2012, 2013)

In this paper only the results of the conventional static tests in compression on the three types of piles are considered.

4 STATIC TESTS RESULTS

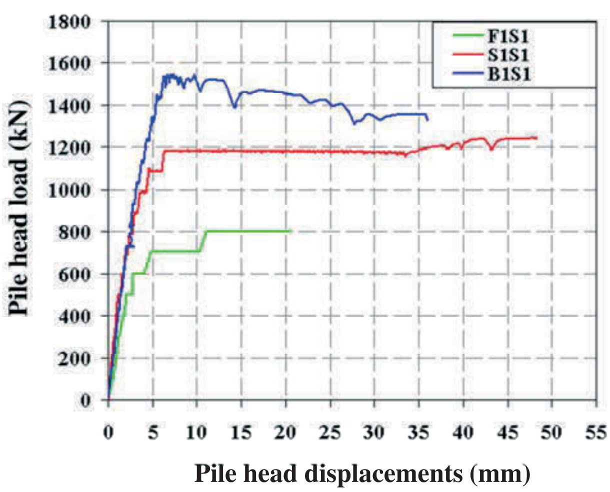

Figure 3: Pile head displacement curves for reference static tests on piles F1, B1 and S1

A conventional static test in compression was performed on a virgin pile of each type. Pile head displacement curves are compared in Figure 3. Due to the high degree of lateral homogeneity of the clay at the Merville site, any differences in the test results can be solely attributed to the different installation methods.

The following is observed:

- Large differences in the peak ultimate capacity of the piles: respectively 1530 kN, 1250 kN and 800 kN for the driven pile B1, the screwed pile S1 and the bored pile F1. The difference is even higher if one considers that the frictional capacity of the driven pile is zero on the upper 4 m (predrilled hole).
- Different pile behaviours at large displacements: the driven pile shows strain softening whereas failure for the bored and screwed piles is of the ductile type. Tension tests on driven pile B4 (Benzaria et al. 2012) indicate that strain softening develops until 80 mm to 100 mm of pile head displacement;
- Pile head displacements at failure are about 6 mm (1.5% of pile diameter) for displacement piles B1 and S1. They are larger for the bored pile F1 (about 12 mm or 3% of pile diameter).

The global behaviour is confirmed by the local friction analysis. Figure 4 shows three typical curves of friction mobilisation at the same level (between 8.4 m and 9.4 m) for each pile. By considering the whole set of results, it can be concluded that the local displacement required to mobilise the maximum friction is smaller for the displacement piles (3 mm for B1 ; 4 mm for S1) than for the bored pile (6 mm).

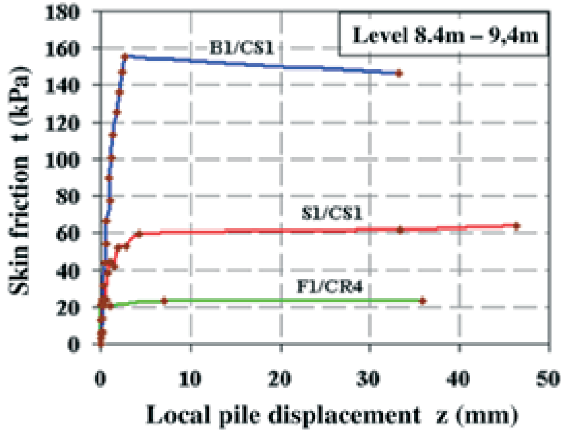

Figure 4: Typical mobilisation curves of soil-pile friction at same level (between 8.4 and 9.4m) for each pile type

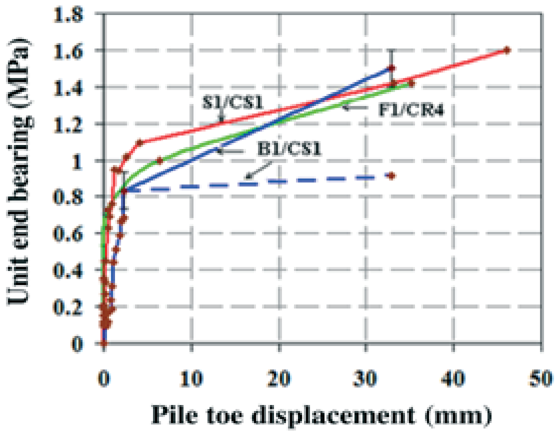

Figure 5: Mobilisation curves of the end bearing for each pile type

Mobilisation of the end bearing for each pile is shown in Figure 5. Responses are very similar with a rapid reaction of the toe, which indicates a careful execution of the base grouting for the bored pile F1. At Zp = 0.1 D, the bearing pressure under the three piles is close to 1.5 MPa, which is in good agreement with the theoretical pressure $q_p = 9.Cu$. The measurement point at 33 mm for the driven pile is most likely unreliable (dotted line). When comparing ultimate capacities of piles B1 in compression and pile B3 in tension, a difference of 200 kN to 250 kN can be attributed to the end bearing, which is corresponds with the other two piles (continuous line).

5 COMPARATIVE INTERPRETATION

Experimental data i.e. the distribution of ultimate local friction may be compared to some of the predictive methods considered the most pertinent as follows:

-for the driven pile, data are compared with: 1) methods based on a direct interpretation of in situ tests (pressuremeter and static penetrometer) as recommended in the new French normative document NF-P 94 262, 2) the API RP2 GEO method based on a total stress approach and 3) the ICP method developed at Imperial College (Jardine et al., 2005).

- for the bored piles, only the methods included in the NF-P 94 262 standard are considered.

In the API RP2GEO approach, the ultimate friction along a closed ended pipe pile is given by (Eq. 1).

$$f = \alpha . C_u \tag{1}$$

where:

C_u : undrained shear strength

$\alpha = 0.5\,\psi^{-0.5}$ if $\psi \leq 1$ and $\alpha = 0.5\,\psi^{-0.25}$ if $\psi > 1$

$\psi = C_u / \sigma'_{v0}$ with σ'_{v0} = effective vertical stress

The Imperial College approach (Jardine et al., 2005) is an effective stress approach. The friction in compression along a driven pile is given by (Eq. 2):

$$\tau_f = 0{,}8\,\sigma'_{rc} . tan\delta_f \tag{2}$$

where: δ_f = soil-pile interface friction angle obtained from ring shear tests simulating the pile roughness and the level of radial effective stress σ'_{rc} acting on the pile wall

σ'_{rc} : radial effective stress acting on pile wall after dissipation of pore pressures generated by driving.

The radial effective stress is expressed by :

$$\sigma'_{rc} = K_c . \sigma'_{vo} \tag{3}$$

with:

$K_c = [2 + 0.016\ YSR - 0.870\ \Delta I_{vy}]\ YSR^{0.42}\ (h/R)^{-0.2}$

YSR is the apparent degree of consolidation (OCR)

$\Delta I_{vy} = \log_{10} S_t$ with S_t = sensitivity

h/R is the normalised distance of the pile toe to the point of estimation of the radial stress. This term quantifies the degradation of the friction during driving ("friction fatigue").

The values of measured maximum (peak) local frictions on pile B1 are compared with corresponding values from prediction methods in Figure 6

NF-P 94 262 standard methods for driven piles based on CPT or PMT data yield very low friction values, which confirm the conservatism of the French standard approach concerning driven piles.

The API RP2GEO method applicable to offshore foundations gives more realistic values although still much lower than those measured.

The ICP method was applied considering the OCR values indicated in Table 1 and soil-pile interface friction values derived from three Bromhead ring shear tests performed in accordance with the procedure described in Jardine et al. (2005). Peak values δ_{peak} and values at large relative displacements δ_{res} are respectively close to 21° and 14°. These values are in good agreement with those obtained by Bond and Jardine (1991) on the London clay and available data bases (Jardine et al. 2005)

Friction values obtained by the ICP method using the δ_{peak} value are the closest to the measured values. The high frictions mobilised in the intact Flanders clays below 7 m penetration are approached and the effect of the friction fatigue due to the driving process in the upper layer between 4 m and 7 m is partially reproduced.

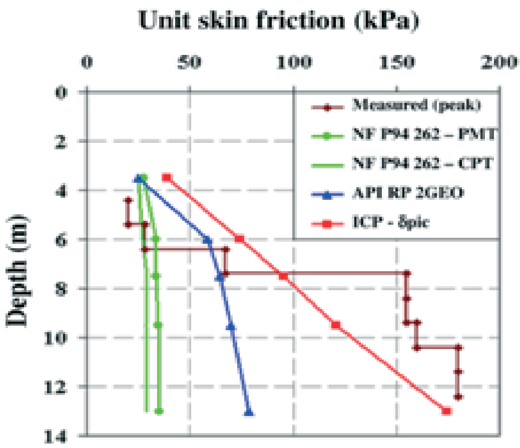

Figure 6: Comparison of measured and calculated local friction values for driven pile B1

Figure 7 compares measured and calculated local friction values on bored pile F1 and screwed pile S1.

Methods included in standard NF-P 94 262 yield realistic friction values for screwed piles and slightly overestimated values for bored piles in Flanders clay.

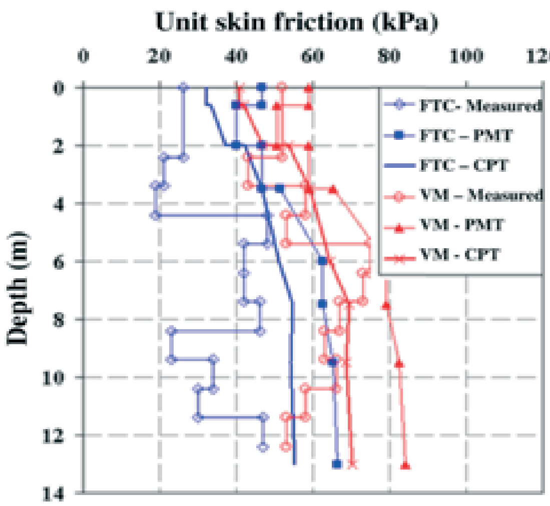

Figure 7: Comparison of measured and calculated local friction values for bored pile F1 and screwed pile S1

6 CONCLUSIONS

The static capacity of piles in fissured, highly plastic and overconsolidated clays, such as Flanders clays, is strongly dependent on the pile installation method.

The driven closed ended steel pipe pile, which generates full soil displacement, mobilises very high friction values (> 150 kPa) equal or even in excess of the undrained shear strength of the clay.

The CFA bored pile, a non-displacement pile, mobilises much lower friction values (of the order of 40 kPa).

The screwed pile, which generates partial soil displacement, mobilises significantly higher friction values (at about 60 kPa)

The ICP effective stress method is the only considered method capable of reproducing the very high friction values observed with driven piles in this type of soil formation.

The methods included in the French standard NF-P 94 262 and based on in situ tests give a realistic assessment of frictions for screwed piles and a slight overestimate for CFA piles. They significantly underestimate the friction values for closed ended driven steel pipe piles.

7 ACKNOWLEDGEMENTS

The results presented in this paper were obtained through the French National Project SOLCYP. SOLCYP is a research project into the behaviour of piles under cyclic loading involving 14 contracting companies from the civil engineering and energy sectors and 6 academic institutions. The project is driven by IREX with funding from private partners, ANR (National Research Agency), MEDDE (Ministry for Ecology, Sustainable Development and Energy) and FNTP (Fédération Nationale des Travaux Publics). The authors are very grateful to the project partners for authorizing publication of the data.

8 REFERENCES

AFNOR.1999. NF P 94-150-2. Norme Française. Sols: Reconnaissance et Essais – Essai statique de pieu sous effort axial – Partie 1: en compression et Partie 2: en traction.

AFNOR. 2012. NF P 94 262. Norme d'application de la Norme Française NF EN 1997-1. Fondations profondes.

API RP2GEO (2011) API Recommended Practice, Geotechnical and Foundation Design Considerations, First Edition, April 2011.

Benzaria O., Le Kouby A. and Puech A. 2012. Cyclic axial load-tests on driven and bored piles in overconsolidated clay, *Offshore Site Investigation and Geotechnics*, SUT, London.

Benzaria O., Puech A. and Le Kouby A. 2013. Essais cycliques axiaux sur des pieux forés dans une argile surconsolidée. *Proceedings 18th ICSMGE, Paris.*

Bond A.J. and Jardine R.J. 1991. Effects of installing displacement piles in a high OCR clay. *Géotechnique*, 41(3) 341-363.

Bond A.J. and Jardine R.J. 1995. Shaft capacity of displacement piles in a high OCR clay. *Géotechnique,* 45: 3–23.

Borel S. and Reiffsteck P. 2006. Caractérisation de la déformabilité des sols au moyen d'essais en place. *Géotechnique et Risques Naturels,* LCPC, GT81.

Jardine R., Chow F., Overy R. and Standing J. 2005. ICP design methods for driven piles in sands and clays. *Thomas Thelford Publishing*, London.

Josseaume H. 1998. Propriétés mécaniques de l'argile des Flandres à Dunkerque et Calais. Revue Française de Géotechnique, N°84.

Mayne P.W. 1991. Determination of OCR in clays by piezocone tests using cavity expansion and critical state concepts. *Soils and Foundations.* 31(2), 65-76.

Powell J.J.M., Quaterman R.S.T. and Lunne T. 1988. Interpretation and use of the piezocone test in UK clays. *Proc. Geot. Conf. Penetration Testing in the UK*, Birmingham, 151-6, Thomas Telford, London.

Puech A., Canou J., Bernardini C., Pecker A., Jardine R., and Holeyman A. 2012. SOLCYP: a four year JIP on the behaviour of piles under cyclic loading. *Offshore Site Investigation and Geotechnics*, SUT, London.

Cyclic axial load tests on bored piles in overconsolidated Flanders clay

Essais cycliques axiaux sur des pieux forés dans l'argile surconsolidée des Flandres

O. Benzaria
Fugro GeoConsulting, Nanterre, France - IFSTTAR, Paris, France

A. Puech
Fugro GeoConsulting, Nanterre, France

A. Le Kouby
IFSTTAR, Paris, France

ABSTRACT: As part of the national project SOLCYP, four bored piles were installed in the highly overconsolidated Flanders clay. The 13 m length, 420 mm diameter instrumented piles were submitted to extensive series' of static and cyclic load tests. This paper presents key results from conventional static tests and cyclic one-way and two-way tests in compression.

RÉSUMÉ : Dans le cadre du projet national SOLCYP, quatre pieux forés instrumentés ont été installés dans l'argile fortement surconsolidée des Flandres. Ces pieux de 13 m de fiche et 420 mm de diamètre ont été soumis à des séries d'essais de chargements statiques et cycliques axiaux. Cette communication présente les principaux résultats des essais statiques conventionnels et des essais cycliques en compression répétés et alternés.

KEYWORDS : SOLCYP, bored piles, overconsolidated clay, cyclic loading

MOTS-CLES: SOLCYP, pieux forés, argile surconsolidée, chargements cycliques.

1 INTRODUCTION

The main objective of the French National Project SOLCYP (Puech et al., 2012) is to develop a methodology for designing cyclically loaded piles. As part of the project field tests were conducted on two experimental sites located in northern France: the Merville site consisting of Flanders clay and the Loon-Plage site consisting of dense sand. At the Merville site four driven metallic piles, four bored piles and two screwed piles were installed.

A description of the experimental conditions and a presentation of the results obtained on the driven tubular piles can be found in Benzaria et al. (2012). This paper presents the results of the static and cyclic tests performed on the bored piles.

2 FLANDERS CLAY

The test site is located in Merville in northern France. The stratigraphy consists of a top cover of 3.5 m of sandy to clayey silts underlain by the Flanders clay formation which is very homogeneous across the site and extends to at least 40 m below ground level (BGL). The water table fluctuates within the upper silt according to the seasons but was approximately 2 m BGL at the time of testing.

The Flanders clay, geologically similar to the London clay and to the Boom clay, was deposited 50 million years ago (Eocene) in a marine gulf extending over northern France, Belgium and south-east of England. The clay was covered by tertiary formations. Sedimentation continued until the Upper Pleistocene period and the ground level was probably some 200 m higher than it is today. The underlying formations were eroded and Flandrian alluvions were deposited during the Quaternary period. The sediments were submitted to glacial loading and unloading during periods of ice advance and retreat. These periglacial processes,chemical cementation and ageing processes have resulted in the high apparent degree of overconsolidation (Josseaume, 1998).

The physical characteristics of the Flanders clay are similar to those of the London and Boom clays (Borel and Reiffsteck, 2006): low water content (about 30%); high plasticity (PI close to 50); significant fissuring particularly below 5 m depth.

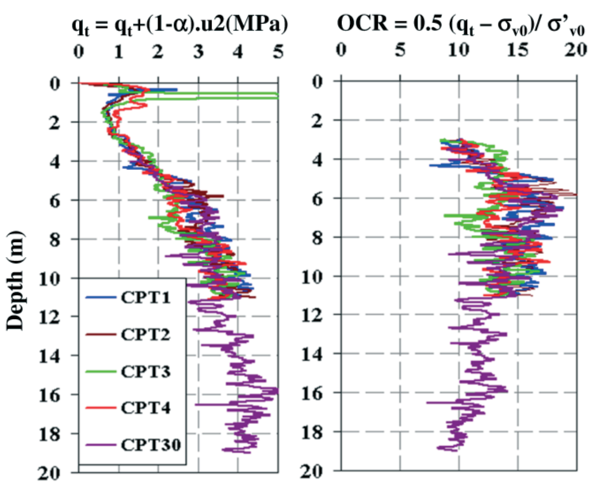

Figure 1: Cone resistance q_t and OCR profiles at Merville

A specific geotechnical site investigation was carried out over the pile testing area including piezocone tests (CPTUs), Ménard pressuremeter tests (PMTs), continuous high quality sampling and standard and advanced laboratory tests on recovered samples.

The OCR was estimated from CPT data using the relationship proposed by Mayne (1986): OCR = k. $(q_t-\sigma_{v0}) / \sigma'_{v0}$ with k = 0.5. The factor k depends on the type of soil. A value of 0.5 was selected as giving OCR values compatible with both the assumed past overburden and the gradient of the cone resistance $q_n = q_t - \sigma_{v0}$ in the deep clay (beyond 8 m BGL). In the London clay Powell et al. (1989) suggest that k values may be higher than 1.

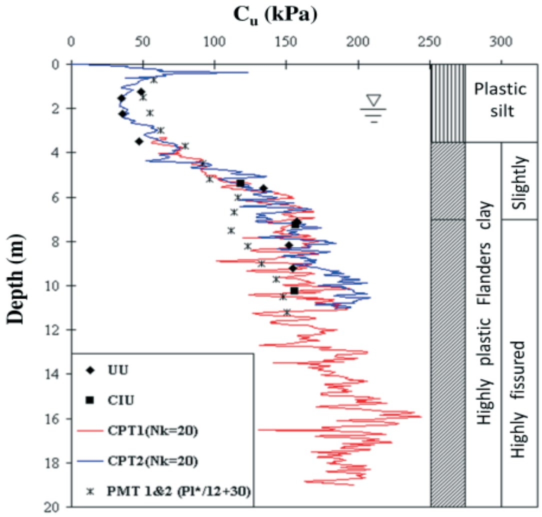

Figure 2: Soil conditions at the Merville pile test location

Unconsolidated undrained (UU) or isotropically consolidated, undrained (CIU) triaxial tests show fragile premature failures of the samples as frequently observed in this type of fissured and highly overconsolidated plastic clays. Failure is characterized by the formation of shear planes containing reoriented particles as noted by Bond and Jardine (1991) in the London clay. Undrained shear strength C_u values correlate with cone resistance values using a high cone factor N_{kt} , [$N_{kt} = (q_t - \sigma_{vo}) / C_u = 20$], compatible with the nature of the material. Net limit pressure values pl* are relatively well linked to C_u using the relationship proposed by Amar and Jezequel (1998): $C_u = p_l^* / 12 + 30$, with C_u in kPa and pl* in MPa.

3 PILE INSTALLATION AND LOADING CONDITIONS

The four piles were geometrically identical (D = 420 mm, length = 13 m). They were bored using a hollow auger that penetrated the soil by rotation (Continous Flight Augering or CFA piles) and was then removed without rotation while grout was poured through the hollow stem (Figure 3a). A telescopic nose was used to improve grouting at the base. Piles were equipped with a set of LCPC removable extensometers lowered into a reservation tube fixed to the reinforcement cage (Figure 3b).

Piles were tested two months after installation. The loading programme included static reference tests with one hour increments according to ISSMGE or NF P 94-150 (AFNOR, 1999), rapid static load tests (load increments maintained only 3 mn) and axial one-way and two-way cyclic load tests. A more detailed description of the testing set up (Figure 4) and loading modes can be found in Benzaria et al. (2012).

The complete characterisation of a cyclic loading requires the definition of the following parameters:

Q_m: mean value of the load during cycling,

Q_c : half -amplitude of the cyclic load,

Q_{max}: maximal cyclic load ($Q_{max} = Q_m + Q_c$)

N: number of cycles (tests were conducted to failure or to a great number of cycles N > 1000)

f: frequency of cycles (normally 0.5Hz)

Q_{us}: ultimate static capacity for the mode considered (tension: Q_{ut} or compression: Q_{uc}).

Loading is in one-way mode when $Q_c < Q_m$ and two-way mode when $Q_c > Q_m$.

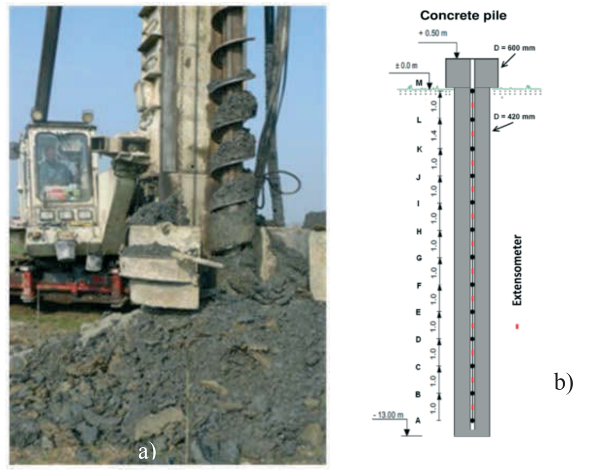

Figure 3: Bored piles at Merville a) hollow auger b) sketch of pile instrumentation using LCPC removable extensometers

Figure 4: Set-up for compression load tests

4 STATIC TESTS

A static reference test was performed on pile F1 before any other load was applied (virgin pile). The load –displacement curve at pile head and the creep curve representing the rate of displacement of the pile head during each one-hour load increment are shown on Figure 5.

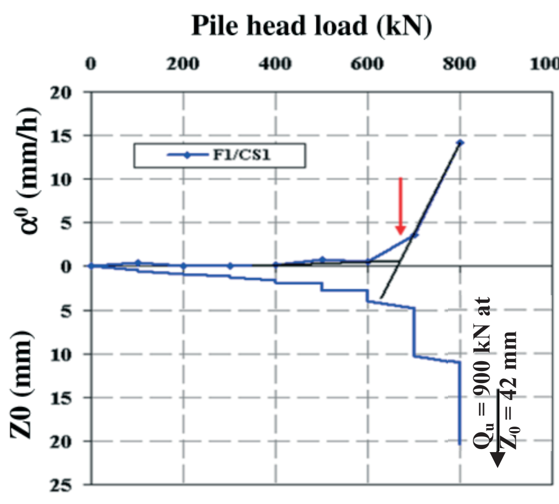

Figure 5: Load-displacement curve and creep curve at pile head for static reference test on pile F1

The following observations were made:
- Failure is of the ductile type (unlike observations made on the driven piles; Benzaria et al. 2012);
- Large plastic deformations start for a pile head displacement of about 3% of pile diameter. The conventional pile capacity at 10% of pile diameter can be extrapolated with confidence at 900 kN ;
- Creep load Q_F is well identified at 670 kN with Q_F/Q_{uc} # 0,75.

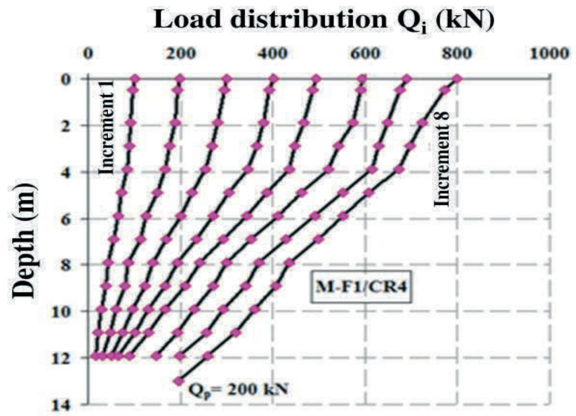

Figure 6: Load distributions obtained at each load increment for static reference test on pile F

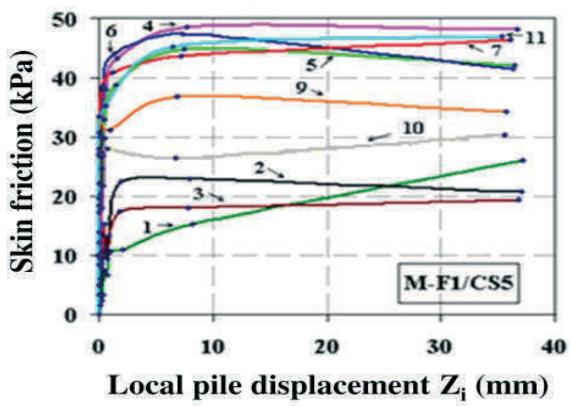

Figure 7: Local shear transfer (t-z) curves obtained for last load increment of static reference test on pile F1

Strain gauge measurements obtained from the removable extensometers allow the load distribution along the pile (Figure 6) and the local load transfer curves to be determined according to the procedure described by Benzaria et al. (2012). A set of local load transfer curves (called t-z curves) is presented on Figure 7. Mobilisation of skin friction is very rapid (between 1% and 2% of pile diameter). The ductile character of the failure phenomenon is confirmed. Limit friction values are moderate (f < 50 kPa) and much lower than observed on tubular closed ended piles driven on the same site.

5 CYCLIC TESTS

5.1 *One-way cyclic tests*

Series of cyclic and rapid load tests were applied on pile F2 as shown on Figure 8. Details of cyclic batches are given in Table 1.

The main observations can be summarised as follows :
- The response of the pile is controlled by the maximum load level (Q_{max});
- As long as Q_{max} remains below a critical level (threshold) pile head displacements are negligible even for large numbers of cycles (N > 1000). Hysteresis loops are closed (Figure 9) ;
- As soon as the threshold is reached or exceeded, permanent pile head accumulate which causes the pile to fail. Tests CC3, CC8, CC9 et CC10 exceeded 12 mm (0.03 D) of permanent displacement, which can be considered as the cyclic failure criterion (Figure 8) ;
- The threshold value is very close to $Q_{max}/Q_{uc} = 0.9$
- The post-cyclic capacity of the pile is not significantly affected by cyclic loads even in case of high amplitude loads leading the pile to failure.

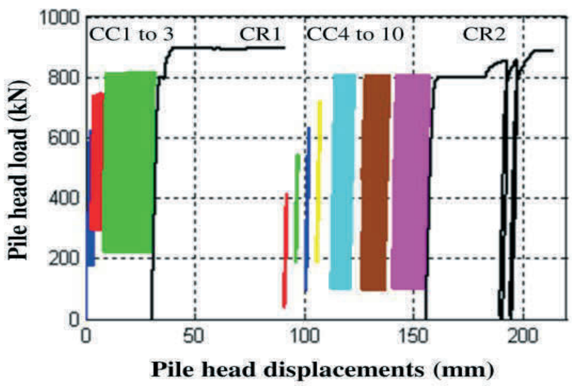

Figure 8: Pile head load-displacement curves obtained for rapid static and cyclic tests on pile F2

It has been noted that frequency may slightly impact the evolution of pile head displacements in the near-failure domain as illustrated on Figure 9. Tests CC9 and CC10 were performed with similar load characteristics but different frequencies (respectively 0.1 Hz and 0.5 Hz); failure is accelerated when frequency drops.

Table 1 : Characteristics of loads applied on pile F2
C : cyclic R : rapid static Q_{uc} = 900 kN (pile F1)

Pile F2	Type	Date	f (Hz)	Q_m / Q_{uc}	Q_c / Q_{uc}	N
Installation		16/03/2011				
CC1	C	16/05/2011	0,5	0,50	0,25	3408
CC2	C	17/05/2011	0,5	0,58	0,25	4834
CC3	C	17/05/2011	0,5	0,58	0,33	2021
CR1	R	17/05/2011				
CC4	C	17/05/2011	0,5	0,25	0,20	1013
CC5	C	17/05/2011	0,5	0,40	0,20	1000
CC6	C	17/05/2011	0,5	0,40	0,30	1088
CC7	C	17/05/2011	0,5	0,50	0,30	602
CC8	C	17/05/2011	0,5	0,50	0,40	81
CC9	C	17/05/2011	0,1	0,50	0,40	24
CC10	C	17/05/2011	0,5	0,50	0,40	85
CR2	R	17/05/2011				

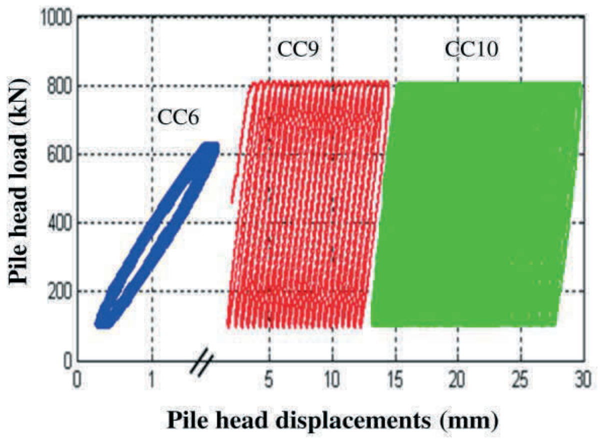

Figure 9: Pile head load-displacement relationships obtained for three cyclic tests on pile F2

5.2 *Two-way cyclic tests*

Nine two-way cyclic tests were performed on pile F3. All tests were conducted under the following load conditions: $Q_m / Q_{uc} < 0.2$ and $0.2 < Q_c / Q_{uc} < 0.5$. For hydraulic system considerations (two jacks used in opposite mode), it was not possible to apply maximal cyclic loads Q_{max} in excess of 0.7 Q_{uc}.

All such tests remain in the stable domain characterised by negligible permanent displacements and closed hysteresis loops as illustrated on Figure 10.

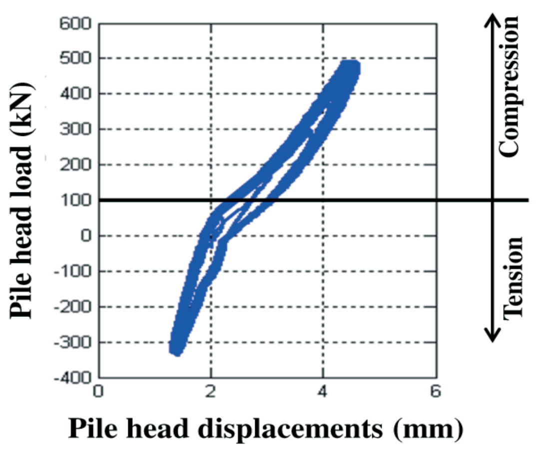

Figure 10: Pile head load-displacement relationship obtained for two-way test CC9 on pile F3

5.3 *Concept of cyclic stability*

A preliminary analysis of the complete set of test results obtained in one-way and two-way compression (but also in one-way and two-way tension) suggests that, in the type of soil considered, two regimes can be clearly differentiated:

- A regime where cyclic loads, even at large number (N > 1000), do not affect significantly the behaviour of the pile : negligible permanent pile head displacements, constant cyclic rigidity ;
- A regime where the pile reaches failure under a small number of cycles.

The stability domain is relatively large in comparison with other soils. It is affected by the loading mode (one-way versus two-way).

The next step is to propose cyclic stability diagrams in the sense of Poulos (1988) or Karlsrud et al. (1986). This should be feasible after a more complete analysis of the dataset and a precise definition of failure criteria.

6 CONCLUSIONS

Bored CFA piles were installed in the overconsolidated Flanders clay at the Merville test site. Results of static and one-way or two-way cyclic compression tests performed on these piles are presented.

Under static loading a ductile failure is observed whereas fragile failure was noted for driven piles (Benzaria et al. 2012). Friction values are much lower for bored piles than for driven piles.

Results suggest the existence of a large domain of cyclic loads where the stability of the pile is ensured for a large number of cycles. The threshold, at least in one-way mode would be close to $Q_{max}/Q_{uc} = 0.9$. The post-cyclic capacity is not significantly affected by cyclic loads even when cyclic pile failure was reached.

A companion paper presented at the same conference (Puech and Benzaria, 2013) analyses the static response of both types of piles, driven and bored, with respect to the mechanical behaviour of the Flanders clay.

7 ACKNOWLEDGEMENTS

Results presented in this paper were obtained in the framework of the French National Project SOLCYP. SOLCYP is a research project on the behaviour of piles under cyclic loading involving 14 contracting companies of the civil engineering and energy sectors and 6 academic institutions. The project is driven by IREX with funding from private partners, ANR (National Research Agency), MEDDE (Ministry for Ecology, Sustainable Development and Energy) and FNTP (Fédération Nationale des Travaux Publics). The authors are very grateful to the project partners for authorising publication of the data.

8 REFERENCES

AFNOR. 1999. NF P 94-150-2. Norme Française. Sols: Reconnaissance et Essais – Essai statique de pieu sous effort axial – Partie 1: en compression et Partie 2: en traction.

Amar S. et Jezequel J.F. 1972. Essais en place et en laboratoire sur sols cohérents. Comparaison des résultats. Bulletin de Liaison des Ponts et Chaussées, N° 58.

Benzaria O., Puech A and Le Kouby A. 2012. Cyclic axial load-tests on driven and bored piles in overconsolidated clay, *Offshore Site Investigation and Geotechnics*, SUT, London.

Bond A.J. and Jardine R.J. 1991. Effects of installing displacement piles in a high OCR clay. *Géotechnique*, 41(3) 341-363.

Borel S. and Reiffsteck P. 2006. Caractérisation de la déformabilité des sols au moyen d'essais en place. *Géotechnique et Risques Naturels,* LCPC, GT81.

Josseaume H. 1998. Propriétés mécaniques de l'argile des Flandres à Dunkerque et Calais. Revue Française de Géotechnique, N°84.

Karlsrud, K., Nadim F. and T. Haugen. 1986. Piles in clay under cyclic loading: Field tests and computational modelling. Proc. 3rd Int. Conf. on Numerical Methods in Offshore Piling, 165-190, Nantes, France, May 1986.

Mayne P.W. 1986. CPT indexing of in situ OCR in clays. Proceedings ASCE Spec. Conf. "In situ 86", Blacksburg, Virginia.

Powell J.J.M., Quaterman R.S.T. and Lunne T. 1989. Interpretation and use of piezocone test in UK. *Proc. Geotechnology Conference: penetration testing in UK, Birmingham,* Thomas Telford, London

Puech A., Canou J., Bernardini C., Pecker A., Jardine R., and Holeyman A. 2012. SOLCYP: a four year JIP on the behaviour of piles under cyclic loading. *Offshore Site Investigation and Geotechnics*, SUT, London.

Puech A. et Benzaria O. 2013. Effet du mode de mise en place sur la réponse statique de pieux dans l'argile surconsolidée des Flandres. *Proc. 18 ICSMGE*, Paris, 2-5 Sept. 2013.

Cyclic axial load tests on bored piles in dense sands

Essais cycliques axiaux sur des pieux forés dans des sables denses

O. Benzaria
Fugro GeoConsulting, Nanterre, France – IFSTTAR, Paris, France

A. Puech
Fugro GeoConsulting, Nanterre, France

A. Le Kouby
IFSTTAR, Paris, France

ABSTRACT: As part of the national project SOLCYP, five bored piles were installed in dense Flanders sands. Two 8 m long, 420 mm diameter instrumented piles were submitted to series of static and cyclic load tests in compression. This paper presents key results from the conventional static tests and cyclic one-way tests in compression.

RÉSUMÉ : Dans le cadre du projet national SOLCYP, cinq pieux forés instrumentés ont été installés dans les sables denses des Flandres. Deux pieux de 8 mètres de fiche et 420 mm de diamètre ont été soumis à des séries d'essais de chargements statiques et cycliques axiaux en compression. Cette communication présente les résultats les plus significatifs des essais statiques conventionnels et des essais cycliques en compression.

KEYWORDS: SOLCYP, bored piles, dense sands, cyclic loading.

MOTS-CLES: SOLCYP, pieux forés, sables denses, chargements cycliques.

1 INTRODUCTION

The aim of the French National Project SOLCYP (Puech et al., 2012) is to develop a methodology for designing cyclically loaded piles. As part of the project field tests were conducted on two experimental sites located in the North of France: the Merville site consisting of Flanders clay and the Loon-Plage site consisting of dense sand. Five bored piles and two driven tubular piles were installed at the Loon-Plage site.

The results obtained with driven and bored piles on the Merville site are partially published (Benzaria et al., 2012 and 2013; Puech and Benzaria, 2013). This paper focuses on the results of the static and cyclic tests in compression performed on the bored piles at the Loon-Plage site.

2 FLANDERS SAND

The test site is located at Loon-Plage near Dunkirk in northern France and a short distance from the site used by Imperial College for the pile tests performed in the nineties (e.g. Jardine and Standing 2000). The stratigraphy consists of a thin cover of man-made materials (0 m to 0.6 m) and recent sandy clays (0.6 to 2.2 m) overlying the Flanders sand formation. The water table at the time of pile testing was approximately at 2 m BGL.

A specific geotechnical site investigation was performed at the pile testing area including four piezocone tests (CPTUs), two Ménard pressuremeter tests (PMTs), three continuous samplings and standard and advanced laboratory tests on the recovered samples (Figures 1 and 2). The sand is a siliceous sand, very fine (D_{50} close to 0.15 mm) and poorly graded (uniformity coefficient CU = 0.98). The formation is laterally homogeneous and characterised by net cone resistances q_n increasing from 5 MPa to 40 MPa at about 8 m depth to stabilise in the range 30 MPa to 50 MPa until 11.5 m. Between 12 m and 16.5 m penetration is found an interbed of soft clay with very poor mechanical properties. According to Jamiolkowski et al. (2003) the density index I_D derived from CPT data (Figure 2) ranges from 0.7 to 0.9 (dense to very dense sand).

A series of monotonic triaxial tests gave constant volume friction angles $Ø_{cv}$ close to 31° in good agreement with values found by Kuwano for the Dunkirk sand (Kuwano, 1999; Jardine and Standing, 2000).

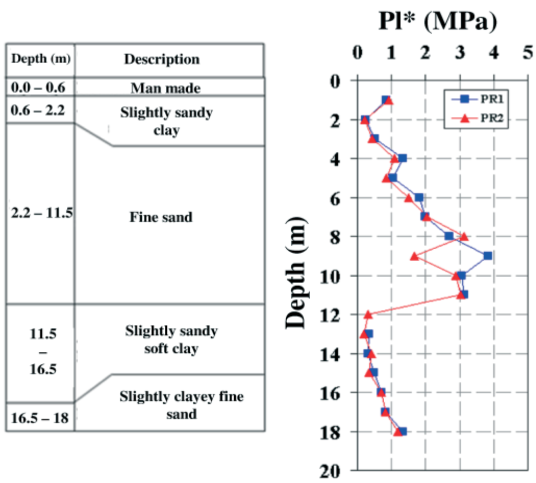

Figure 1: Stratigraphic and PMT profiles at Loon-Plage

3 PILE INSTALLATION AND LOADING CONDITIONS

The two piles F4 and F5 are geometrically identical (OD = 420 mm, length 8 m). They were bored using a hollow auger that penetrated the soil by rotation (Continuous Flight Augering, CFA pile) and was removed without rotation while grout was poured through the hollow stem (Figure 3a). Piles were equipped with a set of LCPC removable extensometers lowered into a reservation tube fixed to the reinforcement cage (Figure 3b).

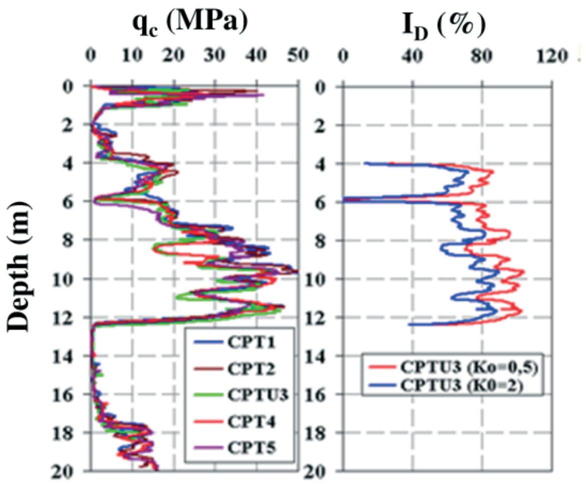

Figure 2: CPT profiles at Loon-Plage: cone resistance q_c and density index I_D

Piles were tested approximately three months after installation. The loading programme included reference static tests with one-hour increments according to ISSMGE or NF P 94-150 (AFNOR, 1999), rapid monotonic load tests (load increments maintained only 3 mn) and axial one-way cyclic load tests. A more detailed description of testing set up (Figure 4) and loading modes can be found in Benzaria et al. (2012).

The complete characterisation of a cyclic loading requires the definition of the following parameters:

Q_m: mean value of the load during cycling,

Q_c : half -amplitude of the cyclic load,

Q_{max}: maximal cyclic load ($Q_{max} = Q_m + Q_c$)

N: number of cycles (tests were conducted to failure or to a great number of cycles N > 1000)

f: frequency of cycles (normally 0.5Hz)

Q_u : ultimate static capacity for the mode considered (tension or compression).

Loading is in one-way mode when $Q_c < Q_m$ and two-way mode when $Q_c > Q_m$.

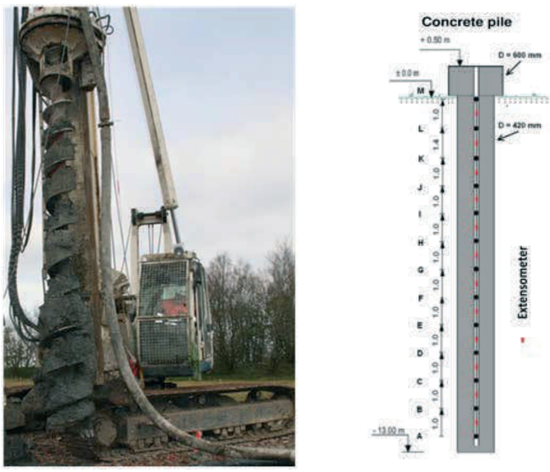

a) b)

Figure 3: a) construction of a CFA pile and b) sketch of pile instrumentation using LCPC removable extensometers.

The pile test set up is similar to the pile test set-up used at the Merville site, described Benzaria et al. (2012).

Figure 4: Pile test set-up used at Loon-Plage

4 STATIC TESTS

A static reference test was performed on pile F4 before any other load was applied to the pile (virgin pile). The load-displacement curve at pile head and the creep curve representing the rate of displacement of the pile head during each one-hour load increment are shown in Figure 5.

The following observations can be made:

- The failure is of the ductile type
- Large plastic deformations start for a pile head displacement of about 5% of pile diameter. The conventional pile capacity Q_{uc} at 10% of pile diameter (42 mm) can be extrapolated with confidence at about 1100 kN
- The creep load Q_F is close to 850 kN with Q_F / Q_{uc} # 0.77
- The mobilisation of the end bearing capacity is delayed, then quasi linear to 8% of relative pile head displacement suggesting further increase after the conventional value at 0.1 D.

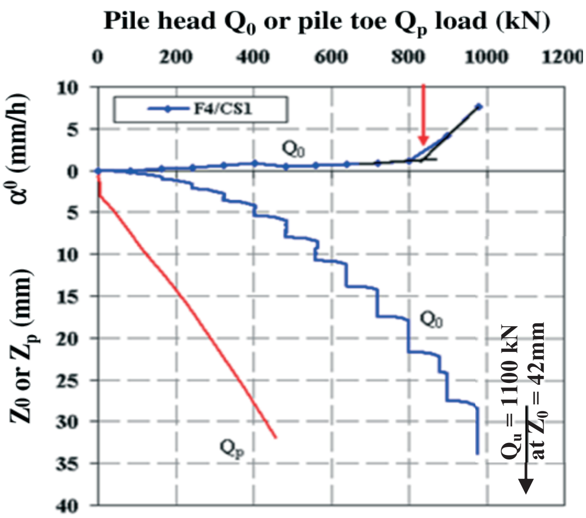

Figure 5: Static reference test on pile F4. Pile head load displacement curve, end bearing mobilisation curve and creep curve

Strain gauge measurements obtained from the removable extensometers allow the load distribution along the pile and the local load transfer curves to be determined according to the procedure described by Benzaria et al. (2012). Local load transfer curves (t-z curves) corresponding to the sand levels are presented in Figure 6. Mobilisation of skin friction is progressive: local relative displacement at failure is of the order of 1% and 2% of pile diameter. The ductile character of the failure phenomenon is confirmed. Limit friction values are moderate (f < 45kPa).

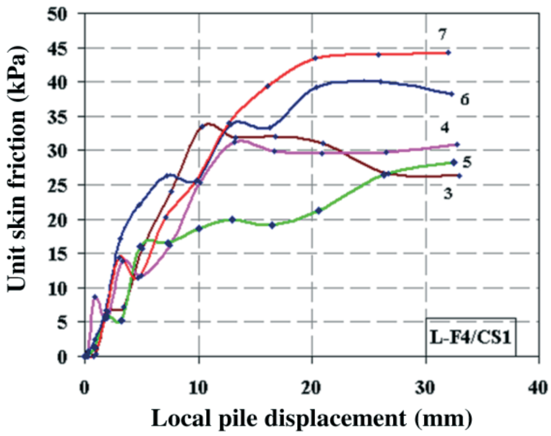

Figure 6: Local shear transfer (t-z) curves in Flanders sand for last increment of reference static load test on pile F4

5 CYCLIC TESTS

5.1 *Cyclic tests on virgin pile*

The response of pile F5 to the cyclic batches applied before any other load was applied to the pile is shown on Figure 7. Details of load characteristics are given in Table 1.

Table 1: Characteristics of loads applied to pile F5
C = cyclic Q_{uc} = 1100 kN (pile F1)

Pile F5	Type	Date	f (Hz)	Q_m / Q_{uc}	Q_c / Q_{uc}	N
Installation		25/11/11				
CC1	C	08/03/12	0.5	0.36	0.27	14
CC2	C	08/03/12	0.5	0.27	0.09	5000
CC3	C	08/03/12	0.5	0.36	0.18	280

The cyclic load ratio applied in test CC1 is relatively small (Q_{max} / Q_{uc} = 0.63). The test had to be stopped prematurely due to unexpected movements of a reaction pile but it is obvious that the pile was close to cyclic failure after only 14 cycles. Cyclic failure is defined for permanent pile head displacements of 3% of pile diameter i.e. 12 mm.

Cyclic load amplitude was significantly reduced for test CC2 (Q_{max} / Q_{uc} = 0.35). Five thousand cycles could be applied but they induced an additional permanent displacement of more than 16nmm.

Test CC3 (Q_{max} / Q_{uc} = 0.54) caused another 6 mm of permanent displacements after only 280 cycles.

It is observed that the rate of displacements of the pile head for a given number of cycles increases with the maximum cyclic load ratio. However, for each individual test, the rate of displacement decreases with the number of cycles (Figure 8). This observation makes it difficult to define pile failure.

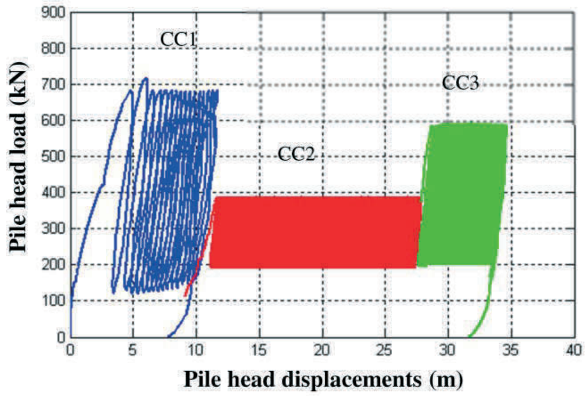

Figure 7: Pile head load-displacement relationships for cyclic tests performed on virgin pile F5

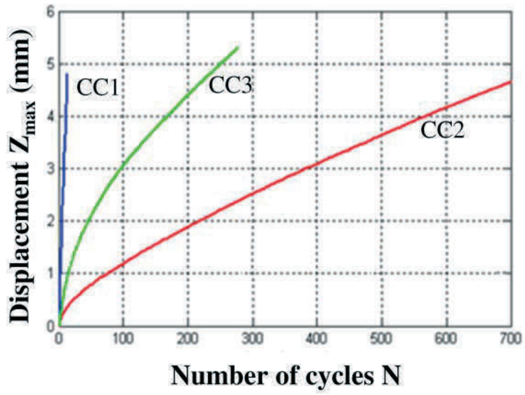

Figure 8: Pile head displacements versus number of cycles for cyclic load tests performed on pile F5

This apparent paradox can be explained by observing in detail the phenomena generated by cyclic loads on pile in sand. Cycles induce small relative soil-pile slips at the interface. The global pile head displacement is the result of these successive slips. The rate of displacement is function of the load amplitude and the maximum load level, but these parameters also determine the evolution of the friction. The friction can degrade (large amplitude cycles) or improve (small amplitude cycles). If the pile is loaded in tension, the rate of displacement is modified accordingly to lead the pile towards cyclic failure or stabilisation (Tsuha et al., 2012). Failure can be defined either in a conventional manner (e.g. 0.1 D) or in terms of allowable pile head displacement. If the pile is loaded in compression, the displacement generates a progressive mobilisation of the end bearing so that in any case the pile tends to stabilise. Consequently, for piles in compression, the failure criterion should be expressed in terms of allowable pile head displacement and not in a conventional manner. The criterion can be reached either under increasing or decreasing rate of displacement. In the first case, failure is reached after a small number of cycles. In the second case, a large number of cycles may be required to reach failure. This explains the significance of stable and metastable domains introduced in cyclic interaction diagrams (e.g. Puech et al., 2013).

5.2 *Effect of loading history*

The history of the loading sequences applied on pile F4 is illustrated on Figure 9 and detailed in Table 2.

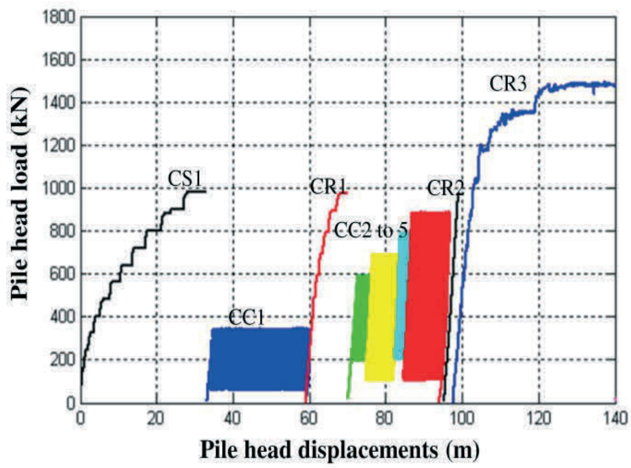

Figure 9: Pile head load-displacement relationships for static and cyclic tests performed on pile F4

The cyclic test CC1 was performed after a conventional reference static test (CS1) conducted to inception of pile failure. Despite a very low cyclic load ratio (Q_{max} / Q_{uc} = 0.31), the failure displacement criterion (set at 3% of pile diameter) was reached before 2000 cycles. The post-cyclic capacity (test CR1) is apparently not affected whereas drops in skin friction (not shown here) are detected by the extensometers.

Tableau 2: Characteristics of loads applied to pile F4
S: reference static R : rapid static C : cyclic

Pile F4	Type	Date	f (Hz)	Q_m / Q_{uc}	Q_c / Q_{uc}	N
Installation		25/11/11				
CS1	S	01/03/12				
CC1	C	02/03/12	0.5	0.18	0.13	1819
CR1	R	02/03/12				
CC2	C	02/03/12	0.5	0.36	0.18	200
CC3	C	02/03/12	0.5	0.36	0.27	200
CC4	C	02/03/12	0.5	0.47	0.25	100
CC5	C	02/03/12	0.5	0.45	0.36	200
CR2	R	02/03/12				
CR3	R	27/03/12				

Successive batches with increasing amplitudes and mean load levels (CC2 to CC5) were then applied. They generated significant permanent displacements (about 25 mm for only 700 cumulated cycles). The rapid static test CR2 conducted to 1000 kN reveals a net increase in the rigidity of the pile response. A static test CR3 was then conducted to failure, showing a post-cyclic capacity of the pile at 1480 kN, i.e. an increase of 27% by reference to the initial reference capacity on the virgin pile (test CS1).

6 CONCLUSIONS

This paper presents the results of static and cyclic load tests in compression performed on bored CFA piles installed in dense to very dense Flanders sand at Loon-Plage.

Under static loading, failure is of the ductile type and large local displacements are required to mobilise the skin friction (between 3% et 5% of pile diameter).

The cyclic response of the piles is highly dependent on the loading history. Globally bored piles appear very sensitive to one-way cyclic loading in sand. Large permanent displacements must be generated before a sufficient end bearing can be mobilised to stabilise the pile. Failure must be defined in terms of allowable displacements and not in a conventional manner.

A more detailed interpretation of the results needs to be done after full processing of the data (including two-way and tension tests) and due consideration of the mechanical behaviour of the Flanders sand.

7 ACKNOWLEDGEMENTS

Results presented in this paper were obtained in the framework of the French National Project SOLCYP. SOLCYP is a research project on the behaviour of piles under cyclic loading involving 12 contracting companies of the civil engineering and energy sectors and 6 academic institutions. The project is driven by IREX with funding from private partners, ANR (National Research Agency), MEDDE (Ministry for Ecology, Sustainable Development and Energy) and FNTP (Fédération Nationale des Travaux Publics). The authors are very grateful to the project partners for authorising publication of the data.

8 REFERENCES

AFNOR.1999. NF P 94-150-2. Norme Française. Sols: Reconnaissance et Essais – Essai statique de pieu sous effort axial – Partie 1: en compression et Partie 2: en traction.

Benzaria O., Puech A., and Le Kouby A. 2012. Cyclic axial load-tests on driven piles in overconsolidated clay, *Offshore Site Investigation and Geotechnics*, SUT, London

Benzaria A., Puech A. et Le Kouby A. 2013. Essais cycliques axiaux sur des pieux forés dans l'argile des Flandres. *Proceedings 18th ICSMGE, Paris*

Jamiolkowski, M.B., Lo Presti, D.C.F. and Manassero, M. 2003. Evaluation of Relative Density and Shear Strength of Sands from CPT and DMT. Soil Behavior and Soft Ground Construction, ASCE, GSP No. 119, 201-238.

Jardine, R.J., Standing, J.R.: OTO 2000. 008 - Pile Load Testing Performed for HSE Cyclic Loading Study at Dunkirk, France; Volume 1".

Kuwano R. 1999, The stiffness and yielding anisotropy of sand. *PhD Thesis*, University of London (Imperial College).

Puech A., Canou J., Bernardini C., Pecker A., Jardine R., and Holeyman A. 2012. SOLCYP: a four year JIP on the behaviour of piles under cyclic loading. *Offshore Site Investigation and Geotechnics*, SUT, London

Puech A. et Benzaria O. 2013. Effet du mode de mise en place sur la réponse statique et cyclique de pieux dans l'argile surconsolidée des Flandres. *Proceedings 18th ICSMGE, Paris*

Puech A., Benzaria O., Thorel L., Garnier J., Foray P. et Jardine R. 2013. Diagrammes de stabilité cyclique de pieux dans les sables. *Proceedings 18th ICSMGE, Paris*

Tsuha C.H.C., Foray P.Y., Jardine R.J., Yang Z.X., Silva M. and Rimoy S. 2012. Behaviour of displacement piles in sand under cyclic axial loading. *Soils and Foundations 52(3), June 2012, 393–410,*

Influence of cyclic axial loads on the behaviour of piles driven in sand

Influence des chargements cycliques axiaux sur le comportement et la réponse de pieux battus dans le sable

Matias Silva and Pierre Foray
Laboratoire 3SR, Grenoble, France

Siya Rimoy and Richard Jardine
Imperial College London, London, UK

Cristina Tsuha
University of Sao Paulo, Sao Paulo, Brazil

Zhongxuan Yang
Zhejiang University, Zhejiang, China

ABSTRACT: This paper presents a new cyclic stability diagram for the lateral friction and the effect on the tensile capacity of instrumented model piles subjected to axial cyclic loading across a wide range of calibration chamber testing in silica sand. Local measurements of stresses in the soil mass (vertical, radial and orthoradial) at different distances from the axis of the pile, as well as shear and radial stresses at the soil-pile interface, provide a detailed analysis of the evolution of local stress paths around the pile and the soil mass during cyclic and post-cyclic loading.

RÉSUMÉ: Cet article présente un nouveau diagramme de stabilité cyclique pour le frottement latéral ainsi que l'effet sur la capacité en traction des pieux modèle instrumentés soumis à des chargements cycliques axiaux suite à une large série d'essais en chambre d'étalonnage dans du sable siliceux. Les mesures locales des contraintes dans le sol (verticales, radiales et orthoradiales) à différentes distances de l'axe du pieu, ainsi que les mesures tangentielles et radiales à l'interface sol-pieu, permettent une analyse détaillée de l'évolution des chemins de contraintes locaux autour du pieu et au sein du massif lors des chargements cycliques et post-cycliques.

KEYWORDS: Calibration chamber, axial cyclic loading, sol-pile interaction, cyclic stability diagram.

1 INTRODUCTION

The piled foundations of oil/gas platforms and wind/water turbines are subject to long term environmental cyclic loading. Deep driven piles experience large numbers of full load-unload cycles that contribute to shaft capacity degradation during installation (Lehane et al. 1993, Kolk et al. 2005). The latter degradation may be reversed partially by the time-dependent "ageing" processes observed in full scale tests (Chow et al. 1998, Jardine et al. 2006). The piles are also subject to extensive cyclic loading in service (due to waves, vibrations, storms) that may also affect their shaft capacity.

The cyclic response of the soil-pile interface has been studied using laboratory model piles installed in pressurized calibration chambers (Chan and Hanna 1980, Al-Douri and Poulos 1994, Chin and Poulos 1996, and Le Kouby al. 2004). These tests showed degradation of shaft shear stress capacities that grew as the amplitude of the loads and displacements increased. Jardine et al. (2006) showed from full-scale tests performed at Dunkirk (Chow et al. 1998) that while high amplitude two-way cycles degrade the piles' shaft capacity, low amplitude cycles can accelerate beneficial "ageing" capacity increases with time. Le Kouby et al. (2004) found similar results with laboratory tests on a 20 mm diameter model displacement pile.

This paper aims to improve understanding of the main results obtained with full-scale piles in Dunkirk by Jardine and Standing (2000) through a laboratory scale investigation performed under controlled environmental conditions. Local stress path measurements were made along the model pile shafts and in the sand mass during the phases of installation, ageing and static / cyclic loading. This was achieved by means of intensive instrumentation of the calibration chamber and the pile. This work is part of a joint research programme between the Grenoble Laboratory 3SR and Imperial College London, and the French National SOLCYP research project.

2 TESTING ARRANGEMENTS

2.1 *Calibration chamber*

The large Laboratoire 3S-R calibration chamber was adapted to provide closely controlled environmental conditions (temperature, pressure and electrical power) during periods of several months to investigate the phenomena of pile shaft friction gains through both "ageing" and under low level cycling. Full insulation of the chamber and a temperature control regulation system installed over the external walls were employed to minimize variations during testing, while the membrane pressurizations system was designed to keep operating even in the event of a power failure.

The Grenoble calibration chamber is composed of three cylindrical elements, each 500 mm high and with a 1.2 m internal diameter. The chamber base and top cover are made of rigid 100 mm thick plates. A vertical pressure of ~150 kPa is imposed by a rubber membrane filled with water. This membrane is fixed under the top cover and controlled by an air/water interface regulation system. A single latex membrane (2 mm thick) was installed on the chamber's inner wall to provide K_o conditions at the border of the chamber. A layer of silicone grease provided between the membrane and the wall reduced the friction with the sand mass to ensure better stress homogeneity within the chamber.

A thermal control system consisting of water circulating copper tubes running around the chamber make it possible to work with nearly constant temperatures controlled between 18° and 19^{o} C.

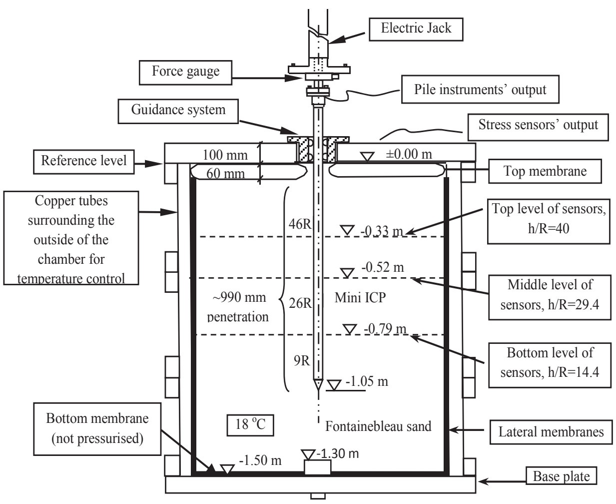

Figure 1: Schematic of the 3SR-calibration chamber

The calibration chamber was filled with NE34 Fontainebleau silica sand for the tests presented. The chamber was filled by air pluviation to give a dense medium to dense state with average Dr = 72%. Table 1 shows the index properties of the sand.

Table 1: Index properties of NE34 Fontainebleau sand

G_s	D_{10} (mm)	D_{50} (mm)	D_{60} (mm)	e_{max}	e_{min}	γ_{max} (kN/m^3)	γ_{min} (kN/m^3)
2.65	0.150	0.210	0.230	0.90	0.51	17.2	14.2

Several standard cone penetration tests (CPT) were performed on NE34 sand samples under a 150 kPa vertical stress. The steady penetration tip resistance traces obtained were almost constant around 23 ± 2 MPa. Further details on the mechanical properties of the NE34 sand are described by Yang et al. (2010).

2.2 *Model pile Mini-ICP*

The Mini-ICP model pile developed by Imperial College London and described by Jardine et al. 2009 was employed for the testing. It is a stainless steel, closed-ended pile of 36mm diameter with a solid cone of 60° at the pile tip. It has three levels of instrumentation (or clusters) identified according to their distance from the tip as: A (9R), B (24) and C (44), R being the pile radius. Each cluster contains an axial load cell, which can be used to calculate the mean friction in the pile shaft; surface stress transducers (SST) for local measurement of total radial and shear stresses; a temperature sensor and an MEMS inclinometer. A tip axial load cell was implemented from ICP03 onwards to better assess the relative contributions of the tip and the shaft friction to the total capacity of the pile.

The pile was installed to a final embedded depth of 0.98 m by cyclic jacking. The installation cycles simulated the aspects of driving that contribute to radial stress degradation during pile driving. The penetration rate varied between 0.5 mm/s and 2 mm/s and the amplitude of the successive jack strokes varied between 5, 10 and 20 mm. The pile head loads were reduced to zero between each stroke.

2.3 *Stress measurements in the soil mass*

Three levels of 12 Kyowa and TML mini-soil stress sensors of different capacities, ranging from 500 kPa to 7 MPa (according to their distance to the pile) were deployed in the soil mass to measure the vertical, radial and circumferential stresses at concentric lines from distances between 2 R and 16 R. Cell action is highly significant with these devices and cyclic loading calibrations were performed at Imperial College following the protocol established by Zhu et al. (2009). The response of each sensor is represented by a series of hysteresis curves that depend on the history of prior loading.

3 EXPERIMENTAL PROGRAMME

After a post-installation ageing period, a first compression test and then a tension load test were conducted to determine the pile capacity prior to cyclic loading. Series' of low and high level cyclic loading tests were then performed, interspersed with tension tests to evaluate the effect of cyclic loadings in the pull-out capacity of the pile.

Cyclic loading tests were characterized by two loading parameters, Q_{cyclic} and Q_{mean}, corresponding respectively to the amplitude of each cycle and the average value of loading. One-way cyclic loading tests were carried out under load-control (LC) involving only tensile conditions, mobilizing up to 60% of the total capacity of the pile in tension, Qt. Two-way (compression and tension) high level cyclic tests were conducted under both load and displacement control (DC). Load cycles were applied at a relatively low frequency, ranging from less than 0.5 cycles per minute in higher levels two-way cycles to almost 2.5 cycles per minute for low level-load controlled tests.

Static tensile tests were performed after each series of cyclic loading at a displacement rate of 0.01 mm/s to assess the available pull-put capacity of the pile. Jardine et al (2006) reported that prior testing could affect the piles' responses to subsequent tests. Table 2 summarizes the different series of cyclic tests performed.

Table 2: Summary of cyclic loading programme

ID	N of cycles	Description	Q_{cyclic} $/Q_T$	Q_{mean} $/ Q_T$
ICP1-OW1 (LC)	1000	0 to -4.0 kN	0.22	0.22
ICP1-TW1 (DC)	100	-4 to 5 mm	0.41	0.06
ICP2-OW1 (LC)	1000	0 to -3.0kN	0.12	0.12
ICP2-OW2 (LC)	1000	0 to -4.8 kN	0.20	0.20
ICP2-OW3 (LC)	500	0 to -6.8 kN	0.28	0.28
ICP2-TW1 (DC)	100	-2.0 to 3.0 mm	0.48	0.15
ICP3-OW1 (LC)	100	0 to -9.6 kN	0.38	0.38
ICP3-TW1 (LC)	287	-5.0 to +8.0kN	0.54	0.08
ICP3-TW2 (LC)	199	-5.0 to +5.0kN	0.40	0.06
ICP3-TW3 (LC)	50	-5.0 to +7.0 kN	0.44	0.02
ICP3-TW4 (LC)	37	-5.0 to +10.0kN	0.44	0.02
ICP4-OW1 (LC)	7000	0 to -3.5 kN	0.15	0.15
ICP4-TW1(LC)	600	-4.0 to +4.0kN	0.23	0.06
ICP4-OW2 (LC)	50	-2.3 to -4.6 kN	0.21	0.63

OW = one-way cycles, and TW = two-way cycles

4 RESULTS FROM ONE-WAY LOW AMPLITUDE CYCLIC TESTS

4.1 *Evolution of stresses along the pile and in the sand mass*

The stress measurements made in the soil mass and along the pile shaft clarify the mechanisms leading to improvement or degradation of the piles' shaft capacities. Figure 2 shows the radial stresses measured in the dry soil at different distances from the pile axis. There is a decrease of the radial stresses with the number of cycles which is accentuated under high-level two-way cycling. Local radial stresses measured on the pile surface present similar trends. Figure 2 also shows the stress changes developed during static tests performed between the two sets of cycling, indicating clear increments in local radial stresses related to greater dilatancy developing in the local stresses after the low level cycling.

The stress distributions developed in the surrounding soil mass are reported in more detail by Jardine et al. (2013) who integrated thousands of measurements to produce a series of summary contour plot diagrams.

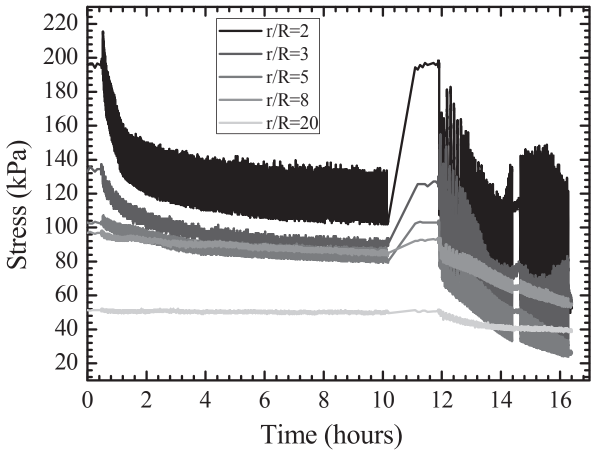

Figure 2: Evolution of radial stresses in the soil mass. From 0 to 9.6 hour: 1000 one-way low amplitude cyclic loading (ICP1-OW1); static tension testing from 9.6 to 10.4 hours and 100 two-way high amplitude cyclic loading from 10.4 to 14.7h (ICP01-OW1).

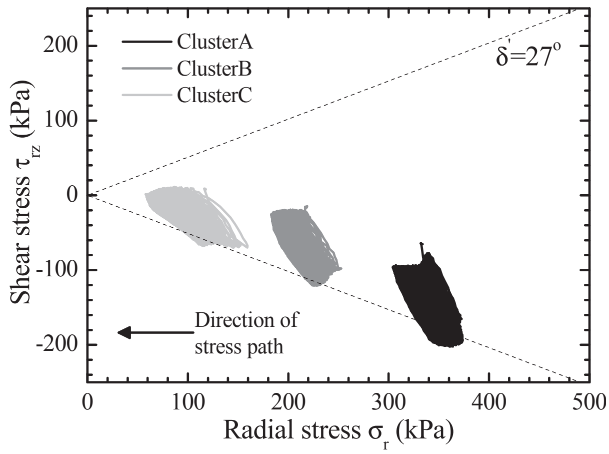

Figure 3: Local stress path at pile surface test Mini-ICP2. One-way low amplitude cycles

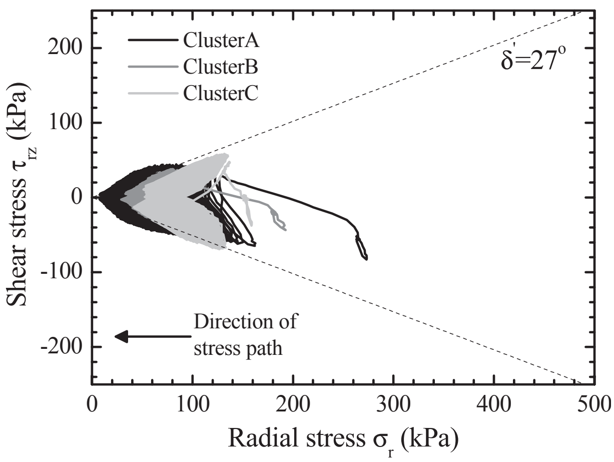

Figure 4: Local stress path at pile surface, test ICP04. Two-way high level cycles

Simultaneous measurements of radial and shear stresses made on the shaft allow us to trace the local stress paths followed on the pile surface. One-way low level cycles, such as those shown in Figure 3 for the three clusters along the pile, cause a slow migration of the effective stress paths to the left as cycling continues, indicating an overall tendency to contract at the interface related to local densification. The latter is interpreted as the main factor leading to increases in the shaft capacity seen during further testing. As the amplitude of the one-way cycles increases, the stress paths migrate more rapidly and reach the static interface shear failure envelope more rapidly (Yang et al. 2010).

The effective stress paths developed under two-way high amplitude cycling follow different paths. They engage, from an early stage, the equivalent of a 'phase transformation line', leading to alternating dilatancy/contractancy of the soil around the interface. These stress paths show 'butterfly wing' patterns similar to those observed during cyclic shear tests conducted under constant volume or normal stiffness conditions (Fakharian and Evgin 1997, Mortara et al. 2007).

4.2 *Tension loading tests*

Table 3 shows the static tests performed after each cyclic loading series to evaluate their effects on the pull-out capacity of the piles.

Table 3: Static pile load testing programme

Test	*Previous test (after Table II)*	Q_T *(kN)*	*Variation between tests (%)*
ICP1-T1	1st compression	9.2	-
ICP1-T2	ICP1-OW1	10.8	17.4%
ICP1-T3	ICP1-TW1	4.9	-54.6%
ICP2-T1	1st compression	12.1	-
ICP2-T2	ICP2-OW1	13.2	9.1%
ICP2-T3	ICP2-OW2	14	6.1%
ICP2-T4	ICP2-OW3	13.7	-2.1%
ICP2-T5	ICP2-TW1	8.7	-36.5%
ICP3-T1	1st compression	12.5	-
ICP3-T2	ICP3-OW1	10.9	-12.8%
ICP3-T3	ICP3-TW1,2,3,4	4.8	-56.0%
ICP4-T1	1st compression	11.5	-
ICP4-T2	ICP4-OW1	13.9	20.9%
ICP4-T3	ICP4-TW1	5.5	-60.4%
ICP4-T4	ICP4-OW2	6.0	9.1%

It is clear that low amplitude cyclic loading can lead to significant increases in the piles' tension capacities, as seen by Jardine et al (2006) in full-scale tests.

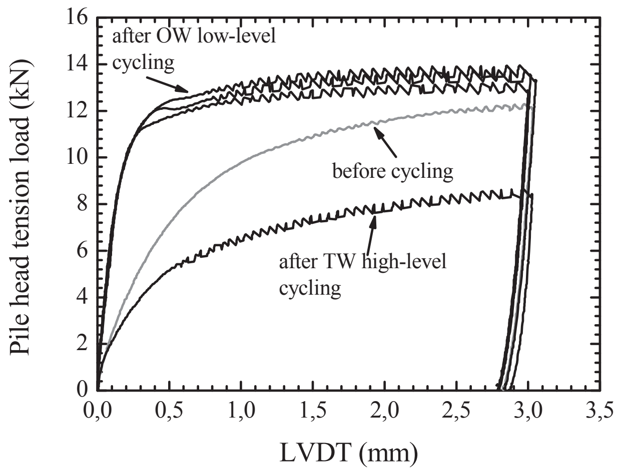

Figure 5: Tensile load-displacement curves of ICP02 before and after cycling

The pullout tests performed before and after cycling are illustrated in Figure 5 tests on Mini ICP02. The load-displacement curves show the effects of local densification near the interface which gives benefits that outweigh the parallel (marginal) losses in radial stresses. However, high-level two-way cycles, which involve both tension and compression loads, damage in the capacity markedly, primarily through the very significant losses they sustain in local radial effective stress.

4.3 *Shaft Stability Diagram*

The first phase of cyclic loading experiments was reported by Tsuha (2012), who analyzed the evolution of the piles' shaft capacities as functions of the number and the type of cycles (one-way or two-way) applied, the cyclic amplitudes and the mean load during cycling. Figure 6 shows the cyclic stability diagram established from all their tests. Three zones of behaviour were identified:

- Stable, corresponding to a region of low amplitude cycling where the pile can sustain more than 1000 cycles without accumulating significant displacements
- A Meta-stable region, corresponding to significant permanent displacement or failure between 100 and 1000 cycles
- An Unstable region, where piles fail in less than 100 cycles.

Cyclic failure was defined in any test when: i) permanent displacements reached 10% of the pile diameter (i.e. 3.6 mm); or ii) displacement rate showed a sharp increment. In this context 'slow' signifies a rate less than 1 mm/10^4 cycles, and 'fast' a rate greater than 1 mm / 100 cycles.

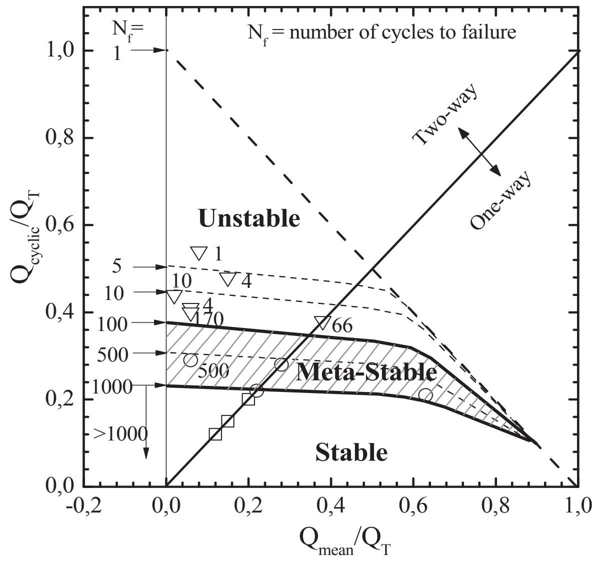

Figure 6: Shaft stability chart derived from tests ICP1-4 (after Tsuha et al. 2012)

5 CONCLUSIONS

Local measurements made of the effective stress paths developed along an intensively instrumented displacement pile, and in the sand mass around the pile, allow a better understanding of the mechanisms that govern the degradation or improvement of shaft friction during cyclic loading of piles driven in sand. In particular, the measurements help to relate the '*stable*', '*metastable*' and '*unstable*' states defined in classical cyclic stability charts to the fundamental behaviour of soils and interfaces, defining for example local 'phase transformation lines' and 'characteristic lines'.

The experiments showed applying a large number of one-way low-level cycles led to a densification at the soil-pile interface which led in turn to more marked interface dilation during further loading and shaft capacity gains for the piles.

However, high-level cycling leads to severe local stress reductions at the interface and to marked reductions in the dilatant response during further testing. Both processes cause degradation in the pull-out capacity of displacement piles in sands. This phenomenon is related to the degradation of the shaft friction along driven piles during installation.

The model pile observations are fully consistent with the behaviour seen at Dunkirk in full scale tests on steel piles driven in silica sand.

6 ACKNOWLEDGEMENTS

The authors acknowledge gratefully the support provided for the research described by Total France, Shell U.K. Limited, the French Program ANR-SOLCYP, Becas Chile, the Commonwealth Commission, the UK Health and Safety Executive, Centre National de la Recherche Scientifique, and the UK Engineering Physical Sciences Research Council.

7 REFERENCES

Al-Douri R. and Poulos H.G. 1994. Cyclic Behaviour of Pile Groups in Calcareous Sediments. *Soils and Foundations* 34, 49-59.

Chan S. and Hanna T. H. 1980. Repeated loading on single piles in sand. American Society of Civil Engineers. *Journal of the Geotechnical Engineering Division* 106 (2), 171-188.

Chin J. T. and Poulos H.G. 1996. Tests on model jacked piles in calcareous sand. *Geotechnical Testing Journal* 19(2), 164-180.

Chow F.C., Jardine R.J., Brucy F. and Nauroy J.F. 1998. Effects of time on capacity of pipe piles in dense marine sand. *Journal of Geotechnical and Geoenvironmental Engineering* 124(3), 254-264.

Fakharian K. and Evgin E. 1997. Cyclic simple-shear behavior of sand-steel interfaces under constant normal stiffness condition. *Journal of Geotechnical and Geoenvironmental Engineering* 123(12), 1096-1105.

Foray P., Tsuha C.H.C, Silva M., Jardine R.J. and Yang Z. 2010. Stress paths measured around a cyclically loaded pile in a calibration chamber. Proc. Int. Conf. on Physical Modelling in Geomechanics, ICPMG 2010, Zurich, Switzerland.

Jardine R.J. and Standing J.R. 2000. Pile load testing performed for HSE cyclic loading study at Dunkirk, France. Two Volumes. Offshore Technology Report OTO 2000 007. Health and Safety Executive, London. 60p and 200p.

Jardine R.J., Chow F., Overy R. and Standing J. 2005. ICP Design Methods for Driven Piles in Sands and Clays, Thomas Telford.

Jardine R.J., Standing J.R. and Chow F.C. 2006. Some observations of the effects of time on the capacity of piles driven in sand. *Géotechnique* 56 (4), 227-244.

Jardine R.J., Zhu B.T, Foray P. and Dalton C.P. 2009. Experimental arrangements for the investigation of soil stresses developed around a displacement pile. *Soil and Foundations* 49(5), 661-673.

Jardine R., Zhu B., Foray P. and Yang Z., 2013. Interpretation of stress measurements made around closed-ended displacement piles in sand. *Géotechni*que. DOI: 10.1680/geot.9.P.138

Kolk H.J, Baaijens A.E and Vergobbi P. 2005. Results of axial load tests on pipe piles in very dense sands: the EURIPIDES JIP Proc. 1st Int. Symposium on Frontiers in Offshore Geotechnics, ISFOG 2005, Perth, W.A.,pp. 661- 667.

Lehane B. M., Jardine R. J., Bond A. J. and Frank R. 1993. Mechanisms of shaft friction in sand from instrumented pile tests. *Journal of Geotechnical Engineering* 119(1), 19-35.

Le Kouby, A., Canou, J., and Dupla, C. 2004. Behaviour of model piles subjected to cyclic axial loading. Cyclic Behaviour of Soils and Liquefaction Phenomena: 159-166. Triantafyllidis (ed).

Mortara G., Mangiola,A. and Ghionna, V.N. 2007. Cyclic shear stress degradation and post-cyclic behaviour from sand-steel interface direct shear tests. *Canadian Geotechnical Journal* 44(7), 739-752.

Tsuha C.H.C., Foray P., Jardine R.J., Yang Z.X., Silva M. and Rimoy S. 2012. Behaviour of displacement piles in sand under cyclic axial loading. *Soils and Foundations* 52(3), 393-410.

Yang Z.X., Jardine R.J., Zhu B.T., Foray P. and Tsuha C.H.C., 2010. Sand grain crushing and interface shearing during displacement pile installation in sand. *Géotechnique* 60(6), 469-482.

Zhu B.T., Jardine R.J. and Foray P., 2009. The use of miniature soil stress measuring sensors in applications involving stress reversals. *Soils and Foundations* 49(5), 675-688.

Cyclic stability diagrams for piles in sands

Diagrammes de stabilité cyclique de pieux dans les sables

A. Puech and O. Benzaria
Fugro GeoConsulting, Nanterre, France

L. Thorel and J. Garnier
IFSTTAR, Nantes, France

P. Foray and M. Silva
3S-R, Grenoble, France

R. Jardine
Imperial College, London, UK

ABSTRACT: Cyclic stability diagrams are a useful tool for the preliminary assessment of the effects of cyclic loading on the pile behaviour. This paper presents cyclic stability diagrams obtained from various experimental sources: in situ tests on actual piles, laboratory tests on model piles in a large calibration chamber and model piles in a centrifuge. Driven piles in tension and bored piles in compression are discussed.

RÉSUMÉ: Les diagrammes cycliques de stabilité sont des outils précieux pour une première estimation de l'effet des chargements cycliques sur le comportement axial des pieux. Cette communication rassemble des diagrammes de stabilité cyclique obtenus dans des sables siliceux denses et par des moyens expérimentaux variés : essais in situ sur pieux réels, essais sur pieux modèles en grande chambre d'étalonnage et essais sur pieux modèles centrifugés. Elle couvre le cas des pieux battus en traction et celui des pieux forés en compression.

KEYWORDS: driven pile, bored pile, axial cyclic loading, cyclic stability diagrams

MOTS-CLES: pieu battu, pieu foré, chargement cyclique axial, diagramme de stabilité cyclique

1 INTRODUCTION

Cyclic interaction diagrams can be used to present synthetically the response of piles under axial cyclic loading. This concept was introduced in the nineteen-eighties by Karlsrud et al. (1986) for clays and by Poulos (1988) for sands.

It is recognised that stability diagrams can be useful tools to make a first appraisal of the potential effect of cyclic loads on pile response (Jardine et al., 2012)

Data in sands are scarce. This paper proposes cyclic stability diagrams applicable to driven piles and bored piles in dense sands.

1 TESTS IN TENSION

1.1 *Dunkirk pile tests (ICL)*

Seven open-ended non-instrumented tubular piles were tested by Imperial College London (ICL) on a site located in the western industrial sector of the Port of Dunkirk, France (Jardine and Standing, 2000). The soil profile consists of 3 m of hydraulic fill overlying Flanders sands. The marine sand is mainly composed of quartz (84%), albite and microcline (8%), and shell debris ($CaCO_3$: 8%). Cone resistances (q_c) vary from 10 MPa to 35 MPa depending on location and depth. The relative density is about 75%. Direct shear tests and triaxial tests gave peak friction angles φ' of between 35° and 40º and a constant volume friction angle $\varphi'_{cv} \sim 32º$. More details on site conditions and laboratory test results can be found in Jardine et al. (2006).

Cyclic tests were performed using the facilities of the GOPAL project (Parker et al., 1999). A total of 21 static tests and 14 cyclic tests were conducted on 6 GOPAL reaction piles. These piles were driven to a penetration of about 19 m with a space/diameter ratio of approximately 15. All piles had a diameter of 457 mm.

Several series of cyclic loads were applied, separated by reference static load tests in tension. Most of the cyclic tests were applied in tension for a better distinction between friction and end bearing.

The detailed response of piles to axial cyclic loading is described in Jardine and Standing, 2012 ; Tsuha et al., 2012; Rimoy et al., 2013.

1.2 *Calibration chamber tests (3SR-ICL-SOLCYP)*

In the framework of a collaborative programme between ICL, the 3SR Laboratory of the University of Grenoble and the SOLCYP project, several series of tests have been performed on an instrumented model pile in the large calibration chamber of the 3SR Laboratory in Grenoble. The first objective was to try to reproduce at a laboratory scale and in a controlled environment the results obtained by Jardine and Standing (2000) on piles driven in the Dunkirk sand.

The calibration chamber is 1.5 m high with a diameter of 1.2 m. A latex membrane and a film of silicon grease were applied on the internal wall to eliminate parasitic friction and facilitate the application of K_0 conditions to the sand mass. An insulation system kept the temperature between 18° and 19° throughout the testing period

The sand was a NE34, Fontainebleau sand (d_{50} = 0.2 mm, γ_{max} = 17.2 kN/m^3 et γ_{min} = 14.2 kN/m^3). For the tests considered, the sand was deposited by pluviation so as to obtain a relative density between 0.65 and 0.70. The sand mass was submitted to a vertical pressure of 150 kPa applied at the surface. The resulting cone resistance q_c ranged between 20 MPa and 23 MPa.

The model pile, developed at ICL, is described in detail in Jardine et al. (2009). This is a closed-ended 36 mm diameter pile instrumented at three levels along the shaft to measure tangential and radial stresses acting on the pile wall. Each instrumented level also includes a load cell. For the last tests the pile was equipped with a load cell at the toe.

The piles were installed to 1 m penetration by applying successions of cycles, 5 mm to 20 mm in amplitude at a rate of 0.2 mm/s, followed by a complete unloading. This procedure aims to simulate a driving process.

The experimental programme included 14 cyclic tests in tension, controlled in force or displacement, and in one-way or two-way mode.

A set of cyclic test results was already presented by Tsuha et al. (2012). More detailed information can be found in Rimoy et al., 2013

1.3 *Failure criteria*

The application of cycles on a pile installed in sand generates a succession of small relative slips at the soil-pile interface. The global displacement results from the addition of these slips. The initial rate of displacement depends on the load amplitude Q_c and on the maximal load level Q_{max} but these same parameters also control the evolution of the skin friction which can degrade for large amplitude cycles or increase for small amplitude cycles (Tsuha et al., 2012). On a pile loaded in tension, the initial rate of displacement changes in two possible ways:

- either the rate increases and the pile reaches failure. Failure can be defined in a conventional manner (e.g. for a pile head displacement of 0.1D) or for a rapid acceleration of the rate of displacement ;
- or the rate decreases and the pile tends to stabilise. The rate slows continuously to a level where it can be considered that cumulated permanent displacements become negligible.

1.4 *Cyclic stability diagrams*

The following parameters are required to fully characterise a cyclic load test:

Q_m= average value of the cyclic load
Q_c = half amplitude of the cyclic load
N_f = number of cycles to failure
N = number of cycles applied to the pile without causing failure
f = frequency of cycles (typically 0,5 Hz).

The test is in one-way mode when $Q_c< Q_m$ and two-way mode when $Q_c > Q_m$. For mormalising data the following parameter is required:

Q_u : ultimate static capacity under the mode considered (Q_{ut} in tension or Q_{uc} in compression).

The results of cyclic load tests can be conveniently presented in a diagram where each batch of cycles is identified by a pair of normalized parameters Q_m/Q_u and Q_c/Q_u. The zones where the pile is in one-way or two-way mode are clearly identified. By assigning to each representative point the number of cycles to failure N_f or the number of cycles N applied without causing failure, the domains of stability or instability for the pile can be defined. The size of these domains depends on the failure criterion selected.

Figures 1 and 2 present the cyclic diagrams obtained for the Dunkirk field tests (Jardine and Standing, 2012) and the calibration chamber tests (Tsuha et al., 2012). In both cases, failure is reached for a pile head displacement of 0.1D. The *unstable* zone delineates tests for which the failure criterion was reached before 100 cycles. The *stable* zone corresponds to small amplitude cycles where the piles were submitted to more than 1000 cycles and did not accumulate significant permanent displacements (both cases) or where the rate of displacement remained below 1 mm per 1000 cycles (Dunkirk field piles). In between the stable and the unstable zone is a so-called *metastable* zone where piles reach failure between 100 and 1000 cycles or cumulate displacements at rates suggesting possible failure beyond 1000 cycles.

It is interesting to note that the three zones would remain unchanged if the failure criterion of 0.03D as used for compression piles was adopted.

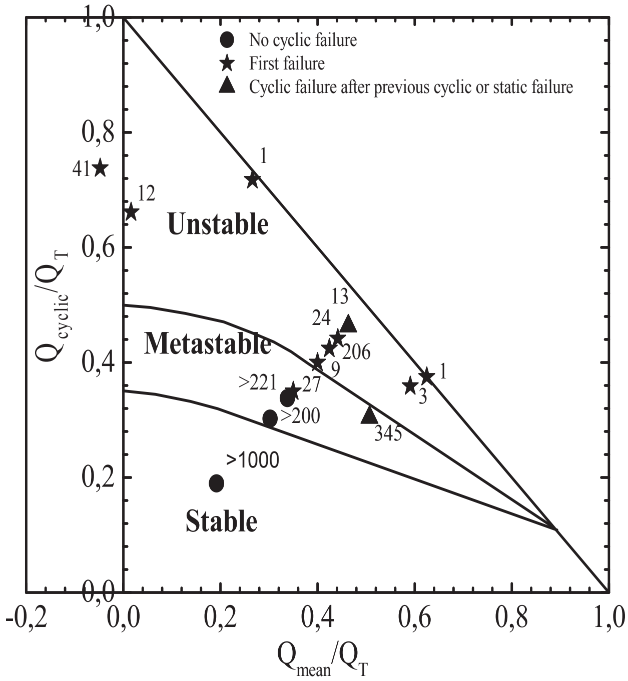

Figure 1: Cyclic stability diagram for driven piles at Dunkirk (after Jardine and Standing, 2012). Piles loaded in tension

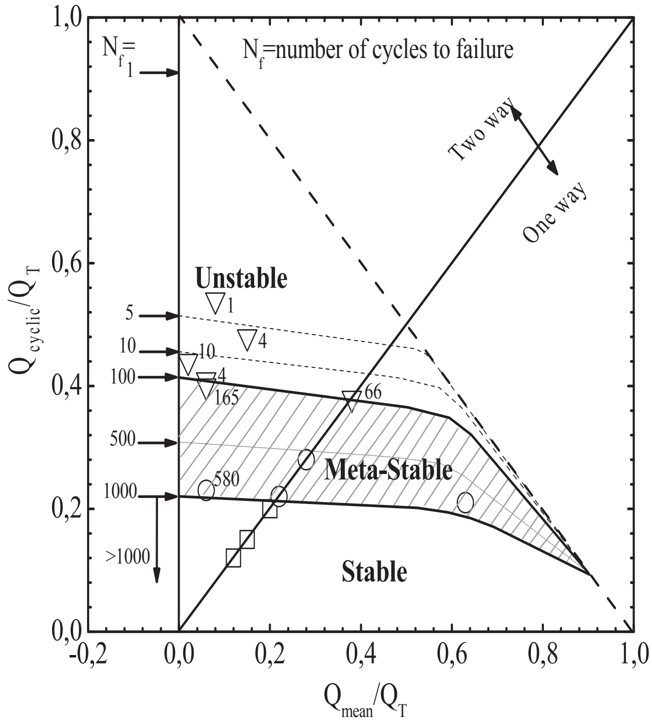

Figure 2: Cyclic stability diagram for model piles in calibration chamber (after Tsuha et al., 2012). Piles loaded in tension

2 TESTS IN COMPRESSION

2.1 *Loon-Plage tests (SOLCYP)*

As part of the National Project SOLCYP (Puech et al., 2012) field tests were conducted on the experimental site of Loon-Plage. Five bored piles and two driven metallic piles were installed in dense to very dense sands and submitted to series of static and cyclic load tests. Results for bored piles are presented in Benzaria et al. (2013).

The Loon-Plage site is located near Dunkirk in northern France. The Flanders sand formation is encountered below a cover of man-made fill (0 m to 0.6 m) and sandy clay (0.6 m to 2.2 m). The water table is about 2 m below ground level (BGL).

The sand is a very fine siliceous material (D_{50} of approximately 0.15 mm), poorly graduated (coefficient of uniformity CU=0.98), very similar to the Dunkirk sand where the ICL tests were performed (same origin). The formation is laterally homogeneous and characterised by cone resistances q_n increasing from 5 MPa to 40 MPa at 8 m depth then oscillating between 30 MPa and 50 MPa down to 11.5 m. The density index I_D derived from CPT measurements is comprised between 0.7 and 0.9 (dense to very dense sand).

The critical angle of internal friction φ'_{cv} obtained from monotonic triaxial tests is close to 31° in good agreement with values previously found on Dunkirk sand (Jardine and Standing, 2000).

Piles F4 and F5 are geometrically identical (D = 420 mm, length 8 m). They were constructed used the CFA technique: a hollow auger penetrates the soil by continuous rotation and is then extracted without rotation while grout is poured through the hollow stem. Piles were equipped with a set of removable extensometers installed in reservation tubes welded to the reinforcement cage.

The piles were tested three months after installation. The loading programme included static reference tests according to the incremental procedure (load steps maintained 1 hour) as recommended by ISSMGE or AFNOR NF P 94-150, rapid load tests (load steps maintained only 3 mn) and cyclic load tests at a frequency of 0.5 Hz. A more detailed description of the loading process can be found in Benzaria et al. (2012).

2.2 *Centrifuge model tests (SOLCYP)*

Extensive model tests were conducted in the IFSTTAR geotechnical centrifuge in Nantes (Guefrech et al., 2012). Piles had a length-to-diameter ratio of 31 and were at a scale of 1/23^{d} with a diameter of 18 mm. The surface was perfectly rough. They were cast in place, i.e. pre-positioned in the container before the surrounding sand mass was formed by the pluviation method. This technique aims at representing bored CFA piles as used in Loon-Plage.

The dry NE34 Fontainebleau sand is identical to the sand used in the 3SR Laboratory for their calibration chamber tests and has physical and mechanical properties similar to the Flanders sand.

The tests discussed below were performed in a dense sand ($I_D \sim 0.7$) at a frequency of 1 Hz. Only one-way cyclic tests in compression are analysed.

2.3 *Failure criterion*

Defining failure criteria in compression is more complex than in tension. In compression, the pile will tend to stabilize irrespective of the rate of displacement generated by the first cycles. This observation is valid for both the field tests (Benzaria et al., 2013) and the model tests (Guefrech et al., 2012). Even in the case of rapid degradation of the interface friction, the resulting displacement of the pile toe generates a progressive mobilisation of the end bearing and a decrease of the rate of displacement and the pile tends to stabilise.

The failure criterion can no longer be defined in a conventional manner (e.g. pile head displacements reaching 0.1D) but should be expressed in terms of allowable permanent displacements. The criterion may be reached for a small number of cycles in case of very severe cyclic loading (and possibly under increasing rate of displacement) but more generally after a more or less important number of cycles and under decreasing rate of displacement.

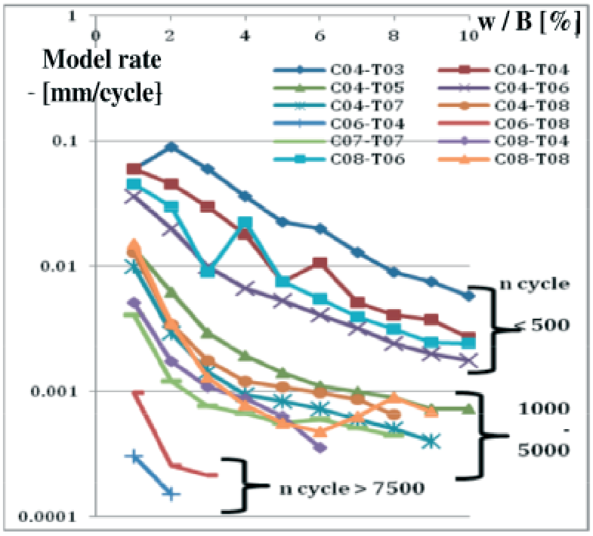

Figure 3: Rate of pile head displacements for one-way cyclic compression tests in the centrifuge

The analysis of the rate of pile head displacement observed in the centrifuge model tests illustrates the phenomena (Figure 3). Three types of results may be identified: a) tests where pile displacements have reached 0.1D in less than 500 cycles and with a permanently decreasing rate of displacement; b) tests where the criterion is reached for only 1000 to 5000 cycles with a rate of displacement tending to stabilise; c) tests showing a rapid drop in the rate of displacement which reaches very low values (< 0.5 mm per 1000 cycles). Further evolution towards significant displacements is unlikely.

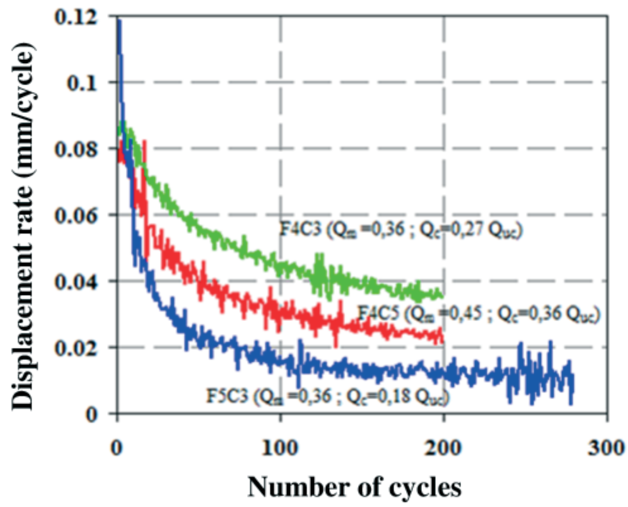

Figure 4: Rate of pile head displacements for one-way compression tests at Loon-Plage

Figure 4 shows similar trends for plots of pile head displacements for the field tests at Loon-Plage.

2.4 *Cyclic stability diagrams*

Cyclic stability diagrams obtained for one-way compression tests for the Loon-Plage bored piles and the centrifuge cast-in-place piles are presented on Figures 5 and 6.

The diagrams in Figures 5 and 6 were constructed assuming a failure criterion defined at 0.03 D of pile head displacement. The *unstable* zone characterises tests where the failure criterion was reached in less than 100 cycles. The *stable* zone corresponds to small amplitude cyclic load tests where piles could not reach the criterion and the rate of displacement was very low. In the *metastable* zone the piles reached failure for a number of cycles between 100 and 1000.

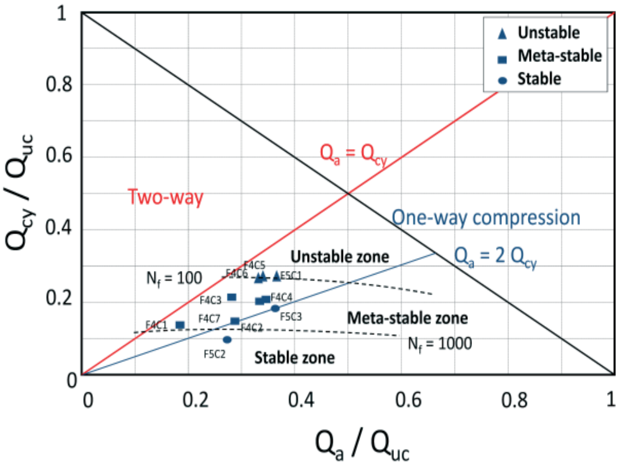

Figure 5: Cyclic stability diagram for one-way compression tests on Loon-Plage bored piles

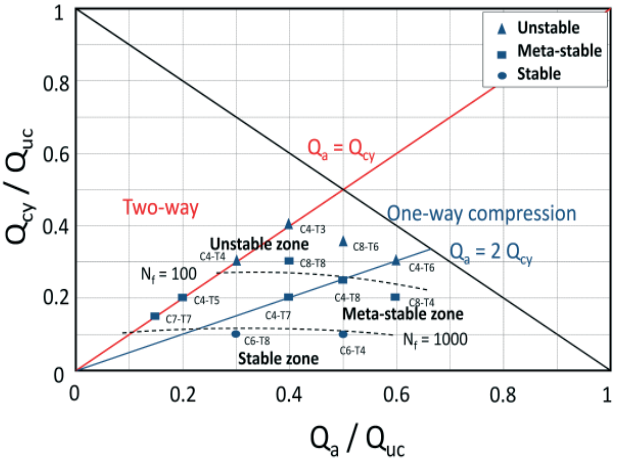

Figure 6: Cyclic stability diagram for one-way compression tests on cast in place centrifuge tests

The diagrams in Figures 5 and 6 are very similar. More details on the methodology used to establish the diagrams can be found in Puech (2013). It is recommended that these diagrams are not extrapolated in the two-way domain. Available data (not shown here) indicate a significant reduction of the stable and metastable zones under alternate cyclic loading.

3 CONCLUSION

This paper presents cyclic pile stability diagrams obtained in dense silica sands and using various experimental sources: in situ tests on real piles, model tests in calibration chamber, centrifuge model tests. The cases of driven piles in tension and of bored piles in compression are addressed.

Cyclic stability diagrams are useful tools for making a preliminary appraisal of the degradation potential of cycles on the response of axially loaded piles.

Attention is drawn to the difficulty in defining pertinent failure criteria, particularly in compression. Cyclic stability diagrams should be interpreted with due consideration to the criteria used to create the diagram.

4 ACKNOWLEDGEMENTS

This paper results from a fruitful collaboration between many researchers and several organisations. The authors are particularly grateful to their colleagues for their valuable inputs and to the partners of the SOLCYP project for authorising publication of the data.

5 REFERENCES

AFNOR.1999. NF P 94-150. Norme Française. Sols: Reconnaissance et Essais – Essai statique de pieu sous effort axial – Partie 1: en compression et Partie 2: en traction

Benzaria O., Puech A., and Le Kouby A. 2012. Cyclic axial load-tests on driven piles in overconsolidated clay, *Offshore Site Investigation and Geotechnics*, SUT, London

Benzaria A., Puech A. et Le Kouby A. 2013. Essais cycliques axiaux sur des pieux forés dans des sables denses. *Proceedings 18th ICSMGE,* Paris

Guefrech A., Rault G, Chenaf N., Thorel L., Garnier J., Puech A. 2012 Stability of cast in place piles in sand under axial cyclic loading . *Proc. 7th Int. Conf. Offshore Site investigation and Geotechnics*. London. 12-14 sept. pp.329-334.

Jardine, R.J. and Standing, J.R. 2000. Pile load testing performed for HSE cyclic loading study at Dunkirk, France. Two Volumes. *Offshore Technology Report OTO 2000 007; Health and Safety Executive*, London. 60p and 200p.

.Jardine, R.J., Standing, J.R. and Chow, F.C. 2006. Some observations of the effects of time on the capacity of piles driven in sand. *Geotechnique,* 56 (4), 227-244.

Jardine, R., Bitang, Z., Foray, P., and Dalton, C. 2009. Experimental Arrangements for Investigation of Soil Stresses Developed around a Displacement Pile. *Soils and Foundations*, 49(5), 661–673.

Jardine, R.J. and Standing. 2012. Field axial cyclic loading experiments on piles driven in sand. *Soils and Foundations*, 52(4), 723–736.

Jardine R, Puech A and Andersen K. 2012. Cyclic loading of offshore piles: potential effects and practical design. *Proc.7th Int. Conf. on Offshore Site Investigations and Geotechnics,* SUT,. London.

Karlsrud K., Nadim F. and Haugen, T. 1986. Piles in clay under cyclic axial loading - Field tests and computational modeling. *Proc. 3rd Int. Conf. on Numerical Methods in Offshore Piling,* Nantes, France

Parker, E. J., Jardine, R.J., Standing, J.R. and Xavier, J. 1999, Jet grouting to improve offshore pile capacity. *Offshore Technology Conference*, Houston, OTC 10828.

Poulos H.G. 1988 Cyclic stability diagram for axially loaded piles. *Journal of Geot. and Geoenv. Eng.* 114 (8): 877-895 .

Puech A. 2013. Advances in axial cyclic pile design: contribution of the SOLCYP project. *Proceedings TC 209 Workshop.* 18 ICSMGE, Paris, Ed. Presses des Ponts et Chaussées. To be published

Puech A., Canou J., Bernardini C., Pecker A., Jardine R., and Holeyman A. 2012. SOLCYP: a four year JIP on the behaviour of piles under cyclic loading. *Offshore Site Investigation and Geotechnics*, SUT, London

Rimoy S., Jardine R. and Standing J. 2013. Displacement response to axial cyclic loading of driven piles in sand. *Proceedings 18th ICSMGE,* Paris

Tsuha, C., Foray, P., Jardine, R., Z.X., Y., Silva, M., and Rimoy, S. 2012. Behaviour of displacement piles in sand under cyclic axial loading. *Soils and foundations*, 52(3), 393–410.

Pile in sand under lateral loading: Development of degradation laws for describing cyclic load effects

Pieu sous charge latérale dans les sables : développement de lois de dégradation pour prendre en compte l'effet des cycles

F. Rosquoët
Laboratoire LTI (AE3899), Amiens, France

L. Thorel and J. Garnier
LUNAM Université, IFSTTAR, Nantes, France

ABSTRACT: The design of piles under lateral cyclic loads has for long assumed that the soil was in a state of failure (limit state calculation). Calculation methods have improved and the design can now be done in displacement but without being able to take into account cyclic loads (except for offshore piles). To analyse the cyclic effects two methods have been developed: the global method which focuses on pile head displacements and maximum bending moments and the local method which relates to P-y curves. For the global method, it is shown that the effect of cycles is essentially related to the ratio of the cyclic load amplitude to the maximum cyclic load. An empirical law is proposed which allows pile head displacements under cyclic loads to be evaluated from displacements calculated under static loading. In sands, maximum bending moments were found marginally affected by cyclic loads. For the local method based on P-y curves, a reduction coefficient (p-multiplier) is given which may be applied to the static P-y curves to take the cyclic effect into account.

RÉSUMÉ : Le dimensionnement des pieux sous une charge latérale a longtemps supposait que le sol était à l'état de rupture (calcul aux états limites). Les méthodes de calcul ont progressé et le dimensionnement peut maintenant être réalisé en déplacement mais sans possibilité de tenir compte de l'effet des cycles de chargement (sauf dans le cas des ouvrages offshore). Pour corriger cette lacune, nous proposons deux méthodes : une méthode globale axée sur le déplacement en tête de pieu et sur le moment maximum, et une méthode locale basée sur les courbes P-y. Pour la méthode globale, nous montrons que l'effet des cycles sur le déplacement est essentiellement lié au rapport entre l'amplitude de la charge cyclique et la charge maximale. Nous proposons une loi de type logarithme donnant le déplacement relatif en fonction du nombre de cycles. On notera que, dans les sables, l'effet des cycles sur le moment maximum est faible. Pour la méthode locale, nous introduisons un coefficient d'abattement qui permet de prendre en compte l'effet des cycles en modifiant la réaction des courbes P-y statiques.

KEYWORDS: Pile – Lateral cyclic loading

1 INTRODUCTION

The lateral cyclic loading of piles is generally caused by waves or wind on offshore structures, berthing and mooring forces on quays, tidal variations or operational loads on coastal or harbour facilities, traffic loads or thermal variations on onshore structures. Cyclic loading sequences are characterized by four parameters: the maximum applied load F, the load variation amplitude DF, the number of cycles n, and the loading mode (one-way or two-way).

To study the pile behaviour under cyclic loads, centrifuge model tests were performed. This method allows parametric studies and improves the understanding of phenomena governed by multiple variables. A better knowledge and quantification of pile behaviour under lateral cyclic loading may help improve the design of piles under lateral loads.

In the geotechnic field, scaling laws state that a model at a reduced scale 1/n must be tested under acceleration n times the earth gravity. At IFSTTAR, centrifuge modelling was applied to the study of pile under lateral cyclic load in sand (Rosquoët, 2004 and Rakotonindriana, 2009) or in clay (Khemakhem, 2012).

An important research programme on piles under cyclic load is currently in progress in France. The lateral cyclic load testing described in this paper forms part of the SOLCYP project.

The ultimate aim of this research is to devise a method for designing piles under cyclic loads. This method must quantify the influence of the cyclic loads on the pile head displacement y, the maximum bending moment M and the relation, at any depth z, between the soil reaction P(z) and the lateral pile displacement y(z) called P-y curve.

The research is limited to service load conditions (maximum load less than one third of the ultimate lateral static resistance). In the tests considered, the piles are flexible (or long) which means that the pile response is not affected by soil-pile interactions concerning pile sections located at depth larger than 3 times the transfer length l_0 (Frank, 1999). Pile behaviour is mainly governed by the upper section, between the soil surface and depths of four to five times the pile diameter B. For comparison, in the API (2002) rules, the effects of cyclic loads in sands are limited to depths less than 2.625B.

1 TEST PROCEDURE

Homogeneous dry Fontainebleau sand samples, at density of 1630 kg/m^3 (relative density I_D = 86%), were prepared using a raining technique and an automatic hopper.

The flexible model pile (at scale 1/40) was instrumented with 20 pairs of strain gauges. Tested under an acceleration of 40-g, it represented a prototype (true scale pile) with a diameter B = 0.72 m, an embedded length of 12 m and a bending stiffness of 476 MN.m^2 (Figure 1). The pile was driven into the sand sample at 1g (earth gravity) before rotating the centrifuge.

The pile was loaded horizontally whilst the vertical load was kept constant (pile dead weight). The load was applied at an elevation of 40 mm (model scale) above the ground surface with a servo jack and transmitted to the pile through a cable (for the one-way cyclic loading).

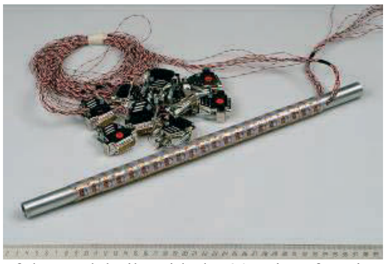

Figure 1: View of the model pile with the 20 pairs of strain gauges

The pile head displacement and rotation were measured using two horizontal displacement sensors located at 20 mm and 65 mm above the ground (Figure 2).

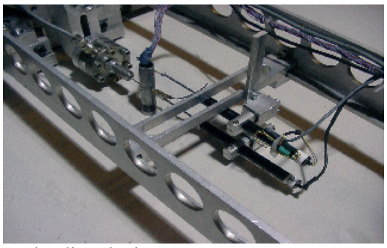

Figure 2: One way loading device

In one-way cyclic loading, the load was always applied in the same direction and varied between F and F minus DF.

2 GLOBAL METHOD

2.1 *Pile head displacement*

The cyclic effect on pile head displacement depends on the load amplitude (DF) and on the maximal applied load (F). Figure 3 shows a plot of the ratio of the pile displacement at cycle n (y_n) to the pile displacement at first loading (y_1) with the number of cycles n.

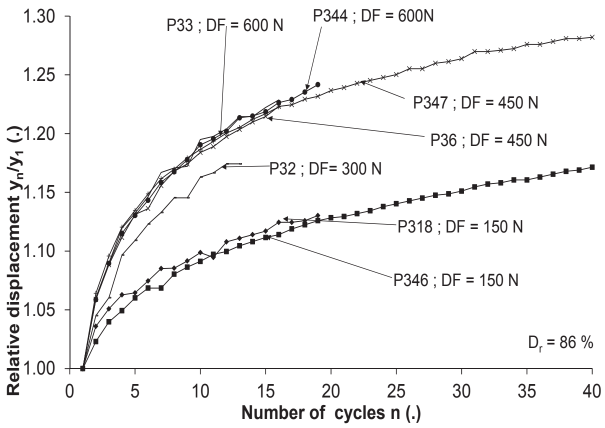

Figure 3: Relative displacement y_n/y_1 versus number of cycles for different amplitudes DF and same maximum load F = 960 kN

As already observed by several authors, a logarithmic law represents correctly the relation between the relative displacement y_n/y_1 and the number of cycles (Equation 1):

$$\frac{y_n}{y_1} = 1 + b\ln(n) \tag{1}$$

where b is a positive parameter and n the number of cycles.

All test data could be fitted with the proposed logarithmic law (1) with a correlation coefficient R² = 0.98. Each test can therefore be characterized by a unique value of the b parameter.

Table 1 gives b values for different cyclic load amplitudes DF. The b parameter is taken equal to 0 for DF = 0 because pile displacements in sand under constant load (as observed from creep tests) are negligible. This table also gives the calculated uncertainty σ_b on the parameter b (Taylor, 1982) assuming that the uncertainty on the variable y_n/y_1 follows a Gaussian distribution (Rosquoët 2004).

Tableau 1: Values of the parameter b and the calculated uncertainty σ_b

Test	*Number of cycles*	*F (kN)*	*DF (kN)*	*b (.)*	*σ_b (.)*
P33	14	960	960	0.082	0.019
P344	14	960	960	0.081	0.017
P36	18	960	720	0.078	0.017
P347	40	960	720	0.075	0.01
P32	15	960	480	0.071	0.021
P318	25	960	240	0.044	0.017
P346	40	960	240	0.049	0.01

The degradation parameter b increases with the cyclic load amplitude DF and can be closely correlated to the ratio DF/F between the amplitude of cycles DF and the maximum applied load F (Figure 4) according to Equation (2):

$$b = 0.08\left(\frac{DF}{F}\right)^{0,35} \tag{2}$$

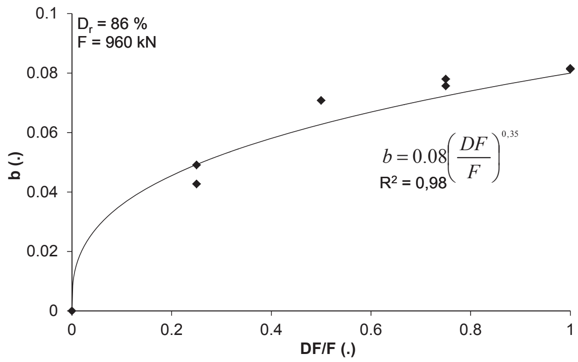

Figure 4: Degradation coefficient "b" versus cyclic load ratio DF/F

The effects of cyclic loads on the pile head displacement may finally be calculated by Equation (3).

$$\frac{y_n}{y_1} = 1 + 0.08 \times \ln(n) \times \left(\frac{DF}{F}\right)^{0,35} \tag{3}$$

Table 2: Values proposed in the literature for the parameter b

Author	*Soil*	*Pile tested*	*Number of cycles*	*Degradation parameter b*
Hettler (1981)	Dry sand	Rigid (1-g model test)		0.2
Bouafia (1994)	Dry sand	Rigid (centrifuge tests)	5	0.18 < b < 0.25
Lin and Liao (1999)	Different sites	In situ tests	100	0.02 < b < 0.24
Hadjadji et al. (2002)	Clay and sand	In situ tests	10000	0.087
Verdure et al. (2003)	Dense dry sand	Flexible (centrifuge tests)	50	0.04< b < 0.18
Rakotonindriana (2009)	Dry sand	Flexible (centrifuge test)	500	0.12
Li et al. (2010)	Dense dry sand	Rigid (centrifuge tests)	100 to 1000	0.17< b < 0.25
Peralta (2010)	Dry sand	Flexible (1-g model tests)	10000	0.21

Table 2 presents the range of values proposed by different authors for the parameter b.

The largest values of b were obtained in 1-g model tests (Hetler, 1981; Peralta, 2010) or in tests where very large moments were applied to the pile head in addition to the lateral loads for simulating offshore wind turbines foundation (Li et al., 2010; Peralta, 2010).

For usual onshore conditions, the relationship given in Equation (4) is suggested:

$$\frac{y_n}{y_1} = 1 + 0.1 \times \ln(n) \times \left(\frac{DF}{F}\right)^{0,35} \qquad (4)$$

2.2 *Maximum bending moment*

From an engineering point of view, the maximum bending moment is a key parameter in laterally loaded pile design. The test data are presented in Figure 5 which shows the effect of the number of cycles on the ratio M_n/M_1.

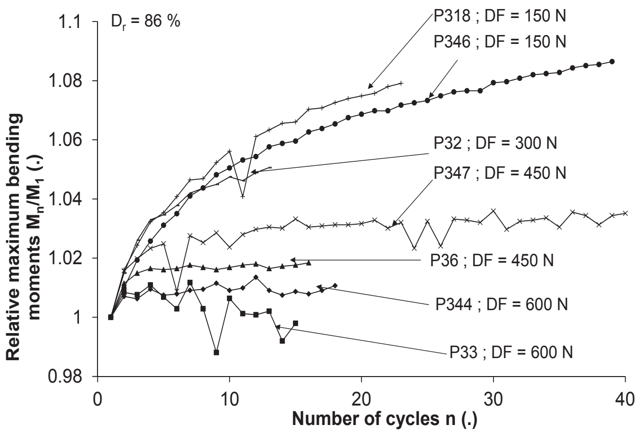

Figure 5: Relative maximum bending moment M_n/M_1 versus number of cycles for several DF and F = 960 kN

As already proposed for pile head displacement, the relative bending moment M_n/M_1 can be correlated to the number of cycles n by a logarithmic expression of the type (Equation 5):

$$\frac{M_n}{M_1} = 1 + a\ln(n) \qquad (5)$$

However, the effect of cyclic loading on the maximum bending moment is small: the ratio M_n/M_1 remains close to 1 and always below 1.1 (Figure 5). In all cases, the value of the parameter a derived from the tests (Table 3) is of the same order of magnitude as the calculated values of uncertainty on this parameter a. For much larger numbers of cycles, Rakotonindriana (2009) found similar results and observed an increase of the maximum bending moment at 75000 cycles of 12% (from the value recorded under the initial static maximum load). Consequently, it is proposed that for dry and dense sand cyclic loading is accounted for by applying conservatively a 10% increase on the maximum bending moment calculated under the maximum static loading.

Table 3: Coefficient a and uncertainty σ_a (F = 960 kN, I_D = 86 %)

Test	*Number of cycles*	*DF/F (.)*	*a (.)*	*σ_a (.)*
P33	14	1	0	/
P344	14	1	0	/
P36	18	0,75	0.0047	0.0038
P347	40	0,75	0.0069	0.0052
P32	15	0,5	0.019	0.017
P318	25	0,25	0.026	0.014
P346	40	0,25	0.025	0.006

3 LOCAL METHOD

As already proposed by several authors and adopted in offshore rules (API RP2GEO, 2011), it may also be possible to model the effect of cyclic loading by reducing the soil reaction P in the static P-y curves of the surface layers. This method may be implemented in any software used for calculating piles under lateral static load. To quantify the cyclic effect on the soil reaction degradation, a proportional transformation is applied to the static P-y curves using a reduction coefficient r sometimes called P-multiplier. This P-multiplier depends on five parameters: the depth z, the pile displacement y, the number of cycles n, the maximum applied load F and the load amplitude DF.

3.1 *Determination of soil degradation parameter r*

The reduction coefficient of soil reaction r (P-multiplier) is determined through an iterative process using the Pilate-LCPC software for lateral pile loading (Romagny, 1985).

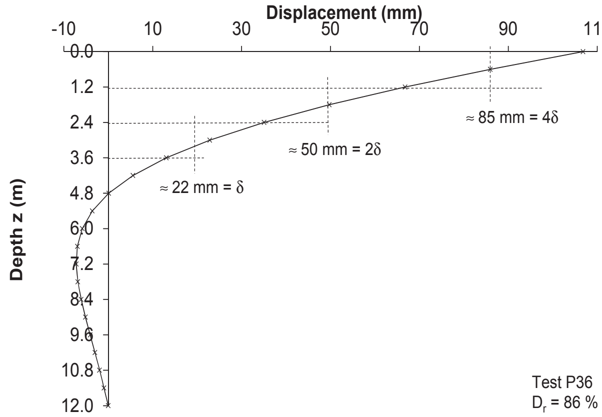

Figure 6: Typical pile lateral displacement profile

Figure 6 shows an example of lateral displacement versus depth profile for a laterally loaded pile. If the pile displacement at depths between 2.4 m and 3.6 m (about 3.5 B to 5 B) is noted δ, the displacement is close to 2δ at depths between 1.2 m and 2.4 m (2 B to 3.5 B) and to 4δ between 0 and 1.2 m (0 to 2 B).

It is assumed that, at any depth, the reaction degradation is proportional to the pile lateral displacement. If so, the reduction coefficient r must follow the same distribution with depth as observed in Figure 6. An iterative process was used to determine the values of the degradation parameter r at any depth for each pile loading test.

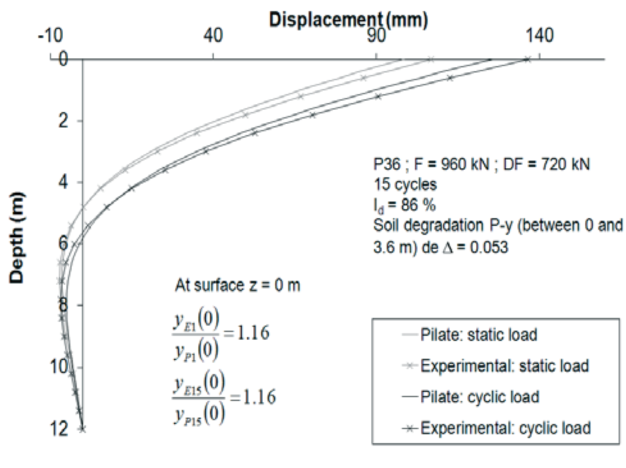

Figure 7: Comparison of measured and calculated pile displacements

An example is shown in Figure 7 where the pile lateral displacement recorded during the test is compared to the calculated pile displacement. These displacements are calculated first with the static P-y curves and then with these P-y curves modified in the upper layers from 0 to 5 B by the reduction coefficients r. In this example, the P-multiplier r was found equal to 0.79 at depths between 0 to 2 B, 0.89 at depths between 2 B to 3.5 B and 0.95 at depths between 3.5 B and 5 B.

Good agreement is observed between the test data and the predicted values ($y_{15}/y_1 = 1.16$ in both cases) for the effect of the cyclic loads (F = 960kN, DF = 720kN) on the pile displacement. Other tests performed with the same maximum load F = 960kN and different cyclic load amplitudes DF were analysed and show that, for dense sands ($I_D = 86\%$), the P-multiplier r depends on DF, a high DF generating a substantial degradation of the P-y curves (Figure 8).

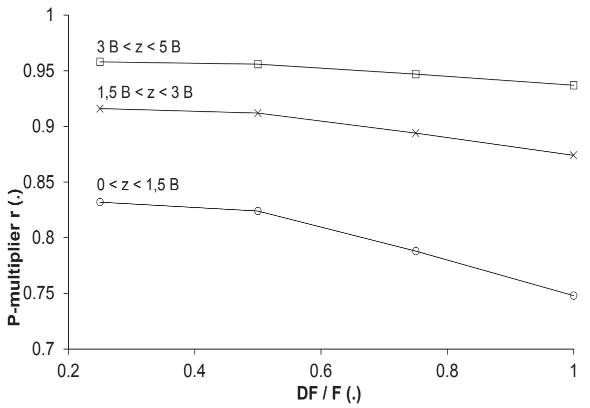

Figure 8: P-multiplier r versus DF/F (for 15 cycles)

Table 4 gives a simple approximate linear expression of the r coefficient versus DF/F at different depths between 0 and 5 B.

Table 4: Expression of P-multiplier r at different depths (for 15 cycles)

Depth z	*Relationship* r = *f(DF / F)*
$0 < z < 1{,}5B$	$r = 0.87 - 0.12\dfrac{DF}{F}$
$1.5B < z < 3B$	$r = 0.94 - 0.058\dfrac{DF}{F}$
$3B < z < 5B$	$r = 0.97 - 0.029\dfrac{DF}{F}$

4 GLOBAL AND LOCAL METHODS COMPARISON

A comparative example of the two methods is given in Figure 9 for a pile in dry dense sand (I_D = 86%) and a cyclic load sequence characterised by F = 960 kN and DF = 720 kN.

The difference between the local method and global method in the estimation of the pile lateral displacement under the maximum load at cycle n = 15 is very small and is about 2% for the pile head displacement at ground level.

Table 4 gives the values of the P-multipliers for only 15 cycles but it is recognised that most of the cycle effects appear during the first tens of cycles. However, more research is in progress aiming at extrapolating present results to much larger number of cycles.

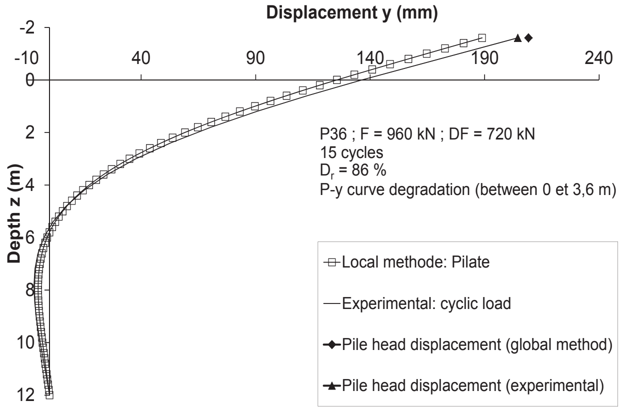

Figure 9: Displacement versus depth (global method vs local method)

5 CONCLUSION

An analysis was carried out on the test data obtained at IFSTTAR on piles in dry dense sands under lateral cyclic load (Rosquoët, 2004; Rakotonindriana, 2009). Two methods were developed for designing piles under lateral cyclic load.

The global method consists of estimating pile head displacement and maximum bending moment under any cyclic load sequence, knowing the maximum applied load F, the pile head displacement and bending moment under static load F, the cyclic load amplitude DF and the number of cycles n.

In the local method static P-y curves already proposed in various codes of practice are modified by applying P-multipliers which account for cyclic degradation effects by reducing the soil reaction. P-multipliers are proposed which are function of depth and ratio DF/F. The local method provides more detailed information than the global method on the pile response to cyclic loads (profiles of pile lateral displacements, rotations, bending moments and soil reactions).

A good agreement was shown between the results obtained by both methods (local and global). However, whereas the global method may be used for large numbers of cycles (>500), the local method has currently be validated only for the first tens of cycles.

6 ACKNOLEDGMENTS

This research was supported by the French national project SOLCYP and by IFSTTAR. Both supports are greatly appreciated.

7 REFERENCES

API RP2GEO. 2011. API Recommended Practice, Geotechnical and Foundation Design Considerations, First Edition, April 2011.

Bouafia A. 1994. Etude expérimentale du chargement latéral cyclique répété des pieux isolés dans le sable en centrifugeuse. *Canadian Geotechnical Journal*, Vol. 31, n°5, 740-748.

Frank R. 1999. *Calcul des fondations superficielles et profondes*. Editions Technique de l'Ingénieur et Presse des Ponts et Chaussées. Paris.

Garnier J. 2001. Modèles physiques en géotechnique. I-Evolution des techniques expérimentales et des domaines d'application. *Revue Française de Géotechnique*. N°97. 3-29.

Hadjadji T., Frank R. and Degny E. 2002. Analyse du comportement expérimental de pieux sous chargements horizontaux, LCPC, Collection Etudes et Recherches, GT74, 303 p.

Hettler. A. 1981. Verschiebungen starrer und elastischer Gründungs körper in Sand bei monotoner und zyklischer Belastung. *Institut für Boden-und Felsmechanik der Universität Karlsruhe*, Heft Nr. 90.

Khemakhem M. 2012. Etude expérimentale de la réponse aux charges latérales monotones et cycliques d'un pieu foré dans de l'argile. *Thèse de Doctorat. Ecole Centrale de Nantes Université de Nantes*. 336 p.

Lin S.S.and Liao J.C. 1999. Permanent strains of piles in sand due to cyclic lateral loads. *Journal of Geotechnical and Geoenvironemental Engineering*, Vol. 125, n°9, 798-802.

Li Z. Haigh S. K. and Bolton M. D. 2010. Centrifuge modelling of mono-pile under cyclic lateral loads. *7th International Conference on Physical Modelling in Geotechnics*. Zurich. Vol. 2, 965-970.

Peralta P. and Achmus M. 2010. An experimental investigation of piles in sand subjected to lateral cyclic loads. *7th International Conference on Physical Modelling in Geotechnics*. Zurich. Vol. 2, 985-990.

Rakotonindriana M. H. J. 2009. Comportement des pieux et des groupes de pieux sous chargement latéral cyclique. *Thèse de doctorat. Ecole Nationale des Ponts et Chaussées*. 381p.

Romagny J.C. 1985. Calculation programme for a pile subjected to lateral loads at the head and to lateral thrusts from soil. *LCPC Paris. 1ère version J.L. Bangratz , R. Frank , M. Kutniak, pp 69.*

Rosquoët F. 2004. Pieu sous charge latérale cyclique. *Thèse de Doctorat. Ecole Centrale de Nantes Université de Nantes*. 305 p.

Taylor J. 1982. An introduction to error analysis, 1982, *Univ. Science Books, 315 p r.*

Verdure L. Levacher D. et Garnier J. 2003. Effet des cycles sur le comportement d'un pieu isolé dans un sable dense sous chargement latéral. *Revue Française de Génie Civil*. 7/2003. 1185-1210.